

https://dspace.org/

Design of an acid mine drainage remediation process using by-products from the steel manufacturing and sugar processing industries

Naidu, Tamlyn Sasha

2024
https://hdl.handle.net/10539/37378

Downloaded from a DSpace repository. https://dspace.org/



UNIVERSITY OF THE
WITWATERSRAND,
JOHANNESBURG

Design of an Acid Mine Drainage Remediation Process using By-products from the Steel Manufacturing and Sugar Processing Industries

Chemical Engineering Doctoral Dissertation

Prepared by:
Tamlyn Sasha Naidu
457495

Submitted to:
SCHOOL OF CHEMICAL AND METALLURGICAL ENGINEERING FACULTY OF ENGINEERING AND THE BUILT ENVIRONMENT, UNIVERSITY OF THE WITWATERSRAND, JOHANNESBURG, SOUTH AFRICA

Supervisors:
PROF. CRAIG SHERIDAN & PROF LIZELLE VAN DYK

January 2023

Acknowledgements

My deepest gratitude goes to my supervisors, Prof. Craig Sheridan and Prof. Lizelle van Dyk; my family (and advisors), Trevonica, Thiagaraja (Hi dad!), Tahlia, Teagen, Thoshar, Tamara and all the other Ts; my PhD partner, colleague and confidante, Ruther; my (much more than) friends, Megan and Sean; and most importantly to my baberr, Nikhil.

Thank you for your unending support and guidance, your many, *many* reviews, all the (very) heavy lifting, for seeing me through all the breakdowns you had to witness along the way, the mental health issues you simultaneously caused and cured, and - ultimately - for making this research possible.

And – now that I will have time to tend to relationships – I would also like to thank my two unborn children for their patience. In their absence, this dissertation is dedicated to Teddy, Arabella, Leia, Starlord, Trinny, Vlad, Grey, Didi and Bon. Although they may not be able to understand the content, I hope they will find in it some abstract appreciation.

Declaration

UNIVERSITY OF THE
WITWATERSRAND,
JOHANNESBURG

University of the Witwatersrand, Johannesburg

School of Chemical and Metallurgical Engineering

PLAGIARISM POLICY

Declaration by Students

I, Tamlyn Sasha Naidu, (Student number: 457495), am a student registered for a Doctoral Degree in Chemical Engineering in the year 2023.

I hereby declare the following:

- I am aware that plagiarism (the use of someone else's work without their permission and/or without acknowledging the original source) is wrong.
- I confirm that ALL the work submitted for assessment for the above course is my own unaided work except where I have explicitly indicated otherwise.
- I have followed the required conventions in referencing the thoughts and ideas of others.
- I understand that the University of the Witwatersrand may take disciplinary action against me if there is a belief that this is not my own unaided work or that I have failed to acknowledge the source of the ideas or words in my writing.

Signature: 

Date: **10 May 2023**

Abstract

Acid mine drainage (AMD) and basic oxygen furnace (BOF) steel slag are waste products from the mining and steel refining processes that are produced in large volumes throughout the world. Although both substances possess useful characteristics, they are largely treated as wastes, and dumped or disposed of in waterways and landfills, causing detrimental environmental and health issues. Treatment schemes that have aimed to address the occurrence or presence of AMD, in particular, are limited due to (i) the high cost of remediation (when compared to the relatively low cost of water), and (ii) variation in AMD characteristics which makes a standard/uniform treatment approach difficult to achieve. The technology explored within this dissertation has the potential to combat both challenges: (i) the cost of the treatment scheme would be substantially lower due to very little envisioned operational involvement, as well as the cost of reagents being kept low (through the use of waste and by products, and through potential valorisation of these wastes); (ii) the technology is aimed to be deployed at the source of production – individual mining sites – in a modular manner, allowing for alteration of treatment schemes to combat a wide variety of AMD strengths and qualities.

BOF slag and AMD combined in an optimized process allowed for the rise in pH of the AMD to neutral levels, as well as the removal of substantial amounts of metals and sulfates. Following this initial physical and chemical treatment, the partially treated AMD stream was then suitable for biological treatment using by-products from the sugar industry, allowing for further removal of sulfate, bringing the water closer to discharge and even drinking water limits: at a laboratory scale, sulfate was shown to reach levels of below 200 mg/L and levels of below 10 mg/L were reached for Al, Fe, Mg and Mn. Operation of a pilot-scale plant treating 200-1000 L/day demonstrated Al, Fe, Mn and SO_4^{2-} removals of 97%, 87%, 100%, and 87% respectively – showing that treatment occurred even in fluctuating AMD conditions. The configuration of the treatment scheme that yielded the best results was suggested for the final design and included a modular system in which BOF slag was used to increase the pH of the system before bacteria sugarcane derivatives were used to polish the sulfate leftover in the stream to below 400 mg/L.

The system which was proposed, designed and tested in this study was successful in treating AMD. It proved to be able to serve as a precursor to multiple other treatment regimes (reverse osmosis, membrane filtration, ionic exchange), or as a stand-alone system to service smaller, isolated areas that aim to reuse the AMD affected water in processes or for irrigation.

Contents

Acknowledgements i
Declaration ii
Abstract iii
List of Tables vii
List of Figures ix
1. Introduction 1
1.1 Background and motivation for study 1
1.2 Problem Statement 4
1.3 Research Objectives 4
1.4 Novelty of Research 5
1.5 Structure and Outputs of the Dissertation 5
2. Literature Review 9
2.1 Acid Mine Drainage 9
2.2 Sugarcane Bagasse 23
2.3 BOF Slag 24
3 Methods and Materials 59
3.1 Materials 59
3.2 Equipment 59
3.3 Methodology 60
3.4 Analytical Techniques 63
3.5 Facilities Used 64
4 BOF Slag Dissolution – Harnessing Alkalinity for AMD pH Modification 65
4.1 Introduction 65
4.2 Methodology 65
4.3 Mechanism of pH Increase 66
4.4 BOF slag Dissolution in Pilot and Laboratory Scale Operation 74
4.5 Conclusion 75
5 Sulfate and Metal Precipitation in AMD treatment 77
5.1 Abstract 77
5.2 Introduction 78
5.3 Experimental Procedure 79
5.4 Results and Discussion 81
5.5 Conclusions and Recommendations 94
6 Sulfate Reducing Micro-organism treatment of AMD in a BOF Slag Neutralized Solution 95
6.1 Part 1: Biological sulfate reduction of AMD in a small-scale batch reactor – kinetics and conditions 95
6.2 Part 2: Biological sulfate reduction of AMD in a continuous system using sugarcane bagasse as a substrate and nutrient source 100

7 Determination of the optimal configuration of a system incorporating and integrating all three processes (pH rise from BOF slag action; precipitation of metals, sulfates, and sulfides; reduction of sulfate and formation of sulfide through SRB action) 114
7.1 Executive Summary 115
7.2 Background 115
7.3 Overview of process 116
7.4 Site Selection and layout 119
7.5 Process flow diagrams 122
7.6 Equipment design 125
7.7 Piping, Valves and Pumps 131
7.8 Control philosophy 133
7.9 Waste Management 136
7.10 Costing 137
7.11 Appendix A (WRC Report 1): Bagasse reactor sizing (literature based) 140
7.12 Appendix B (WRC Report 1): Sedimentation tank sizing 141
8 The design, construction and monitoring of a laboratory scale system treating up to 25 L/day. 142
8.1 Abstract 143
8.2 Introduction 144
8.3 Materials 146
8.4 Methods 147
8.5 Results and Discussion 149
8.6 Conclusions 159
8.7 Acknowledgments 160
9 The design, construction, monitoring and assessment of the long-term performance of a pilot plant used to treat 1000L/day of AMD on-site 161
9.1 Abstract 162
9.2 Introduction 162
9.3 Methods 163
9.4 Results and discussion 167
9.5 Conclusions 171
9.6 Acknowledgements 171
10 Preparation of a process for scale-up on site based on the pilot and lab scale studies 172
10.1 Executive Summary 173
10.2 Design Methodology 177
10.3 Laboratory Scale Plant 186
10.4 Pilot Scale Plant 195
10.5 Complementary Data 201
10.6 Proposed Design for Scale Up 218
10.7 Waste Generation, Disposal and Re-use Routes 225

10.8 Summary 228
11 Conclusions 230
11.1 Application of Research 230
11.2 Fulfillment of objectives 230
11.3 Recommendations 232
11.4 Concluding Remarks 233
12 References 234
Appendix I: Author Contributions 269

List of Tables

Table 2-1: Composition in %weight of BOF-S of varying particle sizes obtained from different sites32
Table 2-2: Physical Properties for BOF-S (Xue *et al.*, 2009) 36
Table 4-1: Free oxide content in quicklime, dolomitic lime, hydrated lime and BOF Slag with particle aperture between 2000-3350 microns (determined via SEM and Energy dispersive X-ray analysis (EDA)) where Wollastonite found on the surface of the particle was not considered a free oxide (due to its insolubility in water) 66
Table 4-2: Oxide content of BOF slag used in the experiment. 68
Table 4-3: Summation of Kinetic Model Fitting for Leaching Experiments 70
Table 4-4: Summary of the Kinetic Constants obtained for the Best Fit Models in each Case 71
Table 5-1: Concentrations of components of interest in two different types of AMD sourced from two different AMD dams in Emalahleni, South Africa 81
Table 5-2: Major oxides in BOF slag used for AMD treatment. 81
Table 5-3: Free oxide content in quicklime, hydrated lime (Tolonen *et al.*, 2014) and BOF slag with particle aperture between 2000-3350 microns (determined via SEM and EDA) where Wollastonite found on the surface of the particle was not considered a free oxide (due to its insolubility in water).82
Table 5-4: Solubility of sulfate compounds % weight/weight in water at 25° C 89
Table 5-5: Equations governing the concentration of ionic metal species in solution as a function of pH when the pH is altered via addition of BOF slag 91
Table 5-6: Qualitative results of presence of elements on the surface of BOF slag before reaction and surface of BOF slag after reaction with AMD for 32 hours. 92
Table 5-7: Cost of raw material when treating 1L of AMD to a pH of 7 in 30 - 55 minutes. 94
Table 5-8: Summation of metal and sulfate removal percentage using BOF Slag added to an AMD Type A sample until a pH of 7 was reached 94
Table 6-1: Initial compositions of effluent in 5 L jar reactors with nutrient availability (carbon, nitrogen and phosphorous) being calculated using LECO analysis results 97
Table 6-2: Standard deviation (coefficient of variance) for results used to determine sulfate reduction kinetics 98
Table 6-3: Oxide Content of BOF slag sourced from Phoenix Slag Services 107
Table 6-4: Elemental composition of AMD used in study 108
Table 6-5: AMD sourced from Mpumalanga, South Africa characteristics 108
Table 6-6: LECO elemental analysis of Sugarcane Bagasse from Illovo Sugar 109
Table 7-1: Key for Process flow diagram 122
Table 7-2: Piping materials of different streams and respective lengths 131
Table 7-3: Key for piping and instrumentation diagram 134
Table 7-4: Parts and pricing list for pilot plant 137

Table 8-1: XRD analysis of BOF slag 146
Table 8-2: Carbohydrate content of Illovo sugarcane bagasse 146
Table 8-3: Composition and pH of AMD sourced from two different AMD sources in Emalahleni, Mpumalanga, South Africa 147
Table 8-4: Residence time, recycle ration and flowrates of the inlet and recycle streams in the system for different particle sizes and AMD qualities 157
Table 8-5: Metal Concentration for size 1 (8 μm <d< 13 μm), 2 (1.7 μm <d< 3.35 μm), Size 3 (d< 1 μm) and Type B in untreated AMD and the outlet for sedimentation vessel (V2), DSR vessel 1 (V3) and DSR vessel 2 (V4) 158
Table 9-1: Description of Process flow diagram elements (Figure 9-2) 166
Table 9-2: Flowrate and Residence Time in System 168
Table 9-3: Extent of Remediation across each Process Vessel (%removal of components) 170
Table 10-1: Description of process flow diagram elements in Figure 10-3 182
Table 10-2: Composition and pH of AMD sourced from two different AMD sources in Emalahleni, Mpumalanga, South Africa 187
Table 10-3: Residence time, recycle ration, and flowrates of inlet and recycle streams in system for different particle sizes and AMD qualities 188
Table 10-4: Particle size distribution of BOFS from Phoenix Slag Services 190
Table 10-5: Standard deviations and repetitions for outlet conditions from laboratory scale plant operation 193
Table 10-6: Flowrate and residence time in system 196
Table 10-7: Average composition and pH of AMD in storage dams 196
Table 10-8: Extent of remediation across each process vessel (%removal of components) where bold text indicates an increase in concentration and plain text indicates a decrease 198
Table 10-9: Free oxide content in quicklime, hydrated lime and BOFS with particle aperture between 2000-3350 microns (determined via SEM and Energy dispersive X-ray analysis (EDA)) where Wollastonite found on the surface of the particle was not considered a free oxide (due to it's insolubility in water) (Tolonen *et al.*, 2014). 202
Table 10-10: Oxide content of BOFS used in the experiment 203
Table 10-11: Solubility of sulfate compounds % weight/weight in water at 25° C 214
Table 10-12: Description of schematic of upscale design shown in Figure 10-21 223
Table 10-13: WHO and SANS 241 drinking water standards compared to quality of slag vessel outlet 226
Table 10-14: South African irrigation water standards compared to quality of slag vessel and DSR vessel outlet 227

List of Figures

Figure 1-1: Flowchart showing structure of dissertation and relationship between objectives 6
Figure 2-1: Speciation of Al as a function of pH (Calculated with PHREEQC 2.7 (25°C, 1 bar)) 13
Figure 2-2: %Mass composition of elements in BOF slag 19
Figure 2-3: Total worldwide steel production from 1950 to 2016 in million tonnes 26
Figure 2-4: Steelmaking routes, raw materials and possible finished products 29
Figure 2-5: Average Elemental composition of BOF-S from 58 steel mill sites 31
Figure 2-6: Molecular/phase composition of different samples of BOF-S in %mass 31
Figure 2-7: Average TCLP) of BOF-S 35
Figure 2-8: Concrete mixtures made with BOF-S that had been chelated with oxalic acid after four days steam curing process 39
Figure 2-9: Waste quantity prediction of LCD in China using the market supply method and comparing to waste quantity produced in 2011 41
Figure 2-10: Schematic of Vertical Section of Constructed Floating Wetlands 48
Figure 2-11: Percentage removal and addition of metals and sulfates between the inlet and outlet of the system using BOF-S leachate and sugarcane bagasse to remediate two types of severely polluted AMD, sourced from a dam and stream in Emalahleni, South Africa (patterned region indicates an increase) 52
Figure 4-1: pH change over time in 800 mL of AMD in a constantly agitated reactor when 80 g of slag with particle aperture between 2000-3350 microns has been added 67
Figure 4-2: pH in water solutions during dissolution of BOF slag of particle size 1 (2 mm to 3.35 mm in diameter); 2 (4.75 mm to 6.7 mm in diameter) and 3 (6.7 mm to 9.5 mm in diameter) 70
Figure 4-3: Total acidity of solutions before and after reaction of 80 g of BOF slag with 800 mL of water or HCl or AMD, expressed in terms of $CaCO_3$ concentration. 72
Figure 4-4: Precipitation layer on top of the BOF slag in the BOF slag reactor 72
Figure 4-5: SEM images of (i) and (iv) unreacted BOF slag; (ii) water leached BOF slag; (iii) AMD leached BOF slag; (v) and (vi) HCl leached BOF slag 73
Figure 4-6: Removal (%) of Al, Ca, Fe, Mg, Mn and Sulfate across the laboratory and pilot-scale systems with Ca exhibiting an increase in the pilot-scale system (shown in grey) 74
Figure 4-7: Concentrations of Mg and Ca ions in water and AMD solutions that are reacted with slag fines in a CSTR 75
Figure 5-1: pH change over time in 800 mL of AMD in a constantly agitated reactor when 80 g of slag with particle aperture between 2000-3350 microns has been added 83
Figure 5-2: Aluminium concentration in AMD over varying pH levels (when pH is altered via addition of BOF slag) 85
Figure 5-3: Magnesium concentration in AMD over varying pH levels (when pH is altered via addition of BOF slag) 86

Figure 5-4: Calcium concentration in AMD over varying pH levels (when pH is altered via addition of BOF slag). 87
Figure 5-5: Iron concentration in AMD over varying pH levels (when pH is altered via addition of BOF slag). 88
Figure 5-6: Manganese concentration in AMD over varying pH levels (when pH is altered via addition of BOF slag). 89
Figure 5-7: Sulfate concentration in AMD over varying pH levels (when pH is altered via addition of BOF slag). 90
Figure 5-8: pH of an AMD system with different loading rates of BOF slag. 90
Figure 5-9: Left: SEM of unreacted BOF slag particle (aperture < 1 cm), Right: SEM of precipitate formed on surface (of BOF slag with aperture size < 1cm) after reaction of BOF slag and AMD for a period of 32 hours. 92
Figure 5-10: Mass of sludge formed (after drying) in a Type A AMD solution containing different concentrations of BOF slag. 93
Figure 6-1: Average sulfate concentration over time for the sealed AMD/SRM vessels 98
Figure 6-2: Integrated rate law for first order sulfate reduction reaction 99
Figure 6-3: Biochemical pathway of dissimilatory and assimilatory reduction 104
Figure 6-4: Sulfate Reduction Continuous Process Set-up Process Flow and Instrumentation Diagram 106
Figure 6-5: Difference in metal concentration between Raw AMD, AMD that had been BOF slag neutralized to a pH of 5,7 and given at least 1 hour settling time, and AMD after having undergone sulfate reduction via microbial action 109
Figure 6-6: Sulfate and COD concentration of samples taken from the outlet of the Bagasse Tank over time 110
Figure 6-7: Mass of sulfate removed in a 50L system via biological functioning per day (non-cumulative) where sugarcane bagasse is used as the carbon, nitrogen and phosphorous source, and AMD is used as the sulfate source 111
Figure 7-1: Top view of AMD tailings dam with area of construction outlined 119
Figure 7-2: Top view of area to be used for construction of pilot plant at AMD tailings dam 120
Figure 7-3: Plant layout top view 121
Figure 7-4: Process flow diagram 123
Figure 7-5: Process Flow Diagram depicting process equipment 124
Figure 7-6: Gravity Settling tank to be used for heavy metal oxide/sulfate/sulfide/carbonate settling 125
Figure 7-7: Side view of bagasse reactor 127
Figure 7-8: Side view of slag reactor 129
Figure 7-9: Piping and instrumentation diagram 135

Figure 8-1: Schematic of laboratory set-up with sampling points and vessels labelled (circled numbers denote sampling locations) 148
Figure 8-2: Concentrations of Mg and Ca ions in water and AMD solutions that are reacted with slag particles in a CSTR 150
Figure 8-3: SEM imaging of (a) unreacted BOF slag compared to (b) slag reacted with AMD (particle size: 2 μm < d < 3.35 μm) 151
Figure 8-4: (a) Laboratory set-up with two slag chambers (V6.1 and V6.2) leading into the sedimentation vessel (V2) and then into the DSR 1 vessel (V3) which contains sugarcane bagasse; (b) top view of samples taken from each sampling point for AMD Type A and slag 152
Figure 8-5: pH at the outlet of the slag (S5), sedimentation (S2), DSR 1 (S3) and DSR 2 (S4) vessels over the 106-day period 154
Figure 8-6: The concentration of aluminium, calcium, iron, magnesium, and manganese an AMD solution with pH change occurring through reaction with BOF slag 154
Figure 8-7: Formation of precipitation accompanying a pH rise in Type B AMD. (a) 1.5 L Untreated AMD, (b) 1.5 L AMD with addition of 3 g of slag, (c) Removal of top liquid after 2 minutes settling time (image by authors) 155
Figure 8-8: Percentage sulfate removal over entire system, sedimentation (V2), DSR1 (V3) and DSR2 (V4) vessels for system using slag with particle size 1, 2 and 3 and for AMD Type A and B 155
Figure 8-9: Sulfate concentration at the outlet of the sedimentation vessel (S1) and the DSR vessels (S2, S3) from start of experiment to Day 44 156
Figure 8-10: Sulfate concentration at the outlet of the sedimentation vessel (S1) and the DSR vessels (S2, S3) from Day 30 to Day 106 156
Figure 8-11: Samples from system. Left to right - Untreated AMD (Type A) (S0), sedimentation inlet (S1i), sedimentation middle (S1ii), sedimentation outlet (S1), DSR 1 outlet (S2), DSR 2 outlet (S3), slag vessel outlet (S5) 159
Figure 9-1: (i-ii) Joint AMD dams in Emalahleni, South Africa where pilot plant is constructed (photographs by authors) 164
Figure 9-2: Process flow diagram (PFD) of pilot plant to treat AMD constructed at site 166
Figure 9-3: ((i) and (ii)) AMD remediation pilot plant at mine dam site 167
Figure 9-4: (i) pH and sulfate concentration in the water reservoir (TK-101) over the 196-day period (ii) Metal concentrations in the water reservoir (TK-101) over the 196-day period 169
Figure 10-1: Preliminary design block flow diagram 178
Figure 10-2: Laboratory scale set-up with vessels and sampling points denoted 179
Figure 10-3: Process flow diagram (PFD) of pilot plant to treat AMD constructed at site 182
Figure 10-4: AMD remediation pilot plant at mine dam site 183
Figure 10-5: Dissolved metal concentration in AMD solutions at different pH levels when pH is altered using BOFS fines 191

Figure 10-6: Percentage of (i) removal of total Al, Fe, Mg, Mn and sulfate in the laboratory scale system when different particle sizes and AMD qualities are used, and (ii) addition of Ca to the treated water due to BOFS dissolution (data prepared using averages for the 106-day period)..... 192
Figure 10-7: pH and sulfate concentration of the treated water from the pilot scale plant over the 196-day period (samples taken from TK-101 - treated water reservoir)..... 197
Figure 10-8: Metal concentrations in the water reservoir (TK-101) over the 196-day period..... 197
Figure 10-9: pH change over time in 800 mL of AMD in a constantly agitated reactor when 80 g of slag with particle aperture between 2000-3350 microns has been added..... 203
Figure 10-10: pH in water solutions during dissolution of BOFS of different particle sizes..... 205
Figure 10-11: Total acidity in 800 mL of water, HCl and AMD solutions before reaction with 80 g of BOFS total alkalinity after as $CaCO_3$ 206
Figure 10-12: Precipitation layer on top of the BOFS in the BOFS reactor 207
Figure 10-13: SEM images of (i) and (iv) unreacted BOFS; (ii) water leached BOFS; (iii) AMD leached BOFS; (v) and (vi) HCl leached BOFS 208
Figure 10-14: Removal (%) of Al, Ca, Fe, Mg, Mn and Sulfate across the laboratory and pilot-scale systems with Ca exhibiting an increase in the pilot-scale system (shown in grey) 209
Figure 10-15: Concentrations of Mg and Ca ions in water and AMD solutions that are reacted with slag fines in a CSTR..... 210
Figure 10-16: SEM of precipitate formed after reaction of BOFS and AMD for a period of 32 hours. 215
Figure 10-17: (i) Process control with recycle flowrate controlled using the pH in the settling tank; (ii) Process control with the AMD flowrate controlled using the pH in the settling tank; (iii) Process control with both the AMD and recycle flowrates being controlled using the pH in the settling tank; (iv) Process control with recycle flowrate controlled using the pH in the secondary bioreactor 216
Figure 10-18: Process control with the recycle flowrate controlled using the pH setpoint in the slag reactor 217
Figure 10-19: Basic design of the proposed settling vessel 219
Figure 10-20: Schematic of HDS system with recycle stream proposed to be used in the larger scale design, using BOFS as a lime source..... 222
Figure 10-21: Schematic of proposed larger scale (10000 L/day) design..... 224

1. Introduction

1.1 Background and motivation for study

Mining has played a key role in the development and growth of humankind and the progress and evolution of human society. It has shaped the way the modern world functions - from the first colonial powers seeking gold to the continuing importance of natural mineral resources in economies and societies (Silbergeld, 2016). Mining provides access to mineral commodities that all countries on Earth find essential in order to maintain acceptable standards of living for their inhabitants – materials that are mined play a vital role in the automobile industry, building and construction sector, technology assembly (phones, computers, etc.), road construction, electricity generation, and the production of many other goods and commodities which are vital for consumers (National Research Council, 2002). In addition, mining is economically important, providing employment and generating wealth and income for masses of individuals and corporations. Mining accounts for a significant portion of gross domestic product (GDP) and gives rise to several downstream, associated activities (manufacturing of mining equipment, provision of engineering and environmental services, and the development of universities in the fields of geology, mining engineering, and metallurgy). Mining economic opportunities and subsequent generation of wealth are substantial, and thus mining activities have continued well into the 21st century, despite its intrinsically non-sustainable nature.

In South Africa (SA), mining activity has been an important contributor to the development and advancement of the economy (Durand, 2012) with mineral extraction occurring at numerous industrial sites across the country. Although much wealth has been generated because of the gold, coal, iron ore, and copper mining industries, these mining activities have also resulted in detrimental environmental problems that have had adverse effects on both the environment and the population of SA. Examples such as (i) dust and air pollution from mine tailings (linked to higher levels of asthma, pneumonia, emphysema, chronic bronchitis, wheezing and chronic cough among both young and elderly people living close to the affected areas (Nkosi, 2018)), (ii) uranium poisoning (a big risk due to the 600 000 tonnes of uranium waste that has accumulated in waste dumps throughout the city of Johannesburg (in Gauteng) (Al Jazeera, 2019)) and (iii) relocation of families, livestock and farming activities due to the establishment of mines and mine-related operations (large scale impact being reported on local and indigenous communities in some areas in SA (Mtero, 2017)), are just a few of the hard-hitting issues associated with mining. Another wide reaching problem, one that has been overlooked in the past, is that of Acid Mine Drainage (AMD) or Acid Rock Drainage (ARD) (Mccarthy, Africa and Africa, 2011).

AMD around the globe is considered an environmental hazard (Sheoran and Sheoran, 2006) due to its long term impairments to waterways and to the biodiversity of ecosystems that rely on these waterways (Akcil and Koldas, 2006). In 2017, following the Gold Fields Mine water spill which led to the

poisoning of the Animas river in the United States of America (USA) (Chief *et al.*, 2016), a United Nations (UN) spokesperson classified AMD as the second biggest problem that the Earth faces – second to global warming (Tuffnell, 2017). There are multiple closed and abandoned mine sites in countries such as Australia, Canada, Russia and the USA which are also afflicted by this environmental challenge (Naidoo *et al.*, 2009). In September 2015, all 193 Member States of the UN's General Assembly resolved to "shift the world on to a sustainable and resilient path" by agreeing upon and accepting the 2030 Agenda for Sustainable Development – a plan of action for the planet to improve and "transform our world" for the better (United Nations, 2018). The Agenda established 17 Sustainable Development Goals (SDGs), 30% of which relate directly to water and water management and sanitation, and 53% of which relate to waste management. Solving or establishing proper management of AMD which falls into both these SDG categories, is thus of vital importance to begin establishing a sustainable world.

For South Africa, AMD presents a particular problem, as the minerals which have been discovered and extracted here have accounted for a large portion of the world's mineral resources and reserves: gold, platinum-group metals, chrome ore, manganese ore, zirconium, vanadium and titanium, amongst others (Ministry of Economic Development NZ Petroleum & Minerals, 2013). For this reason, mining of these minerals is critical to the South African economy (Kearney, 2012). This is juxtaposed with regional (and national) water scarcity challenges whereby the leaching and extraction of these minerals from mines (whether open pit or shaft mines) is a complicated process which often results in waste water and effluent generation (Akcil and Koldas, 2006) that can impact surface waters. Accordingly, in the early 2000's, the South African government shifted their focus to mining companies and mine managers controlling AMD release in a bid to minimize the impact that AMD had on the environment (Morrissey, 2003). Because of the high cost of AMD treatment however, a trend developed in SA (and many other countries throughout the world) in which mining companies submitted to the closure of an AMD-affected mine rather than incurring the costs associated with water treatment (Labuschagne, Usher and Matfield, 2005). Consequently, cost-effective passive treatment systems were and are still strongly needed within the global context (and particularly within SA) to prevent the further contamination of already stressed water resources. For the past two decades (2000 – 2020), research into this field of water treatment has been extensive, and numerous new technologies have emerged with the potential to prevent and treat AMD. However, in SA this problem has persisted until the present and remains unresolved, with environmental issues continuing to arise at both large and small sites around the country (the Vaal River contamination, Middelburg Dam pollution, Grootdraai Dam contamination and the overflowing of smaller AMD tailings dams in Mpumalanga (du Toit, 2018)). Treatment methods for AMD have still not been effectively implemented in many areas of the country due to (i) costs associated with the treatment method, (ii) the volume of AMD needed to be treated (which makes certain types of treatment schemes unfeasible) and (iii) the fact that the characteristics of AMD vary

widely across the different mining areas – posing a challenge to the development of a ubiquitous treatment scheme.

However, one treatment scheme that has shown promise in combatting AMD pollution, despite the above-mentioned challenges, is a technology which incorporates the use of multiple waste or by-products, and which ensures that all streams resulting from the process have reuse avenues that can combat or assist in combatting other mining related issues (thereby contributing to the formation of a circular economy). In SA two industrial by-products are available in large volumes with the potential to passively remediate AMD: Basic Oxygen Furnace (BOF) Slag (a by-product of the steel manufacturing industry) and sugarcane bagasse (the shredded cane stalk material remaining after sugar extraction) (Ziemkiewicz and Skousen, 1997; Ziemkiewicz, 1998; Grubb, Landers and Hernandez, 2000; Ziemkiewicz, Skousen and Simmons, 2003).

Name and Sheridan (2014) conducted a study on the use of BOF slag and which determined that it had significant potential as a reagent for treating AMD and could potentially be used to replace lime as a primary neutralizing reagent in many AMD treatment schemes. The BOF slag was shown to effectively remove all iron from solution and demonstrated removal of sulfate to a final concentration of approximately 400 ppm from a starting concentration of 6000 ppm (>90% removal).

Other research has shown that sugarcane-bagasse has the potential to serve as a host media for a multitude of microorganisms (including sulfate-reducing micro-organisms (SRM)) with the ability to remediate raw, untreated AMD (pH~3) to levels below 400 ppm of sulfate by converting it to sulfide in various processes (dissimilatory sulfate reduction (DSR) or assimilatory sulfate reduction (ASR)) (Canfield, 2004). Sulfide can then form insoluble precipitates (Grubb, Landers and Hernandez, 2000; Hussain and Qazi, 2016) which effectively remove them from solution, lowering the sulfur content.

Thus, using BOF slag and bagasse either together or in series could have significant advantages for the purposes of improving mining wastewater quality. The coal-based AMD challenges and sources of BOF slag and sugarcane bagasse are all co-located within south-eastern Mpumalanga and Kwa-Zulu Natal in South Africa. In addition, using these materials in differing configurations or amounts could treat many different AMD qualities, either as a full treatment scheme or as a pre-treatment step. With regards to cost, the use of regionally available waste materials or by-products to treat AMD is a desirable option as it could substantially lower the cost of treatment – especially in areas where mines are no longer operational or active (in many instances it is not sustainable to create new plants to treat old AMD problems (Moodley et al., 2018)). The use of by-product or waste materials – in conjunction with lowering costs - has the added advantage of benefitting more than one industry simultaneously.

A process that could combine these two by-products (BOF slag and sugarcane bagasse) would result in an overall treatment system that consists of four processes which are chemical and biological in nature; (i) the pH rise of treated water via alkaline addition through contact with BOF slag particles, (ii)

sedimentation of metals and sulfates present in the AMD via precipitation reactions facilitated by the rise in pH and the presence of counter-ions in the solution, (iii) production of sulfide and reduction of sulfate via DSR or ASR through the action of biological components using waste sugarcane bagasse as a substrate, and (iv) the subsequent precipitation of metal sulfides. Some of these processes have been studied in-depth (biological sulfate reduction and precipitation reactions) and some have only been the subject of preliminary studies.

This research therefor focusses on the integration of all these process into a continuous AMD treatment system either as a stand-alone process or a pre-treatment step.

1.2 Problem Statement

Several studies have confirmed the use of BOF slag and sugar cane bagasse in AMD treatment, but the scope of these studies were limited in that: (i) they did not determine if any minerals/metals were leaching from the slag into the remediated AMD, (ii) they did not seek to determine ways to polish the effluent below 400 ppm sulfate when BOF slag was used, (iii) they did not assess the removal of other metals that are commonly found in AMD (only iron), (iv) they did not determine the dissolution kinetics or behaviour of the slag leachate; and (v) they did not evaluate the combination of the slag and bagasse in a treatment scheme.

Thus, although these bodies of literature have demonstrated a proof of concept, little research has been conducted into the design and optimization of a process that incorporates both treatment methods (SRM/sugarcane bagasse and BOF slag) and can be implemented on a larger scale. Specific areas that need further investigation for the design and scaling up of the process are:

1. Evaluation of points (i) – (v);
2. Configuration of the process;
3. Kinetics for all reactions and units of the process system;
4. Reaction and reactor yields;
5. Optimization of the consolidated process; and
6. Waste generation and management for the process.

For the purpose of this dissertation, these areas are assessed. These are expanded upon in the research objectives, below.

1.3 Research Objectives

The objectives of the research presented in this dissertation were to perform and discuss the following:

1. Determine the kinetics of the slag dissolution reaction in acidic and neutral solutions.
2. Identify and study the kinetics of the precipitation reactions which occur when the pH of the AMD treatment system rises.

3. Determine the kinetics of the sulfate reducing micro-organism (SRM) reactions in a BOF slag neutralized solution.
4. Determine the optimal configuration of a system incorporating and integrating all three processes (pH rise from BOF slag action; precipitation of metals, sulfates and sulphides; reduction of sulfate and formation of sulfide through SRM action).
5. Design, construct and monitor a laboratory scale system for treating up to 25 L/ of AMD per day.
6. Design, construct, monitor and assess the long-term performance of a pilot plant to process and treat 1000L/day of AMD on-site.
7. Design and propose a process for scale-up on site based on the pilot study.

1.4 Novelty of Research

The integration of the proposed processes into one system, and research into the mechanisms of the various processes, are novel for several reasons:

- The kinetics of BOF slag dissolution in any medium have not been studied.
- The kinetics of the precipitation reactions that occur after pH increase in AMD using BOF slag as a source of alkalinity have not been studied.
- SRM kinetics in a BOF slag neutralized solution have not been studied.
- The combination of the three processes to remediate AMD has never been applied and studied before, and the simultaneous optimization of these processes will result in new knowledge in the field.

In addition to the specific areas in which novel research aspects can be found and to which will be contributed, a shifted approach to many other mining related problems could also be achieved through this research: (i) the management of waste products, (ii) the potential to derive value out of closed/abandoned mines and waste material (producing cleaner water and valorised slag, the latter of which can be used in construction), and (iii) the method with which waste from this solution is proposed to be dealt (contributing to alleviating food shortage and land unavailability through the use of hydroponics) could contribute to establishing a circular, bio-based economy in the mining and mineral processing industry (Westensee *et al.*, 2018).

1.5 Structure and Outputs of the Dissertation

The objectives of this dissertation have been achieved through a stepwise fashion, and will therefore be presented in the same order, according to the flowchart presented in Figure 1-1. The introductory, review and methodology sections are presented first, followed by the three preliminary/informative studies which (upon fulfilment) contribute to the achievement of the first 3 objectives as listed in section 1.3. These three studies were then used as a basis to inform the subsequent objective (combining all

three processes into one operation). This operation was then tested at a laboratory scale (objective 5), and the results from this study were used to inform the design detailed in objective 6. The results from all 6 objectives were then used to compile a final design, in fulfilment of the final objective (7).

A content summary of each chapter is given after Figure 1-1.

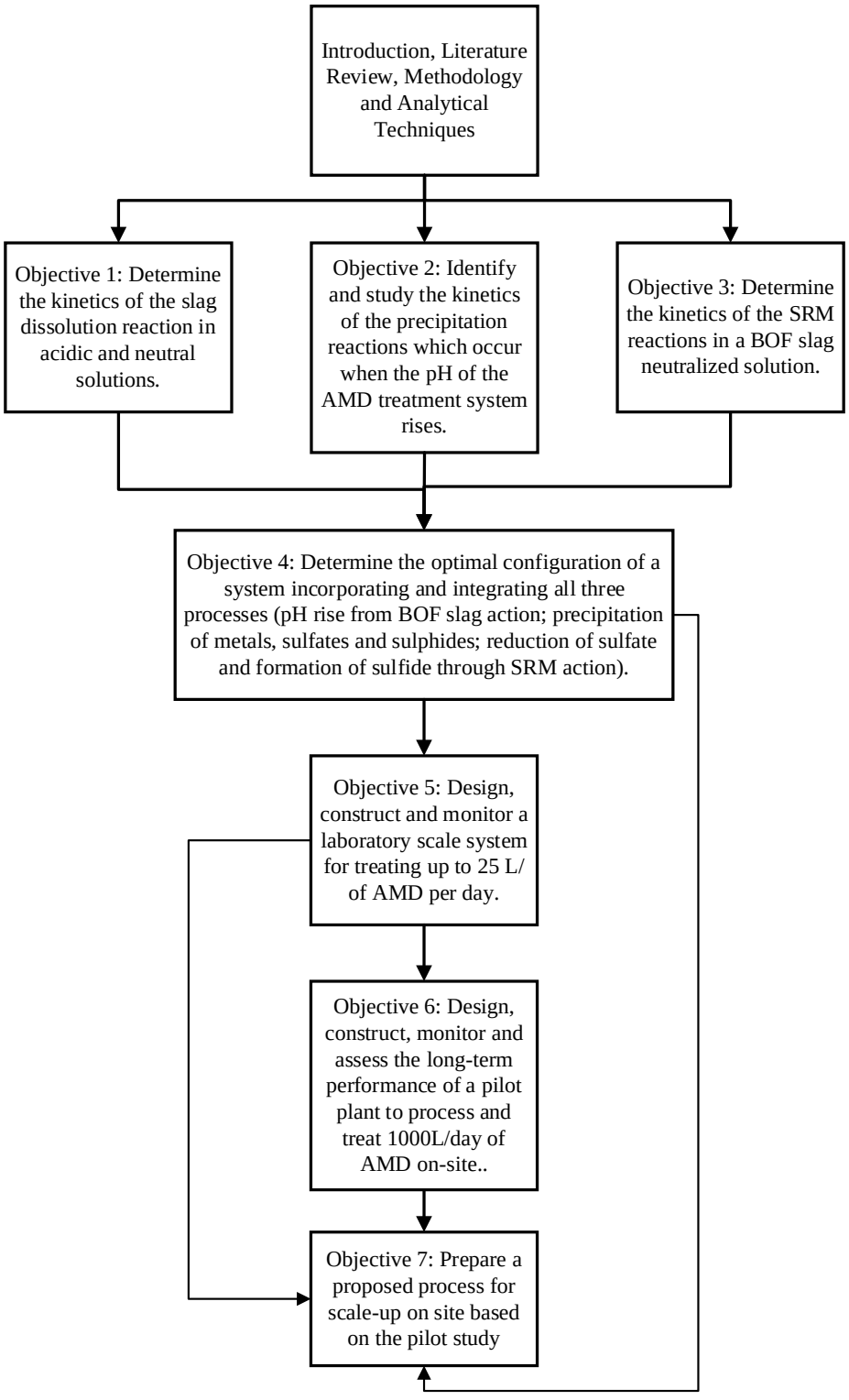


Figure 1-1: Flowchart showing structure of dissertation and relationship between objectives

It must be noted that the fulfilment of the objectives of this dissertation was done primarily through various publication outputs. The content of each chapter is summarized below, with reference to the type of publication that is used as either partial or complete fulfilment of the relevant objective.

- Chapter one contains an introduction into the topic, a statement regarding the areas that are currently lacking in existing literature, a description of the novelty of the topic as well as a problem statement and list of specific research objectives that – being achieved – will allow for a contribution to this field of knowledge.
- Chapter two contains an extensive literature review and includes an in-depth study into AMD, BOF slag, carbon sources, SRM and lime dosing. This section is partly presented as a published review article detailing the current uses of BOF slag (Naidu, Sheridan and van Dyk, 2020). This article was published in the Journal of Minerals Engineering in 2020.
- Chapter three details the methodology followed, experimental procedures used, and investigative techniques employed throughout the duration of the research period. This chapter lists the materials used and the sources of these materials. This section also includes a description of analytical techniques, different testing procedures and different equipment used to achieved each of the objectives.
- Chapter four addresses the first objective: "Determining the kinetics of the slag dissolution reaction in acidic and neutral solutions". This is presented in the form of a published conference article (peer reviewed and presented) which has been extended with additional information pertaining to the achievement of the objective (Naidu, Chauhan, *et al.*, 2020). The article that this chapter is based on was published in the South African Institute for Mining and Materials' (SAIMM) Tailing storage conference 2020 proceedings.
- Chapter five addresses the second objective: "Identify the kinetics of the precipitation reactions which occur when the pH of the AMD treatment system rises". This is presented in the form of a journal article which is an extended form of an already published conference paper. The paper that this chapter expands upon was published in the South African Institute of Chemical Engineer's (SAIChE) South African Chemical Engineering Congress 2021 proceedings.
- Chapter six addresses the third objective: "Determine the kinetics of the SRM reactions in a BOF slag neutralized solution". This is presented in the form of a technical note and journal article.
- Chapter seven addresses the fourth objective: "Determine the optimal configuration of a system incorporating and integrating all three processes (pH rise from BOF slag action; precipitation of metals, sulfates and sulphides; reduction of sulfate and formation of sulfide through SRM action)". This is presented in the form of a design report submitted and approved by the Water Research Council (WRC) of South Africa (Naidu *et al.*, 2017).

- Chapter eight addresses the fifth objective: “Design, construct and monitor a laboratory scale system for treating up to 25 L/day”. This chapter is presented solely as a published journal article (peer reviewed), which was published in The Journal of Hazardous, Toxic and Radioactive waste in 2020 (Naidu, van Dyk, *et al.*, 2020). This journal article is an extended form of a published (peer reviewed and presented) conference paper published in the Aristotle University of Thessaloniki’s Protection and Restoration of the Environment conference in 2018 (Naidu *et al.*, 2018).
- Chapter nine addresses the sixth objective: “Design, construct, monitor and assess the long-term performance of a pilot plant to process and treat 1000L/day of AMD on-site”. This is presented as a published conference paper (peer reviewed and presented) which was published in the International Mine Water Association’s (IMWA) Biennial Mine Water conference held in 2019 (Naidu *et al.*, 2019).
- Chapter ten addresses the seventh objective: “Prepare a proposed process for scale-up on site based on the pilot study”. This is presented as a final design report submitted, approved and published by the WRC of South Africa (Naidu, Sheridan and van Dyk, 2021).
- Chapter eleven is presented as a concluding chapter, summarizing the impact of the study, limitations of the research, and detailing future prospects for this work.

Due to the format of this dissertation (being presented as publications), duplication of data, tables, figures, equations and findings is to be expected in all chapters and the author requests the readers’ patience and indulgence with any repetition.

2. Literature Review

The research involved and presented in this dissertation, as mentioned, incorporates the use of multiple waste streams, namely AMD (primary focus), BOF slag (secondary focus) and sugarcane bagasse. A review of the literature that exists regarding each of these materials, their current and historical uses, limitations, sources, and prospects is presented below. Tertiary topics related to these materials and relevant to the aims and objectives of this dissertation, are presented and discussed where necessary, within each section.

2.1 Acid Mine Drainage

AMD (also ARD or Industrial acid mine drainage (I-AMD) (Vélez-Pérez *et al.*, 2020)) is formed when rocks or waste mine materials that contain sulfide components oxidize on exposure to water or air (Naicker, Cukrowska and Mccarthy, 2003). Pyrite (FeS_2), the main component that contributes to the formation of AMD, is the most abundant metal sulfide mineral in the Earth's crust and is generally concentrated in coal deposits, hydrothermally altered rocks and mineral zones containing zinc, copper, gold, silver, lead and uranium (Tatsuhara *et al.*, 2012). The oxidation of pyrite is the dominant process that gives rise to the acidification of natural waters (whether the source of pyrite is natural or anthropogenic). The weathering of this mineral can result in the acidification of large tracts of stream, river, and lake systems leading to the destruction of living organisms (Rimstidt and Vaughan, 2003). Pyrite oxidation is an electrochemical process that generally consists of three distinct steps: (i) cathodic reaction involving aqueous species (oxidants like Cl_2, H_2O_2, NO^{3-} or – the most abundant ones – O_2 and Fe^{3+}) that accept electrons from an Fe(II) site on the pyrite surface, (ii) transport of electrons through the pyrite from the anodic site to the cathodic site from which they are transferred to the oxidant and (iii) anodic reaction involving oxidation of the pyrite which removes seven electrons from di-sulfide sulfur (or eight electrons from sulfide sulfur) to form a sulfate group. It should be noted that the sulfur atoms in step 3 pass through several oxidation states during the process, thus many different sulfur compounds might be involved (Rimstidt and Vaughan, 2003).

If pyrite has been exposed to oxidative conditions as a direct result of mining activities (coal or other mineral deposit mining where pyrite is concentrated), this acidic water is termed AMD and is no longer associated with the naturally (and more slowly) occurring, ARD (Brumleve and The United States Geological Survey, 2011). Although pyrite is the most common sulfide containing mineral (Vaughan, 2005; Vaughan, D.J. and Corkhill, 2017), other minerals such as Marcasite (FeS_2), Pyrrhotite ($Fe_{1-x}S$), Chalcocite (Cu_2S), Covelite (CuS), Chalcopyrite ($CuFeS_2$), Molybdenite (MoS_2), Millerite (NiS), Galena (PbS), Sphalerite (ZnS) and Arsenopyrite (FeAsS) also contain sulfide and when oxidised, contribute to the formation of both naturally occurring ARD and "manmade" AMD.

The mechanism of formation or generation of AMD is important as it gives an indication of the contaminant properties that AMD possesses. AMD (or waters that have been contaminated with AMD) are characterized by a low pH, high acidity (due primarily to the oxidation of pyrite) and high concentrations of sulfates and metals such as iron, manganese, aluminium, magnesium, calcium and iridium (due to the counterions found in pyrite and other sulfidic compounds) (Feng, Deventer and Aldrich, 2004). Each of these undesirable aspects need to be addressed/eradicated in order to fully treat or remediate AMD.

2.1.1 Acidity, pH and buffering capacity of AMD

The oxidation reaction of pyrite (or other sulfide containing minerals) (shown by Equation 2-1), causes a release of hydrogen ions which decreases the pH of the liquid waste stream. Equation 2-1 is a depiction of the oxidation of sulfide (Ptacek *et al.*, 2003). It should be noted that in the first step of AMD generation, ferrous iron (Fe^{2+}) is not oxidized to ferric iron (Fe^{3+}).

$$2FeS_2 + 7O_2 + 2H_2O \rightarrow 2Fe^{2+} + 4SO_4^{2-} + 4H^+$$

Equation 2-1

If the mineral is in a favourable environment for oxidation to occur (presence of sufficient oxidant species, sufficient exposure of metal sulfide surface, sufficient bacterial activity and exhibiting correct pH levels and temperature (Akcil and Koldas, 2006)), Equation 2-1 will be followed by Equation 2-2, which effectively reduces the H^+ concentration but produces ferric iron which can either precipitate or will be used as an oxidant for further oxidization of more sulfide bearing minerals. These reactions are shown in Equation 2-3 and Equation 2-4, respectively (Akcil and Koldas, 2006; Simate and Ndlovu, 2014). In many cases the oxidation of iron and sulfate is accelerated by the presence of iron and sulfate oxidizing bacteria (Schippers and Sand, 1999; Fan *et al.*, 2019).

$$Fe^{2+} + \frac{1}{4}O_2 + H^+ \rightarrow Fe^{3+} + \frac{1}{2}H_2O$$

Equation 2-2:

$$Fe^{3+} + 3H_2O \rightarrow Fe(OH)_{3\ solid} + 3H^+$$

Equation 2-3

$$FeS_2 + 14Fe^{3+} + 8H_2O \rightarrow 15Fe^{2+} + 2SO_4^{2-} + 16H^+$$

Equation 2-4

Similar reactions occur facilitating the oxidation of other sulfide bearing minerals, but the predominant cause of AMD generation is the oxidation of pyrite. The oxidation of other sulfide minerals also liberates H^+ ions and in a similar way to pyrite, decreases the pH of the aqueous environment. The pH

of AMD usually ranges between 2.5 and 6 (Vallero, 1970) but there have been cases where the pH is lower, reaching levels of 2.38 or 2 (Naidu *et al.*, 2018; Keterew and Brilliance Mamba, 2020). The pH of AMD is the most common aspect that is targeted in treatment schemes with the main aim of treatment being to neutralize or at least increase the pH to near neutral conditions via addition of alkaline reagents (Pereira *et al.*, 2020).

Acidity is also an important (but not very well understood (Morel and Hering, 1993; Kirby and Cravotta III, 2005)) characteristic of AMD and will change in the solution depending on the amount of dissolution of metals and sulfate (Akcil and Koldas, 2006). Acidity (or titratable acidity) – the measure of the amount of strong base that is needed to neutralize an acidic solution to a pH of 8.3 – is not solely dependent on the pH of the AMD and thus samples with a higher pH can still exhibit highly acidic characteristics due to the presence of other components that are able to react with the hydroxide group (OH^-) from a strong base. The computed, theoretically approximated acidity of an AMD sample is given by

Equation **2-5** and shows how the acidity is theorized to be dependent on other species in the AMD solution (Kirby and Cravotta III, 2005). Other chemical species can also affect the acidity of AMD however,

Equation **2-5** (Kirby and Cravotta III, 2005) only shows the effect of certain species of iron, manganese and aluminium (the most prominent contaminants in AMD).

$$\mathbf{acidity_{calculated}} = \mathbf{50}\left\{\mathbf{1000}\left(\mathbf{10^{-pH}}\right) + \frac{\left[\mathbf{2}\left(\mathbf{Fe^{II}}\right) + \mathbf{3}\left(\mathbf{Fe^{III}}\right)\right]}{\mathbf{56}} + \frac{\mathbf{2}(\mathbf{Mn})}{\mathbf{55}} + \frac{\mathbf{3}(\mathbf{Al})}{\mathbf{27}}\right\}$$

Equation 2-5

The acidity of AMD contributes to its buffering effect – the higher the acidity of the solution, the higher the amount of alkaline reagent that will be needed to raise the pH. High acidity and low pH are detrimental characteristics of water streams and can have a devastating effect on plant, aquatic and human life. These are generally the first factors that are addressed in a treatment scheme. In addition to this, a change in acidity and pH also influences the other characteristics (sulfate and metal concentration) of AMD. For these reasons, this measurement is extremely important in AMD remediation schemes and should be constantly monitored to ensure that over or under-dosing of alkaline reagents does not occur (Qin *et al.*, 2019). A measure of both the pH and acidity of an AMD sample is needed in most types of remediation systems and these measurements will depend heavily on the source of AMD and the conditions that the sulfide bearing minerals were under during oxidation.

2.1.1.1 Treatment/Remediation Options for Metals in AMD

Multiple treatment options exist which are aimed at combatting the pH and high acidity of AMD; almost all of these options use the basis of dosing with, or the addition of, alkaline agents. Skousen et al. (2019) recently stipulated six chemicals which are commonly used to treat AMD: (i) limestone—$CaCO_3$, (ii) hydrated lime—$Ca(OH)_2$, (iii) pebble quicklime—CaO, (iv) soda ash—Na_2CO_3, (v) caustic soda—NaOH, and (vi) ammonia—NH_3 (Skousen, Ziemkiewicz and McDonald, 2019). The choice of the best pH range to attain – which could range from 6 to 9 – depends on the dissolved metals that are present in the AMD (Carneiro *et al.*, 2020). Economic factors predominantly influence the choice of which dosing agent to use, with the alkali cost of treatment raging between R2.80/m^3 of AMD in the case of limestone and hydrated lime treatment and R5.83/m^3 of AMD if only lime is used (Maree *et al.*, 2013). For treatment of large volumes of water (85 mL/d as in the case with the Western and Central Water Basins of Gauteng) this difference will amount to a cost difference of approximately R76 million per annum between the two options. For comparison, soda ash and caustic soda cost more that lime products, whereas ammonia is cheaper but is much more dangerous to use than lime products. All products, if used correctly – given enough reaction time, agitation and product – are capable of increasing the pH of an AMD stream to pH levels of between 6 and 9. The cost of treatment using alkaline agents would substantially decrease if a waste or by-product was used – BOF slag costs R100/tonne (Vermuelen, 2019) (at specific conditions this would mean a cost of R1/m^3 of AMD (Naidu, van Dyk and Sheridan, 2021)) whereas the cost of lime ranges between R168 and R408/tonne (Kalkor, 2021).

2.1.2 Metals concentration

Another characteristic of AMD that is dependent on its source is the concentration of metals. The types of metals (usually termed “heavy metals” in literature and conventionally defined as elements with metallic properties and an atomic number greater than 20 (Tangahu *et al.*, 2011)) present will depend on both the geochemistry of the mineral ore body from which the sulfide minerals originate as well as the source of water. Metals of highest concern are Iron and Aluminium which can occur in excess of 1g/L. Other metals, such as Zinc, Magnesium, Manganese, Calcium, Cadmium, Lead, Nickel, Chromium and Copper also commonly occur, generally in lower concentrations, but always depending on the type of mine and geographical area in which it is situated. A list of common heavy metals found in AMD and their sources are described in the following section, with focus on their mineralogy, speciation, and their environmental significance.

2.1.2.1 Aluminium

Of all the heavy metals contained within AMD, Aluminium (Al) is the most sensitive to low pH and high electrical conductivity. It is readily leached from soil and rock into the water source (Chamier *et al.*, 2015). Al minerals which are abundant (found at multiple different mine types (Bilski *et al.*, 2014))

generally dissolve at levels below pH 4.5 – 5.0 and Al species tend to precipitate at any pH above this – precipitation of aluminium in the presence of sulfate, can occur in the form of several oxyhydroxysulfates, namely hydrobasaluminite, basaluminite and gibbsite (Sánchez-España *et al.*, 2005). It is important to note that the precipitation of Al compounds generally results in retention by adsorption and/or coprecipitation of many other toxic elements which may be present in the mine effluents (As, Pb, Cr, Cu, Zn, Mn, Cd, Co, Ni, or U). Al activity thus acts simultaneously as a strong buffering system of the AMD solutions (at pH 4.5 – 5.0) and as a natural "scavenger" or remover of toxic trace elements (Romero *et al.*, 2015).

AMD normally exhibits high concentrations of sulfate ions, the presence of which strongly determines the complexation of Al – thus precipitation is usually dominated by metal-sulfate and metal-bisulfate species of the type Al–SO_4^{2-} (Nordstrom, 1982). At typical AMD pH and sulfate concentration conditions (pH ~2.5 – 3.5 and 0.1 M SO_4^{2-}), Al(III) is chiefly present in the form of sulfate complexes ($AlSO_4^+$, $Al(SO_4)^{2-}$) with a minor presence of the free aqueous ion (Al^{3+}), and with the hydroxyl-containing ionic complexes being negligible (Sánchez España *et al.*, 2006). However, this ionic speciation strongly varies with pH and the activity of the sulfate anion. This is presented in Figure 2-1 which plots the distribution of different ionic species of Al in a solution with 0.1M SO_4^{2-} as a function of pH. This figure shows that the free aqueous cations (Al^{3+}) are only dominant at extremely acidic conditions (pH < 1.0), while the metal-sulfate complexes are dominant in the pH ranges 1.5 – 6. As pH increases, the sulfated ionic complexes are replaced by hydroxide species ($Al(OH)_3$, $Al(OH)_4^-$), which become dominant at near-neutral conditions (pH > 6).

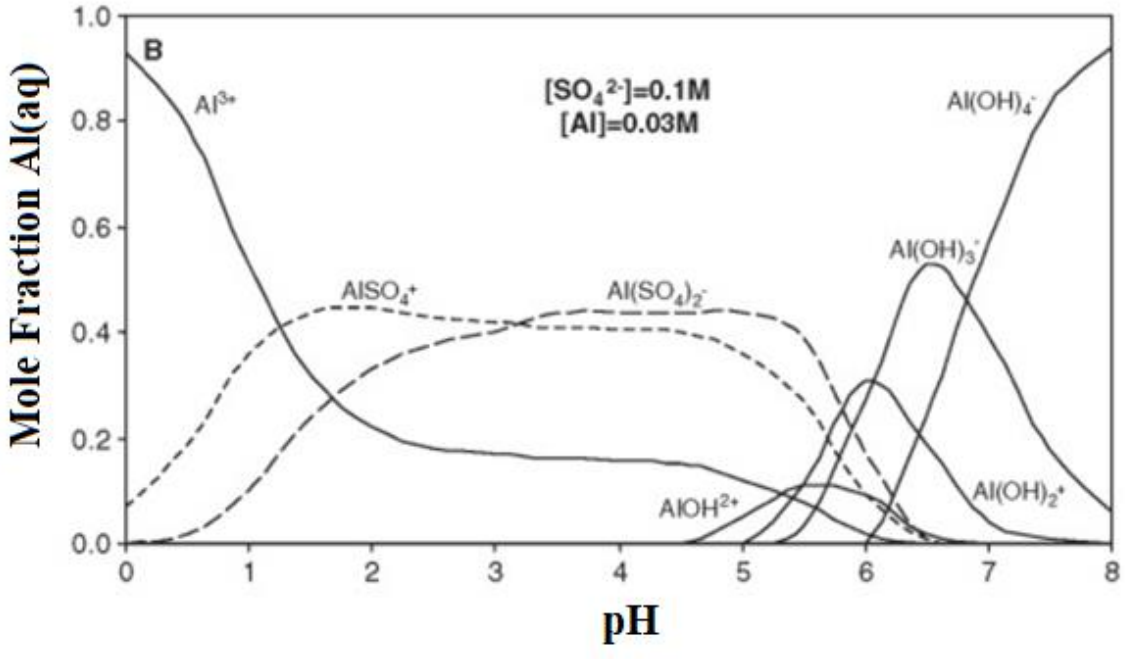


Figure 2-1: Speciation of Al as a function of pH (Calculated with PHREEQC 2.7 (25°C, 1 bar)) (España, 2007)

Depending on the area, Al entering AMD can be due to the natural water source (Momot and Synzynys, 2005) or due to the geology of the surrounding rock and soil in the area. AMD can have concentrations of Al as high as 497 mg/l (Naidu, van Dyk, *et al.*, 2020) whereas natural groundwaters have Al concentrations of between 0.1 and 0.8 mg/L (Patil *et al.*, 2013). According to aquatic life protection standards, the allowable limit in water that sustains aquatic life is 0.005 mg/L if pH < 6.5, 0.1 mg/L if pH > 6.5 (Solomon, 2008) – a substantial amount of Al thus needs to be removed before AMD can be returned to natural waters.

Removal of Al from AMD streams is also essential as exposure to Al is linked to multiple health and environmental problems - neurological disorders, bone disease, cellular immune impairment (Hellström *et al.*, 2006), and toxicity in aquatic organisms (The Water Center, 2018). In South Africa and other HIV afflicted countries, immunity compromising metals are of special concern, due to a large vulnerable population consisting of children, the elderly and HIV infected persons.

Alternatively, if the water is to be used for irrigation, a concentration limit of 20 mg/L must be adhered to (or the water can only be used for a short period of time on a site specific basis) (Department of Water Affairs and Forestry, 1996c). Treated AMD can also be used as industrial water but the concentration guidelines for this will be dependent on the proposed use.

2.1.2.2 Calcium

The calcium (Ca) content of AMD is dependent almost solely on the characteristics of the groundwater or aquifer water that comes into contact with the sulfide bearing minerals at the mine of origin. Calcium minerals are present in almost all rocks or solids and generally will dissolve from limestone, dolomite, and gypsum, increasing the calcium (and magnesium) concentration of the water stream (The Groundwater Association, 1999). Dissolution of calcium minerals is accelerated by the presence of carbonic acid in natural waters, and is also attributed the chemical breakdown of calcic-plagioclase feldspars (silicate minerals) and pyroxenes (Ganyaglo *et al.*, 2010).

The normal concentration of calcium in groundwater ranges from 10 to 100 mg/L (Nag, 2009). In addition to natural rock formations, calcium in water can also originate from agricultural fertilizers which sometimes contain calcium compounds (Saha, Reza and Kanti Roy, 2019). The concentration of calcium in AMD thus would start at a similar level as the groundwater, however the increased acidity would further the dissolution of any calcium containing rocks that are present, increasing this initial concentration. Calcium can therefore be present in all types of AMD, regardless of the type of mine in which it is generated. Calcium can occur in AMD at concentrations of up to 250 mg/L (Gogoi *et al.*, 2021) and although there are no reported detrimental side effects of consuming calcium rich water (with concentration levels greater than 80 mg/L), at these levels severe scaling occurs in pipework or plumping and the effectiveness of soap is diminished (Department of Water Affairs and Forestry,

1996a) – thus treatment needs to occur to keep Ca levels at between 0 and 32 mg/L for potable use. Calcium impacted waters can generally still be used in irrigation as well as in industry as process water.

2.1.2.3 Iron

Iron (Fe) is the most predominant metallic species found in AMD due primarily to the prevalence of pyrite around the world. Iron pyrite is the most widespread and abundant sulfide on Earth and can be found in tens of thousands of localities in multiple different mining areas (Mineralpedia, 2020). In addition, iron is the fourth most abundant element and is found in multiple minerals – such as haematite (Fe_2O_3), pyrite (FeS_2) siderite ($FeCO_3$), magnetite (Fe_3O_4), goethite ($Fe_2O_3.3H_2O$) and limonite ($2Fe_2O_3.3H_2O$). Iron is also found in a number of mixed ores and thus it is ubiquitous in most kinds of AMD.

Iron is found in three oxidation states, namely, 0, II and III of which the III oxidation state is the most common. In unpolluted water, iron is present as dissolved ferric iron, Fe(III), as ferrous iron, Fe(II) or as suspended iron hydroxides and is generally found in concentrations between 0.001 and 0.5 mg/L (Department of Water Affairs and Forestry, 1996a). In the case of AMD however (implying a high concentration of sulfate and a pH of below 3.5), the complexation of Fe is usually of the type Fe-SO_4^{2-} ($FeSO_4$, $Fe(SO_4)_2^-$) with the free aqueous ion (Fe^{3+}), and hydroxyl-containing complexes ($FeOH^{2+}$, $Fe(OH)_2^+$, $Fe_3(OH)_4^{5+}$, etc.) having a very minor presence (Sánchez-España *et al.*, 2005; Sánchez España *et al.*, 2006). As the pH increases to 5, sulfate iron complexes are replaced by the hydroxide forms (España, 2007).

The concentration of dissolved iron in AMD is dependent on the pH, redox potential, turbidity, suspended matter content (Lyde *et al.*, 2014), the concentration of aluminium and the occurrence of several other heavy metals (most notably manganese) (Nolan and Udall, 1962; Department of Water Affairs and Forestry, 1996a). Precipitation of iron may also result in the coprecipitation of trace metals such as arsenic, copper, cadmium, and lead – similar to Al coprecipitation. For Fe polluted waters to be used in irrigation, an ideal concentration of 5 mg/L (maximum 20 mg/L (Department of Water Affairs and Forestry, 1996c)) must be attained, thus AMD must be treated to remove the iron content. Total Fe concentrations in AMD can reach up to 3500 mg/L and thus extensive remediation must be undertaken to ensure water is safe for re-use (Naidu, van Dyk, *et al.*, 2020).

2.1.2.4 Magnesium

Magnesium (Mg) is not generally considered an element of concern in AMD streams due to its low concentration at many AMD sites and its relatively high allowable intake in humans (70 mg/L in drinking water (Department of Water Affairs and Forestry, 1996a)) and high allowable concentration in water streams used for irrigation. Magnesium (Mg) can be dissolved from many types of solids and rocks but especially from dolomite and magnesite – which occur worldwide (Warren, 2006). Mg is also present in large quantities in sea water and other brines, and along with Ca causes most of the hardness

and scale-forming properties of water – the main reason for treatment before use in irrigation, industry or domestic use (due to the formation of scale in boilers, water heaters, and pipes, and to the objectionable "curd" in the presence of soap) (The Groundwater Association, 1999). Mg containing minerals (magnesite, dolomite and magnesium oxide) seem to be prevalent in coal mines and AMD in these regions can reach concentrations of up to 396 mg/L (Keterew and Brilliance Mamba, 2020).

2.1.2.5 Manganese

Manganese (Mn) is the third most abundant transition metal in the Earth's crust and is found in a number of commonly occurring minerals, including pyrolusite (MnO_2), manganite ($Mn_2O_3.H_2O$), rhodochrosite (MnC_3O) and rhodonite ($MnSiO_3$) (Department of Water Affairs and Forestry, 1996a; Mihaela and Rosa, 2019). Manganese is found as the manganous Mn(II) ion in solution, which can be stabilized via complexation with various humic acids (that are important components of humus (Barrett, 2015)). Upon oxidation of Mn(II) to manganic Mn (Mn(IV)), manganese tends to precipitate to form a black hydrated oxide (Brant and Ziemkiewicz, 1997). Manganese is not a necessary constituent of the common silicate or carbonate minerals (as is the case with calcium), but can act as a substitute for iron, magnesium, calcium, and other divalent elements which occur in mineral structures (Hem, 1985). In some kinds of sedimentary rocks however, Mn will substitute for Fe in siderite and pyrite, and can also act as a substitute for certain cations in clays. As these minerals undergo natural (or accelerated due to mining activities) weathering, manganese is dissolved into solution and can exist in a variety of oxidation states (2+ ,3+, 4+ ,6+, and 7+), with the 2+ state being the most common in AMD (Brant and Ziemkiewicz, 1997).

The treatment of Mn in AMD is challenging due to (i) the high solubility of its minerals relative to other metal containing minerals, (ii) the inhibition of Mn precipitation at a molar ratio of Fe/Mn > 4 due to the presence of Fe, (iii) the reductive dissolution of Mn oxides by organic matter, sulfides and Fe (II), and (iv) the high pH (>8) required for the formation of insoluble Mn compounds (Mihaela and Rosa, 2019). Remediation of Mn rich waters (like AMD) is essential as natural waters generally have concentrations of Mn in the range of 0.02 - 130 µg/L whereas Mn in AMD can reach levels of 200 mg/L (Department of Water Affairs and Forestry, 1996a; Naidu, van Dyk, *et al.*, 2020). For AMD to be treated for domestic use, irrigation use or industrial use, the concentrations of Mn that would need to be reached would be 0.05 mg/L, 10 mg/L and < 2 mg/L respectively (Department of Water Affairs and Forestry, 1996b, 1996a, 1996c).

2.1.2.6 Treatment/Remediation Options for Metals in AMD

Because of their high solubility in aquatic environments, heavy metals can easily be absorbed by living organisms (Barakat, 2011), causing disturbances in their natural functioning which can result in illness, mutation and death (Malkoc and Nuhoglu, 2006). The control of metal concentration in water bodies is therefore essential, and many regulations and laws are in place that govern the maximum metal content

that can be contained in industrial wastewater discharges. Government agencies give limits for the concentrations of metals, taking into consideration the effect they have on biological organisms. Specific limits have been discussed in detail in the sections above and the total electrical conductivity reading (which is an indicator of total dissolved solids (TDS) and mineralization in a water sample) should not exceed 70 mS/m (Fatoki and Awofolu, 2004). Mining wastewater streams will invariably contain larger quantities of metals than this, and thus removal of these metals – before allowing the mine water to enter back into a natural water body, to be used in irrigation or as industrial water – is required. Several treatment methods are currently used by mines for metal removal. These include (amongst others) precipitation using pH adjustment, solvent extraction and ion exchange (Zhang *et al.*, 2016). Metal removal is generally a costly process and even when passive and low-cost methods are used, there remains the problem and added cost of waste management. New methods that aim to provide more effective, cheaper means to facilitate metal removal that result in less waste production are thus continuously being researched and improved.

One such method, biomaterial adsorption and accumulation (a process that uses biological waste materials (such as eggshells (Zhang *et al.*, 2016) or dead biomass containing lipids and proteins (Kaduková and Virčíková, 2005)) to remove heavy metals) is reported to be highly effective. This is because biomaterials such as eggshells are generally benign, abundant, and cost effective. Adsorbent loss in these methods however is high and continual replenishing needs to be undertaken in order to maintain a process (Chern and Chien, 2002). In addition, the sourcing of the adsorbents is often difficult and/or expensive.

Another method, removal via ion exchange resins, is also a developed method of treatment for heavy metal rich waters. The use of resins is beneficial as there is the potential of lowering costs of treatment via product recovery (Desilva, 1996). Ion exchange, however, is a costly option and large treatment volumes (which are needed) are difficult to accomplish. Resins are also highly specific (meaning multiple resins may be needed to remove all undesirable contaminants in a water stream) and can be easily fouled which increases the cost of maintenance (Alchin, 2006).

The use of waste metallurgical slag as an adsorbent and alkaline reactant is useful as it is readily available in large quantities, and many steel companies are actively pursuing methods in which to eliminate this by-product – making sourcing of the reagent much easier. Use of metallurgical slag has been approved in biological systems (soil systems) (Aydilek, 2015; Strandkvist, 2016) and thus incorporation of this treatment into the treatment program will allow for further biological means, in particular sulfate reducing microbes (SRM), to be used to lower the sulfate content of the AMD.

The five metals discussed above (Al, Ca, Fe, Mg and Mn) are the metals that will be assessed in this study. These metals have been selected due to the nature of the treatment scheme – using slags which are rich in calcium and magnesium species and may dissolve into the AMD solution, increasing the Mg

and Ca content – and also due to the nature of the metals. Aluminium and iron undergo precipitation that facilitates the coprecipitation of several other metal species and thus monitoring these metals gives an indication of the overall efficacy of the treatment scheme. The monitoring of Mn was also deemed necessary due to the concentrations at which it was present and due to its relationship and similarity (in terms of chemical characteristics) with Fe and Al.

The precipitation of metals in this study is facilitated by pH rise. Metal hydroxides, sulfides, sulfates and oxides form at different pH's and will precipitate out of the solution, settling under the action of gravity. Iron precipitates form at pH values greater than 3.5 and aluminium precipitates form at pH values greater than 5 (Balintova and Petrilakova, 2011). A pH of greater than 7 should therefore almost completely remove these two metals. Manganese begins to precipitate at between pHs of 6.5 and 9, and copper precipitates between the pH's of 4 and 6. Magnesium begins precipitation at a pH of 8 (Irving, 1926; Yamagata and Paschoal, 2001). Magnesium and manganese will therefore only partially precipitate at a pH of 7.5. This research incorporates the use of a DSR system for sulfate removal and thus sulfides will also be present in the system for the metal ions to bind to and precipitate with and thus precipitation of metals will occur faster. Hydrogen sulfide reacts with dissolved metals in the AMD via the reaction shown in Equation 2-6 below (Taylor, 2005):

$$H_2S + M^{2+} \rightarrow MS + 2H^+$$

Equation 2-6

$$S^{2-} + M^{2+} \rightarrow MS_{(s)}$$

Equation 2-7

At suitable pH values this results in the precipitation of metals as metal sulfides. As indicated by the research objectives, this research also aims to determine whether any metals or other elements leach out of the slag into the water during treatment. Studies which have assessed the composition of various BOF samples show compositions similar to that presented in Figure 2-2. With the exception of calcium and silicon, any of the other prominent elements which are present in the slag which are leached into solution should precipitate due to the high pH that will be achieved.

It must be noted that treatment of AMD (treatment that addresses heavy metals, sulfate concentration, pH level and acidity) generally incorporates many different steps and processes (Macías *et al.*, 2012), each process targeting at least one problematic aspect of the acidic water. The main aspects of treatment involve raising the pH of the system (Pereira *et al.*, 2020), removing high concentrations of heavy and other toxic metals, removing sulfate (Jafaripour, Rowson and Ghataora, 2015), and finally removing any other toxins and contaminants which may be present in the water and which are specific to the area and type of mine from which it was generated.

A critical part of any treatment method is also management of any waste that may be produced during operation (Ryan, Kney and Carley, 2017). Treatment targeting pH and metal concentration has been discussed, the subsequent sections below address the high sulfate concentration in AMD as well as the waste management aspect of the system.

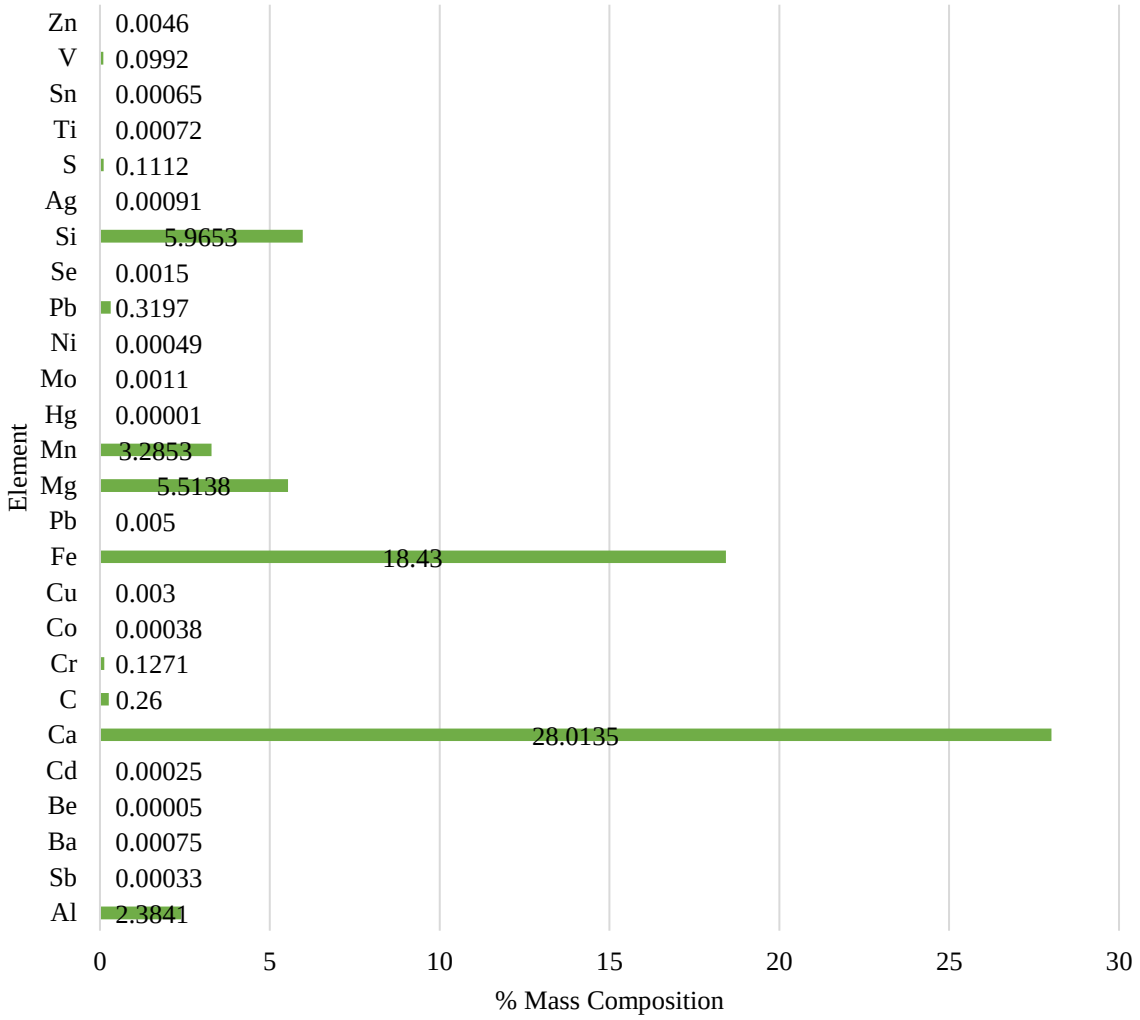


Figure 2-2: %Mass composition of elements in BOF slag (Proctor et al., 2000)

2.1.3 Sulfate Concentration

The final characteristic of AMD (relevant in treatment schemes and dependent on the source of AMD) is the concentration of sulfate that is contained within the stream.

2.1.3.1 Occurrence of Sulfate in AMD

Similar to the ores containing metal species that contribute to the formation of AMD, ores containing sulfidic metal compounds (pyrite, sphalerite, chalcopyrite, and pendanlite) are chemically stable and will undergo oxidation slowly during the natural weathering of rocks. Under anthropogenic activities however (such as mining), the exposure of these ores to oxygen and water occurs much faster and

sulfide oxidation occurs at an accelerated rate (Blodau, 2006). The presence of hydroxyl ions and CO_2 also act as sulfide oxidizers (Evangelou and Zhang, 1995) further accelerating the formation of AMD. Both biotic and abiotic sulfide oxidation can occur, the abiotic oxidation following similar reactions as presented in Equations 2-1 to 2-4 (differing slightly where other metal sulfide compounds – other than pyrite – are present). Microorganisms (such as *Leptospirillum ferrooxidans, Acidithiobacillus ferrooxidans, Acidimicrobium ferrooxidans* and *Sulfolobus metallicus* (Johnson and Hallberg, 2003)) are well known for the ability to oxidize metal sulfides this exacerbates the production of sulfuric acid, lowering the pH and causing further increase in sulfate concentration due to further dissolution of solid sulfides (Norris *et al.*, 1996). Sulfate generation also occurs via the microbial polysulfide mechanism followed by microbial elemental sulfur oxidation to produce sulfate (as detailed in Equations 2-8 to 2-10).

$$\mathbf{2MS_{(s)} + 2Fe^{3+}_{(aq)} + 2H^{+}_{(aq)} \rightarrow 2M^{2+}_{(aq)} + H_2S_{(aq)} + 2Fe^{2+}_{(aq)}}$$

Equation 2-8

$$\mathbf{4H_2S_{(aq)} + 8Fe^{3+}_{(aq)} \rightarrow S_{8(s)} + 8Fe^{2+}_{(aq)} + 8H^{+}_{(aq)}}$$

Equation 2-9

$$\mathbf{S_{8(s)} + 12O_{2(g)} + 8H_2O_{(l)} \rightarrow 8SO^{2-}_{4(aq)} + 16H^{+}_{(aq)}}$$

Equation 2-10

The presence of sulfate in AMD is proportional to the amount of metal species contained within which have occurred based on oxidation of metal sulfide minerals.

2.1.3.2 Treatment/Remediation Options for Sulfate in AMD

Sulfate control in mine waters is primarily achieved by one of two methods: (i) removal through membrane separation of salts from water or (ii) removal of sulfate by salt precipitation through ion exchange. Other methods and technologies that are used to a lesser degree are permeable reactive barriers, biological reduction technologies and dosing technologies which allow for the formation of insoluble mineral precipitates (Bowell, 2004). As discussed in the previous chapter, this study will incorporate biological reduction and the formation of insoluble metal precipitates facilitated by pH rise.

2.1.3.2.1 Biological Sulfate Reduction

Bioremediation processes (processes which use living organisms to combat the harmful effects of AMD) can function naturally or can be enhanced by supplementing the process with electron acceptors, nutrients or by altering other factors (Lin and Lin, 2005). In the case of biological sulfate reduction for AMD treatment, this process can be enhanced by providing a carbon source and by maintaining a favourable pH level – due to the excessive presence of sulfate in AMD streams, supplementing the process with more electron acceptors is not necessary. Other than the presence of a substrate and a

favourable pH level, biological sulfate reduction relies almost solely on the presence of different sulfate reducing microorganisms, which are able to live together within the reaction vessel (Goldhaber, 2003). SRM are the most ubiquitous of the sulfate reduction facilitating organisms (Keller, Wall and Chhabra, 2011), but other types of microorganisms may be present in these types of systems that will assist either directly with the sulfate reduction or indirectly via creating a greater availability of nutrients. Competition between microorganisms (methanogenic organisms) in this environment may also be a factor (Jing *et al.*, 2013). SRM are suitable for AMD treatment as they are able to oxidize organic matter, produce bicarbonates that raise pH and the alkalinity of the media in which they reside, and reduce any sulfates which are present to sulfides under anaerobic conditions (Zagury, Neculita and Management, 2007). Sulfides can then combine with metals to form insoluble metal sulfides.

The rate of biological sulfate reduction or DSR relies almost solely on the presence of different – but complementary – microorganisms which are able to live together within systems that contain suitable concentrations of sulfate. These organisms form an ecosystem that releases volatile fatty acids (VFAs) via degradation of carbon containing substrates and further use these to reduce sulfates within the sulfate rich sample. Although SRM are the most well-known of the DSR facilitating bacteria, other types of microorganisms are present in these types of systems that will assist either directly with the sulfate reduction or indirectly via creating a greater availability of nutrients (via degradation of the substrate). SRM generally use VFAs as a substrate (although they are able to use other carbon sources), and thus the presence of other microorganisms within the system is essential, as the sugars released from complex carbohydrates must first be further broken down into VFAs before use by the SRM. Many organisms are able to accomplish this. Acidogenic bacteria are able to facilitate a process known as acidogenesis (Alexiou and Panter, 2004). which is the process whereby sugars and complex carbohydrates are converted into VFAs via fermentation (Henze *et al.*, 2008). One percent of all known bacteria fall into the category of fermentative bacteria (Henze *et al.*, 2008) and thus there is no documented specific species or strain that is particularly apt at performing in the conditions imposed by AMD. In terms of SRM, based on their substrate utilization, they can be divided into two metabolic groups. These include complete oxidizers such as the genera Desulfomonas, Desulfobacter, Desulfosarcina and Desulfoacium which are capable of oxidising the substrate to produce carbon dioxide, while the other group which include the genera Desulfovibrio, Desulfomicrobium, Desulfobolotus (and others) can only oxidise the substrate to acetate (Brahmacharimayum et al., 2019).

SRM reduce sulfate to sulfide by oxidizing organic or carbon containing material (Munawar and Riwandi, 2010). The effectiveness of the SRM at reducing sulfate depends on the following characteristics: (i) population size, (ii) the pH and temperature of the solution, (iii) the exposure to air, and (iv) the distribution of the SRM throughout the reaction vessel/bioreactor (Barton and Fauque, 2009). Different strains of SRM function optimally over a range of pHs and thus selection of the suitable strain or cultivation thereof is recommended before commencement of treatment. SRM also do not

function at very low or high temperatures and thus the sulfate reduction must occur at largely neutral conditions (Hao *et al.*, 1996). SRM are known to develop and migrate into a biofilm layer, which usually forms at the surface of the liquid (Labrenz *et al.*, 2000). Although this film is not essential to SRM functioning, if a film does develop, the DSR will be most effective in regions which are close to this film. Sulfate removal will also occur via metal sulfate precipitation as mentioned.

The overall sulfate reduction (and subsequent sulfide and hydroxide precipitation mechanisms) are described in Equation 2-11, Equation 2-12 and Equation 2-13 below and in Equation 2-6 and 2-7 (Tuttle, Dugan, & Randies, 1969), however it should be noted that other types of carbon containing compounds can be substituted into Equation 2-10. It is also important to note that the concentration of different sulfur species within solution is dependent on pH. At pH levels between 0 and 4, H_2S is predominant; at pH levels between 9 and 14, HS^- is the predominant species and at pH levels above 13, S^{2-} is the predominant species. Equation 2-6 and 2-7 can occur with each of the species to form metal sulfides. Manganese and magnesium sulfides reportedly exhibit high solubility at pH levels below 7, thus these metal sulfides are not expected to precipitate (Lewis, 2010).

SRM can use a wide range of electron donors to facilitate anaerobic respiration which in turn utilizes sulfate as a terminal electron acceptor (the process known as biological sulfate reduction). These electron donors include hydrogen, methanol, ethanol, acetate, lactate, propionate, butyrate, sugar, molasses and other simple organics (Cao *et al.*, 2012). Commercially available simple organic compounds like the ones listed above (ethanol, butanol, lactate, and simple sugars) have been successfully used at a laboratory-scale; however, the cost of these materials prohibits their application at a larger scale. This has led to the search for cheaper substrates with many organic rich effluents having been tested with varying levels of success. These wastes include (amongst others) compost, domestic, agricultural and industrial wastes.

$$SO^{2-}_4 + 2CH_2O \rightarrow H_2S + 2HCO_3^-$$

Equation 2-11

$$HCO_3^- + H^+ \rightarrow CO_2(g) + H_2O$$

Equation 2-12

$$Al^{3+} + 3H_2O \rightarrow Al(OH)_3(s) + H^+$$

Equation 2-13

The type of electron donor that is used has a substantial impact on the rate of sulfate reduction achieved by the SRM that are present. Different electron donors can result in different bacterial biomass yields of SRM (Liamleam and Annachhatre, 2007) and in addition, the substrate consumption rate of the SRM is dependent on the concentration of both the electron donor and sulfate (the electron acceptor). This in

turn affects the competition between SRM and methanogenic bacteria. Low molecular weight compounds produced from anaerobic fermentation such as organic acids, VFAs and alcohol are ideal for use as electron donors for SRM, however, many considerations, including price, ease of the handling and purchasing, have to be taken into account when choosing a substrate for use in industrial processes or (as in this case) for use in wastewater treatment. Thus, although using alcohol as a substrate would allow for the best functioning of the SRM in the system, this would not be feasible due to the cost of procuring this reagent. In this research, sugarcane bagasse (which is a waste material in the sugar industry and is readily available in South Africa) is chosen as the substrate as it is cheaper than other reagents and it has shown promise in the treatment of AMD (Li *et al.*, 2018).

2.2 Sugarcane Bagasse

Sugarcane has considerable economic significance in multiple countries, being the principal feedstock for sugar and ethanol production (Souza *et al.*, 2014). Two main wastes are generated in sugarcane processing, namely straw and bagasse. Sugarcane straw is composed of the dry leaves (approximately 60%) and green tops (approximately 40%) that surround the sugarcane stalk (Aguiar *et al.*, 2021). Sugarcane bagasse is the solid, fibrous waste from sugarcane milling. It consists of fibre bundles vessels, parenchyma, and epithelial cells (Bizzo *et al.*, 2014). It is produced in large amounts around the globe, with a reported production of 280 million tons/year (Ortiz and Oliveira, 2014). The main re-use avenue for sugarcane bagasse is as a source of energy and electricity in sugarcane mills (Dantas, Legey and Mazzone, 2013), however other avenues include use in biorefineries in the production of bio-ethanol, use in paper and animal feeds manufacturing (Tongaat Hulett and Department of Energy (RSA), 2013) and there has also been research where bagasse has shown potential in the treatment of AMD (Cherubini, 2010; Bardone *et al.*, 2014; Westensee *et al.*, 2018)

Sugarcane bagasse is a rich source of cellulose, hemicellulose and lignin (containing 32–45%, 20–32% and 17–32% respectively) (Alokika *et al.*, 2021). The large volume of sugarcane bagasse generation has been a challenge to many industries as well as the environment at a global level for many years as, although cellulosic and hemicellulosic fractions in bagasse makes it a potential raw substrate for the production of value-added products at large scale, the presence of lignin hampers its degradation which leads to low yields of value-added products (Mokhena *et al.*, 2017). Pre-treatment of sugarcane bagasse is therefore important and will allow for solubilization of lignin that will exposes cellulose and hemicellulose for enzymatic action. Sugarcane bagasse has shown in promise in serving as a nutrient medium for the cultivation of diverse microorganisms and for the production of organic acids and biofuels. It's use in AMD treatment schemes is ideal, as the acidic AMD could initially be used to solubilize lignin in the sugarcane bagasse (as a pre-treatment step) and the resulting cellulose and hemicellulose rich stream can be used as a substrate for the various reducing microorganisms.

In nature simple organic feedstocks (electron donors) are provided by the activities of cellulose degraders and fermenters. The breakdown of cellulose is a slow process and is generally the rate limiting step, thereby slowing the treatment process.

As mentioned prior, the sulfate reduction facilitated by SRM and other microorganisms is aimed to occur after the sulfate concentration reaches values of approximately 400 ppm and below. The removal of sulfate at levels higher than this will be facilitated by pH and counterion presence-based precipitation. The altering of the pH and the provision of counterions will be provided by the addition of an alkaline reagent – namely BOF slag.

2.3 BOF Slag

This section of the literature review is presented in the form of a Critical Review Article that has been published in the Journal of Minerals Engineering (Naidu, Sheridan and van Dyk, 2020), titled "Basic oxygen furnace slag: Review of current and potential uses". The background, associated cost, current uses and hypothesized use in AMD treatment is presented sectionally in this article.

The full reference for this article is as shown below.

Naidu, T. S., Sheridan, C. M. and van Dyk, L. D. (2020) 'Basic oxygen furnace slag: Review of current and potential uses', *Minerals Engineering*, 149(February), p. 106234. doi: 10.1016/j.mineng.2020.106234.

.

Basic oxygen furnace slag: Review of current and potential uses

2.3.1 Abstract

Steel slag, in particular, basic oxygen furnace slag (BOF-S) - a by-product in the steelmaking industry - is an environmental challenge due both to the large volume of the material that is produced annually and its potentially detrimental environmental impacts. Globally, waste generation and management has become a critical issue with waste prevention and recycling rates reportedly too low to keep up with the growing rate of production. In this regard, considerable research has been done to improve traditional applications as well as explore possible reuse options of BOF-S. Multiple, innovative, new technologies and uses have emerged, including BOF-S reuse as a cement binder, a neutralizing agent, an anti-microbial additive or as a carbon sequestration material. Many applications involve the treatment or processing of other waste products such as wastewater, contaminated soils or thin film transistor liquid crystal display waste. Even so, much still needs to be done for sizeable implementations and noticeable differences to be made in the BOF-S reuse field. Large slag dumps continue to exist and grow in many parts of the world as the global steel production rate increases on an annual basis.

This paper presents an overview of BOF-S characteristics and composition and discusses how these qualities contribute to the range of possible applications of the by-product. The applications for use of BOF-S presented herein, range from novel, small-scale applications and extends to well-established, large-scale uses.

2.3.2 Introduction

The iron and steel manufacturing industries are fundamental to the economies of many countries (RSA Department of Trade and Industry, 2018). They provide the basic materials needed for the development and maintenance of infrastructures, vehicles, buildings, industrial facilities, and many other daily necessities (Ko, Chen and Jiang, 2015). Global steel production has been growing rapidly for the past 60 years - in 1967, the total world steel production was reported to be just less than 500 million tonnes (World Steel Association, 2017), but during 2015, the total steel production was reported to be 1599.5 million tonnes, showing an increase of more than 200% in 48 years. This number increased substantially again in 2016, where 1666.2 million tonnes of crude steel was reported to have been produced (Worldsteel Association, 2016). As shown in Figure 2-3, worldwide steel production has experienced an average growth rate of approximately 5% per annum for the last 10 years (Xu and Da-qiang, 2010).

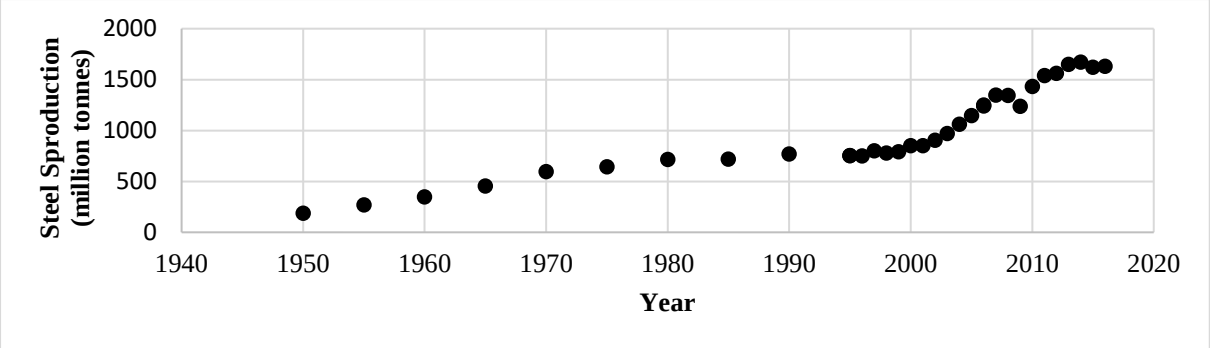


Figure 2-3: Total worldwide steel production from 1950 to 2016 in million tonnes (Xu and Da-qiang, 2010; World Steel Association, 2017)

The steel industry provides substantial employment in the world's top producing countries, namely China, Japan and India (Sawe, 2017), but it is also responsible for large amounts of waste material generation, energy consumption and CO_2 emissions. The proper and efficient reduction and management of waste production, energy use and greenhouse gas (GHG) emissions are essential to achieving sustainable development. Improper management impacts on environmental and public health and affects the development and improvement of future generations. For this reason, research has been conducted in this industry with the aim of (i) reducing energy consumption and lowering CO_2 emissions and (ii) combatting, eliminating, or reducing waste and re-using or recycling waste materials and by-products. These two areas are discussed below.

2.3.2.1 Energy consumption and CO2 emission

Iron and steel manufacturing is the most energy and carbon-intensive industry in the world (Quader *et al.*, 2015) as both the iron and steel making sectors have not yet attempted to fully incorporate renewable energy sources into their production. They are highly dependent on fossil fuels and release substantial amounts of CO_2 during normal operations (Helle *et al.*, 2012). The industry released 2.3 Gt in 2007 and its emissions have subsequently increased (Dhunna *et al.*, 2014). The Intergovernmental Panel on Climate Change (IPCC) has reported that the steel industry accounts for 5% of the total world CO_2 emissions. This is a substantial amount as the International Energy Agency (IEA) reported that CO_2 emissions from manufacturing industries account for approximately 40% of the total CO_2 emissions worldwide. This implies that the steel industry's carbon emissions account for 12.5% of all manufacturing emissions in the world (International Energy Agency, 2010b).

During the steel making process, CO_2 is generated as a by-product in either one of the following two processes: (i) reduction of iron ore with coke in a blast furnace (BF) to produce pig iron, or (ii) from the decarbonisation of limestone ($CaCO_3$) and dolomite ($MgCO_3$) which are added together with coke as fluxing materials to strip oxygen and other impurities from iron ore (Kuwahara and Yamashita, 2013). For the average tonne of steel that is produced, between 1900 kg and 2200 kg of CO_2 is generated (Kundak, Lazic and Crnko, 2009; Kuwahara and Yamashita, 2013). The iron and steel industry is

reportedly the largest consumer of coal in the industrial sector, accounting for between 10 and 18 % of delivered energy (to the industrial sector) consumption worldwide (U.S. Energy Information Administration, 2016). As of 2013, the industry consumed approximately 5–6% of the world's total energy (Kuwahara and Yamashita, 2013). Although efforts have been made to enhance the energy efficiency of the industry with some successes reported (up to 60% reduction in energy consumption (Xu and Da-qiang, 2010) and the specific energy consumption of steel in the U.S. decreasing from 48 to 20 GJ/tonne between 1960 and 2000 (Barati, Esfahani and Utigard, 2011)), more needs to be done in order to ensure the long term environmental sustainability of the industry.

2.3.2.2 Solid waste generation

In addition to energy consumption and CO_2 emissions, the steel industry is also responsible for large amounts of solid waste generation, primarily in the form of steel slag. The worldwide output of steel slag is reported to be over 1600 million tons annually (Liu and Wang, 2017). Slag is a glass (Huang *et al.*, 2013) or gravel like by-product that is left over in steel making processes after the desired metal has been smelted or separated from its ore (Humbert, 2019). It can be categorized by either the process in which it was generated (basic oxygen furnace slag (BOF-S), electrical arc furnace slag (EAFS), ladle refining slag (LFS)), or by the type of steel produced in said process (carbon steel slag or stainless-steel slag) (Yi *et al.*, 2012; Liu and Wang, 2017; Ndlovu *et al.*, 2017). Countries such as Japan, Germany and France have found multiple reuses for their slag production and report waste material reusability rates of close to 100%. However there are still countries that struggle with managing the waste production from this industry (Yi *et al.*, 2012). China was responsible for approximately half the world's steel production in 2010 (Allen, 2010), and generates large amounts of slag that do not currently have reuse avenues. In 2015, 120 million tonnes of steel slag was produced in China with another 1 billion tonnes already accumulated in landfills or in stockpiles where metallic elements present in the slag can leach out and have the potential to cause environmental and health problems (Evarts, 2017; Mo *et al.*, 2017).

Two types of by-products are produced during steel and iron manufacturing, (i) blast furnace slag (BF-S) combined with BOF-S and (ii) converter or refining slag. In 2008 between 230–280 Mt of BOF-S and 130–200 Mt of converter slag were produced globally (Kuwahara and Yamashita, 2013) and current estimates put slag generation at between 200 and 250 kg per tonne of steel that is produced (Kumar *et al.*, 2019). As discussed, slag which is not reused is generally placed in landfill sites which are not closed off or isolated from the surrounding environment. When water comes into contact with the slag, a solution high in alkaline content is produced. When this water seeps back into the environment it has detrimental side effects for aquatic and terrestrial animal and plant life in the surrounding areas (Souter and Watmough, 2017). This is considered the most widespread and chronic impact of alkaline wastes from the steel industry (Gomes *et al.*, 2016).

2.3.2.3 Impact of slag on the environment

The geochemical behaviour and characteristics of the alkaline leachate seeping from landfill sites and stockpiles depends on many factors, including (Roadcap, Kelly and Bethke, 2005; Mayes and Younger, 2006; Mayes, Younger and Aumônie, 2008): (i) the chemistry (pH, conductivity, etc.) of the water before it comes into contact with the slag; (ii) the composition and age of the slag contained in the landfill site; (iii) the flow rates, redox status, and residence time of the water (known as hydrogeological factors); (iv) the nature of any other steel mill wastes also present in the land fill site; (v) the chemical and physical properties of the surrounding ground and lastly, (vi) the chemistry of the body of water that eventually receives the leachate.

Alkalinity generation generally arises from two processes: (i) the rapid hydration and dissociation of calcium and magnesium oxide, and (ii) the slower dissolution of Ca-Silicate minerals like $Ca_3Si_2O_7$ (rankinite), Ca_2SiO_4 (larnite) and $Ca_2Mg(Si_2O_7)$ (akermanite) (Gomes *et al.*, 2016). The release of metals or elements from slags that contribute to alkalinity generation can cause environmental problems such as water and soil pollution (Shen and Forssberg, 2003). There are many impacts of alkaline leachate waters which include increased water pH, increased chemical oxygen demand (COD), increased oxygen depletion, increased salinity, and increased metal concentrations (Mayes and Younger, 2006; Mayes, Younger and Aumônie, 2008). In conjunction with these effects, mineral precipitation also occurs and can suffocate or smother macroinvertebrate communities as well as reduce light penetration into water bodies, further amplifying any ecological impact of the leachate release (Hull, Oty and Mayes, 2014). For these reasons, along with the need to reduce the environmental impact of the steel manufacturing industry as a whole, metallurgical slag reuse and recycling is considered to be essential.

2.3.3 Objective

Since the management of BOF-S use has become a significant environmental engineering issue due to the quantities generated and the high associated disposal costs and constraints (Li, 1999; Stadler, Eksteen and Aldrich, 2007; Tsai, Kao and Hong, 2009), recycling techniques need to be better utilized to reduce the environmental impact of the steel industry. This article reviews the current and some possible future uses and reuses of metallurgical BOF-S.

2.3.4 Steel making process

2.3.4.1 Overview

There are two main processes used in the production of steel: (i) primary steel production which uses iron ore as the main raw material [this includes BF and BOF processes (Steenkamp and Preez, 2015)], and (ii) the direct reduction (DR) process and electric arc furnace (EAF) process. The latter two processes require much less capital than the BF and BOF processes and involves using a combination of steel scrap and iron ore that will be reduced in the DR process (Tanaka, 2015) and purified in the

EAF process. At present, steel production in high output countries, such as in China and Japan, mainly use iron ore as raw materials via the primary BF and BOF route (Wei *et al.*, 2017). A depiction of the possible steel production routes is shown in Figure 2-4.

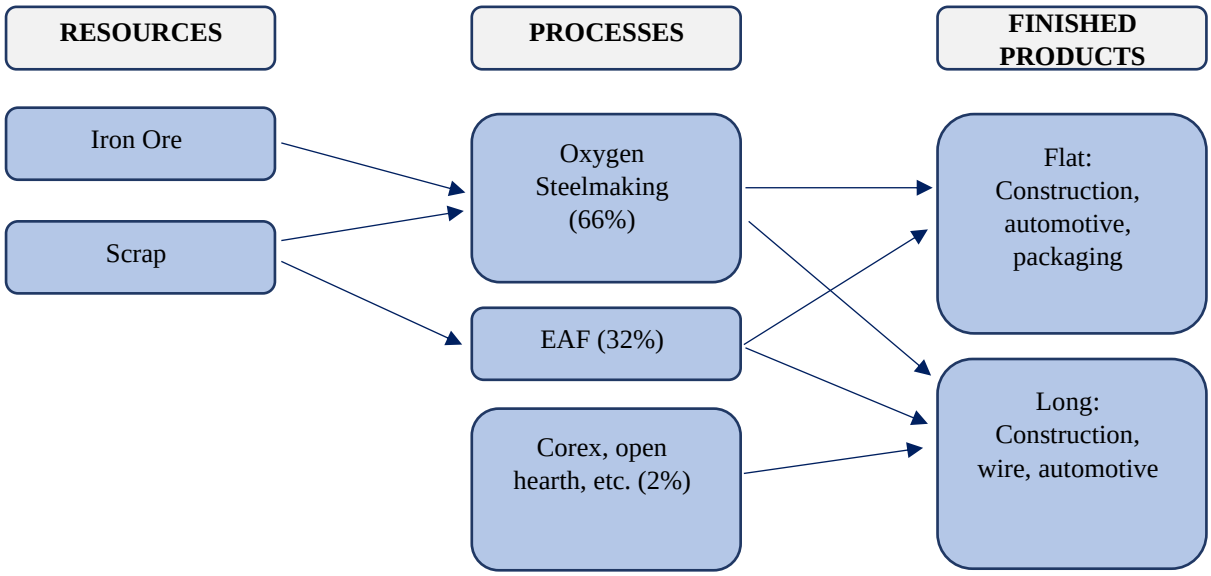


Figure 2-4: Steelmaking routes, raw materials and possible finished products *(World Steel Association, 2017)*

2.3.4.2 The Basic Oxygen Furnace (BOF)

The BOF process forms part of the primary steel production route, which also incorporates the BF process. In a BF, the iron ore, limestone and fuel are continuously supplied through the top section of the furnace, while heated air is forced into the lower section (Geerdes, Toxopeus and Van der fliet, 2009). The end products are usually molten metal and slag, of which the former is fed into a BOF and the latter is considered a waste material or by-product of the process. If the carbon content in steel is too high it could result in defects such as inclusions and blowholes which form during solidification, thus the BOF process is essential in steelmaking as it lowers the carbon content of the molten alloy and changes it into low-carbon steel (Kloppers and Fedotova, 2001). The BOF is essentially a converter in which heat is internally generated by the oxidation of impurities that are found within the molten slag. Along with the molten slag, oxygen is also added to the charge and this leads to the formation of iron oxide and carbon monoxide (which are exothermic reactions). Within the furnace, the temperature level or amount of heat produced is determined by the rate of oxidation of metals and the temperature of molten iron which is received from the BF (Remus and Roudier, 2010; Yildirim and Prezzi, 2011). Due to the increasing amount of accumulated scrap metal, scrap is also sometimes added into the BOF, making up 20% to 30% of the entire charge. Lime and fluorspar [the commercial name for calcium fluorite (Masoudi, Ezzati and Moradzadeh, 2017)] are added to the furnace to form a slag which contains the impurities that are removed from the molten slag. When the carbon content of the molten metal is reduced to a sufficient level, the steel is tapped into a ladle and cast continuously.

At the end of the BOF process, the liquid steel and slag form an immiscible layer which is first separated and then tapped into ladles and slag pots. The BOF-S pots are transported to further processing facilities or directly to solidification and casting facilities, after which they are sent to a disposal or storage site (Ndlovu, Simate and Matinde, 2017). The composition of the hot metal from the BF process, the scrap metal that was added and the chemical reactions that occur during the BOF cycle will determine the composition of the slag as well as the amount produced (Remus and Roudier, 2010; Yildirim and Prezzi, 2011). The BOF process has not undergone any fundamental changes in the last 20 years: the same processes that occur in steel processing plants today were used then (Barker *et al.*, 1998).

2.3.4.2.1 Composition and characteristics of BOF-S

The characteristics and composition of BOF-S varies largely from site to site, as well as over different time periods at the same site. This is due to the varying nature of the sources of ore and scrap used in the process and thus the varying characteristics of the chemical reactions and mechanisms that occur (Teir *et al.*, 2007). In general all BOF-Ss tend to have a high basicity or alkalinity ratio (due to the nature of impurities found in the ore) and a high Iron Oxide content (Reuter, Xiao and Boin, 2004; Remus and Roudier, 2010; Ndlovu, Simate and Matinde, 2017). The alkalinity in slag is found in compounds such as CaO, MgO and SiO_2 in varying degrees (Naidu *et al.*, 2018). Some examples of compositions of BOF-S from around the world at different steel processing plants are shown in Table 2-1. The average elemental and molecular composition of BOF-S is shown in Figure 2-5, and the phases composition of different samples of BOF-S from different sites throughout the world, is shown in Figure 2-6 (where sample 1 is from Newcastle, South Africa (Naidu, van Dyk, *et al.*, 2020); sample 2 is from China (Yi *et al.*, 2012); sample 3 is from Japan (Shen and Forssberg, 2003); sample 4 is from Brazil (Calmon *et al.*, 2013); sample 5 is from Spain (Fernández-gonzález *et al.*, 2019) and sample 6 is from the United States of America (USA) (Barker *et al.*, 1998).

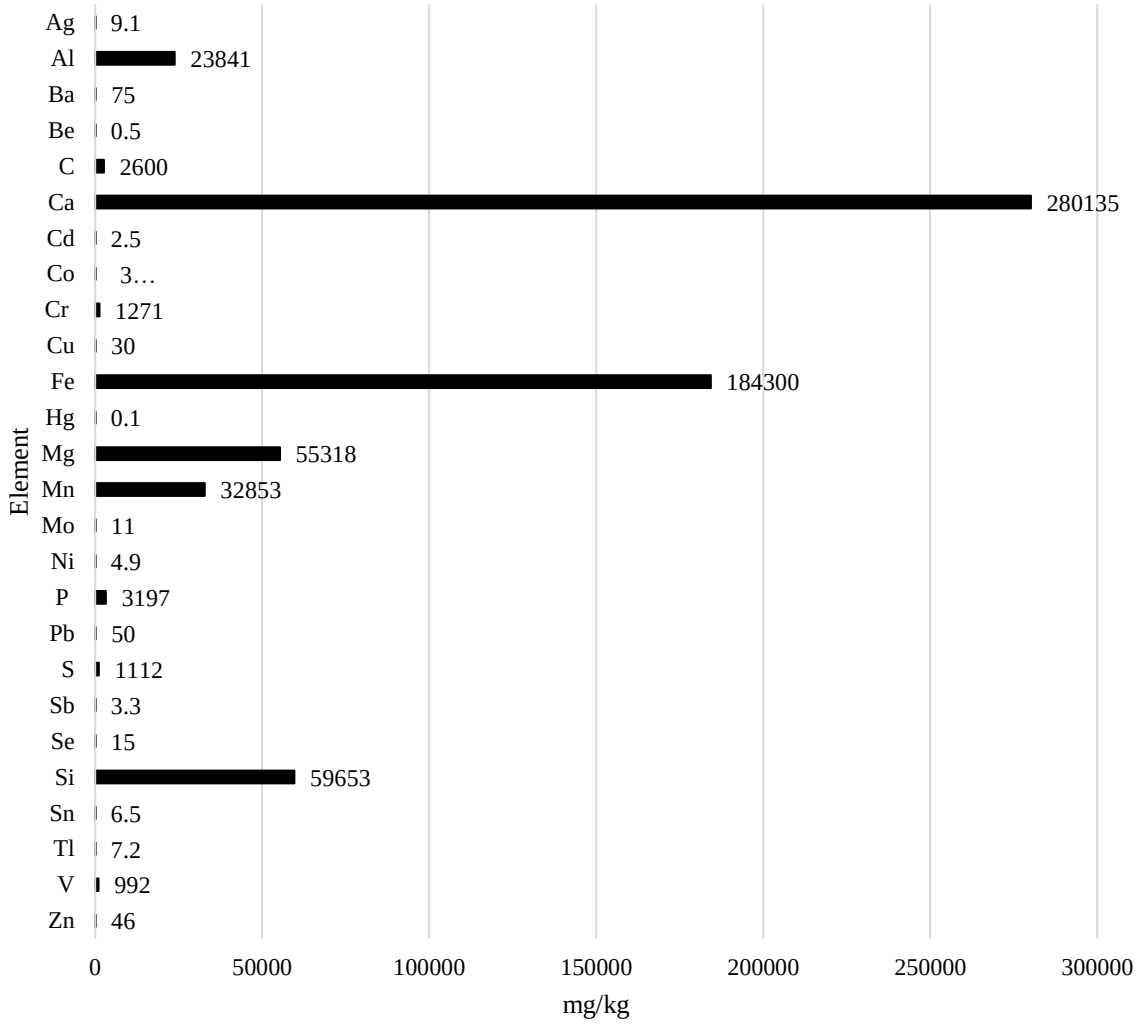


Figure 2-5: Average Elemental composition of BOF-S from 58 steel mill sites (Proctor *et al.*, 2000)

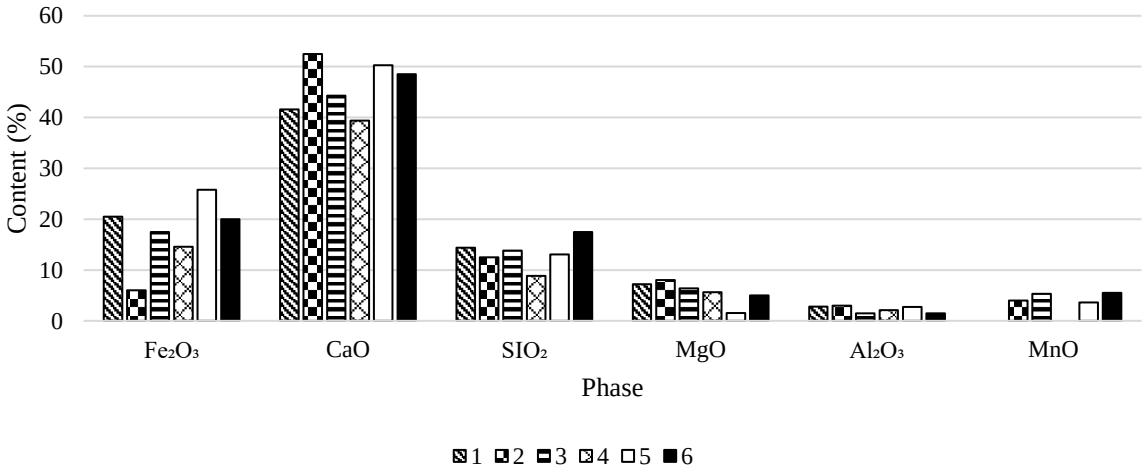


Figure 2-6: Molecular/phase composition of different samples of BOF-S in %mass

Table 2-1: Composition in %weight of BOF-S of varying particle sizes obtained from different sites

Country	Particle Size	Fe_2O_3	FeO	Fe met.	Al_2O_3	CaO	MgO	MnO	SiO_2	TiO_2	P_2O_5	Na_2O	K_2O	Cr_2O_3
Sweden (Tossavainen *et al.*, 2007)	30–40 mm	10.9	10.7	2.3	1.9	45	9.6	3.1	11.1	-	-	-	-	-
France (Windt, Chaurand and Rose, 2011)	> 1 mm	29	-	-	2.5	40	5	6	13	-	1	-	-	-
France (Mahieux, Aubert and Escadeillas, 2009)	0.04 - 1mm	22.6	-	-	2	47.5	6.3	1.9	11.8	-	2.7	0.2	0.1	-
VOEST-VAI steel plant Austria (Chaurand *et al.*, 2007)	> 2 mm	31.2	-	-	2.4	41.3	4.3	6.1	12.5	0.8	-	-	-	-
Kwangyang Iron & Steel Works	-	31.3	-	-	-	34.6	-	-	11	-	-	-	-	-

Country	**Particle Size**	**Fe_2O_3**	**FeO**	**Fe met.**	**Al_2O_3**	**CaO**	**MgO**	**MnO**	**SiO_2**	**TiO_2**	**P_2O_5**	**Na_2O**	**K_2O**	**Cr_2O_3**
plant in Korea (Sung Ahn *et al.*, 2003)														
China (Xue, Hou and Zhu, 2009)	0.6mm	17.8		-	6.8	45.4	7.3	-	13.7	-	-	-	-	-
India (Rashtriya Ispat Nigam Ltd, Visakhapatnam, Andhra Pradesh) (Indian Bureau of Mines, 2016)	10 – 60 mm	16.50			1.07	50.70	10.31	1.05	17.69	-	-	-	-	-
India (Reddy, Pradhan and Chandra, 2006)	-	16.2			1.3	52.3	1.1	0.39	15.3	-	3.1	-	-	0.2
South Africa (Doucet, 2010)	< 0.15mm	16.5			3.4	41.2	8	4.3	18.8	-	1.3	-	-	-

Country	**Particle Size**	**Fe_2O_3**	**FeO**	**Fe met.**	**Al_2O_3**	**CaO**	**MgO**	**MnO**	**SiO_2**	**TiO_2**	**P_2O_5**	**Na_2O**	**K_2O**	**Cr_2O_3**
South Africa (Doucet, 2010)	< 0.15mm	17.3			2	49.9	7.7	1.2	16.9	-	0.3	-	-	-
South Africa (Doucet, 2010)	< 0.15mm	26.9			7.5	38.1	9.4	3.2	13.9	-	1	-	-	-
Japan (Doucet, 2010)	< 0.15mm	17.5			1.5	44.3	6.4	5.3	13.8	-	-	-	-	-
Finland (Doucet, 2010)	< 0.15mm	24.1			1.8	43.6	1.4	2.4	13.9	-	-	-	-	-
USA (Brand and Roesler, 2015)	-	26.2			2.3	11	12.7	1.8	9.3	0.3	0.3	-	-	-

As indicated in Figure 2-4, Figure 2-5, Figure 2-6, and Table 2-1, the most abundant substance found in BOF-S is calcium oxide (CaO) followed by iron containing compounds and silicon dioxide (SiO_2). Magnesium oxide is also found in BOF-Ss and this, along with the presence of calcium and silicon containing compounds, are the main factors that give BOF-S the ability to increase the pH and the alkalinity of solutions that are allowed to percolate through it (Roadcap, Kelly and Bethke, 2005; Riley and Mayes, 2015). In addition to the oxides presented in Table 2-1, a number of different minerals can be found in BOF-S, including Larnite, β-Ca2SiO4 and different types of CaMg Oxides (Tossavainen *et al.*, 2007). The chemical mechanism by which the pH of the solution rises is the hydration of CaO by water molecules. This results in the formation of calcium hydroxide, which then dissociates to form both Ca^{2+} and OH- ions, the latter of which is responsible for the increase in pH (Roadcap *et al.*, 2006). Other oxides present in the slag (MgO, SiO_2) undergo the same progression, further increasing the pH rise. Water that has been allowed to seep through BOF-S beds can also leach out certain elements that are found in BOF-S. The mean toxicity characterization leaching potential (TCLP) of BOF-S is shown in Figure 2-7.

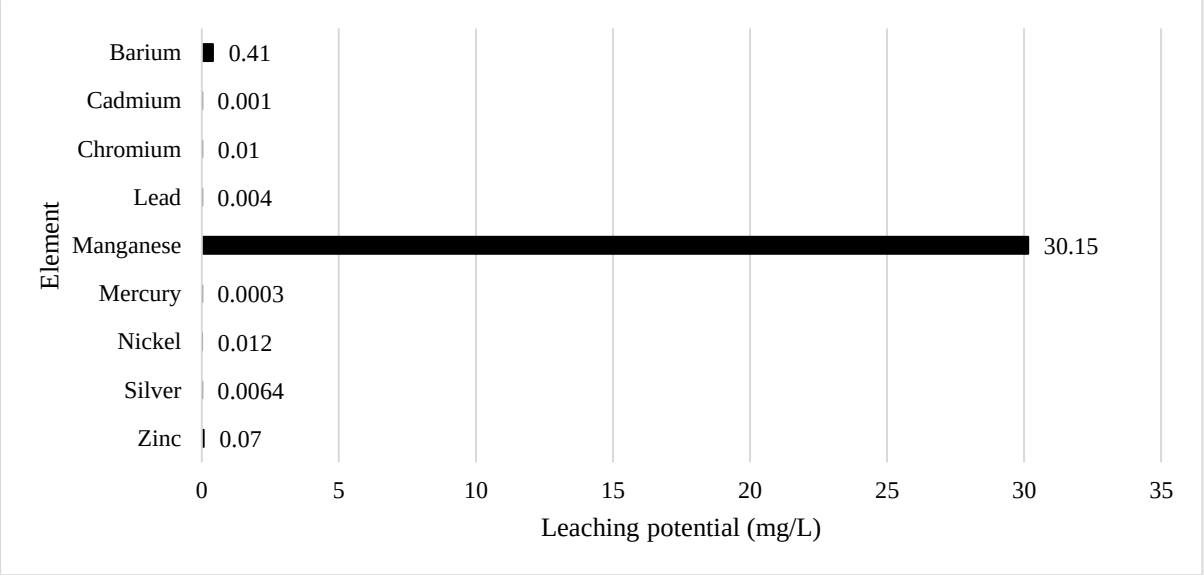


Figure 2-7: Average TCLP) of BOF-S (Proctor *et al.*, 2000)

2.3.4.2.2 Primary Physical Characteristics of BOF-S

BOF-S has three structures, namely supercooled liquid, glassy or crystalline (solid) (Mills, Yuan and Jones, 2011), each of which have different porosities and structural characteristics. The physical properties of slag depend on the chemistry (discussed previously) as well as the method of cooling. Slow cooling generates crystalline slag whilst quenching generates a vitreous/glassy slag. In addition to influencing the structure of the slag, the cooling mechanism and speed also influences the size of the slag crystal – slow cooling will generally produce slag with particle size <100 mm and extreme slow cooling will produce slag of particle size <300 mm (Euroslag, 2012). Air-cooled slag (produced by allowing the molten slag to cool under atmospheric conditions) results in a porous and low-density

substance with particular physical properties that make the slag suitable for certain reuses. If the slag is cooled under atmospheric conditions it tends to be hard and dense, making it suitable for reuse in concrete products and other construction applications (Indian Bureau of Mines, 2016).

The particle density of BOF-S can be between 2.5 g/cm^3 and 3.6 g/cm^3 (Grubeša *et al.*, 2016; Euroslag, 2017). BOF-S has high specific gravity, mechanical strength, and abrasion resistance (Ko, Chen and Jiang, 2015). In Table 2-2 the average values for some physical properties of BOF-S are given (Li, 1999; Xue *et al.*, 2006; Euroslag, 2017)

Table 2-2: Physical Properties for BOF-S (Xue *et al.*, 2009)

Binder Adhesion (%)	**Polishing stone value (%)**	**Crushing Value (%)**	**Pile Density (g/cm^3)**	**Bulk Density (g/cm^3)**	**Compressive Strength (N/mm^2)**	**Impact Value (%)**	**Water Absorption (%)**	**MOHS Hardness**	**Los Angeles Abrasion Loss (%)**
>95	57	12	1.92	3.29	200	17	1 – 1.18	7	13.1 - 17.6

Although variable to an extent, the physical and chemical properties of BOF-S are highly relevant, as they determine what type of reuse the slag will be suitable for. These reuses are discussed below.

2.3.5 Uses of BOF-S

Steel Slag reuse generally falls into three main areas of application (Piatak, Parsons and Seal, 2015):

a. Slag as a construction material,
b. Metal recovery from slag
c. Slag use in environmental remediation applications

All uses are discussed according to the above three application areas. Some applications of slag have the potential to detrimentally affect the environment in which they are used, but if done in a controlled manner (i.e. flowrate controlled, residence time controlled, leaching media controlled etc.), none of the components should pose a risk to human or environmental health or groundwater drinking sources (Proctor *et al.*, 2010).

2.3.5.1 Slag as a construction material

2.3.5.1.1 Hydraulic/Cement binder

The use of BOF-S as a raw material for cement production is environmentally, economically and technically viable and desirable to the cement industry, as it has the potential to reduce material consumption, energy costs and waste storage areas (Carvalho *et al.*, 2017). BOF-S as a cement additive is a common reuse for the steel mill by-product with 5 –10% of slag being reused in this manner per tonne that is produced worldwide (Carvalho *et al.*, 2017). Due to regulations however, some countries

still do not allow for large portions of the waste to be used in cement production. Countries such as Brazil use only 2% of their BOF waste as a cement binder (IAB, 2016).

The use of slag as a partial replacement for binder in cement, depends largely on the mechanical properties of the slag. The chemical composition of BOF-S is generally an indication of its mechanical strength. The higher the basicity or alkalinity content of the slag, the better the hydraulic properties tend to be (Akin Altun and Yilmaz, 2002). If the alkalinity is > 1.8, it can be considered as cementitious material (Xuequan *et al.*, 1999). An experiment conducted in Turkey and measured in accordance with the Turkish cement standards, indicated that a Portland cement mixture with a 30% addition of BOF-S had a compressive and bending strength comparative to normal (100%) cement mixtures after 2, 7 and 28 days (Akin Altun and Yilmaz, 2002). Experiments showed that slag with low MgO content was ideal for use in cement mixtures as the MgO was found to retard the initial hydration of cement and increase the setting time of the mixture (Akin Altun and Yilmaz, 2002).

Use of BOF-S as a cement binder is an established method of reuse, but research is still being conducted regarding: (i) ways to improve the cementitious qualities of the slag, and (ii) ways in which the addition of BOF-S changes the properties of cement (Li *et al.*, 2013; Wang, 2016; Xiang *et al.*, 2016; Zhao *et al.*, 2016; Lu *et al.*, 2018; Olsson *et al.*, 2018). In a recent study, the rheological qualities of cement were changed by the addition of BOF-S, which resulted in the mixture requiring less water to initiate flow in cement pastes (Calmon *et al.*, 2013). Another study showed that the cementing properties of quenched slag products were improved (when compared to non-quenched products) due to the hydration of dicalcium silicate and had considerable strength improvement after 28 days of water curing (Reddy, Pradhan and Chandra, 2006). Studies such as these indicate that the use of BOF-S as a partial or total replacement for cement binder is not only beneficial for the steel industry in terms of waste recycling and reuse, but also for the cement industry as it could add structural benefits to the cement and lower the water requirements.

2.3.5.1.2 Concrete Aggregates

Due to increased environmental concerns and more restrictive regulations in some countries (China and India), a substitute for sand and gravel as natural aggregate use in the civil construction and concrete industries is highly sought after (Somvanshi, 2015; Wang, 2016). Since more than 15 million tons of natural aggregate resources like gravel, limestone and other rocks are used annually, the search for natural aggregate replacement has become an important and urgent issue (Ding *et al.*, 2017). Like steel, concrete is a major construction material, reportedly the most widely and extensively used man-made material in the world (Brito and Saikia, 2012). This large scale production of concrete has many negative environmental effects, some of which arise from the concrete industry's use of natural stones as aggregates (Brito and Saikia, 2012).

Concrete comprises of three major fractions, namely aggregate, binder and water – aggregate constitutes approximately 75 % of the total concrete volume and therefore plays a vital role in the performance of the final concrete product (Brito and Saikia, 2012). Concrete properties such as workability, strength, dimensional stability and durability are all, in part, due to the quality and characteristics of the aggregate used. Conventional concrete contains sand as fine aggregate and gravel (in various sizes) as coarse aggregate. Materials that are used as aggregates are mined, and this process as well transporting the aggregate to the cement plant, are both fuel and labour intensive (Ayenagbo *et al.*, 2011). For this reason, the use of waste materials as an aggregate is an attractive alternative to traditional aggregate avenues.

BOF-S is an example of a waste material that has shown potential for use as an aggregate substitute in concrete. The physical properties of slag (Table 2-2), are highly comparable to those of natural aggregates. The California bearing ratio, compressive strength, and Mohs' scale of hardness value of slag are even reported to be better than that of natural aggregate (Ding *et al.*, 2017). In addition to this, the Toxicity Characteristic Leaching Procedure (TCLP) test showed that there are no toxic materials which exist in BOF-S that can be classified as general industrial waste (Yildrim and Prezzi, 2009). The bulk density of BOF-S qualifies it for use as a construction material and the L.A. Abrasion and crushing indices indicate that BOF-S has good crushing and abrasion resistance. These qualities, amongst others, make it suitable for use in concrete (Maslehuddin *et al.*, 2003; Manso *et al.*, 2006). When compared to limestone and basalt, a BOF-S mix showed comparable results for fatigue life, low temperature cracking resistance, water sensibility (damage due to water freezing and thawing cycles), and high temperature stability (Xue *et al.*, 2006).

A drawback that has been reported in the use of BOF-S as an aggregate is that it contains many hydratable oxides (shown in Table 2-1). These can result in volumetric instability or expansion – a characteristic not allowable in concrete aggregates for safety and structural soundness.

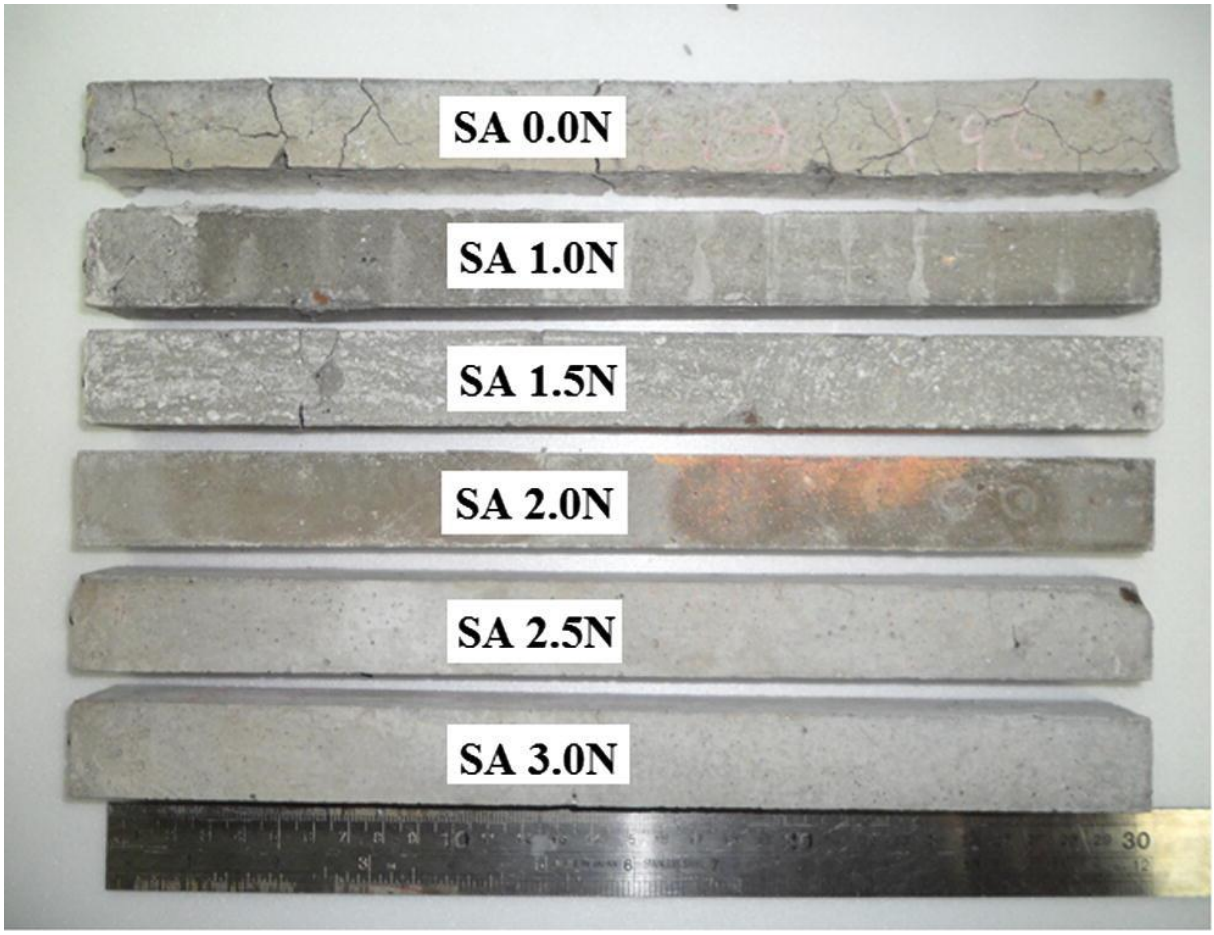


Figure 2-8: Concrete mixtures made with BOF-S that had been chelated with oxalic acid after four days steam curing process *[photograph by Ding (2017)]*

This remains an issue and studies are currently underway that aim to remove or lower the free lime content of the slag before use as a concrete aggregate. By reducing the hydratable oxide content through attrition and chelating processes (using oxalic acid as a chelating agent), the volume expansion of BOF-S decreases from 4.7 % to 2.8 % (approximately a 40 % volume expansion reduction). Aside from possible volume instability, the physical and mechanical properties of cement mortars made with BOF-S has great potential as a civil construction resource (Ding *et al.*, 2017). A depiction of the effect of volume instability is shown clearly in Figure 2-8, where different concentrations of oxalic acid were used to chelate the BOF-S prior to preparation of the concrete mixture. Sample SA 0.0N contained slag that was not pre-treated at all and the subsequent samples (from top to bottom) show samples which received increasing pre-treatment. Understandably, volume instability is a major issue in the reuse of slag in cement, concrete and road filler and more research is needed to combat this.

2.3.5.1.3 Road filler

BOF-S aggregates show many favourable technical and environmental characteristics, especially in comparison to natural stone aggregates. In addition to being suitable for concrete aggregate reuse, this also makes them potentially valuable road construction materials. BOF-S-bitumen mixes have shown

better structural and resilient characteristics than mixes with natural aggregates. These characteristics include rutting resistance, bonding and moisture damage resistance and stripping resistance.

Assessments made on a 2 km long and 24 m wide BOF-S and asphalt test road, showed that a road with natural aggregates replaced by BOF-S performs as well as a conventional asphalt pavement (Xue *et al.*, 2006; Kambole *et al.*, 2017). After nearly 2 years, the slag-asphalt section showed no signs of any rutting, cracking or stripping. The performance of a porous asphalt and BOF-S mixture was evaluated and showed a higher Marshall Stability, lower abrasion, and a better stripping and rutting resistance than that of equivalent crushed stone and asphalt mixtures (Shen, Wu and Du, 2009). Tensile strength measurements made on all the mixtures also exceeded the minimum requirements. Furthermore, slag asphalts exhibited sound absorption characteristics which could have potential benefits in reducing traffic noise generated from tyre-road interactions. Other similar studies that were conducted suggested that the replacement of natural aggregate with steel slag in paving mixes should be done for either the fine or the coarse aggregate fraction but not both (Asi, Qasrawi and Shalabi, 2007). This is due to the fact that if slag is used to replace both the coarse and fine aggregate components the mix is likely to have a lot of air voids necessitating the use of high quantities of bitumen which in turn could lead to bulking and flushing problems in the road pavement.

In some countries road specifications do not cater for slag reuse which results in limited BOF-S reuse. This is likely due to pavement performance problems that arise from some chemical constituents in some slag. Free calcium and magnesium oxides which are present in large quantities in slags, react with water, resulting in large volume expansions which can in turn lead to structural and failure when used in roads (volume stability issues as discussed above). Thus, hydration treatment or other chelating treatment before use as road aggregates must be undertaken to ensure allowable expansion (Kambole *et al.*, 2017).

2.3.5.1.4 Glass-Ceramics

The manufacture of glass-ceramic materials has been a potential route for BOF-S commercial re-use for the past 16 years (Ferreira, Zanotto and Scudeller, 2002) and has grown in importance due to the increase in slag production (Karamanov *et al.*, 1994; Romero and Rincón, 1999). Glass-ceramics produced using BOF-S exhibit good fracture strength, chemical resistance and aesthetic appeal suitable for wall and floor tile application (Ferreira, Zanotto and Scudeller, 2002). Methods for reuse in this manner are discussed below.

2.3.5.1.5 Thin film transistor liquid crystal display recycling

Thin film transistor liquid crystal display (TFT-LCD) is a type of LCD used in televisions, computer monitors, mobile phones and navigation systems (Lin *et al.*, 2009). Recent developments in the field of information technology (IT) have led to a considerable increase in the demand for TFT-LCD panels and in 2013 the demand for TFT-LCD was estimated to be 364 million m^2 (panel area) (Jang *et al.*,

2014). In conjunction to this, the Environment Agency classified LCD waste as 'hazardous' in 2010 (Environment Agency, 2018), and multiple waste regulation schemes have been put into place in an attempt to manage the production, storage and recycling of this waste. A prediction of LCD waste production (as per display area) compared to the amount of LCD waste produced in 2011 is shown in Figure 2-9.

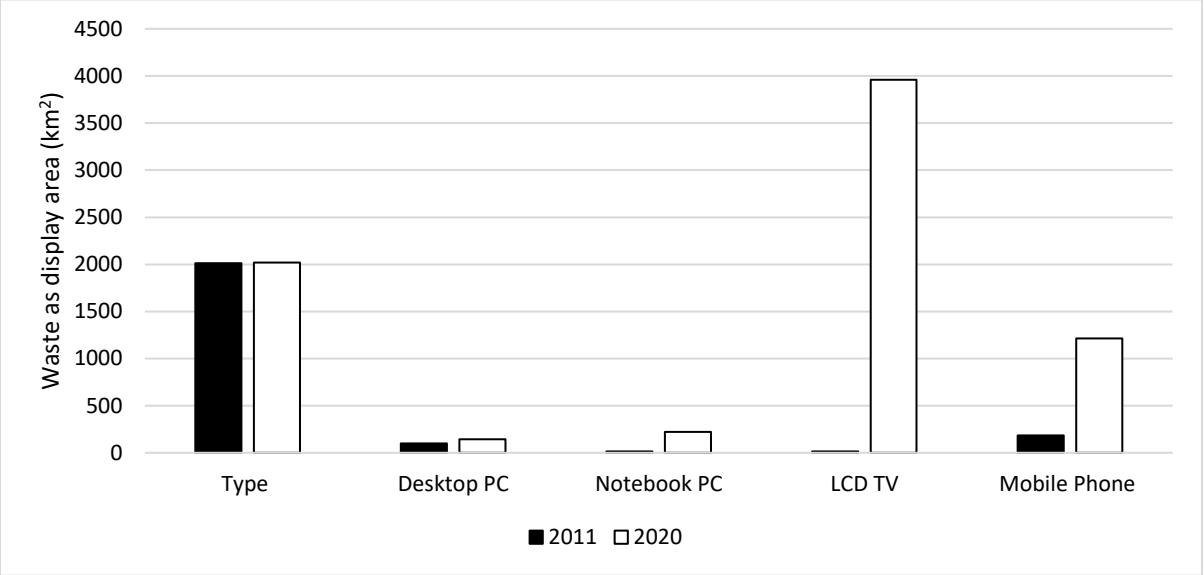


Figure 2-9: Waste quantity prediction of LCD in China using the market supply method and comparing to waste quantity produced in 2011 (Liu *et al.*, 2015)

As shown, waste quantity is growing exponentially, with LCD TV waste predicted to increase almost 260 times over 9 years. Many studies aiming to find a feasible reuse or recycling avenue to reduce this waste production are thus currently underway (Fan and Li, 2014).

Success has been reported in combining this waste material with BOF-S to produce CaO–MgO–Al_2O_3–SiO_2 (CMAS) glass-ceramic products via vitrification and heat treatment methods. Tests with a TFT-LCD waste glass to BOF-S ratio of 7:3 and an added 20 wt% of MgO, resulted in a produced ceramic that exhibited optimal composition in terms of flexural strength and electrical insulation. This glass-ceramic had a primary crystalline phase of anorthite ($Al_2CaSi_2O_8$) and contained diopside ($MgCaSi_2O_6$). due to the presence of excess MgO. The resulting product had a flexural strength of 140 MPa and a dielectric constant in the range of 10–12 at 1 MHz. Both these values meet the criteria for glass ceramics that are used as insulating glass (Fan and Li, 2014), meaning this method could potentially reduce both the TFT-LCD waste glass and BOF-S waste reserves.

2.3.5.1.6 BOF-S

Multiple studies have explored the suitability of BOF-S as a glass-ceramic material. BOF-S with higher iron and lower silicon dioxide content than traditional slag was used to obtain glass-ceramics using an open hearth furnace (Kislitsyn, Sas and Golius, 1981; Ferreira, Zanotto and Scudeller, 2002). Their

design incorporated 60 wt% of BOF-S added to sodium nitrate at temperatures between 1450 ℃ and 1470 ℃. Crystallization occurred after treatment, between 800℃ and 1000 ℃, and all glass produced showed internal crystallization. Cr_2O_3 was required to enhance nucleation and avoid deformation. Physical properties of the product were reportedly as good as those of commercial BFS glass ceramic. Different quality glass-ceramic was produced from a process using 60 wt% slag, 35 wt% commercial grade sand (to increase the SiO_2 composition) and 5 wt% Na_2O. The product reportedly exhibited a high degree of crystallization and a marble like appearance (Ferreira, Zanotto and Scudeller, 2002). With appropriate adjustments (such as treatment temperatures), BOF-S can be used to produce glass-ceramics with high standards and an attractive appearance, suggesting that it would be suitable for a range of applications in the construction/building industry (Ferrerira, Zanotto and Fredericci, 2000).

2.3.5.1.7 BOF-S as an additive in antimicrobial mortar/alkali activated cement

Microbial induced corrosion of concrete (MICC), cement or epoxy-based pipes is a costly yet common occurrence in many urban centres around the world (Vasil, V., Lapšev, N., Stolbichin, 2013; Wu, Hu and Liu, 2018). A substantial number of underground water transfer mechanisms involve the use of pipes or sewers made from partially from concrete or cement, which are responsible for safely transporting wastewater away from homes and buildings for appropriate treatment. Over the last century, there have been considerable investments in this wastewater infrastructure, however due to the sheer volume of pipes contained in this network, monitoring is scarce and substantial corrosion has occurred at many sites (Hernandez, 2018). Pipes which allow for the flow of microbially rich waters (sewage pipes, wastewater pipes) generally exhibit anaerobic conditions in many areas, giving rise to the formation of hydrogen sulfide gas (H_2S) through various biological processes. This gas forms sulfates and acidic H^+ ions upon oxidation which in turn can cause severe damage to the structure and appearance of the pipes. This has been confirmed in studies where the examination of pipe materials exhibiting various extents of degradation revealed the presence of biogenic sulfuric acids (Mori *et al.*, 1991; Valixa *et al.*, 2012; Jiang *et al.*, 2016). Engineers have been unable to find feasible and effective methods to control systemic corrosion, which is rapidly consuming this infrastructure – and most rehabilitation and prevention technologies focus on applying acid-resistant materials instead of targeting the acidogenic microbes responsible for the process. Recent research, however, suggests that BOF-S could offer a viable solution. Formulations of novel cementitious mixtures known as alkali activated cements (AAC's) are less permeable to water and chlorides and more resistant to corrosive media (chlorides, acid) than conventional ordinary Portland cement (OPC) (Shi, Jiménez and Palomo, 2011). Cements spiked with BOF-S have shown a significant reduction in surface microbial activity and corrosion. AAC's made with 66% metakaolin (MK) and 33% BOF-S can be used as a base for AAC (Gevaudan *et al.*, 2019) but any amount of slag can be used to dose the cement mixture with varying results. One study that assesses this phenomenon shows BOF-S (or more specifically the metals present within BOF-S) acting as a microbial inhibitor (Hernandez, 2018).

2.3.5.2 Metal Recovery

2.3.5.2.1 Magnetic metal recovery

Steel slag (BF-S and BOF-S) usually goes through a metal recovery process prior to application outside of iron and steel works. In general, the recovery process includes crushing or grinding, screening, magnetic separation, and removal of phosphorus (Gavrilovski, Radossavljevic and Milic, 1996; Yi *et al.*, 2012). There is a variety of different metals that can be extracted from the slag.

2.3.5.2.1.1 Vanadium

In addition to volume instability issues, BOF-S also contains small amounts of vanadium (Figure 2-2). For use as a construction material, different countries have different vanadium allowance levels for BOF-S. According to Swedish standards for example, it is expected that for use in the cement industry and for road construction the vanadium content of slag should be lower than 0.1 % by mass and 0.3 % by mass, respectively (Lindvall, Rutqvist and Ye, 2010). The potential value of vanadium in discharged BOF-S annually amounts to more than US$ 100 million (Ye, Kärsrud and Lindvall, 2011), and thus recovery of vanadium from slag is beneficial for two reasons: (i) it results in increased reuse potential of BOF-S and (ii) it can generate income. It has been demonstrated in a pilot scale experiment which treated 13 tonnes of BOF-S, that recovery of Vanadium of up to 98% can potentially be achieved using a two-step reduction procedure. Carbon based reductants were used as a pre-reduction step and a final reduction was achieved by means of injection of ferrosilicon and/or aluminium powder. The obtained reduced slag had a low vanadium, iron, phosphorus and chromium content which made it suitable for other uses. The V, Fe and Cr were extracted into a metal phase using this method (Lindvall, Rutqvist and Ye, 2010).

2.3.5.2.1.2 Iron

Magnetic separation is used for separating metallic iron and iron minerals from the slag using magnetic machines (cross-belt magnetic separator, drum magnetic separator and magnetic- pulley separator) (Alanyalı *et al.*, 2006). To improve magnetic separation efficiency, the classification of slag fed to magnetic separation is carried out. A single or double-deck vibrating screen is used for this process. It is possible to produce steel scrap (Fe: 90%) and iron concentrate (Fe>55%) from slag using this method (Shen and Forssberg, 2003).

2.3.5.2.1.3 Other metals

BOF-S contains a number of other elements, but recovery of metals such as Cu, Al, Pb, Zn, Co, Ni, Nb, Ta, Au, and Ag is not performed [recovery of these metals generally occurs in incineration, stainless steel and non-ferrous slag (Shen and Forssberg, 2003)].

2.3.5.2.2 Neutralizing agent in bioleaching processes

Bioleaching is an effective and relatively simple technology used for the extraction of metal species from their ores using the functioning of living organisms, generally bacteria, and their various associated reactions (Bosecker, 1997). The technology is widely used to recover or remove metals from

mine ores (Pradhan *et al.*, 2008), but has also recently been increasingly applied to the recovery of metals from solid waste materials such as ore, mine tailings, electronic waste, and sediment (Zhu *et al.*, 2011). Bioleaching is low cost, simple, safe and has the potential to be environmentally friendly (Chen and Lin, 2009).

The microorganisms that are used in bioleaching processes are chemolithotrophic [(using CO_2 as their principle source of carbon and obtaining energy by oxidizing inorganic compounds (Lewis, 1998)] and acidophilic (thriving in acidic media). These bacteria generally have optimum activity at a pH of approximately 1.5. In highly acidic solutions (pH < 1.5), the addition of neutralising agents is required to maintain the desired pH and ensure bacterial functioning (Sekhar, Lucelinda and Sandström, 2009). The neutralisation of the acid produced during bioleaching processes is generally done via the addition of limestone at three different stages of the process (neutralisation is required at multiple stages): (i) primary neutralisation to a pH of 1.5 using limestone for bioleaching to occur, (ii) secondary neutralisation to a pH between 3 and 4 using lime for precipitation of iron and arsenic, and (iii) neutralization to a pH between 7 and 8 for overall effluent neutralisation. The cost of this neutralisation is normally the second largest operational cost in bioleaching plants (mainly due to transportation) and thus research is continuously being conducted to determine if other, more cost-effective options, would be viable.

BOF-S has recently been used with success to effectively neutralize the entire bioleaching process of a pyrite concentrate. The study showed that BOF-S had a high neutralisation capacity and did not negatively impact the bioleaching process, despite the presence of vanadium found in the slag. The amount of slag used in the reaction resulted in a higher pH than desired – testament to how alkaline the BOF-S is. Taking this into account, much less BOF-S may have been needed to reach the pH of 1.5 and this, in conjunction with having achieved a higher pyrite oxidation than that of lime, makes BOF-S a good substitute for bioleaching neutralization reagents. The study proved BOF-S to be a functional alternative to limestone for pH control in bioleaching operations (Sekhar, Lucelinda and Sandström, 2009).

2.3.5.3 Environmental Remediation Applications

2.3.5.3.1 Waste stabilization

BOF-S can stabilize or solidify carbon steel electric arc furnace (EAF) waste. The dust that is produced from the EAF often contains hazardous metals such as lead, cadmium, chromium or zinc and these waste products need to be immobilized before being considered safe or benign. Geopolymeric reagents such as sodium hydroxide, potassium hydroxide, sodium silicate, potassium silicate, kaolinite, metakaolinite and BF-S have been studied to immobilize this waste and the stabilization/solidification of the dust was determined using compressive strength values and testing for leachability. In both cases the geopolymer systems performed better than traditional systems and as such show promising results

in the stabilization/solidification technology. Due to its high silicate and hydroxide content, BOF-S is a possible reagent in this immobilization technology although research has only been carried out that confirms heavy metal immobilization in this dust through the use of geopolymerization using BF-S (Pereira, 2009).

2.3.5.3.2 Carbon capture and storage/sequestration

Carbon capture and storage (CCS) is a process made up of three main steps: the separation of CO_2 from gaseous waste streams, the transport of the separated CO_2 to storage locations, and the long-term isolation of CO_2 from the atmosphere. There is growing interest in CCS around the world due to heavy dependency on fossil fuels, and it is viewed as a method that will allow CO_2 emissions to be managed. BOF-S can reportedly be used in mineral carbon sequestration technology, a type of CCS which is based on the process of natural rock weathering. During this process, carbonic acid is generated through the dissolution of CO_2 in rainwater. This acid is then neutralized with mineral alkalinity to form carbonate minerals (Lackner *et al.*, 2002; Huijgen and Comans, 2003; Bobicki *et al.*, 2012). The carbonate minerals which form are stable and will remain in the solid state. Mineral carbonation reactions are exothermic and occur spontaneously via the reactions listed below (Huijgen and Comans, 2003; Working group III of the IPCC, 2005; Bobicki *et al.*, 2012):

$$CaO + CO_2 \rightarrow CaCO_3 \quad (+ 179\ kJ/mol)$$

Equation 2-14

$$MgO + CO_2 \rightarrow MgCO_3 \quad (+ 118\ kJ/mol)$$

Equation 2-15

$$CaSiO_3 + CO_2 \rightarrow CaCO_3 + SiO_2 \quad (+ 90\ kJ/mol)$$

Equation 2-16

$$Mg_2SiO_4 + 2CO_2 \rightarrow 2MgCO_3 + SiO_2 \quad (+ 89\ kJ/mol)$$

Equation 2-17

$$Mg_3Si_2O_5OH_4 + 3CO_2 \rightarrow 3MgCO_3 + 2SiO_2 + 2H_2O \quad (+64\ kJ/mol)$$

Equation 2-18

The oxide and hydroxide components that react with CO_2 are all found in abundance in BOF-S.

Aqueous carbonation of steelmaking slags has been studied by many researchers (Huijgen, Witkamp and Comans, 2005; Bonenfant *et al.*, 2008; Lekakh *et al.*, 2008) and carbonation can be accomplished successfully. At ambient conditions, 24.7 g of CO_2 was captured using 100 g of slag and at elevated temperatures approximately 74% of carbonate conversion occurred (Huijgen, Witkamp and Comans, 2005). The extent of carbonation achieved in these experiments depended primarily on the elemental

and mineral composition of the slag. As shown in the reactions above, slags with a higher oxide content are more reactive (especially if the calcium oxides are present rather than silicates). Slag containing a high percentage of free calcium in oxide form can form carbonates more readily than slag which has its calcium present in silicate compounds. Generally, however, the calcium content of BOF-S makes it an ideal candidate for mineral carbon sequestration. It is estimated that steelmaking slags (including BOF-S) could store up to 171 Mt of CO_2 every year worldwide (Eloneva *et al.*, 2008), which is approximately 0.6% of global CO_2 emissions from fuel combustion (International Energy Agency 2010). Temperature and pressure were also important variables, as well as particle size. Smaller slag particles carbonate significantly better and faster than larger ones.

According to these studies, if this technology is correctly implemented, it could potentially reduce CO_2 in the atmosphere, reuse BOF-S wastes and create energy (due to exothermic nature of the reactions) simultaneously. One drawback of BOF-S use for CCS (as mentioned above) is that they have to undergo comminution to be suitable for mineral carbon sequestration. This can be energy intensive.

2.3.5.3.3 Mitigation of landfill gas emissions

Landfilling of waste is considered unsustainable and much effort is being made to reduce the amount landfilled annually, however it remains the primary waste management technique in the USA and many other countries. Of the 258 million tonnes of municipal solid waste (MSW) generated in 2014, about 136 million tonnes was landfilled in the USA (USEPA, 2016) – meaning more than half of the MSW that is produced, is landfilled. MSW in landfills undergoes anaerobic decomposition which produces methane (CH_4) and carbon dioxide (CO_2) as by-products. Gas collection systems are employed at many landfill sites to reduce gas emissions, but emissions which are not targeted by these systems escape into the atmosphere – landfills are thus large anthropogenic sources of CH_4 and CO_2. The landfill cover soil plays an important role in mitigating emissions as it is responsible for microbial oxidation of CH_4 to CO_2 (thereby reducing the CH_4 emissions to atmosphere). In recent years, biochar as an organic amendment has shown promise in enhanced microbial oxidation in landfill sites, and success has been reported in converting substantial amounts of CH_4 to CO_2 (Reddy *et al.*, 2018). However, this CO_2 still escapes into the atmosphere in undesirable amounts and this emission must now be controlled (Reddy *et al.*, 2018; Reddy, Grubb and Kumar, 2018).

BOF-S has shown promise in this regard, due to its high alkalinity and carbonation potential (as discussed). Batch experiments have been undertaken to assess the performance of this application and the results have shown carbonation in the range of 53-68 mg CO_2/g BOF-S after 24 hours. Further studies are being performed to analyse the carbonation mechanism and evaluate the effects of various system parameters on carbonation capacity of BOF-S (Reddy *et al.*, 2018).

2.3.5.3.4 Wetland Applications

Constructed wetland (CW) technologies were developed in the 1970s as an alternative ecological method for wastewater treatment (Kadlec, 2009). The most significant design parameters of constructed floating wetlands are: (i) the type of vegetation that will be present, (ii) the percent of vegetation coverage, (iii) the growth media, (iv) the depth of the wetland, and (v) methods for achieving buoyancy. Applications of BOF-S in this field have been successful and the use of slag in this regard contributes to both the treatment of contaminated water and the reduction of waste materials. It is able to act as a stable support medium for vegetation, as well as effectively reduce acidity levels in the wastewater (Sheridan *et al.*, 2012). BOF-S wetland applications are discussed below.

2.3.5.3.4.1 Phosphate removal

Rapid cooled basic oxygen furnace slag (RC-BOF-S) is derived from a new slag process called Baosteel Slag Short Flow, which involves treating molten steel slag with compressed air and cooling water (Wang and Chen, 2016). This treatment method lowers the calcium content in the slag, allowing it to maintain a lower pH and have a higher affinity for phosphate adsorption (Park *et al.*, 2016). This was tested in a small-scale CW consisting of horizontal flow beds packed with 75% coarse sand and 25% RC-BOF-S (filter media). Phosphate adsorption by RC-BOF-S was reportedly rapid in the first 30 minutes and followed a pseudo-second-order kinetic model. Phosphate adsorption capacities of RC-BOF-S under different pH levels were 3.57 mg P/g for a pH of 5; 2.47 mg P/g for a pH of 7 and 1.46 mg P/g for a pH of 9. RC-BOF-S with a particle size of between 0.8 mm and 2.3 mm demonstrated a 23% higher phosphate adsorption than RC-BOF-S with a particle size between 2.3 mm and 4.6 mm (Park *et al.*, 2017). Adsorption of phosphate ions was dominated by the metal oxide content in the slag and the addition of the slag is predicted to increase the longevity of the CW from 292 days to 1349 days (Park *et al.*, 2017). The study confirmed BOF-S as a wetland additive for treating phosphate rich waters.

2.3.5.3.4.2 Constructed Floating Wetlands

In natural floating wetlands, self-buoyancy occurs either by the entrapment of gases within the mat (frame) or by air spaces that occur between the roots (Hogg and Wein, 1988) (

Figure **2-10**). A great number of alternative technologies have been tested to ensure that the floating frame has buoyancy, and there are many patented mats which are commercially available in parts of Europe and the USA (Pavlineri, Th and Tsihrintzis, 2017). These mats are constructed from buoyant materials and have a series of holes that are essential for plantation of wetland vegetation.

One concept, which combines dredged lake sludge, BOF-S and expanded perlite [siliceous volcanic rock that is expanded up to 20 times its original volume when heated (Rashad, 2016)] in order to achieve flotation has been introduced to this field and has since shown success (Hu *et al.*, 2010; Pavlineri, Th and Tsihrintzis, 2017).

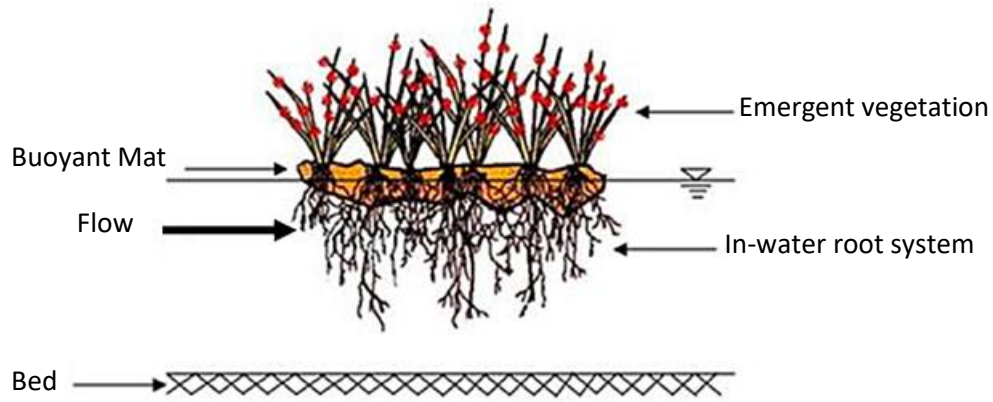


Figure 2-10: Schematic of Vertical Section of Constructed Floating Wetlands (Pavlineri, Th and Tsihrintzis, 2017)

The optimum mixing ratio of the three components to achieve a floating bed was 72.5% dredged sludge, 15% expanded perlite and 12.5% BOF-S. With this configuration (and using Sweet Flag (*Acorus calamus)* as the type of vegetation) minimal leaching was observed and a maximum removal of 36.3% total nitrogen (TN), 35.7% total phosphorus (TP), and 44.3% ammonium nitrogen achieved. The growth of the vegetation (by relative growth rate) was reported to be 0.31.

A similar study conducted by Sheridan et al. (2012) used BOF-S as the sole constructive material for a CW bed matrix designed to treat AMD (using Arum-lily (*Zantedeschia aethiopica)* and Paper Reed (*Cyperus papyrus)*). The bed matrix was effective at supporting vegetation and resulted in overall wetland functioning of 75% sulfate removal across the CW and a rise in pH from 4 and 1.35 to between 6 and 7 (Sheridan *et al.*, 2012).

2.3.5.3.5 Soil enrichment and treatment

2.3.5.3.5.1 Fertilizer

BOF-S was officially approved as an ordinary lime fertilizer in 1981. Steel manufacturers currently supply BOF-Ss to be used as silicate, lime and phosphate fertilizers as well as special fertilizers containing iron (Horii, 2015). BOF-S has been reported to contain over 20% silicic acid (which of all the other components in slag, has the most potent fertilizer effect), and because of this can be used a raw material for silicate fertilizer (Ito, 2015). Experiments conducted on rice plants have shown growth improvements of over 1000 % (determined by measuring the difference in nitrogen uptake). Silicic acid also reportedly enhances the quality and flavour of rice as well reduces the occurrence of certain plant diseases. The use of BOF-S as a fertilizer may become even more necessary in future due to possible nutrient deficient fields throughout the world (Japanese Society of Soil Science and Plant Nutrition, 2002). Sugarcane, corn, wheat, and barley also benefit from the presence of silicic acid fertilizer. Other components of the slag that can also benefit the soil structure and plant growth include (Ito, 2015):

1. Calcium oxide - neutralizes acidic soil, assisting with resistance of plants against pathogens. In addition, Ca makes the roots strong and promotes the absorption of potassium.

2. Magnesium oxide - assists with neutralization of acidic soil and promotes photosynthesis.
3. Phosphoric compounds - promote plant growth, stooling, root extension, blossoming, and fruit bearing.
4. Manganese - promotes photosynthesis.
5. Iron - assists with stabilizing sulfidic compounds in the soil by forming iron sulphide. This reduces the toxicity which has favourable effects on plant growth.

2.3.5.3.5.2 Wine grape irrigation water

Nutrition is a cost-sensitive issue in many vineyards. In recent years nutrient additives have increased in price by up to 80% (Proffitt and Campbell-Clause, 2012). Nutrition is an important part of managing a vineyard since it impacts vine growth, crop yield, berry composition, must and wine quality. BOF-S leachate has recently been used with intermediate success (research ongoing) as a nutrient additive for wine grape growth (Proffitt and Campbell-Clause, 2012; Lategan and Grubb, 2018). Macro and micro-nutrients needed in vineyards (calcium, magnesium, manganese and iron) are all contained in BOF-S and BOF-S leachate, thus the use of this by-product could potentially, substantially lower the cost of vineyard maintenance grape plant growth.

2.3.5.3.5.3 Treatment of contaminated soil

Marine oil spills have had detrimental impacts on both shorelines and seas in the past century due to the hazardous properties of oil (Lim, Lau and Poh, 2016). The toxicity of oil spills is of great environmental concern and is an issue which has been highlighted by multiple researchers (Tang *et al.*, 2011; Hentati *et al.*, 2013; El-Sheshtawy *et al.*, 2014; Kanarbik *et al.*, 2014; Ma *et al.*, 2014; Gao *et al.*, 2015). Soil contamination resulting from oil spills causes earthworm, plant and bacterial death which ultimately results in the destruction of habitats and ecological development (Hentati *et al.*, 2013; Ramadass *et al.*, 2015). Clean-up efforts for oil spills at present, require mechanical and labour-intensive methods but have many disadvantages and are considered costly and timely. Therefore, there is an urgent need to investigate other environmentally friendly remediation methods to remove oil contaminants in soil.

BOF-S used as a catalyst for oxidation of oil may be one such method. Different types of oxidants have been investigated for the remediation of oil contaminated soil via chemical oxidation reactions. These chemicals include hydrogen peroxide, Fenton's reagent, persulfate, peroxymonosulfate, permanganate, and ozone. Many oxidants have reportedly had negative impacts on the natural attenuation of the oil (by the soil) but use of BOF-S as a catalyst has rendered these impacts null. Tsai and Kao (2009) successfully used BOF-S as a catalyst to enhance Fenton-like oxidation for the remediation of petroleum-hydrocarbon contaminated soil. Results showed that BOF-S was much more effective than hematite and goethite as the Fenton-like catalysts – most likely due to the fact that BOF-S contains significant amounts of extractable iron. The iron oxide compounds naturally found in BOF-S (such as amorphous and soluble iron) allow for Fenton-like oxidation and have shown removal efficiency of

96% for fuel oil contaminated soil (Lim, Lau and Poh, 2016) and 76% in another similar study (Tsai and Kao, 2009).

2.3.5.3.5.4 Treatment of saline contaminated soils

Salinization caused by human activities (also known as secondary soil salinization), is a widespread occurrence caused by improper use of irrigation systems, poor drainage conditions and over-pumping of groundwater which leads to seawater intrusion (Askri *et al.*, 2016; Daliakopoulos *et al.*, 2016). Recently, it has been identified as a major threat to global food security - with an estimated 76 million hectares of land is currently affected around the globe (FAO and ITSP, 2015) and monetary set-backs anticipated to be as high as $300 per hectare (Munns and Gilliham, 2015). Saline soil is a term used to describe soils that have: (i) high salt content, (ii) high sodium cation content and/or (iii) high pH (frequently due to the presence of excess carbonate) (van Beek *et al.*, 2012). These soils are termed: saline, sodic and alkaline soils respectively. Soil salinization is considered a serious environmental issue as it can lead to the alteration and destruction of the natural biological and biochemical processes (Decock *et al.*, 2015; Smith *et al.*, 2015) and in arid coastal regions, can limit crop production, change soil structure and promote desertification. Due to these possible detrimental effects, preventative measures have been proposed in the Soil Framework Directive (Naidu *et al.*, 2015), but adoption of this framework has not been successful in some countries (Daliakopoulos *et al.*, 2016). Remediation of saline soils is thus highly relevant and research into methods by which rectification can be achieved are currently being explored (Li *et al.*, 2016; Swallow and Sullivan, 2019).

BOF-S has shown potential in this regard, and a study assessing the functionality of the slag as a sodium cation remover has been conducted. The study was conducted along the coastal region in Italy and involved a three-year lysimeter trial using both wheat and tomato crop areas which were treated with slag (Pistocchi *et al.*, 2017). Soil which was dosed with BOF-S was compared [in terms of exchangeable sodium percentage (ESP)] to soil which was not dosed. ESP is an expression of sodicity and is calculated as the percentage of exchangeable sodium with respect to Cation Exchange Capacity (CEC) (Chun-ming *et al.*, 2011). It is used to describe the risk associated with the level of sodium in the soil. If the ESP is >15%, the soil is classified as sodic (Güler *et al.*, 2014). In the study by Pistocchi (2017), soils which were enriched with 3.5 g of slag per kg of soil per year, resulted in a 40% decrease in ESP (and soils which were enriched with 2.7 g slag per kg of soil per year resulted in a 45% decrease in ESP (in comparison to the sodium content from unchanged soils) – a decrease which was attributed to slag competing with sodium for sorption sites within soil (Pistocchi *et al.*, 2017).

The study also resulted in an increase in calcium, magnesium and vanadium content of the soil which had a positive effect on the tomato crops (higher yield than when compared to the unchanged soil) but had an unfavourable effect on wheat production which was lower in the soil that was amended with slag. The study concluded that BOF-S was effective in lowering the ESP of soil, but could only be used

in certain crop areas (tomato or corn fields (Wang and Cai, 2006)) or precautions would be needed to avoid vanadium build up.

2.3.5.3.6 Thermal energy storage

Thermal Energy Storage (TES) is a breakthrough concept in industrial heat recovery applications and is an important technology to consider when using renewable energy to reduce energy consumption (J. Park *et al.*, 2019). TES systems can store surplus energy and release energy when supply is insufficient - effectively solving the gap between supply and demand of energy and combatting the irregularity in supply by renewable energy sources (Lin, Alva and Fang, 2018). A wide variety of potential heat storage materials have been identified and several materials have shown high potential (Alva, Lin and Fang, 2018) however, the main drawback in the development and implementation of these materials is their cost – which is generally very high. In this regard, use of waste materials and by-products lower the total cost of the storage system and concurrently valorise the waste industrial materials.

Metallurgical slags are an example of a suitable by-product for this application and have a high thermal stability range of up to 1200 °C, which allows for high operating temperatures and enables them to be used for a wide range of heat storage applications. EAFS and BOF-S have thus been identified as potential TES materials due to their thermophysical properties and research is currently underway that will determine their conditions of use. A recent study which compared BOF-S as a TES material to magnetite was able to show that BOF-S has an above average energy density (higher than EAF slag and lower only than magnetite) and an average thermal conductivity (Grosu *et al.*, 2018). The BOF-S would essentially replace molten salt (the material currently favoured for TES (Herrmann, Kelly and Price, 2004)), which would result in a substantial cost reduction of the storage system since BOF-S is a by-product from the steel industry that does not have clear applicability.

Due to its stability range, BOF-S is not only valid for current storage technologies (which can reach temperatures of up to and 565 °C), but can also be used for next generation powerplants where operation temperatures can reach up to 1000 °C (Gutierrez *et al.*, 2016). BOF-S may need to be subjected to some prior treatment before use in TES, but if correct parameters are identified and put into place, the reuse of the slag could potentially have strong environmental and societal benefits and could result in the reduction of BOF-S in landfills as well as reduction in greenhouse emissions.

2.3.5.3.7 Industrial water treatment.

Effluent waters from industrial processes may contain high concentrations of heavy metals, sulfate, phosphate, arsenic, lead and many other toxins and ions. Due to the absorptive and alkaline nature of BOF-S, it has exhibited effectiveness in treatment of saturated, contaminated waters and is thus ideally suited to be used in this kind of remediation.

2.3.5.3.7.1 Mine water

BOF-S is useful in acid mine drainage (AMD) treatment (Ziemkiewicz and Skousen, 1997; Ziemkiewicz, 1998; Ziemkiewicz, Skousen and Simmons, 2003; Skousen and Ziemkiewicz, 2005). The batch experimental study by Name and Sheridan (2014) which was done on synthetic AMD (synthesized to mimic the Witwatersrand gold basin AMD of pH 2.5 with composition of 5000 mg/L of sulphate and 1000 mg/L of soluble Fe(II)), showed a Fe(II) removal of 99.7% and a sulfate removal of 75% through the addition of BOF-S. The pH of the system increased to 12.1 in a reaction time of 30 min (Name and Sheridan, 2014). Similar studies using BOF-S leachate instead of BOF-S have shown removal of metals and sulfate (Figure 2-11) (Naidu *et al.*, 2018).

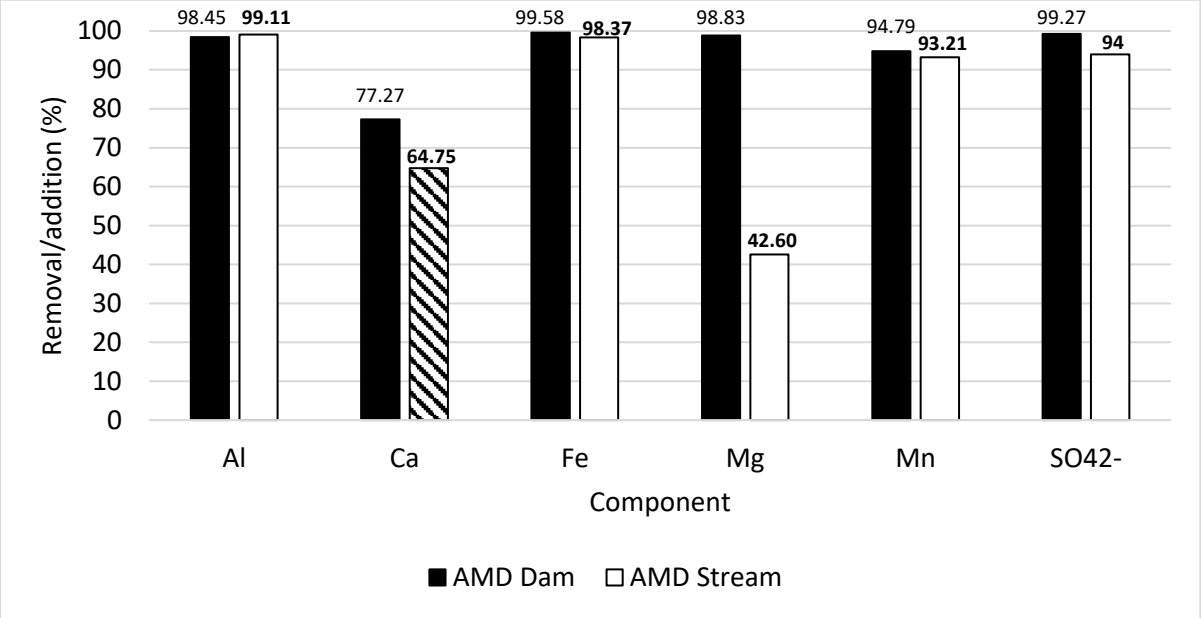


Figure 2-11: Percentage removal and addition of metals and sulfates between the inlet and outlet of the system using BOF-S leachate and sugarcane bagasse to remediate two types of severely polluted AMD, sourced from a dam and stream in Emalahleni, South Africa (patterned region indicates an increase) (Naidu *et al.*, 2018)

The results of Name and Sheridan's (2014) and Naidu et al's (2018 and 2019) experiments indicate that BOF-S is a candidate to replace lime in the remediation of AMD. A further study indicated that the process could have merit when implemented at a larger scale, with operation of a pilot scale system treating 200-1000 L/day showing Al, Fe, Mn and SO_4^{2-} removals of 97%, 87%, 100%, and 87% respectively (Naidu *et al.*, 2019). Other studies have produced comparable results. The production of drinking water and the recovery of valuable minerals from AMD using a mixture of BOF-S, lime and soda ash in a reverse osmosis system was evaluated and it was determined that more than 99% of all initial metals and 75% of initial sulfate could be removed (Masindi, Suhail and Abu-mahfouz, 2017). In addition to this the pH increased to above 8 and the hardness of the water was reduced. This treatment option has shown great potential to replace costly lime slaking plants that are generally used in South Africa.

The possibility of the metals that have precipitated leaching out due to the high created pH's and the method of metal recovery from the sediment sludge have been identified as future research opportunities for this treatment method (Kefeni, Msagati and Mamba, 2017). It is important to note that there is a limit to the removal of sulfate ions using BOF-S as a reagent.

2.3.5.3.7.2 Copper rich industrial waters

Industrial wastewater streams, rich in Cu from the dye, paint, printing, photography, paper, and petroleum refining industries are a major environmental issue, as these effluent streams often enter larger natural water bodies, polluting them and causing adverse effects on the surrounding ecological systems. Unlike organic contaminants, copper is not biodegradable and tends to accumulate in living organisms (Huang *et al.*, 2017). It is known to be toxic and carcinogenic and causes many diseases in animal and aquatic life. Hence, copper needs to be removed from industrial effluent prior to discharge in water streams.

There are many methods currently being researched that could provide means to remove copper from already polluted streams or directly from the effluent before entering into larger water bodies. The use of BOF-S as a reagent has shown promise by decreasing copper content via adsorptive removal. Results showed that in low concentrations of copper, 0.5 g of BOF could remove up to 1000 mg/L of copper adsorbate (Xue, Wu and Zhou, 2013). The copper or Cu(II) removal has the potential to reach 99.9% if the precipitation effect is used in conjunction with other adsorption techniques such as adsorption using activated carbon (Uzun and Güzel, 2000), fly ash, lignin or red mud (Ahmed and Ahmaruzzaman, 2016).

2.3.5.3.7.3 Trichloroethylene contaminated groundwater

Trichloroethylene (TCE) is a volatile and colourless liquid that is a common groundwater contaminant (Tsai, Kao and Wang, 2011; Dumas *et al.*, 2018). Belonging to the chemical group of chlorinated aliphatic solvents, TCE has been used in multiple industries as an industrial solvent, an extractant in the dry-cleaning industry and as a component in many consumables such as paint, polishes, lubricants and wood finishes (Agency for Toxic Substances and Disease Registery, 2006). Many countries have discovered many serious environmental problems due to the improper storage and disposal of TCE (Interstate Technology and Regulatory Council, 2005; Tsai *et al.*, 2008). TCE compounds have a stable chemical structure, low solubility and high densities; and thus, undergo slow degradation in environmental systems. They are quickly able to form impermeable layers at the bottom of aquifers or groundwater sources, creating longstanding sources of pollution (Fu, Dionysiou and Liu, 2014; Tang *et al.*, 2015). TCE has been linked to increased levels of toxicity in blood, liver and kidney, multiple types of cancer and has recently shown evidence of causing some kinds of respiratory diseases in animals (Dumas *et al.*, 2018).

BOF-S has shown potential in the treatment of TCE, acting as a catalyst to enhance Fenton-like oxidation of the contaminant (Matthaiou *et al.*, 2019). TCE concentrations in groundwater contaminated with TCE waste, dropped from 5 to 1.1 mg/L, and chloride concentrations increased from 0 to 2.7 mg/L after 60 min of reaction with BOF-S in the presence of H_2O_2 (Tsai *et al.*, 2010). TCE oxidation occurred at a greater rate at low pH's and hence acid needs to be present in the reaction (Tsai, Kao and Wang, 2011). The studies also demonstrated that BOF-S can be used to as a continuous catalyst supply and can practically be used via installation of the slag in a permeable barrier system to enhance oxidation. This catalysed reaction occurs due to the presence of measured amorphous iron and extractable iron in BOF-S. When these compounds dissolve, they release Fe^{3+} ions which act as a catalyst in the Fenton-like oxidation process (Tsai *et al.*, 2010).

2.3.5.3.7.4 Arsenic

Arsenic is one of the world's most pressing contamination issues (Fujita *et al.*, 2009). In many countries [Argentina, Bangladesh, Canada, Chile, China, Hungary, India, Japan, Mexico, Poland, USA (Cebrian *et al.*, 1983; Burkel and Stoll, 1999; Mohan and Pittman, 2007)] high levels of contamination are reported and serious health and environmental problems have occurred due to lack of treatment methods.

Most of the arsenic found in groundwater is naturally occurring, and dissolves into the water when soil, bedrock layers and groundwater come into contact. However, due to the increase in water usage and rapid suburban development, arsenic dissolution is increasing (Wisconsin Department of Natural Resources, no date). Acidic drainage from abandoned mines, tailing impoundments, and waste rock piles, contain high concentrations of sulfate and heavy metals and some tailings from gold mining operations contain high amounts of arsenic – adding to the already high concentrations of As in groundwater (Sung Ahn *et al.*, 2003). Remediation techniques and cost-effective treatment methods are continuously being researched in order to combat this problem.

Many of the countries listed above, also produce large amounts of steel slag per annum, which consist of elemental iron, iron oxides, calcium hydroxides, and iron calcium silicates. The surfaces of iron oxides are important adsorption sites for oxyanions such as arsenate, chromate and phosphate. Thus, due to its composition, BOF-S can potentially be used for arsenic treatment by acting as an adsorbent for the element and two studies have shown that it can effectively remove both As(V) and As(III) from waste water streams (Mohan and Pittman, 2007). If a technologically and economically feasible method of treatment using BOF-S can be constructed, many countries (having both BOF-S production and As pollution) would be in an ideal position to implement it.

There are currently several As treatment methods utilizing BOF-S that are being tested and optimized. One such method is that of enriching the slag with iron oxide before using it as a reagent to lower the arsenic content. After being converted into a more oxide rich compound, slag has shown successful

arsenic remediation. Zhang and Itoh (2005) synthesized a slag-based adsorbent that could be used for aqueous arsenic removal using this method. Loading of iron oxide onto slag can increase the surface area by 68%. This adsorbent effectively lowered the concentration both arsenate and arsenite in solution. Approximately 15 g of this slag was sufficient to remove 200 mg As (V) from 1 L of aqueous solution of industrial wastewater discharge and 65 g to remove As (III) from 1 L solution to meet the permissible limit (0.01 mg/L). Arsenic removal in this manner occurs via three processes: (i) affinity adsorption (which depends on surface area), (ii) reaction with iron oxides and (iii) reaction with calcium and other metallic elements initially contained in the slag. In the pH range of 2–7, As (V) may be removed through the reactions with iron oxides and other metallic elements present in the slag, shown in Equation 2-19, Equation 2-20 and Equation 2-21:

$$FeOOH + 3H_2AsO_4^- + 3H^+ = Fe(H_2AsO_4)_3 + 2\ H_2O$$

Equation 2-19

$$2H_2AsO_4^- + Ca^{2+} + nH_2O = Ca(H_2AsO_4)_2 \cdot nH_2O$$

Equation 2-20

The following reaction occurs at pH's of 9 to 11.

$$2H_2AsO_3^- + Ca^{2+} + nH_2O = Ca(H_2AsO_3)_2 \cdot nH_2O$$

Equation 2-21

In other studies, BOF-S reportedly was able to lower As concentrations to <0.5 from 25 mg/L in 72 h. High Ca concentrations and alkaline conditions induced by the BOF, are thought to promote the formation of stable, sparingly soluble Ca–As compounds that precipitate out of solution at high pH levels. Another study showed that when BOF-S was crushed to a particle size of >0.5 mm and continuously shaken, this drop in As concentration occurred after only 24 hours (Sung Ahn *et al.*, 2003).

2.3.5.3.7.5 Phosphorus

Phosphoric acid and its salts have important uses in detergents and fertilizers, often in the form of sodium tripolyphosphate or calcium phosphate which is processed from phosphate containing rocks (Mar and Okazaki, 2012). After phosphate rock has been treated with phosphoric acid, it takes the form of calcium dihydrogen phosphate which is highly soluble and forms the basis of many fertilizers (Brown; *et al.*, 2009). This compound can be assimilated by plants, but due to its high solubility, is also easily washed from the soil by agricultural or rain water and enters into water bodies, contributing to water pollution. Elevated PO_4^{3-} concentrations in water bodies are a major concern due to the process of eutrophication (caused by the presence of the nutrient) which remains a major water quality problem on a global scale (Dubrovsky et al., 2010; Harrison et al., 2010). PO_4^{3-} enters surface waters from wastewater treatment plant effluents, agricultural drainage, and storm water runoff (Boyer *et al.*, 2011).

Much effort has been dedicated to combatting the occurrence of eutrophication and success has been reported using engineered materials, such as ion exchange resins and polymeric adsorbents to remove the phosphate from nutrient rich waters. These materials and methods generally have high costs and require long preparation times which is why new materials and innovative approaches to phosphate remediation are required. Natural materials and waste/by-product materials from industrial processes have shown potential in phosphate removal from surface waters. Advantages of using these materials include their low-cost, abundant supply, and minimal required preparation. BOF-S has been tested in this regard and is considered a potential reagent. During laboratory experiments in which canal water rich in phosphates was treated with BOF-S (added at 4 g/L), 50% PO_4^{3-} removal occurred after 60 minutes due to both precipitation and adsorption. The possibility of using BOF-Ss for phosphate removal has been addressed by many researchers, all reporting success (Meyer *et al.*, 2012; Barca *et al.*, 2014; Han *et al.*, 2015, 2016; Zhou *et al.*, 2016).

2.3.5.3.7.6 Fluoride

Fluoride contamination in ground and surface water is recognized as one of the most potentially hazardous and large-scale health problems worldwide (Amini *et al.*, 2008). Fluoride is widely and naturally present in the geological environment (Abe *et al.*, 2004) and generally released into groundwater via the slow dissolution of fluorine-containing rocks and minerals such as fluorite, biotites, topaz, and their corresponding host rocks (granite, basalt, syenite, and shale) (Banks *et al.*, 1995). Besides the natural geological causes of fluoride enrichment in groundwater, multiple industries also contribute to fluoride pollution, exacerbating the problem (Reardon and Wang, 2000). These include the brick and iron works industries, coal fired power stations, aluminium smelters, the glass and ceramic production industries, the semiconductor manufacturing industries and the electroplating industry (Shen *et al.*, 2003). Generally, waste water that is produced from industry has a much higher fluoride concentration than water bodies containing naturally attained fluoride with concentrations reported to reach 1000 mg/L (Puente *et al.*, 1997). The WHO guideline for safe water fluoride concentrations (suitable for human consumption) is 1.5 mg/L (World Health Organization, 2004), but currently more than 200 million people worldwide are estimated to rely on drinking water with fluoride concentrations that exceed this. Methods in which to remove or lower the fluoride concentration in waters that exceed the recommended concentration are therefore actively being pursued and a method that incorporates the use of BOF-S has reportedly shown success.

BOF-S efficiency in adsorption of fluoride ions has been investigated and results from this study indicate that the adsorption characteristics are a function of pH and ionic strength of solution (Islam and Patel, 2011). The maximum adsorption capacity of BOF-S that had been thermally activated is 8.07 mg fluoride/g BOF-S, the optimum pH range for fluoride removal is reportedly 6 and 10 and the kinetics of the reaction followed a pseudo first order model (Islam and Patel, 2011). It was also found that fluoride adsorption was impeded by the presence of PO_4^{3-}, followed by SO_4^{2-} and NO_3^-.Thermal

activation of the slag was necessary as it resulted in more porous and bigger surface areas than if thermally untreated, however this can also be combatted by using slag particles of different sizes.

2.3.5.3.7.7 Dyes

Excess dyes used in the food and clothing industries are commonly released as pollutants into wastewater streams. BOF-Ss have also shown promising results in the removal of these dyes (Ramakrishna and Viraraghavan, 1997; Xue, Hou and S. Zhu, 2009). Experiments were successfully carried out to remove reactive blue 19, reactive black 5 and reactive red 120 from aqueous solutions in batch systems. The maximum dye uptake was observed at pH 2.0, and the maximum blue, black and red dye uptake capacities at dye concentration of 500 mg/L were 76, 60 and 55 g per gram of BOF-S, respectively. The adsorption kinetic process followed a first order kinetic model. The BOF-S used in this treatment method was exposed to acid beforehand (Bhatnagar and Sillanpää, 2010).

2.3.5.3.7.8 4-Chlorophenol

BOF-S has a relatively high FeO and Fe_2O_3 content (Table 2-1). When in contact with an acidic medium, these compounds dissociate to form ferrous and ferric ions which react with hydrogen peroxide and can generate hydroxyl radicals (Fenton Oxidation). These in turn are able to oxidize 4-chlorophenol, a pollutant found in industrial wastewaters. Studies have shown that within a 30-minute reaction period, a solution containing 4-chlorophenol with a concentration of 100 mg/l 4-cp is completely decomposed by a solution containing 438.7g/l of BOF-S and 8.24 mM hydrogen peroxide at a pH of 2.8. Intermediate oxidative states of 4-chlorophenol (4-chlorocatechol) are also oxidized during the process and the COD value changes from 290 to 90 mg/l after a 40 min reaction period, indicating that the procedure can significantly improve wastewater quality (Li, 1999).

2.3.6 Summary

In approximately 350 BC, Aristotle was recorded to have said: "When iron is purified by fire, there forms a stone known as iron slag. It is wonderfully effective in drying out wounds and results in other benefits" (Ciocan, 2012).

In the 21st century there are many more reuses of slag and methods in which to recycle and regain value from this waste/by-product. With global population and the demand for steel production growing exponentially, efficient waste re-use and striving towards a circular economy is becoming less a desire and more a necessity. Due to the sheer volume of BOF-S produced annually, reuse and recycling avenues for this by-product have been a popular topic of research and discussion for over 50 years. This review article has discussed and consolidated traditional methods as well as upcoming experimental methods for BOF-S reuse that have been researched and published. In particular the following findings are relevant:

a. BOF-S has many reuses in environmental remediation applications. Reuse in this manner will reduce or treat waste in more than one industry. BOF-S valorization in this way can potentially lower the cost of waste management in multiple industries.
b. The main drawback of the use of slag as a construction material is the high oxide content which causes volume instability. If practical methods of removing these oxides are implemented, the use of slag in construction will rise which will in turn lower the need for finite resources in that industry (sand, stone etc.). In this regard, it may be useful to implement an environmental technique that depletes the oxide content of slag in conjunction to its use as a building material.
c. Metal recovery is limited in BOF-S.

The use of waste materials or by-products in applications that have a positive effect on the environment resonates strongly with the concept of sustainability, and the potential use of these materials have been shown to benefit multiple industries other than that of steel manufacturing. Although the cost of transport of BOF-S to the area of application must be considered to ensure economic viability of implementation, in countries where slag production is extensive, the environmental impacts may outweigh the costs. If implemented and managed properly, there is no reason that the bulk of BOF-S produced should not be utilized for other applications.

3 Methods and Materials

This chapter outlines the materials used and the methods followed to achieve each of the objectives stipulated in Chapter 1. Chapters 4 to 11, each address specific objectives, and thus, a detailed methodology is provided in each of these chapters, that describes the processes followed to achieve the objective on which the chapter presents. This chapter provides a brief outline of all these methods.

3.1 Materials

Experimentation and pilot-scale work done during the course of this research involved the use of the three by-products: BOF slag, AMD and Sugarcane Bagasse. These were sourced from South African-based sites and companies.

1. AMD was sourced from a coal mine (at two different sites) in Witbank, Mpumalanga.
    a. Type A AMD was sourced from a dam situated at the base of a mine tailings storage site. Four cubic meters were collected in intermediate bulk containers (IBCs) from this site. Type A AMD was used to perform the continuous laboratory scale experimentation and the continuous pilot plant study.
    b. Type B AMD was sourced from an AMD stream in the same Witbank area. Type B AMD was collected using 25 L vessels. These were stored at 4°C until use.
2. BOF slag was sourced from Phoenix Slag Services in Newcastle, Kwazulu Natal. This slag was milled by Phoenix Slag Services to various particle sizes ranging from < 1mm to < 15 cm. The samples obtained were sieved during experimentation to ensure that only certain ranges were used for each of the tests. The slag was stored in a dry area at ambient temperature throughout the course of experimentation.
3. Sugarcane Bagasse was sourced from an Illovo Sugar mill in Eston, Kwazulu Natal. These samples were refrigerated at 4° C before use. Sugarcane bagasse which was used in the pilot plant study was stored in sealed material bags at ambient temperature at the coal mine site where the study was conducted.

3.2 Equipment

Equipment (vessels, pipe fittings, sensors and process control equipment) needed for the construction of the laboratory and pilot scale processes was sourced from South African based companies.

1. A Siemens Simatic S7-1200 programmable logic controller (PLC) was used to control the pH and flowrate of the pilot plant situated at the mine tailings site.

2. Two Watson Marlow 530UN/R2 automatically controlled peristaltic pumps were used both in the pilot and laboratory scale plants.
3. The following Endress and Hauser equipment were used:
    a. A Liquiline CM444 transmitter used in conjunction with the analytical equipment and the PLC to control the pH and flowrates in the pilot plant.
    b. An Orbipac CPF81D Memosens pH meter to measure pH.
    c. An Orbipac CPF82D Memosens Oxidation Reduction Potential (ORP) meter to measure ORP.
    d. An Indumax CLS50D Conductivity meter to measure conductivity.
4. An Arduino Mega 2560 processing board was used to programme a pH sensor and record continuous pH readings (every 3 seconds)
5. A DF Robot Analog pH Meter V1.0 was used (in conjunction with the Arduino Mega 2560) to measure pH.
6. Temperature Sensors (DS18B20 from MicroRobotics South Africa) were used to monitor temperature both in the laboratory and pilot plants.
7. Generic fishpond pumps were used to circulate the effluent stream in the laboratory scale plant. Clamps were used to control flowrate in these instances.

3.3 Methodology

3.3.1 Objective 1– Kinetics of BOF slag dissolution

- A particle size distribution curve of the BOF slag was determined using sieving techniques and information provided by the company providing the slag.
- A composition of the slag was determined using X-Ray fluorescence (XRF) as well as acid digestion followed by atomic absorption spectroscopy (AAS). Slag was weighed and then submersed in sulfuric acid for 72 hours. The liquid was filtered, diluted and tested using AAS. Mass of solids remining after leaching and filtration were measured.
- Batch, continuously stirred tank reactor (CSTR) and packed bed reactor (PBR) configurations were used. For each reactor type, slag samples were brought into contact with the leaching liquid and samples of liquid and slag were taken at different time intervals. The volume of the reactors was large enough to allow for volume change from sample extraction to be negligible. Where the taking of samples influenced the reaction, experiments were performed as multiple batches with different reaction times at the same operating conditions.
- A variety of liquids were used, including untreated AMD, hydrochloric acid and deionized water.
- Liquid samples were analysed for acidity, metal content and sulfate level and solid samples were subjected to XRF analysis to identify changes in oxide content.

3.3.2 Objective 2 - Kinetics of Precipitation reactions

1. A full elemental and ionic analysis of the AMD before treatment was performed.
2. The AMD was put into contact with BOF slag, and a full elemental and ionic analysis of the resulting high pH eluate was determined. This was done using AAS and Inductively coupled plasma - optical emission spectrometry (ICP -OES).
3. Raw AMD and treated AMD (high pH eluate) were mixed, and samples were taken at different time intervals. Both batch and continuous flow reactors were used.
4. Each sample was tested for pH, acidity, and all known present metals, sulfates, and silicon.
5. Sludge formation was monitored in steps 2 and 3, and samples of sludge were analysed using XRF and – after acid digestion – AAS for metal content.

3.3.3 Objective 3 - Kinetics of DSR reactions

1. A full carbohydrate and sugar analysis was conducted for the sugarcane bagasse. The dry mass of the sugarcane bagasse was also measured.
2. Sulfate reducing microorganisms (SRM) was cultivated using mixed cultures of SRM obtained from the Northern Wastewater Treatment Works, Emmerantia Dam (Johannesburg, South Africa) and from previous AMD experiments. This mixed culture was grown in nutrient rich media (containing 5g of sodium citrate, 4,5 mL of sodium lactate, 1g of yeast extract and 4.5 g of Magnesium sulfate heptahydrate in 1 L of deionized water). To desensitize the culture to AMD and BOF conditions, 3 mL of a BOF slag neutralized AMD samples were added every 2 days.
3. Batch and continuous flow reactors were performed.
4. BOF slag neutralized AMD was contacted with sugarcane bagasse, either in a batch reactor by adding 1.5 L of solution to a beaker containing 150 g of sugar cane bagasse, or in a continuous reactor by pumping 25 L/day of BOF slag neutralized AMD through a 25 L vessel containing 4 kg of sugarcane bagasse (and with a liquid volume capacity of 14.4 L).
5. Liquid samples were taken at different time intervals and analysed for sulfate and sulfide content.
6. Samples of bagasse were also taken, rinsed with de-ionized water and dried at room temperature over a period of a week. These samples were then acid digested to determine if precipitation occurred on the bagasse surface.
7. Sludge that formed was analysed for metal and sulfide content using spectrophotometric and AAS techniques.
8. Spectrophotometric sulfide tests were used to determine the presence and concentration of sulfide in the liquid samples.

3.3.4 Objective 4 - Design, construction, and optimization of laboratory scale AMD treatment system

1. Data obtained from the studies conducted for Objectives 1 – 3 were used to design and construct a laboratory scale AMD treatment system.
2. Experiments were conducted to determine the system outputs to certain changes in the operating variables such as changing the size of BOF particle used, changing the order in which the various unit operations were placed/encountered by the AMD, altering the flowrate of the AMD or the recycle stream.
3. The continued monitoring of the system outputs, analysed as water characteristics (metal, sulfate, sulfide, pH, acidity, silicon, oxide) over time allowed for changes to be made to achieve optimal results in terms of sulfate and metal removal, pH level, sulfide content and acidity for the system. Changes that were made included changing the size of the BOF slag particles, changing the flowrates and residence times of the reactors and allowing for process control (pH) to be installed.

3.3.5 Objective 5 and 6 - Design, construction, and optimization of a process to treat 1000L/day of AMD on-site

1. Traditional chemical engineering design methodology was used to design a pilot plant capable of treating 1000 L/ day of AMD on-site.
2. A mass balance, process flow diagram, piping and instrumentation diagram and control philosophy were prepared.
3. Using data obtained from objective studies 1 – 4, the plant specifications were determined. This included determining and detailing the sizes of all plant units, as well as, detailing a plant layout diagram.
4. A contractor’s manual was assembled, and health and safety training were completed to allow access to the site.
5. The plant was constructed at the stipulated site using locally procured equipment. Small scale civil work was required at this stage.
6. The plant output was monitored using similar methods as in the laboratory scaled system to assess the long-term performance of the pilot plant.
7. Parameters monitored for Objectives 5 and 6:

    7.1 The rate of metal sludge build-up within the settling vessel.

    7.2 The sulfate, sulfide, silicon, acidity, pH, redox, conductivity and metal concentration before and after each reactor.

    7.3 The rate of recycle into the system.

7.4 The outlet specifications (sulfate, metals, silicon, redox and pH).

3.3.6 Objective 7 – Prepare a proposed process for a scaled-up design for AMD treatment on site based on pilot study data.

1. Data from the studies conducted to achieve objectives 5 and 6, was used to prepare a larger scale process.
2. Traditional chemical engineering design methodology was used to fulfill this objective.

3.4 Analytical Techniques

A myriad of analytical techniques and instruments were used to obtain data from the experiments performed in this research. Some analyses were performed by external laboratories. These have been indicated in brackets.

1. Spectrophotometry: A Merck Pharo 300 spectrophotometer was used to analyse iron, sulfate and COD concentrations. Merck test kits were used to analyse for these anions and cations. Additionally, CeBER (Center for bioprocess engineering research, 2016) methods were used to analyse for sulfate.
2. High Performance Liquid Chromatography (HPLC) was used to assess the sugar and other volatile organic acids (VOA) content in the bagasse chamber. An Agilent 1200 series machine with a refractive index detector was used to perform HPLC tests.
3. pH was measured using the Endress and Hauser or DF Robot pH probe.
4. Inductive Coupled Plasma- Mass Spectroscopy (ICP-MS) was used to analyse cation and anion concentrations (external laboratory).
5. Atomic Adsorption Spectroscopy (AAS) was used to assess the heavy metal concentration in the AMD prior to and after treatment. An Agilent Technologies, Series 200 instrument was used.
6. X-ray diffraction (XRD) and X-ray fluorescence (XRF) were used to identify crystaline phases and measure metal element concentrations in the solid metal precipitates that form and the slag particles. These analyses were performed by the Earth Lab at the University of the Witwatersrand using a Malvern Panalytical Axios Wavelength Dispersive (WD) XRF machine. XRD was performed by the School of Chemistry at the University of the Witwatersrand, using a Bruker Discover D8 machine. Sample preparation included drying of the particles and pulverizing them using a crusher.
7. Scanning Electron Microscopy (SEM) was performed on the sugar cane bagasse and slag prior to and after treatment. FEI Quanta 400 E-SEM was performed (external laboratory).
8. A combustion LECO analysis was performed on the sugarcane bagasse to determine the nitrogen, carbon and sulfur content (external laboratory).

3.5 Facilities Used

1. The preliminary benchtop design, initial experiments and monitoring thereof, required the use of peristaltic pumps for pH-controlled dosing and reservoir chambers. These were acquired by the Biochemical Engineering Laboratory in the Chemical Engineering Department of Wits and were available to be used on the premises
2. The larger pilot scale plant required a source of AMD and a site for construction near the AMD source. This site was provided by a mine, and was situated in Witbank, Mpumalanga.
3. As mentioned previously, various analytical instruments and equipment were required to measure and monitor the composition, chemical and physical properties of samples obtained during the study. These were available in the biology laboratory located on the second floor of the Richard Ward Building at Wits University or on the Wits East Campus, in the Bernard Price Building, Earth Sciences lab. Permission was obtained to use all facilities and equipment.

4 BOF Slag Dissolution – Harnessing Alkalinity for AMD pH Modification

This chapter is an extended form of the conference article "An Assessment of Basic Oxygen Furnace Slag Dissolution for Application in AMD Dam Remediation using Waste Products from the Steel Manufacturing and Sugar Industries" which was peer reviewed, presented and published in the SAIMM Mine Tailings Conference in 2020 (Naidu, Chauhan, *et al.*, 2020). The authors contribution for this paper is listed in Appendix I.

4.1 Introduction

Traditional AMD treatment revolves predominantly around neutralization of the acidic waters which in turn leads to removal of sulfate and metals via precipitation reactions. Thus, the manner in which the pH is raised is of importance as it dictates multiple parameters such as reactor type, residence time, manner and frequency of removal of sludge and amount and frequency of neutralizing material addition. For the case of BOF slag used as the neutralizing agent, the kinetics of the dissolution of this material had to be determined. This was done as described in the following section.

4.2 Methodology

Experiments were performed with slag of three different size classes: (i) class 1 (2 mm to 3.35 mm in diameter); (ii) class 2 (4.75 mm to 6.7 mm in diameter) and (iii) class 3 (6.7 mm to 9.5 mm in diameter). This was done to formulate a suitable model to predict the extent of dissolution of BOF slag in media of different pH levels or acidity/alkalinity measurements – in essence slag leaching tests were conducted to ascertain the mechanism of dissolution. Slag samples and leaching liquids (water, AMD and hydrochloric acid with a molarity (M) of ~ 10,2) were weighed and measured out such that the liquid to solid ratio remained constant at 10:1. Initially, 40 g of slag and 400 mL of liquid were used, thereafter, 80 g of slag and 800 mL of liquid were used. The liquid was placed into a 1000 mL beaker on a magnetic stirrer, at 200 rpm at room temperature, and a pH probe was inserted into the liquid. The pH of the liquid after slag was added, was monitored continuously. 1 mL of the leaching liquid was removed as aliquots at varying time intervals for AAS analysis, and titration samples of 20 mL of the leaching liquid were removed at 20 seconds into the experiment and at the end of the experiment, indicated by stable solution pH. The leached slag was then removed from the liquid media and put into an oven for drying at 50°C for 4 hours. Experiments were replicated, and where necessary multiple experiments were run to ensure change in volume after sampling did not affect the experiment – a total maximum volume change of 5% was allowed during sampling. Other experiments were run using the same methodology with different volumes and masses of BOF slag and leaching liquid. The Lagergren and shrinking core kinetic models were applied to the data obtained from these experiments. A comparison between lime

and BOF slag was also performed using data from literature. Where relevant, data from the laboratory and pilot scale plants are also incorporated in the study.

4.3 Mechanism of pH Increase

4.3.1 Comparison of lime and BOF slag

An important note in the comparison between lime (quicklime or hydrated lime) and BOF slag is the availability of free lime in the sample (components that are available to hydrate and raise the pH of the media). Lime and free lime generally refer to the CaO of the sample, however, BOF slag contains multiple other units in oxide and silicate form that dissolve in liquid media and contribute to the neutralization or pH rise of the media.

Table 4-1 shows approximate availability of oxides (that can readily hydrate in liquid media) in lime and BOF slag. Although the free lime content in BOF slag is 13 %, this only refers to the components found on the surface of the solid particle, or that are readily available to react.

As dissolution occurs, more oxide components become available. The size of the BOF slag particle will also affect the amount of free oxide content – smaller particles have a larger availability of neutralizing/alkaline components than larger particles.

Table 4-1: Free oxide content in quicklime, dolomitic lime, hydrated lime and BOF Slag with particle aperture between 2000-3350 microns (determined via SEM and Energy dispersive X-ray analysis (EDA)) where Wollastonite found on the surface of the particle was not considered a free oxide (due to its insolubility in water)

Alkaline material	Oxide content (Total %)	Free oxide content (%)
Quicklime (Tolonen *et al.*, 2014)	94	91
Dolomitic Lime (Dryden, 1982)	53	50
Hydrated lime (Tolonen *et al.*, 2014)	73	71
BOF slag (Tolonen *et al.*, 2014)	87	13

Although the free oxide content of BOF slag is significantly less than that of normal quicklime or hydrated lime, the BOF slag still exhibited success in neutralizing AMD. 80g of slag was able to raise the pH of a sample of Type A AMD with an initial pH of 2.44 to (i) a pH of 7 in 540 minutes and (ii) a pH of 10 in 1365 minutes. This is shown in Figure 4-1.

The experiment – of which results are shown in Figure 4-1 – was repeated multiple times and it was observed that the pH in the system did not stabilize, even after 72 hours of reaction time.

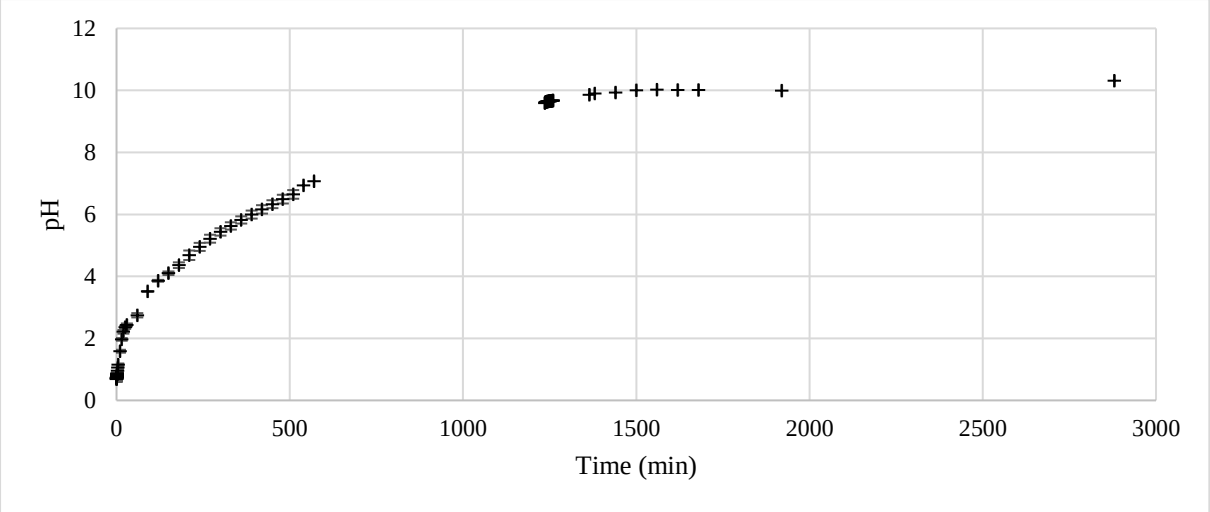


Figure 4-1: pH change over time in 800 mL of AMD in a constantly agitated reactor when 80 g of slag with particle aperture between 2000-3350 microns has been added

The pH rise was causally related to (i) the volume of AMD, (ii) the composition of AMD, (iii) the amount of BOF slag, (iv) the particle size of the BOF slag and the (v) allowed reaction time. For example, 15 g of slag fines (aperture of 1000 microns or less) was able to increase the pH of 1500 mL of Type B AMD (significantly lower initial sulfate and iron concentration) to a pH of 7 in 55 minutes, and similarly 67 g of fine BOF slag was able to raise 200 mL of this Type B AMD to a pH of 7 in 5 minutes. The alkalinity addition corresponding to the last data point collected for the experiment shown in Figure 4-1 was 2897 units of alkalinity as $CaCO_3$ in mg/L.

It should be noted that the dissolution of BOF slag in an acidic medium in the proposed AMD treatment process is the main mechanism of pH rise, with the secondary/supporting mechanism being the hydrolysis of the sugarcane bagasse in the biological reactor.

Mg and Ca concentrations increase within the system, confirming the hydration reaction between the treated AMD and these oxidic species within the slag (this was also seen during operation of the laboratory and pilot scale systems). This is shown in Figure 4-7.

According to literature, alkalinity can be generated from BOF slag via hydration followed by dissociation of calcium, magnesium and other metal oxides (Gomes *et al.*, 2016). The BOF slag obtained directly from Phoenix Slag services was assessed for oxide content and shown to contain 41.6 mass% CaO and 7.2 mass% MgO (shown in Table 4-2) (XRD was performed as per the procedure given in Methods and Materials). The main components of BOF slag were Ca, Fe, Si, Al and Mg oxides and thus Ca and Mg concentrations were primarily used as an indication of dissolution extent, as Fe and Al formed precipitates at the pH levels that were reached in the solutions.

Table 4-2: Oxide content of BOF slag used in the experiment.

Oxide	wt.%
CaO	41.6
Fe_2O_3	20.5
SiO_2	14.4
MgO	7.2
Al_2O_3	2.8
SO_3	0.4
Loss on ignition (LOI)	5

The hydration, dissolution and dissociation reactions that bring about alkalinity from CaO and MgO are described by Equation 4-1, Equation 4-2, Equation 4-3 and Equation 4-4. The iron oxide and aluminium oxide compounds also undergo dissociation similar to calcium and magnesium oxide. However, as mentioned, these components cannot be measured in the solution as they have already formed insoluble compounds and precipitated due to the pH levels that are reached in the system.

$$CaO + H_2O \leftrightarrow Ca(OH)_2$$

Equation 4-1

$$Ca(OH)_2 \leftrightarrow Ca^{2+} + 2OH^-$$

Equation 4-2

$$MgO + H_2O \leftrightarrow Mg(OH)_2$$

Equation 4-3

$$Mg(OH)_2 \leftrightarrow Mg^{2+} + 2OH^-$$

Equation 4-4

The concentrations of H^+ ions (obtained from pH measurements in the media) over time were also used to study the dissolution kinetics (using Equation 4-5). $[H^+]$ was used as this was representative of the dissolution of all oxidic compounds in the slag, regardless of pH induced precipitation.

$$[H^+] = 10^{-pH}$$

Equation 4-5

4.3.2 Chemisorption Behaviour

Equation 4-6 (Lagergren pseudo-1st order), Equation 4-7 (Lagergren pseudo-2nd order), Equation 4-8 (shrinking core diffusion through liquid film), Equation 4-9 (shrinking core diffusion through the ash layer) and Equation 4-10 (shrinking core chemical reaction model) were applied to the experimental data, and evaluated respectively. It should be noted that agitation was used in the batch experiments which reduced the liquid film layer diffusion limitations.

$$\ln\left(\frac{C_t - C_e}{C_o - C_e}\right) = -k_{1,obs}t$$

Equation 4-6

$$\frac{1}{C_o - C_e} - \frac{1}{C_t - C_e} = k_{2,obs}$$

Equation 4-7

Where; C_o is the initial concentration, C_t is the concentration at time t, C_e is the concentration at equilibrium and $k_{1,obs}$ and $k_{2,obs}$ are the apparent rate constants.

$$k_f t = X$$

Equation 4-8

$$k_d t = 1 - 3(1 - X)^{0.67} + 2(1 - X)$$

Equation 4-9

$$k_r t = 1 - (1 - X)^{0.33}$$

Equation 4-10

Where k_f refers to the diffusion through liquid film constant, k_d refers to diffusion through the ash layer constant and k_r refers to the chemical reaction constant.

It was observed that the chemical reaction model did not fit the data of the water and the AMD media dissolution cases. Diffusion through the ash layer was found to apply best to water for Ca (all size classes of slag) and Mg (size class 3) release from the BOF slag. AAS was used to determine the concentrations of Ca and Mg. $[H^+]$ kinetics was used to represent the experiment as a whole and a pseudo-1st order Lagergren model was seen to apply more often. The larger particle sizes underwent a lower rate of dissolution than the smaller particle sizes of BOF slag. This can be seen in the pH data obtained over time for dissolution of different particle sizes shown in Figure 4-2.

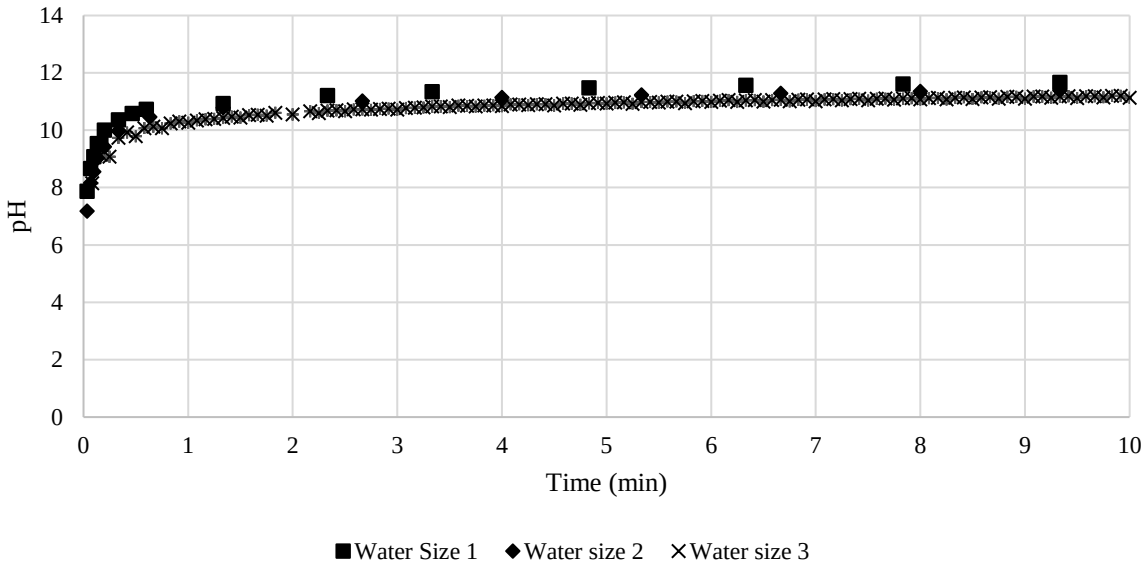


Figure 4-2: pH in water solutions during dissolution of BOF slag of particle size 1 (2 mm to 3.35 mm in diameter); 2 (4.75 mm to 6.7 mm in diameter) and 3 (6.7 mm to 9.5 mm in diameter)

4.3.3 Kinetic Model Fitting

Table 4-3 shows a summation of the kinetic model fitting for the leaching processes performed. The first value of each entry in the Lagergren model indicates whether the pseudo-first order (1) or pseudo-second order (2) was obtained as the best fit, and the first value of each entry in the Shrinking core model indicate whether diffusion through liquid film (F), diffusion through the ash layer (D) or the chemical reaction (R) model is the best fit.

Table 4-3: Summation of Kinetic Model Fitting for Leaching Experiments

Lagergren kinetic model					**Shrinking core kinetic model**				
Liquid	Size	H^+	Ca	Mg	Liquid	Size	H^+	Ca	Mg
Water	1	2; 0.99	1; 0.77	1; 0.43	Water	1	R; 0.26	F; 0.91	D; 0.69
	2	2; 0.96	1; 0.93	1; 0.10		2	R; 0.44	D; 0.97	D; 0.23
	3	1; 0.85	1; 0.93	1; 0.92		3	D; 0.59	D; 0.97	D; 0.97
HCl	1	1; 0.97	2; 0.99	2; 0.97	HCl	1	R; 0.97	D; 0.64	D; 0.72
	2	1; 1.00	2; 0.95	2; 0.99		2	R; 0.88	D; 0.62	D; 0.77
	3	1; 1.00	2; 0.99	1; 0.97		3	D; 0.95	D; 0.59	D; 0.63
AMD	1	1; 0.90	1; 0.84	1; 0.93	AMD	1	R; 0.69	D; 0.72	D; 0.80

In Table 4-3, the second value of each entry indicates the coefficient of determination value of the best fit trendline. In each row, the highest coefficient of determination is highlighted to show which component and model was the best fit for that leaching process. Table 4-4 shows a summary of the kinetic constants obtained for the best fitting models in each case, where $k_{1,obs}$ refers to the pseudo-first

order (white), $k_{2,obs}$ refers to the pseudo-second order (black), k_f refers to diffusion through liquid film (grey) and k_d refers to diffusion through the ash layer (patterned).

Table 4-4: Summary of the Kinetic Constants obtained for the Best Fit Models in each Case

Liquid	Size	H^+		Ca		Mg	
		Constant	Value	Constant	Value	Constant	Value
water	1	$k_{2,obs}$	-7.00E+10	k_f	-0.0003	k_d	3.00E-05
	2	$k_{2,obs}$	-5.00E+10	k_d	0.0004	k_d	4.00E-06
	3	$k_{1,obs}$	-7.8051	k_d	0.0013	k_d	0.0001
HCl	1	$k_{1,obs}$	-0.3575	$k_{2,obs}$	4.00E-05	$k_{2,obs}$	0.0002
	2	$k_{1,obs}$	-0.1589	$k_{2,obs}$	8.00E-06	$k_{2,obs}$	2.00E-05
	3	$k_{1,obs}$	-0.0961	$k_{2,obs}$	6.00E-06	$k_{1,obs}$	-0.0012
AMD	1	$k_{1,obs}$	-0.0733	$k_{1,obs}$	-0.0011	$k_{1,obs}$	-0.0004

By using kinetic model fitting, it was observed that the chemical reaction model did not apply to any case. Diffusion through the ash layer was found to apply to water for Ca and Mg release. H^+ kinetics had the highest coefficient of determination values – leading to the supposition that this may be the best way to determine the kinetics of the dissolution. The pseudo-first order model was seen to apply more often.

4.3.4 Alkalinity

The alkalinity and acidity of water, HCl and AMD were measured before and after reaction with BOF slag of size class 1 (diameter from 2 mm to 3.35 mm) using titration methods. The total alkalinity and acidity calculated is summarized in Figure 4-3.

As shown, the acidity in water before the BOF slag reaction and the alkalinity after the BOF slag reaction are much lower than the acidity and alkalinity of both acidic media. This indicates that more BOF dissolution occurs in acidic media than in neutral solutions. For application in AMD treatment, this potentially means that AMD should be reacted directly with the slag instead of using a recycle stream (as used in the laboratory and pilot-scale systems). Paradoxically, armouring of BOF slag particles, which is due to precipitation of various compounds (especially iron) that form during neutralization reactions (Pathirage *et al.*, 2012), prevents the direct contact between AMD and BOF slag. This was observed during the SEM analysis of the slag and is discussed in the next section.

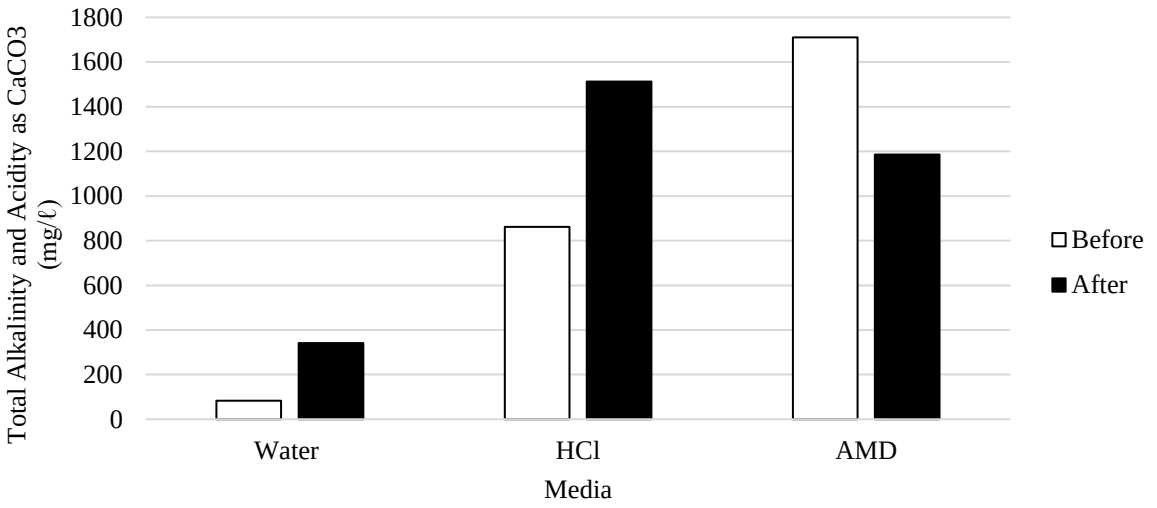


Figure 4-3: Total acidity of solutions before and after reaction of 80 g of BOF slag with 800 mL of water or HCl or AMD, expressed in terms of $CaCO_3$ concentration.

4.3.5 BOF slag Surface Morphology

The surface morphology of the BOF slag was studied before and after leaching. It can be seen from Figure 4-4 that a layer of precipitation formed on the surface of the BOF slag in the reactor.

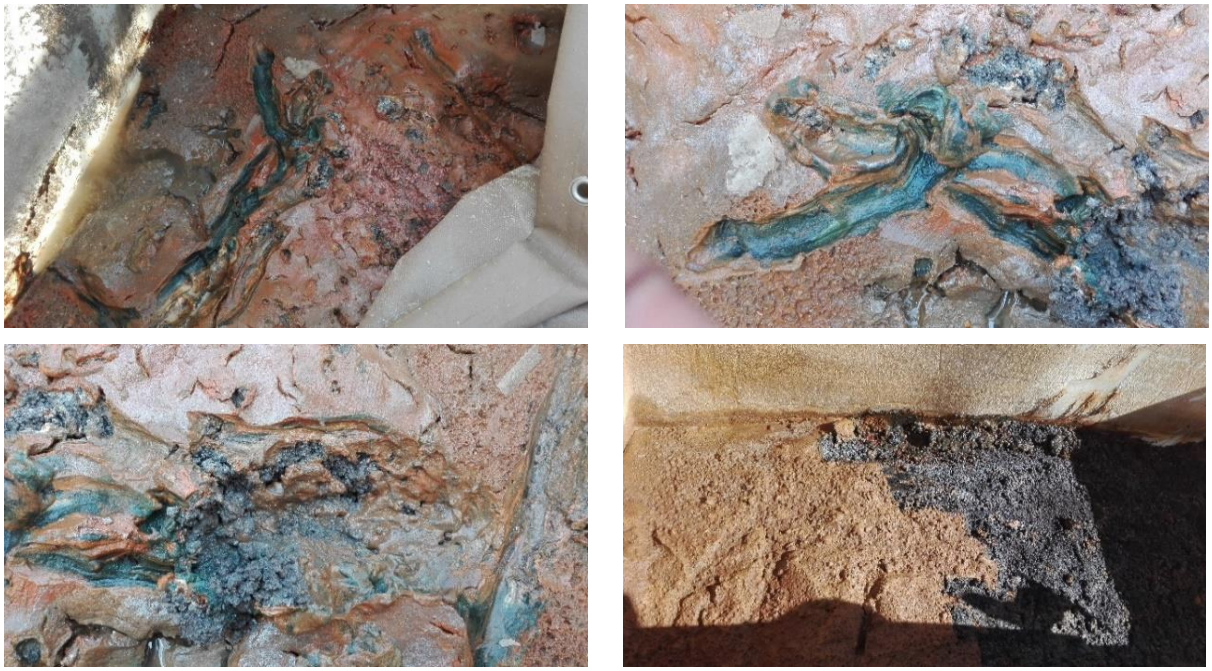


Figure 4-4: Precipitation layer on top of the BOF slag in the BOF slag reactor

SEM images of the BOF slag particles before and after reaction with water, HCl and AMD were obtained and are shown in Figure 4-5. The slag leached by water and the untreated BOF slag look similar, with slightly more porosity being seen in the water leached slag. The particles leached in HCl ((v) and (vi)) display more precipitation spots (shown by the lighter colour) than the others and the AMD particle (iii) appears to be coated in a distinct layer identified as gypsum. It is evident that a

coating of precipitates was formed on the surface of the BOF slag particles which were reacted with acidic media. This coating or armouring of the BOF slag particles was also observed in the continuous process and had a significant impact on the accessibility of the AMD to the slag. An agitated system could be used to prevent settling of the precipitate.

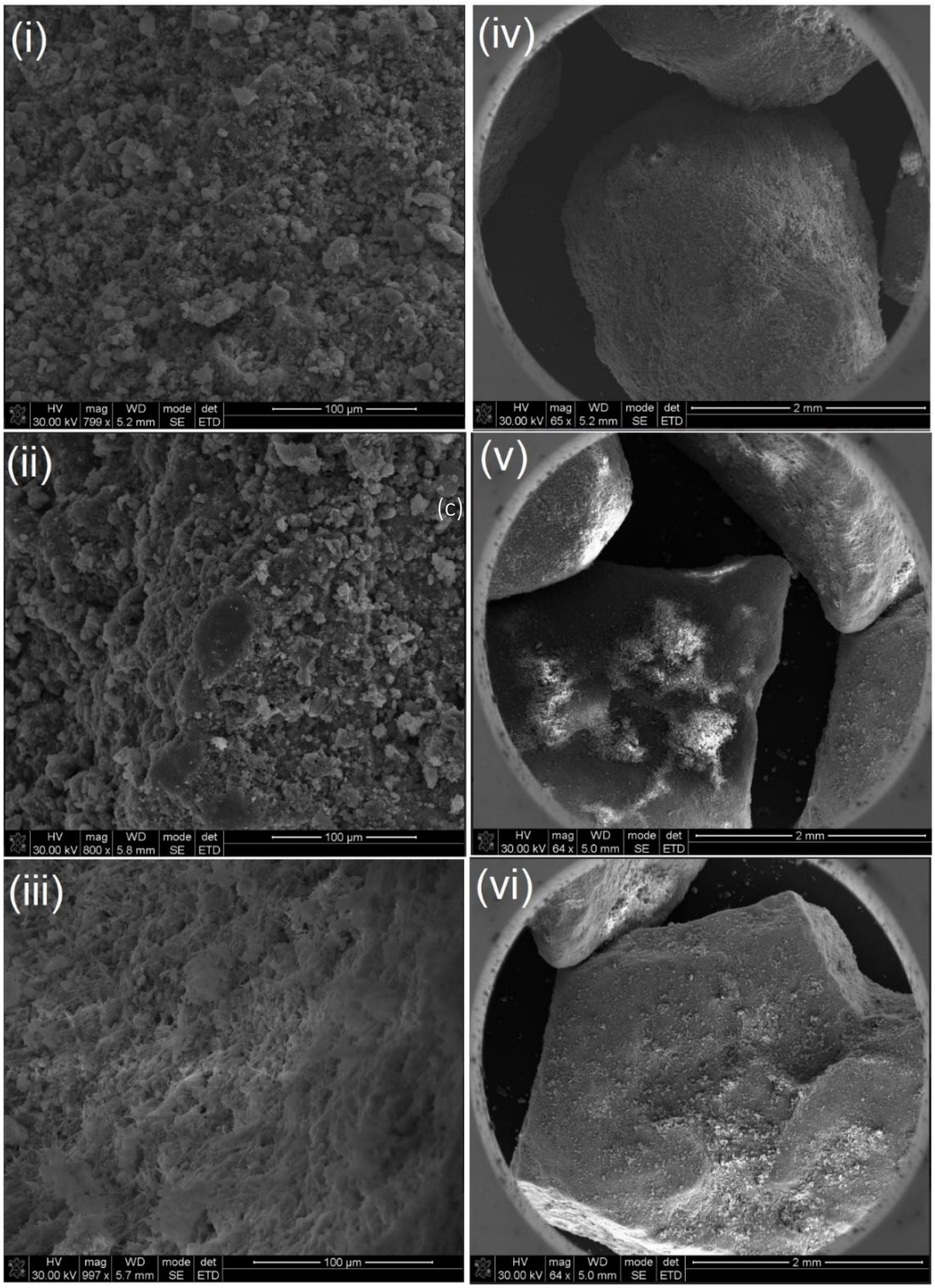


Figure 4-5: SEM images of (i) and (iv) unreacted BOF slag; (ii) water leached BOF slag; (iii) AMD leached BOF slag; (v) and (vi) HCl leached BOF slag

4.4 BOF slag Dissolution in Pilot and Laboratory Scale Operation

During the operation of both the laboratory and pilot-scale plants, it was observed that the pH of the system was the variable that the concentrations of metals and sulfates were dependent on. The pH, in turn, was dependent on the rate of dissolution of the BOF slag.

BOF slag dissolution was deemed the rate controlling step and efforts were made to increase it by (i) increasing the amount of BOF slag used, (ii) decreasing the particle sizes used and (iii) changing the reactor type from packed bed reactor (PBR) to a continuously stirred tank or agitated reactor (CSTR). Each of these changes yielded positive results - the rate of dissolution increased, and more AMD could be treated per unit time.

In the pilot-scale system, it was noted that the calcium concentration increased with pH – an indication that the dissolution of CaO contributed to the rise in pH. Dissolution of other elements (Al, Fe and even Mg) could not be assessed, as all these elements formed insoluble compounds at the pH levels that were reached (8 - 12). The normalised (to 100%) removal or increase in concentration (Ca only) through leaching from the slag is shown in Figure 4-6.

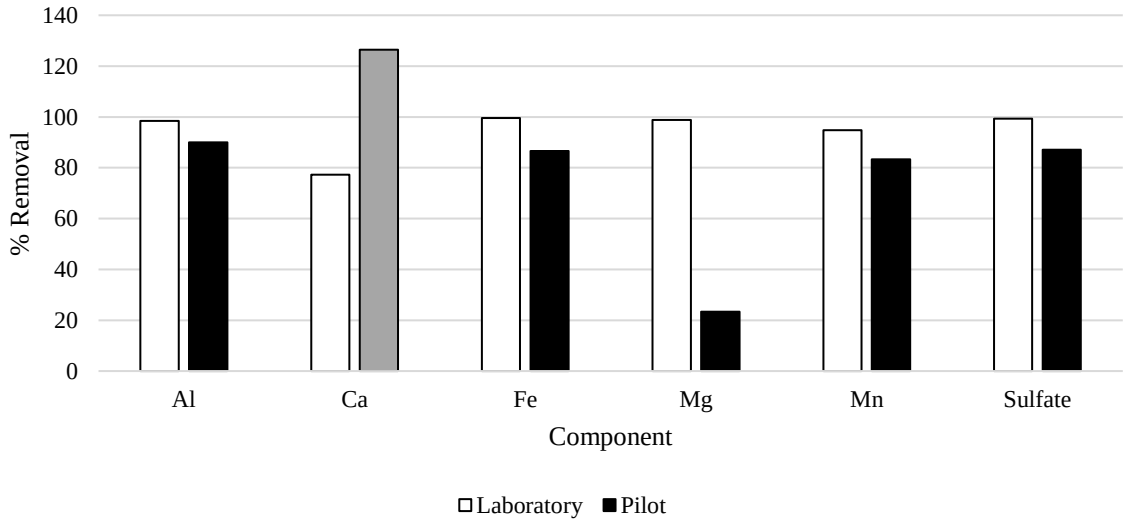


Figure 4-6: Removal (%) of Al, Ca, Fe, Mg, Mn and Sulfate across the laboratory and pilot-scale systems with Ca exhibiting an increase in the pilot-scale system (shown in grey)

As seen, the Ca concentration increased by 126% in the pilot-scale system while decreasing in the laboratory scale system. This was expected as the ratio of BOF slag to AMD in the pilot scale system was much higher than that of the laboratory scale system. This ratio was changed from the laboratory scale to pilot scale to limit the rate controlling effect of the BOF slag dissolution. Consequently, the BOF slag was present in excess in the pilot-scale plant. Mg removal was also much lower in the pilot-scale experiments and this was due to the presence of excess BOF slag as well as the low pH levels in the pilot-scale that did not cause Mg to form insoluble precipitates. Apart from the Ca and Mg, the pilot

scale and laboratory processes functioned comparably.

The higher dissolution rate (than in water) being found in acidic media is demonstrated in Figure 4-7, where the concentration of Ca and Mg ions in solution are much higher in AMD than in water after being reacted with BOF slag at the same conditions for the same period of time.

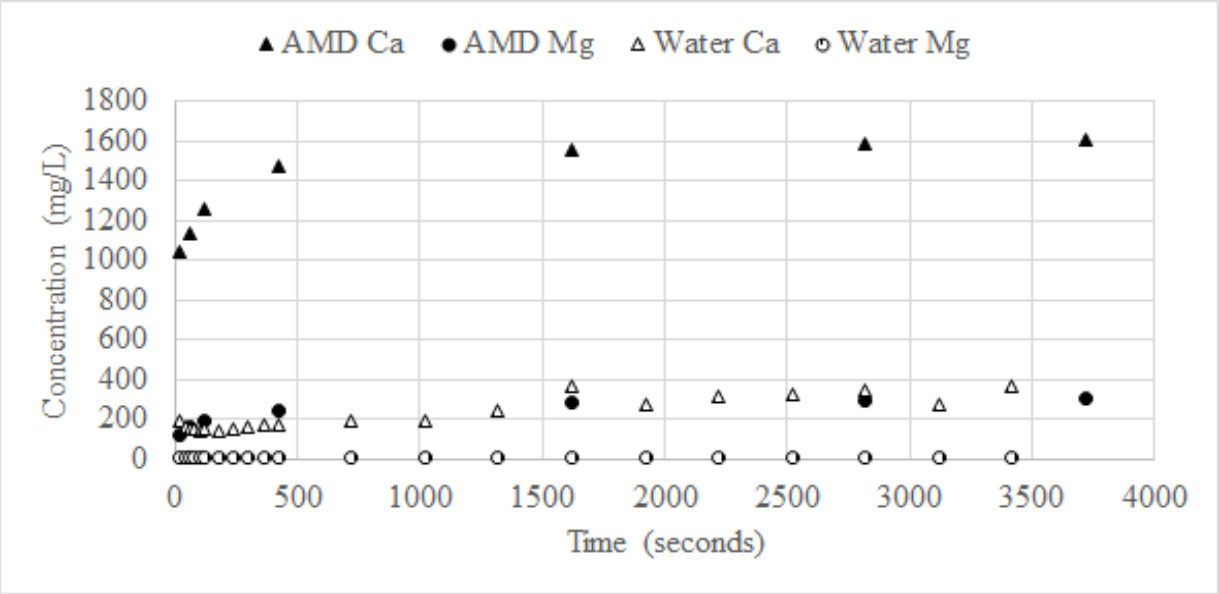


Figure 4-7: Concentrations of Mg and Ca ions in water and AMD solutions that are reacted with slag fines in a CSTR

This corresponds to the findings from alkalinity measurements taken in water, AMD and HCl media after reaction with BOF slag for a period (approximately 1200 minutes) (Figure 4-3). The pH in each of the ms was different (the pH in the water system was the highest, followed by HCl and then AMD) after the same reaction time with the same mass of BOF slag. The alkalinity readings indicate that although a lower pH is recorded in the acidic media, the solutions have a higher alkalinity than that of water. This explains the large amount of water (recycle stream) that is needed to neutralize the AMD. These observations support and explain the findings from the laboratory scale set-up which indicated that a lower recycle rate was maintained when fine particles of BOF slag were stirred into the AMD. It indicates that dosing may be a less energy intensive option when compared to using large particle sizes and a recycle stream.

4.5 Conclusion

The kinetics of the BOF slag dissolution were determined. According to the data obtained from the laboratory and pilot-scale systems, there was substantial dissolution of oxides into the solution from the BOF slag. BOF slag was effective in raising the pH of the AMD, as well as the other leaching solutions (HCl, water), to ranges between 10 and 12. The observed increase in alkalinity of the solution was however, dependent on the initial acidity of the leaching solution. pH rise occurred the fastest in water, but a greater release of alkaline elements was achieved in more acidic solutions. The Lagergren kinetic

model fitted the data of the leaching experiments better than the shrinking core model, with the pseudo-first-order model seeming to better apply to acidic media (using $[H^+]$ as the concentration of interest), and the pseudo-second-order model found to apply better to BOF leaching in a neutral solution such as water. The assessment of the dissolution of Mg and Ca oxides individually, showed converse results, with dissolution in acidic media fitting the pseudo-second-order model better and dissolution in neutral media fitting the pseudo-first-order model better (for both metals). Fitting of the data using shrinking core model was achieved in certain cases. The kinetic rate constants were estimated from the batch tests done; however, pH dependency was not considered in this study. By using pH buffered solutions the primary mineral kinetics may be estimated with more accuracy (Windt et al., 2011).

5 Sulfate and Metal Precipitation in AMD treatment

The precipitation reactions involved in AMD treatment with BOF slag have been studied and the kinetics of precipitation with change in pH have been determined and is presented. This chapter provides a discussion of the objective related to this topic: "Identify and study the kinetics of the precipitation reactions which occur when the pH of the AMD treatment system rises" and is presented in the format of a journal article titled "Acid mine drainage treatment using steel slag as a lime substitute", which will be submitted to the Journal of Chemosphere or Water Resources and Industry. This chapter also contains information that was presented at the South African Chemical Engineering Congress in 2021 (SACEC2021) in the form of a conference paper titled "The Use of Basic Oxygen Furnace Slag as a Substitute for Lime in Acid Mine Drainage Treatment" (Naidu, van Dyk and Sheridan, 2021). The authors contribution for this paper is listed in Appendix I.

5.1 Abstract

Active chemical treatment is the most widely used technique for acid mine drainage (AMD) remediation, combining effluent with an alkaline source (lime or limestone) to promote the chemical oxidation of metal species (predominantly Fe^{2+} to Fe^{3+}) and removing metal ions through the formation of hydroxide and calcium sulfate precipitates. Although limestone is considered a low-cost reagent, the amount of the chemical required to treat the volume of AMD that is produced at individual or collective mining sites results in an exorbitant cost, especially considering that these treatment schemes will have to persist for as long the mine site generates AMD – sometimes decades after closure of the mine. The use of limestone is also known to produce large amounts of sludge that requires disposal – also contributing to the cost of the overall treatment regime. In addition, the opportunity for waste re-use and waste valorization exists in the AMD treatment sphere due to the acidic nature of the waste effluent. The low pH, hydrogen rich nature of the AMD could be used to hydrolyze or hydrate other waste or by-products, treating them whilst simultaneously undergoing treatment itself. This research aimed to ascertain the effectiveness of basic oxygen furnace (BOF) slag in AMD treatment. BOF slag is a cheaper alternative to lime derivatives and requires acid pre-treatment before it can be re-used in construction. The cost benefit as well as the treatment extent (acid neutralizing capacity, metal removal, sulfate removal) of the AMD were determined in this study. BOF slag was found to be effective in the treatment of AMD with respect to pH increase, alkalinity addition and metal and sulfate removal, successfully raising the pH to a range of pH levels and subsequently allowing for high levels of metal and sulfate removal via precipitation. The percentage of removal of aluminium, iron, manganese and sulfate at a pH of 7 was 97.16 %, 99.99 %, 27.27 % and 97.59 % respectively. An increase of magnesium (+ 80.87 %) and calcium (+ 486.36 %) occurred at this pH, however at higher pH levels, a decrease in magnesium was observed. BOF slag was found to be the cheapest alkaline containing material when compared to dolomite, quicklime and hydrated lime used for similar purposes. Characterization of the sludge

produced showed the presence of heavy metal hydroxides and sulfates. This study confirms that BOF slag is a viable alternative to lime for the remediation of AMD.

5.2 Introduction

Lime and limestone dosing (for neutralization) at acid mine drainage (AMD) generating mines is commonly used as a treatment strategy in the remediation of mine affected waters. In the past this method has been widely employed to meet legislative requirements for the discharge of mine effluent into receiving waters (Maree, Tonder and Mitlard, 1996). The first full-scale implementation of limestone neutralization of AMD occurred in 2001 at an Anglo Coal mine in the Witwatersrand, with lime dosing having been carried out at this site and others for decades before this (Günther *et al.*, 2003). Lime and limestone are arguably the most widely used alkaline material for all types of dosing systems (Bosman, 1983), due predominantly to their relatively low cost, availability and simplicity of associated dosing system. Disadvantages of the process however, are (i) the voluminous amount of sludge that is produced via precipitation reactions and settling, (ii) the limited solubility and armouring of the limestone particles and (iii) the challenge associated with raising the pH of the resulting solution to >7 which is linked to inefficient removal of some species of pollutants contained in the mine water (Potgieter-Vermaak *et al.*, 2006). In addition, although the costs of these chemicals are considered to be relatively low, the temporal price variability between the different grades of lime and limestone, is substantial. For example, when the change between lime and limestone occurred at the Anglo Coal mine, a saving of R4.5 million (approximately $320 000 using an exchange rate of R14 to $1 (Google Finance, 2021)) was achieved (Günther *et al.*, 2003). If lower quality, slaked or hydrated lime was used this could result in a difference of between R3500/ton (approximately $250/ton) and R263/ton (approximately $18/ton) (Swartz, 2021). Given these variabilities, multiple studies have been conducted that aim to replace or reduce the amount of lime or lime-derived products that are used at mining sites (Kaur *et al.*, 2018).

A method that has gained use in recent years is the utilization of waste products in neutralizing operations (Moodley *et al.*, 2018; Upadhyay *et al.*, 2021). The re-utilization of waste products as value added “resources” in industrial applications supports the concept of a circular economy by aiming to ensure the recycling and utilization of resources that closes the resource loop. In a world of declining and often scarce natural resources, this increases the opportunities for economic growth as well as decreasing the amount of waste generated in other commercial activities. For the case of neutralizing acid mine waters, many waste materials have been identified, including industrial wastes such as bauxite refining residue (Power, Graefe and Klauber, 2011), paper mill waste (Pérez-López *et al.*, 2010), Portland cement and fly ash (Sephton, Webb and McKnight, 2019), as well as commercial waste such as eggshell powder (Kastyuchik, Karam and Aïder, 2017) and shrimp shell (Núñez-Gómez *et al.*, 2019). Another waste material that has shown promise in this field as well as potential to create a value added product subsequent to its use in AMD treatment, is a type of steel waste known as Basic Oxygen Furnace

(BOF) slag (Ziemkiewicz and Skousen, 1997; Name and Sheridan, 2014; Naidu, Sheridan and van Dyk, 2020).

BOF slag is characterized by its high oxide content, of which calcium and magnesium oxide form the largest percentage (Naidu, Sheridan and van Dyk, 2020). Because of these constituents, BOF slag's neutralizing ability is high, however its reuse in building and construction applications (the traditional reuse avenue for slag products (Reddy, Pradhan and Chandra, 2006; Calmon *et al.*, 2013)) is low as the presence of oxides gives a volume instability factor to the structure that has been built (Aydilek, 2015; Kambole *et al.*, 2017). Because of this, reuse in AMD remediation applications could serve a dual purpose – (i) increasing the pH of the AMD (producing clean or cleaner water) as well as (ii) removing the oxide content of BOF slag (producing a cement or concrete aggregate that exhibits a higher volume stability). This research aims to determine the viability of point (i) above by assessing the following:

1. The neutralizing ability (acid neutralizing capacity (ANC)) of BOF slag.
2. The precipitation reactions that occur in the AMD upon BOF slag addition and reaction.
3. The extent of removal of metal and sulfate species related to pH and alkalinity rise in the AMD BOF slag system.
4. The volume of sludge production in AMD using BOF slag.
5. The difference in cost associated with treating a specific volume of AMD with BOF slag vs. with traditional lime products.

These aims were assessed in the manners described below:

5.3 Experimental Procedure

BOF slag was sourced from Phoenix Slag services in Newcastle, South Africa. The BOF slag was milled to a variety of sizes, all < 15 cm in aperture, by the slag management company. Slag of aperture size < 1 cm and, and < 1 mm were separated from the larger sample via sieving. These size classes were used to perform the study. Two different types of AMD which were sourced from (A) a coal mine tailings storage facility (TSF) and (B) an AMD effluent stream in Emalahleni, South Africa (compositions of the two AMD types are shown in Table 5-1) and were used to perform this study.

Quicklime, dolomite and hydrated lime were obtained in powdered form from a local chemical distributor in Johannesburg, South Africa.

The AMD and BOF slag were contacted in (i) a plug flow reactor (PFR), and (ii) a continuously agitated batch reactor. The reaction using a batch system was allowed to progress for 72 hours, while the PFR system ran continuously for 58 days. The PFR system allowed a constant flow of ~ 25 L/day of AMD through a 3.6 L packed bed containing 3 kg of a mixed slag sample (aperture <1 cm). This allowed for a residence time of just under 3.5 hours. The batch system reacted 1.5L of AMD with 0.25, 0.5, 1, 2, 3 and 4 g of BOF slag fines (aperture < 1 mm).

5.3.1 pH and Acid Neutralizing Capacity (ANC)

The pH changes in both systems were assessed (pH was measured using a DF Robot combined pH and oxidation reduction potential (ORP) meter) and the alkalinity of the batch system was measured using the following titration method:

The total alkalinity calculated was calculated using Equation 5-1.

$$\textbf{Total alkalinity as } \mathbf{CaCO_3} = \frac{\mathbf{B \times N \times 50 \times 1000}}{\mathbf{ml\ sample}}$$

Equation 5-1

Where B was the total volume of H_2SO_4 used to titrate a liquid sample (post treatment) to a pH of 4.5; N was the normality of the acid, 50 was the mg equivalent of $CaCO_3$ and the factor of 1000 was used to convert from mL to L.

5.3.2 Oxide Content

Oxide content on the surface of the slag was evaluated using X-Ray Diffraction (XRD) as well as Scanning electron microscopy (SEM) and Energy Dispersive X-Ray Analysis (EDA). Solid samples were mounted onto a metal plate using carbon tape and coated (carbon and gold palladium) before testing. XRD sample preparation involved grinding 3 g of sample (either slag or dried precipitate) and spiking it with fluorite on a 90:10 weight basis. A Siemens D500 computer automated diffractometer was used to perform XRD.

5.3.3 Identification of metal species removal/precipitation mechanism

Liquid samples (5 mL diluted with deionized water) were taken periodically from the reactors to assess for aluminium, calcium, iron, magnesium, manganese and sulfate concentration (using an Agilent 200 series atomic spectrometer (AAS) for the metal special and turbidimetric spectrophotometric tests (using a Merck Spectroquant Pharo 300) (American Public Health Association, 1975; Center for Bioprocess Engineering Research, 2016) for the sulfate species). Samples were filtered to remove solids using 0,45 μm filters, diluted on a 1:3 ratio with deionized water and acidified with 0.6 mL of nitric acid (with a molarity of 15.6) prior to analysis. This was done to measure the difference in concentration in dissolved and precipitated metals in the samples. Dilution was necessary to ensure the concentrations within the samples were within range of the AAS instrument. Standard concentration solutions were used for each test to calibrate the AAS instrument. Metal species and sulfate concentrations were measured to assess what type of precipitation reactions were occurring. It must be noted that these experiments were run multiple times to ensure volume loss from sampling did not interfere with results. Sampling frequency varied from 10 second intervals to 24-hour intervals.

The “spent” BOF slag was assessed before and after the neutralizing reaction using XRD and Rietveld quantification analyses. XRD was performed to investigate how the chemical makeup of the BOF slag

had changed and what had become available in the AMD solution to act as counterions to facilitate precipitation.

Sludge formed in the reactor was collected, acidified (via the addition of 0.6 mL of nitric acid with a molarity of 15.6 and 15 mL of deionized water to a 0.5 g sample of dried sludge), and assessed using the same AAS and Spectroquant procedures. This was done to determine what types of precipitates had formed and to determine if the elemental species balanced across all evaluations. The sludge formation was also assessed volumetrically (volume AMD:volume sludge).

5.4 Results and Discussion

Two types of AMD were used, each with varying concentrations of sulfates and the metals of interest. The initial pH of both AMD sources was the same. The composition of both AMD sources is presented in Table 5-1.

Table 5-1: Concentrations of components of interest in two different types of AMD sourced from two different AMD dams in Emalahleni, South Africa

AMD Type	pH	Aluminium (mg/L)	Calcium (mg/L)	Iron (mg/L)	Magnesium (mg/L)	Manganese (mg/L)	Sulfate (mg/L)
Type A	2.44	435	111	3040	106	88	12956
Type B	2.47	497	175	3507	94	198	5200

An XRF and XRD analysis was performed on the BOF slag, and the major oxides found are shown in Table 5-2.

Table 5-2: Major oxides in BOF slag used for AMD treatment.

Oxide	wt.%
CaO	41.6
Fe_2O_3	20.5
SiO_2	14.4
MgO	7.2
Al_2O_3	2.8
SO_3	0.4
Loss on ignition (LOI)	5

5.4.1 Acid Neutralizing Capacity (ANC) of BOF slag

An important thing to note in the comparison between lime (quicklime, dolomitic or hydrated lime) and BOF slag is the availability of free lime in the sample (components that are available to hydrate and raise the pH of the media). The ANC of lime and free lime generally refers to the CaO component of the sample, however BOF slag contains multiple other oxides and silicates that dissolve in liquid media and contribute to the neutralization of acid or the increase of pH. Table 5-3 shows the availability of oxides (that can readily hydrate in liquid media) in lime and BOF slag. It is noted that although the free lime content in BOF slag is 13 %, this only refers to the components found on the surface of the solid particle. The free component – unreacted CaO – that is found on the surface of the particle is generally an indication of how quickly the alkaline material can react to form calcium hydroxide – thereby raising the pH of the liquid media or causing volume expansion in the solid. This indicator, however, does not take into account other oxides (FeO) (G. C. Wang, 2016) that are present on the surface nor does it take into account the other alkaline reagents (silicates) that are liberated as the surface of the particle is degraded/reacted. As dissolution and leaching occurs (largely following Lagergren kinetics (Naidu, Chauhan, *et al.*, 2020)), more oxide and silicate components become available from the BOF slag. The size of the BOF slag particle used will also affect the amount of free oxide content – smaller particles have a larger availability of free neutralizing/alkaline components than larger particles and smaller particles are more likely to dissolve completely whereas larger particles are likely to undergo a degree of leaching. This is largely due to the surface area of the particle – access to the other oxidic and silicate components in the BOF slag by an acidic medium could result in a complete hydration of the solid, whereas a larger particle would retain its solid structure.

Table 5-3: Free oxide content in quicklime, hydrated lime (Tolonen *et al.*, 2014) **and BOF slag with particle aperture between 2000-3350 microns (determined via SEM and EDA) where Wollastonite found on the surface of the particle was not considered a free oxide (due to its insolubility in water).**

Alkaline material	Oxide content (Total %)	Free oxide content (%)
Quicklime	94	91
Dolomitic Lime	53 (Dryden, 1982)	50
Hydrated lime	73	71
BOF slag	87	13

Although the free oxide content of BOF slag is significantly less than that of normal quicklime or hydrated lime, the BOF slag was still able to neutralize AMD. 80 g of slag was able to raise the pH of a sample of 800 mL Type A AMD with an initial pH of 2.44, in a continuously stirred batch reactor to (i) a pH of 7 in 540 minutes and (ii) a pH of 10 in 1365 minutes. This is shown in Figure 5-1.

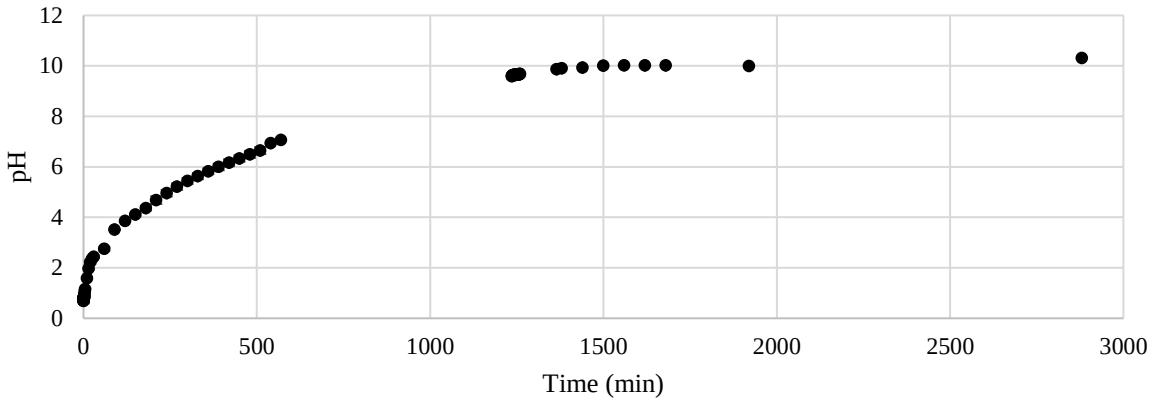


Figure 5-1: pH change over time in 800 mL of AMD in a constantly agitated reactor when 80 g of slag with particle aperture between 2000-3350 microns has been added.

During the experiment (results shown in Figure 5-1) it was observed that the pH in the system did not stabilize, even after 72 hours of reaction time – indicating that the slag remaining in any sludge that is produced in the system (metal sulfate and hydroxide precipitate) has a high potential for reuse and would function well in a high density sludge (HDS) system. The sludge in a HDS system would be recycled to provide alkalinity to a fresh AMD stream. The observed pH rise in the system was directly related to (i) the volume of AMD and amount of BOF slag added (the solids loading of the solution in g of BOF/ml of AMD), (ii) the composition of the AMD, (iii) the particle size of the BOF slag and (iv) the allowed reaction time. An indication of this is the difference between the experiment in Figure 5-1 (80 g of fines in 800 mL to a pH of 7 in 540 minutes), and a similar experiment in which 15 g of slag fines (aperture of 1000 microns or less) was able to increase the pH of 1500 mL of Type B AMD (significantly lower initial sulfate and iron concentration) to a pH of 7 in 55 minutes – showing the difference in behaviour of the system when two AMD sources with different compositions are used.

Similarly, 67 g of fine BOF slag was able to raise 200 mL mL of this Type B AMD to a pH of 7 in 5 minutes – showing the difference that solids loading can have on reaction time. The alkalinity addition corresponding to the last data point collected in the experiment shown in Figure 5-1, was 2897 units of alkalinity as $CaCO_3$ in mg/L. The pH rise in these systems also correspond to a number of precipitation reactions that effectively remove metal species from the AMD solution upon settling. These reactions are dependent on the pH of the system and therefore are dependent on points (i) to (iv) above. The composition of AMD is expected to change at each different mine site and therefore the findings from this study are particular to the AMD found in the Witwatersrand region. The particle size of the BOF slag (point (iii) used in the experiments discussed in this study are all <1 mm in aperture (slag fines) to keep them as comparable as possible to powdered and granular dolomite and lime. Lastly, the reaction time is kept constant at 55 – 60 minutes, however, it is important to note that longer reaction periods will yield more leaching or dissolution of alkali components. The removal of metal species from the AMD solution under the action of pH change is elaborated on below.

5.4.2 Identification of metal species removal/precipitation mechanism and indication of precipitation kinetics as a function of pH

5.4.2.1 Aluminium

The initial concentration of aluminium in the AMD (Type A) was 434 mg/L. Aluminium in acidic media most commonly forms an aqueous cation, with an oxidation number of +3 (Harding, Johnson and Janes, 2002). Addition of an alkaline material (which will hydrate and dissociate to form hydroxide units) to the solution, will first precipitate an insoluble aluminium hydroxide (by Equation 5-2):

$$Al^{3+}(aq) + 3OH^{-}(aq) = Al(OH)_3(s)$$

Equation 5-2

This was considered the main mechanism of aluminium removal in the system. It is important to note that both aluminium oxide and hydroxide species are amphoteric in nature. In acidic solutions, they will dissolve and assist with neutralizing the acid (shown in Equation 5-3):

$$Al(OH)_3(s) + 3H^{+}(aq) = Al^{3+}(aq) + 3H_2O(l)$$

Equation 5-3

Excess hydroxide units in the solution could also cause the aluminium hydroxide to form a tetrahydroxyaluminium ion via reaction shown in Equation 5-4:

$$Al(OH)_3(s) + OH^{-}(aq) = [Al(OH)_4]^{-}(aq)$$

Equation 5-4

Aluminium sulfate or sulfide could also potentially form as there is an excess of sulfate in the AMD. However, aluminium sulfate has a very high solubility product (K_{sp} of 69.2) which means it will not precipitate. Similarly, aluminium sulfide, also with a very high K_{sp} is rapidly hydrolysed in an aqueous solution to form aluminium hydroxide and hydrogen sulfide gas – thus it is unlikely that removal of aluminium occurred in this manner. Aluminium was removed from the solution almost completely (to a concentration of 10.7 mg/L) at a pH of 3.8 and redissolution did not occur even at a pH level of 9. Judging by the solubilities of aluminium compounds as well as the pH at which the system yielded results, it was concluded that the removal of Al involved the formation of Al(oxy)hydroxide, not aluminosilicates or basic aluminium sulphates (Tipping *et al.*, 1988).

Figure 5-2 shows the change in concentration of the aluminium ion in solution of Type A AMD as the pH of the solution changes. As shown, there are three distinct behavioural patterns/slopes – between pH levels 2.5 and 4, between 4 and 9, and between 9 and 10. To remove aluminium, the best pH range for the BOF slag neutralized system is between 4 and 9, corresponding to an addition of between 0.42 – 0.828 g/ml of AMD. The lowest attainable aluminium concentration using BOF slag as an alkaline

source was 10.7 mg/L. Water with this concentration of aluminium may be used as industrial or operational water (depending on the type of process) as well as for irrigation (DWAF, 1996a, 1996b).

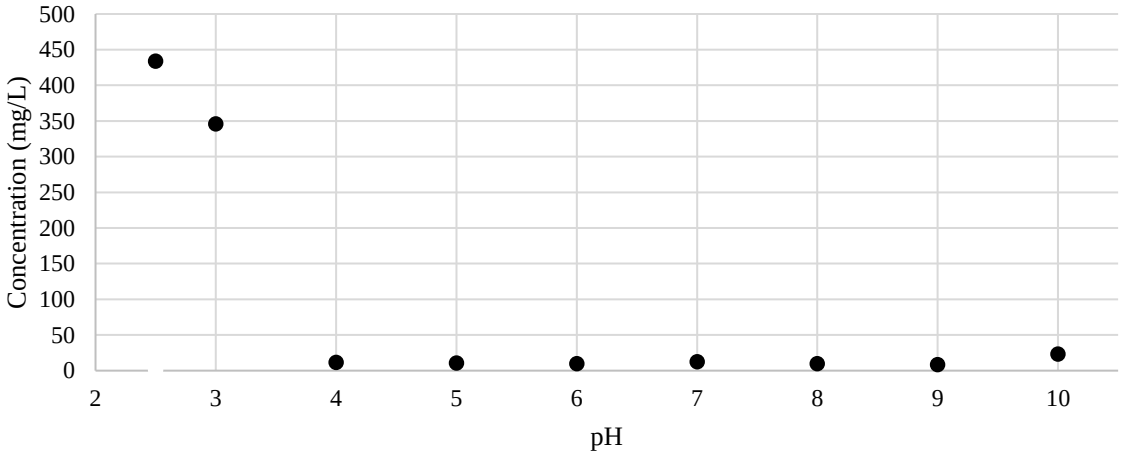


Figure 5-2: Aluminium concentration in AMD over varying pH levels (when pH is altered via addition of BOF slag).

5.4.2.2 Calcium and Magnesium

Calcium and magnesium were present in the AMD at a concentration of 110 mg/L and 115 mg/L (AMD type A) respectively. Calcium (as well as magnesium) was also added to the solution through the dissolution (hydration and dissociation) of the BOF slag. Calcium and magnesium in aqueous solutions are found in the form of a positive cation with an oxidation number of +2. Both calcium oxide and calcium hydroxide have an intermediate solubility in water and calcium will not precipitate out of solution as either of these species. Calcium sulfate has higher solubility than calcium hydroxide (experimentally exhibiting a solubility of 0.274% w/w compared to calcium hydroxide which exhibited a solubility of 0.12% w/w in water at 20 ° C (Royal Society of Chemistry, 2020)), however due to the saturation of the solution with sulfates (initial Type A AMD concentration of 12955 mg/L) and the reaction of the hydroxyl group with multiple other elements – the bulk of the calcium removal is achieved via gypsum precipitation. Despite the precipitation of calcium sulfate, the calcium concentration increased in the system with increasing pH. At a pH of 9 the calcium concentration in the sample was 1348 mg/L.

When the BOF slag comes into contact with liquid, hydration will take place and calcium hydroxide will form. If this hydrated BOF slag is then exposed to air, carbon dioxide will react with this to form calcium carbonate (by Equation 5-5 (Earl and Wiford, 2104)) which has a low solubility in water (National Center for Biotechnology Information, 2022a):

$$Ca(OH)_2\,(aq) + CO_2\,(g) = CaCO_3\,(s) + H_2O\,(l)$$

Equation 5-5

The pH raising capacity of the BOF slag in neutral solutions will thus be lowered if this occurs, however further reaction with an acidic media can result in the formation of carbon dioxide and water (Equation 5-6 (Brown; *et al.*, 2009)):

$$CaCO_3\,(s) + 2H^+\,(aq) = Ca^{2+}\,(aq) + CO_2\,(g) + H_2O\,(l)$$

Equation 5-6

It is thus recommended to keep the BOF slag dry before use as a reagent, and once it is in use keep the particles submerged. Magnesium is most likely removed from the solution in the form of magnesium sulfate (which has a solubility of 33.7% w/w in water) and magnesium hydroxide (which is soluble in acidic solutions but less so in basic solutions (Royal Society of Chemistry, 2020)). Magnesium decreased in solution at a pH of 9 (to a concentration of 61.7 mg/L).

Figure 5-3 and Figure 5-4 show the change in concentration of the magnesium and calcium (respectively) in Type A AMD when solution is gradually neutralized with BOF slag. Magnesium and calcium are expected to behave differently to the other ions in the AMD solution as slag leaching and dissolution may result in an increase of these ions in solution. According to the graphs shown in Figure 5-3 and Figure 5-4, in terms of magnesium removal, a pH of 8,5 and above would be ideal as this allows for the magnesium concentration to be within SANS241 drinking water limits. In the event that the treated AMD is used for irrigation, the ideal pH for magnesium removal would be lower, as the concentration of Mg in water for agricultural use is seemingly negligible (DWAF, 1996b). The calcium concentration rises with increase in pH (and increase in mass of BOF slag added) but experiences a decrease in concentrations between pH 5 and 8. This is attributed to the precipitation of gypsum in the solution once the concentration of calcium has reached a supersaturated zone (for this pH). From a pH of 8 onwards, the concentration once again rises.

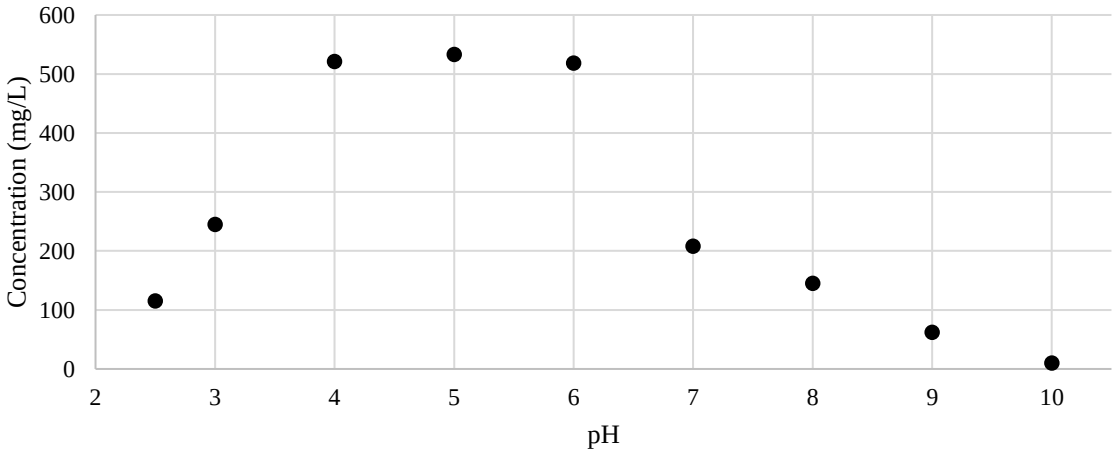


Figure 5-3: Magnesium concentration in AMD over varying pH levels (when pH is altered via addition of BOF slag).

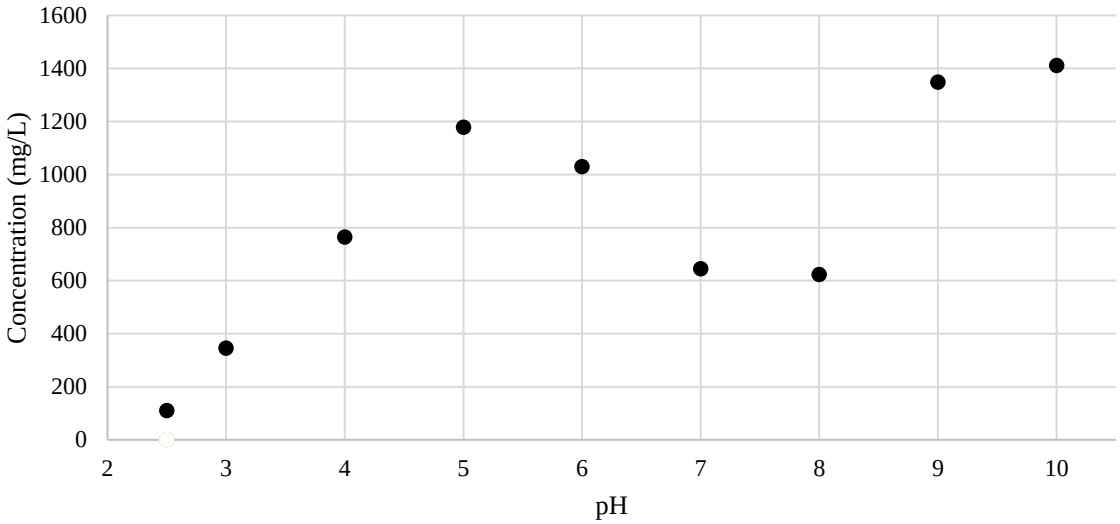


Figure 5-4: Calcium concentration in AMD over varying pH levels (when pH is altered via addition of BOF slag).

There is no ideal pH level for calcium concentration – this water cannot be used as drinking water, but may be used as process water (dependent on the process) or can be discharged to the environment (Department of Water Affairs and Forestry, 1996b).

5.4.2.3 Iron

Under acidic conditions, the most stable oxidation state of iron is 2+. If the AMD is aerated then the redox potential of the water is such that it allows for oxidation of the ferrous iron (2+) contained in the solution to ferric iron (3+) which can then precipitate as iron hydroxide, $Fe(OH)_3$ via reactions described by Equation 5-7 and Equation 5-8 (Silver, 2012).

$$4Fe^{2}\,(aq) + 3O_2\,(g) + 2H^{+}(aq) = 2Fe^{3+}\,(aq) + H_2O\,(l)$$

Equation 5-7

$$Fe^{3+}\,(aq) + 3OH^{-}\,(aq) = 2Fe(OH)_3\,(s)$$

Equation 5-8

Fe^{3+} has a low solubility at certain pH levels and generally precipitates out of solution. In the case that the system is anaerobic – and if excess CO_3^{2-} is available in the solution (as may be the case if BOF slag is hydrated and then exposed to air) – an $Fe(HCO_3)_2$ salt is formed. Upon exposure to air this can lead to the formation of $FeCO_3$ (via the reaction shown in Equation 5-9 (National Center for Biotechnology Information, 2022b). At the right temperatures (> 200 °C) $FeCO_3$ will react with oxygen to form Iron (III) Oxide (Othmer, 1995). This reaction is shown in Equation 5-10.

$$Fe(HCO_3)_2 \rightarrow FeCO_3 + CO_2 + H_2O$$

Equation 5-9

$$O_2 + 4FeCO_3 \rightarrow 4CO_2 + 2Fe_2O_3$$

Equation 5-10

During the experiments described in the method section, iron was almost completely removed at a pH of 7 (from an initial concentration of 3039 mg/L to 0.289 mg/L). This is in line with findings in literature; the Pourbaix diagram predicts very little Fe at this pH (McCafferty, 2010). In Figure 5-5 below, the concentration of iron in solution as the pH is altered using BOF slag addition is shown. The ideal pH for iron concentration would be between a pH of 7 and 8 as this allowed for the greatest removal from solution.

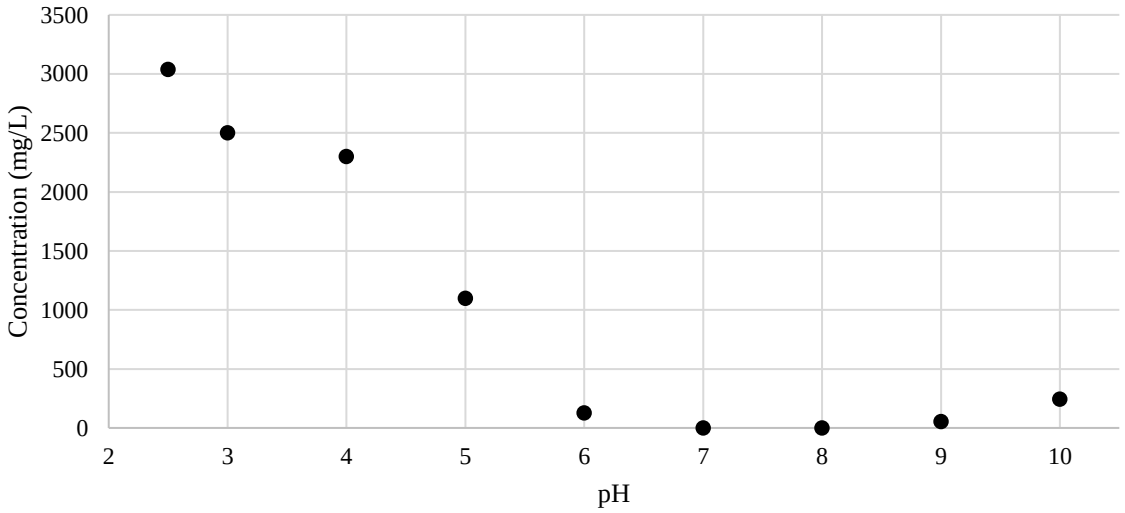


Figure 5-5: Iron concentration in AMD over varying pH levels (when pH is altered via addition of BOF slag).

5.4.2.4 Manganese

Under acidic conditions, the most stable oxidation state of manganese is 2+. In this state, manganese is moderately soluble in the form of $MnSO_4$ and thus very little Mn removal is attributed to $MnSO_4$ formation and precipitation. At pH levels of 8 and above, manganese can precipitate as $MnCO_3$ and $Mn(OH)_2$ (Lei *et al.*, 2009). In aerated systems (under oxidizing conditions), Mn in the 3+ and 4+ can also form MnO_2, Mn_2O_3 and Mn_3O_4 even at lower pH levels – compounds which are all insoluble in water. It must be noted that interactions among metals in the AMD solution influence the rate and degree to which metals precipitate. Precipitation of iron will remove manganese from solution at a pH of 8 due to co-precipitation when the iron concentration is 4 times (or more) greater than the manganese concentration. If the iron concentration in the AMD is less than four times the manganese content, manganese will likely not be removed by co-precipitation at neutral conditions and a solution with a pH of >9 is then necessary to remove this metal (Lehigh Environmental Initiative, 2011). Manganese in the system decreased from 88 mg/L to 52 mg/L at a pH level between 6 and 9. It should be noted that initially manganese increased in the system – this could be attributed to dissolution of manganese containing compounds in the BOFS (XRF analysis shows Mn makes up 3% by weight of BOF slag).

The relationship between manganese and pH is shown in Figure 5-6. Manganese is at its lowest concentration at a pH of 10. Further treatment will have to be undertaken to remove more manganese.

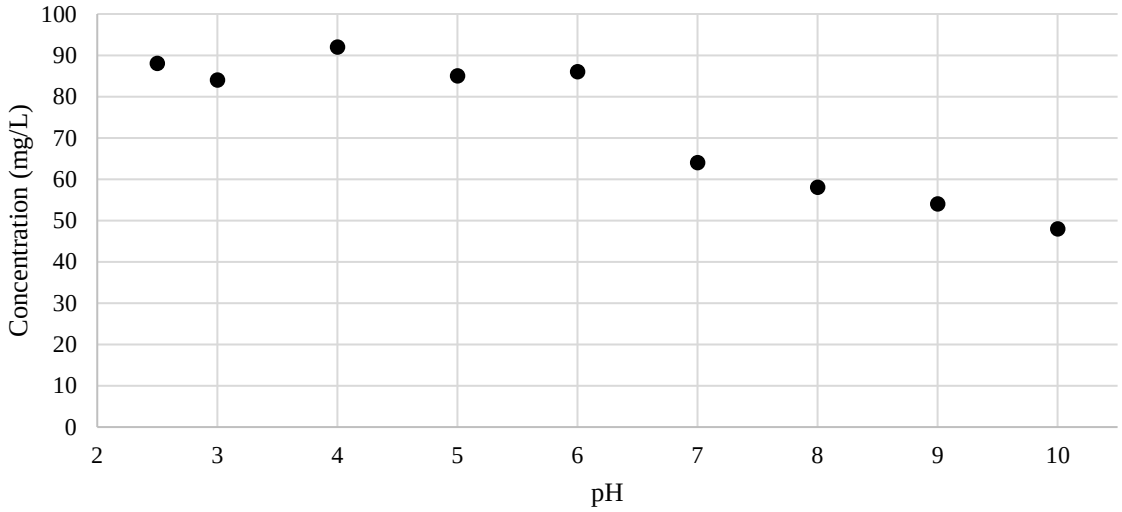


Figure 5-6: Manganese concentration in AMD over varying pH levels (when pH is altered via addition of BOF slag).

5.4.2.5 Sulfate

Sulfate in the system is likely to form any of the compounds found in Table 5-4 (Brown; *et al.*, 2009; Silver, 2012; National Center for Biotechnology Information, 2021). The most likely mechanism for sulfate removal is via the precipitation of calcium sulfate. Calcium becomes abundantly available in the solution through the dissolution of the BOF slag and can then bind with the sulfate ion to form a nearly insoluble product. The solubility of each possible sulfate compound is shown below, and it is likely that a small percentage of sulfate is also removed via formation of small amount of other compounds. Sulfate decreased to 269 mg/L at a pH of 11.4.The manner in which sulfate is dependent on the pH of the system (which in turn is dependent on the amount of BOF slag that is mixed into the solution), is shown in Figure 5-7 below. At a pH of 4, the sulfate concentration is lowered substantially – which corresponds with a plateau in the concentration of magnesium as well as a rise in the concentration of calcium. Therefore, any pH above 5 and below 10 should be sufficient at removing a significant amount of sulfate (to bring the AMD to within environmental discharge limitations).

Table 5-4: Solubility of sulfate compounds % weight/weight in water at 25° C

Magnesium Sulfate	33.7
Manganese (II) Sulfate	62.9
Iron (II) Sulfate	26.3
Calcium Sulfate	0.274
Iron (III) Sulfate	Slightly soluble
Aluminium Sulfate	36.4

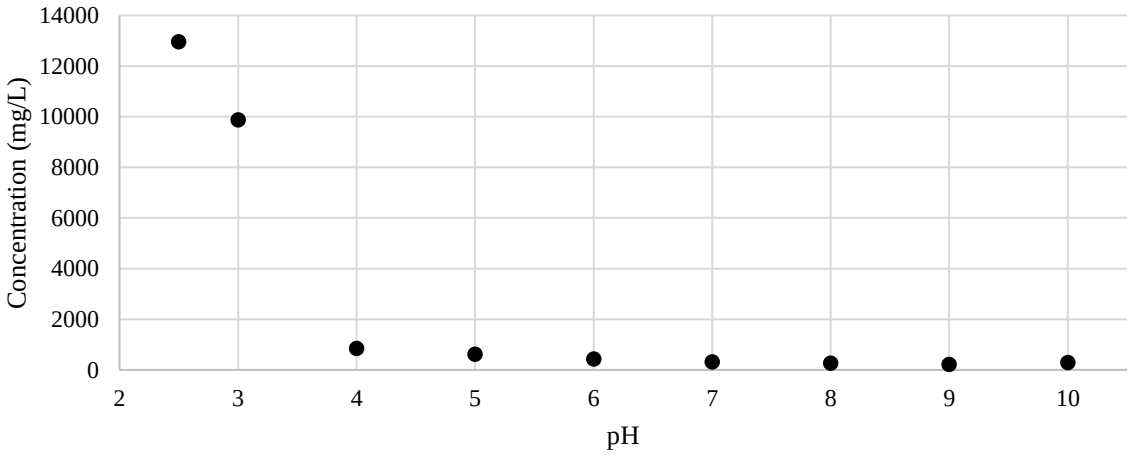


Figure 5-7: Sulfate concentration in AMD over varying pH levels (when pH is altered via addition of BOF slag).

5.4.2.6 Overall Assessment

The observed results discussed thus far have been consolidated in Table 5-5. For this particular system, in which the pH is altered by the addition of different masses of BOF slag (Figure 5-8) the equations presented in Table 5-5 represent the relationship between the pH of the system (which is based on the mass of the BOF slag that is added per mL of AMD) and the concentration of the ionic metal species at that pH. These equations are specific to this type of AMD and depend on the presence of counterions in the solution as well as the pH and alkalinity added by the slag particles.

Taking into account all of the metal species which have been assessed in this study, and the pH levels at which their maximum precipitation (and therefore removal) occurred, the following conclusion can be drawn: a pH of 7 allows for the best combination of removal of ionic species in the solution via precipitation.

According to the findings presented in Figure 5-8, the best addition rate (in accordance with the desired pH of 7) is 0.785 g of BOF slag/ mL of AMD.

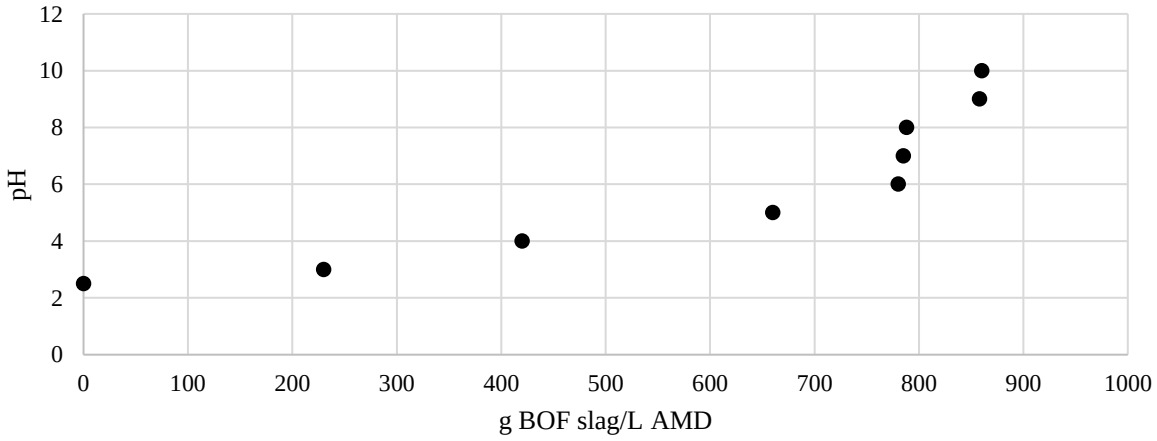


Figure 5-8: pH of an AMD system with different loading rates of BOF slag

The approximate equation that governs the pH change as dosage of BOF slag changes is given by

$$y = 4E - 08x3 - 3E - 05x2 + 0.0106x + 2.3936$$

, where x is the loading rate of BOF slag in AMD in g/L, and y is the resulting pH.

Table 5-5: Equations governing the concentration of ionic metal species in solution as a function of pH when the pH is altered via addition of BOF slag

Species	pH Range	Type of relationship	Co-efficient of Determination	Equation (x is the pH and y is the concentration in mg/L)
Aluminium	2.5 - 4.0	Linear	0.9819	y = -289.21x + 1179.7
	4.0 - 9.0	Polynomial	0.6151	$y = -0.1778x^3 + 3.331x^2 - 20.306x + 50.838$
	9.0 - 10.0	Linear	1	y = 14.7x - 123.8
Calcium	2.5 - 5.0	Linear	0.9995	y = 424.85x - 940.32
	5.0 - 8.0	Polynomial	1	$y = 100x^3 - 1918.5x^2 + 11856x - 22637$
	8.0 - 10.0	Polynomial	1	$y = -331x^2 + 6352x - 29009$
Iron	2.5 - 10.0	Polynomial	0.9586	$y = 95.344x^2 - 1587.7x + 6563.1$
Magnesium	2.5 - 10.0	Polynomial	0.9522	$y = 9.775x^3 - 208.73x^2 + 1317.4x - 2050.2$
Manganese	2.5 - 10.0	Polynomial	0.9503	$y = 0.0402x^4 - 0.6632x^3 + 1.737x^2 + 7.118x + 65.805$
Sulfate	2.5 - 4.0	Linear	0.9926	y = -8210.9x + 33893
	4.0 - 10.0	Polynomial	0.9967	$y = 27.655x^2 - 481.77x + 2332.1$

5.4.3 Sediment/precipitate formed.

An SEM and EDA analysis was performed on the precipitate which had formed on the surface of the BOF slag particle.

An unreacted BOF particle is shown alongside a particle with precipitate formation (after reaction) in Figure 5-9. The notable presence of nanorod structures in the image of the BOF slag particle after reaction with AMD is indicative of the presence of iron oxide and gypsum precipitate (Sayed and Polshettiwar, 2015).

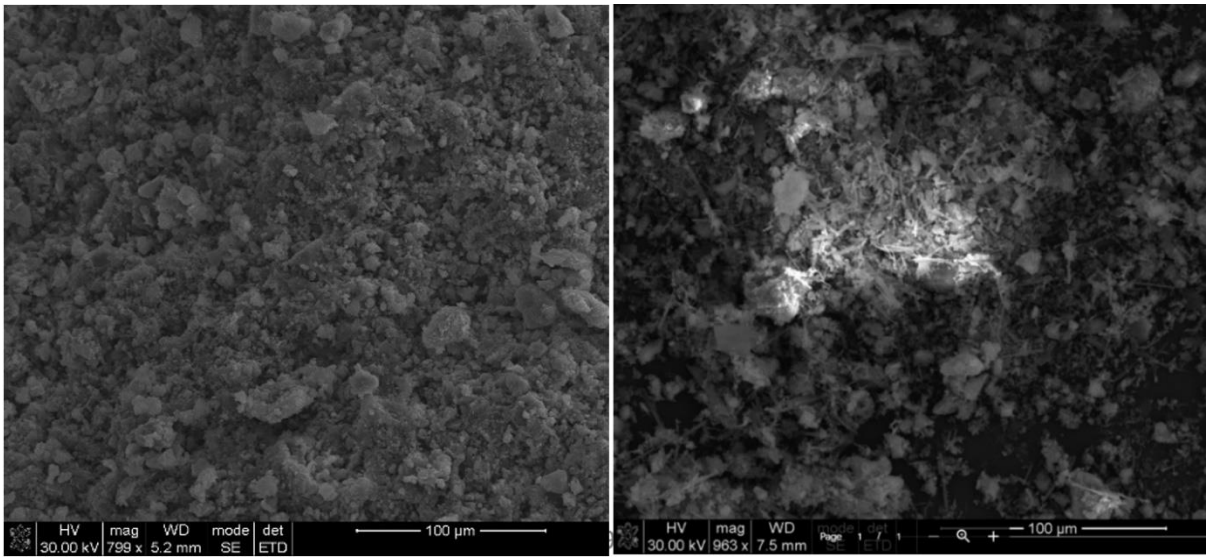


Figure 5-9: Left: SEM of unreacted BOF slag particle (aperture < 1 cm), Right: SEM of precipitate formed on surface (of BOF slag with aperture size < 1cm) after reaction of BOF slag and AMD for a period of 32 hours.

The results from the SEM on the precipitate covered BOF slag particle confirmed a decrease in the presence of oxygen, calcium and magnesium on the surface of the particle after reaction with AMD – indicating that the calcium and magnesium oxides from the surface had undergone reaction. The EDS data also showed an increase in the presence of iron, manganese, aluminium and sulfate – indicating that these elements had precipitated and adhered to the surface of the BOF particle. The decrease in oxygen on the surface and the increase in silicate and sulfate percentage, indicates that some of the metals found on the surface of the particle precipitated as sulfates and silicates. It must be noted that the EDA data is qualitatively and not quantitively meaningful. Table 5-6 shows the difference in the presence of certain elements on the surface of the BOF slag particle before and after AMD reaction.

Table 5-6: Qualitative results of presence of elements on the surface of BOF slag before reaction and surface of BOF slag after reaction with AMD for 32 hours.

Element	BOF Surface before AMD reaction (%)	BOF Surface after BOF reaction (%)
O	15.2	11.1
Ca	6.8	2.4
Mg	0.9	0.4
Fe	0.5	3
Mn	0.2	0.3
Si	1.2	1.8
Al	0.5	0.6
S	0	0.8

It is likely, given the chemistry of the AMD solution and the difference in initial concentration and pH and final concentration and pH, that the majority of precipitates formed were sulfates and hydroxides. This was confirmed by testing the sulfate concentration of the acidified precipitate which resulted in a sulfate content of > 63% by mass. Thus the sludge contains significant amounts of metal sulfate

components. The mass of sludge formed vs addition of BOF slag in 1 L of AMD is presented in Figure 5-10.

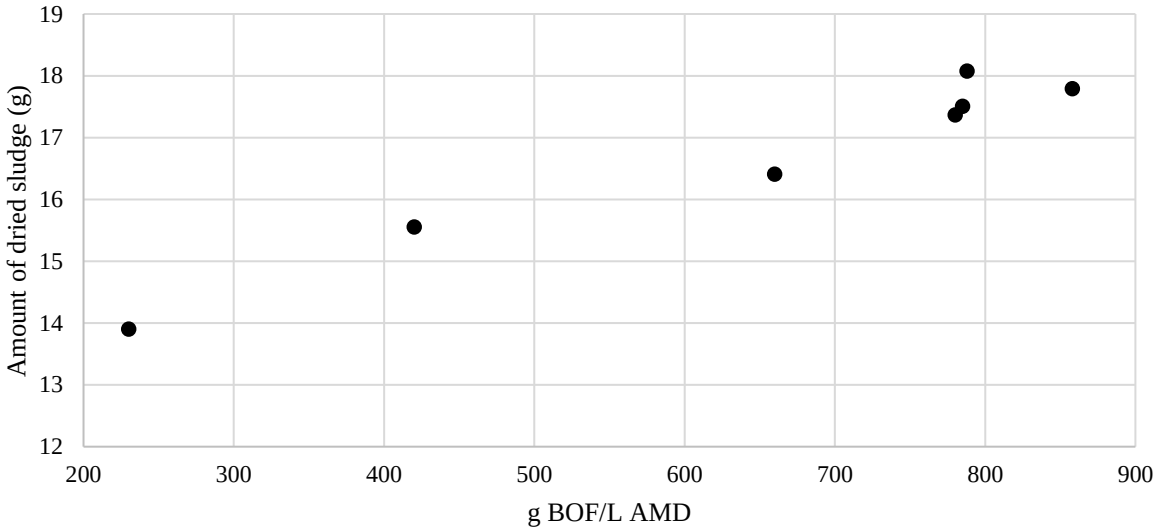


Figure 5-10: Mass of sludge formed (after drying) in a Type A AMD solution containing different concentrations of BOF slag.

This sludge contains heavy metals and hydroxides, and thus can be recycled in an HDS system to lower the dosage and the amount of produced sludge. Furthermore, sludge quantity can be reduced by using larger particles of BOF Slag that can be used in construction subsequent to treatment by AMD (an option with a possibility of this treatment becoming a revenue generating stream). Lastly, this sludge (which contains material that is frequently used as aggregates in the cement and concrete industry can be used as a method to prevent further leaching and AMD generation from exposed rocks and closed/abandoned mine sites (Demers *et al.*, 2015). This sludge has also shown promise in agricultural applications, used as a fertilizer (Naidu, 2020).

5.4.4 Cost Analysis

Slag management companies sell BOF slag at a cost of R121/ton inclusive of value added tax (VAT) (Vermuelen, 2019) cost updated according to a cost increase of 10% per year. This cost is applicable to any particle size as the management company mills the slag to the desired size. Protea Chemicals provides hydrated powdered lime at an estimated cost of R3500/ton (Naidoo, 2021) and dolomitic lime is sold at prices between R302.45 and R408.25 (Swartz, 2021).

The pH of the system (for typical neutralization applications) should be at 7, however if different levels of precipitation for different metal species is desired to be achieved, then higher pH values could be established. The amount of lime in comparison to the amount of BOF slag required to increase the pH of 1L of Type B AMD to a pH of 7 at a reaction time of between 30 and 55 minutes, in terms of the associated cost, is shown below in Table 5-7 (Department of Mineral Resources, 2010; Maree *et al.*,

2013; United States Geological Survey Mineral Resources Program, 2014; Othman, Sulaiman and Sulaiman, 2017; U.S. Geological Survey, 2020).

Table 5-7: Cost of raw material when treating 1L of AMD to a pH of 7 in 30 - 55 minutes.

pH	Dolomitic Lime (R/L)	Quicklime (R/L)	Hydrated lime (R/L)	BOF slag (R/L)
7	0.008	0.0073	0.025	0.00121

According to this data, BOF slag is the cheapest lime source for AMD treatment (of those considered).

5.5 Conclusions and Recommendations

BOF slag was found to be effective in the treatment of AMD with respect to pH increase, alkalinity addition and metal and sulfate removal. It successfully raised the pH (to a range of pH levels depending on mass to volume ratios) and precipitated metal and sulfate compounds. The amount of metal and sulfate removal following the addition of BOF slag to an AMD system until a pH of 7 was reached was as shown in the summary below (Table 5-8)

Table 5-8: Summation of metal and sulfate removal percentage using BOF Slag added to an AMD Type A sample until a pH of 7 was reached

pH	2.5	7	% Removal
Aluminium	434	12.3	97.16
Calcium	110	645	Increase 486.36
Iron	3039	0.289	99.99
Magnesium	115	208	Increase 80.87
Manganese	88	64	27.27
Sulfate	12955	312	97.59

BOF slag was found to be a cheaper alkaline containing material when compared to dolomite, quicklime or hydrated lime used for similar purposes and additionally has the benefit of being a recycled product. Characterization of the produced sludge showed a production of heavy metal hydroxides and sulfates. Further investigation into the use of the sludge in a recycle stream (HDS systems) would need to be conducted to determine whether BOF slag will also be effective in these applications. Investigation into the reuse of the sludge and for agricultural or construction purposes would also need to be done to explore this route.

This study confirms that BOF slag is a viable alternative to lime. The use of this alternative has environmental benefits; reliance on virgin materials is lessened, and waste materials are re-used whilst simultaneously undergoing treatment. The potential for revenue stream generation via the re-use of the BOF slag in construction and the cheaper price of BOF slag (in comparison with other traditionally used alkaline sources) provides an economic benefit as well.

6 Sulfate Reducing Micro-organism treatment of AMD in a BOF Slag Neutralized Solution.

This Chapter is presented in two parts, the first being in the form of a technical note which discusses the kinetics of biological sulfate reduction under specific conditions in a batch reactor, and the second being in the form of a journal article which determined the functionality of SRM in a small-scale continuous system at similar conditions to the batch system. Both experiments confirm that sulfate reduction and removal of sulfate occurred in an AMD stream using biological sulfate reducing agents.

6.1 Part 1: Biological sulfate reduction of AMD in a small-scale batch reactor – kinetics and conditions

6.1.1 Abstract

A small-scale batch reaction was assessed with regard to the rate of sulfate reduction in a basic oxygen furnace (BOF) slag neutralized acid mine drainage (AMD) effluent sample. Untreated sugarcane bagasse was used as a substrate and nutrient source for sulfate reducing microorganisms (SRM) which were added to the system to facilitate biological sulfate reduction. The reaction was duplicated and run over a period of 60 days in two, 5 L, sealed glass containers, each containing 100 g of partially hydrolyzed sugarcane bagasse. The assessment of the reaction confirmed that a first order process was followed with relation to sulfate reduction (following the reaction: Organic matter + $SO_4^{2-} \rightarrow CH_3COO^- + HS^- + HCO_3^-$), with a rate constant of 0.0091 day^{-1} being calculated at a temperature of approximately 26 ° C.

6.1.2 Introduction

Sulfate reducing micro-organisms (SRM) have been used in acid mine drainage (AMD) treatment regimes with success for at least the last 20 years (Utgikar *et al.*, 2002). The use of sulfate reducing bacteria (SRB) and other SRM to treat AMD with high sulfate concentrations is not ideal for the following reasons: (i) the residence time required for this type of biological treatment is high (Magowo, 2014), (ii) the sulfide production from large amounts of sulfate could potentially be high and would pose a risk to nearby industrial processes as well as impede the functioning of the SRM (Reis *et al.*, 1992; Tang, Baskaran and Nemati, 2009), (iii) the nutrient (phosphorous, carbon and nitrogen) requirements for the growth of the SRM to facilitate this level of sulfate removal is high and adds substantial cost to the operation (Metcalf & Eddy *et al.*, 2014). Combining this technology with a traditional dosing scheme, would combat a lot of these issues – with the exception of the additional cost of the alkaline agent. In this regard, basic oxygen furnace (BOF) slag can be used as an alkaline pretreatment reagent substitute, lowering costs, but still allowing for more efficient biological sulfate reduction (due to the more neutral pH's, and lower sulfate and metal concentrations that this gives rise

to). Due to the lower amounts of sulfate that would need to be reduced in this type of treatment scheme (high concentrations of sulfate would be removed via metal sulfate precipitation through a pH increase first), fewer nutrients would be required. Waste or by-product materials can potentially be used to provide these nutrients in an attempt to keep the cost of treatment down. The sulfate reduction facilitated by SRM using organic matter as a carbon source is given by Equation 6-1.

$$\text{Organic matter} + SO_4^{2-} \rightarrow CH_3COO^- + HS^- + HCO_3^-$$

Equation 6-1

The results of a batch test which was run to determine the kinetics of biological sulfate reduction at a pH of > 5 and <7, in an AMD system where BOF slag had been used as an alkalizing agent are discussed in this note. The kinetics of the reaction were determined at a temperature of 26°C, using sugarcane bagasse (a waste product from the sugar industry) as the carbon and nutrient source. The aim of the experiment was to determine the reaction rates of the biological process with specific regard with utilization of reagents. Parameters influencing the kinetics of the reaction (such as metal ion content, nutrient availability, SRM consortium type and growth rate) were not taken into account – the kinetics were determined at a single set of predetermined parameters.

6.1.3 Materials

BOF slag was sourced from a steel slag management company (Phoenix Slag) in Johannesburg South Africa. The slag used in the experiment had an aperture size < 1mm. X-ray diffraction and X-ray fluorescence were used to identify the components and the amount of components in the slag particles. These analyses were performed by the Earth Lab at the University of the Witwatersrand using a Malvern Panalytical Wavelength Dispersive (WD) XRF machine. Sample preparation included drying of the particles and pulverizing them using a crusher. XRD was conducted under contract by the School of Chemistry at the University of the Witwatersrand, using a Bruker Discover D8 machine (external laboratory).

Sugarcane bagasse was sourced from Illovo sugar in Eston, South Africa. This material was not processed in any way before use. A C, N, S, and P analyses were performed on this sugarcane bagasse using a Leco Elemental Analyzer (this was performed by Leco Africa).

AMD was sourced from a coal mine dump in Mpumalanga, South Africa. A Merck Pharo 300 spectrophotometer was used to analyze iron, sulfide and sulfate concentrations. Merck test kits were used to analyze for these anions and cations. Additionally, CeBER (Center for bioprocess engineering research, 2016) methods were used to analyze sulfate. Merck test kits were also used to analyze chemical oxygen demand (COD) content of the AMD stream after it had been put into contact with sugarcane bagasse.

SRM were cultivated using mixed cultures of SRM obtained from the Northern Wastewater Treatment Works, Emmerantia Dam in Johannesburg, South Africa and from previous AMD/SRM experiments. This mixed culture was grown in nutrient rich media (containing 5 g of sodium citrate, 4.5 mL of sodium lactate, 1 g of yeast extract and 4.5 g of Magnesium sulfate heptahydrate in 1 L of deionized water). An attempt was made to desensitize the culture to AMD and BOF slag conditions by adding 3 mL of a diluted BOF slag neutralized AMD to the sample every 2 days for a period of 28 days.

6.1.4 Method

Ten litres of raw AMD was contacted with 300 g of unprocessed sugarcane bagasse for a 3 day period. The AMD was then drained from this solution and mixed with BOF slag fines in a continuously stirred reactor until a pH of 6.5 was achieved. This sample was then allowed to settle under gravity, and the supernatant was drawn off and tested for sulfate, iron, calcium, aluminium, manganese and magnesium. The sample was then divided into 3 L aliquots and doped with 200 mL mL of SRM inoculum. Five-litre glass jars were packed with the equivalent of 100 g of sugar cane bagasse each and filled with the partially treated AMD/SRM mixture (3 L). The 5 L tanks were sealed with parafilm and silicone tape with a single outlet being controlled via syringe. These vessels were allowed to sit for a total of 60 days with a total of 16 x 5 mL samples being taken from each of these vessels at different time intervals. Only sulfate was analyzed from these samples, with the exception of the first sample (20 mL) which was analyzed for sulfate, calcium, manganese, magnesium, iron and aluminium using spectrophotometric and AA techniques (as described in the methods chapter, Chapter 3).

6.1.5 Results and Discussion

One of the 5 L jar's sealing mechanism failed, resulting in aeration of the sample and an environment that could not sustain anaerobic sulfate reduction. Thus, an average of two vessels was used to determine the kinetics of the reaction. The initial composition of species in the jars are shown in Table 6-1. It is noted that the nutrient quantity was the total amount available and not necessarily the total amount that was accessible to SRM culture – some of these nutrients may have been entrained in the cellulosic structure of the bagasse.

Table 6-1: Initial compositions of effluent in 5 L jar reactors with nutrient availability (carbon, nitrogen and phosphorous) being calculated using LECO analysis results

Component	Concentration (mg/L)
Sulfate	440.6
Calcium	302.4
Magnesium	84
Manganese	25
Aluminium	11.5
Iron	89
Available carbon (g)	32.78
Available nitrogen (g)	0.36
Available phosphorous (g)	2.3

The sulfate concentration of the combined systems over time is shown in Figure 6-1, with the error margin (given as coefficient of variance %) displayed in Table 6-2.

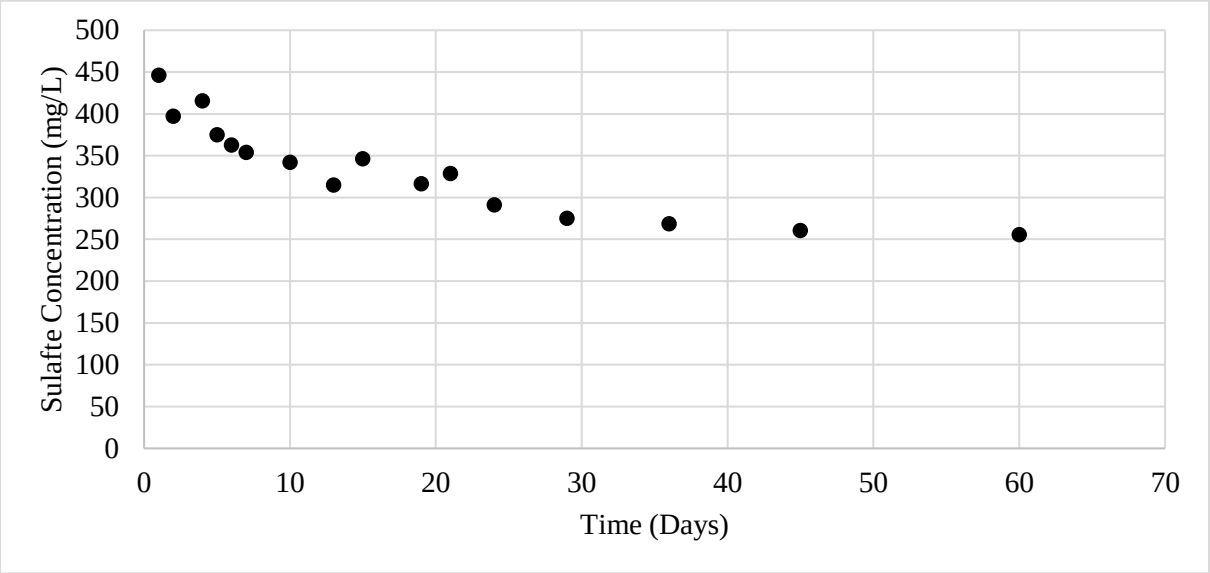


Figure 6-1: Average sulfate concentration over time for the sealed AMD/SRM vessels

Table 6-2: Standard deviation (coefficient of variance) for results used to determine sulfate reduction kinetics

Sample Day	Coefficient of Variance (%)
1	1.27
2	12.25
4	3.93
5	6.45
6	4.46
7	0.56
10	3.85
13	5.40
15	15.11
19	8.32
21	10.55
24	6.24
29	1.82
36	2.43
45	3.27
60	4.94

The results as shown graphically in Figure 6-1, suggest that the reaction progressed as a first order reaction, following the rate law as given by Equation 6-2. This was similar to what was found in literature for bacterial induced sulfate reduction in effluent from a Brazilian oil reservoir (Bernardez *et al.*, 2013).

$$\frac{d([SO_4^{2-}])}{dt} = -k[SO_4^{2-}]$$

Equation 6-2

Where:

d([SO_4^{2-}])/dt denotes the change in the concentration of the first-order reactant '[SO_4^{2-}]' in the time interval dt.

-k is the rate constant of the first order reaction (in this case with unit day^{-1})

[SO_4^{2-}] denotes the concentration of the first-order reactant [SO_4^{2-}]

Using integrated rate law analysis, the rate constant for this reaction was calculated using the data shown in Figure 6-2. The rate constant for this reaction was calculated to be 0.0091 day^{-1}. It is important to note that the coefficient of determination was 0,822 for the reaction shown in Figure 6-1 and Figure 6-2. This is indicative that there are other variables than time which are affecting the rate of this reaction.

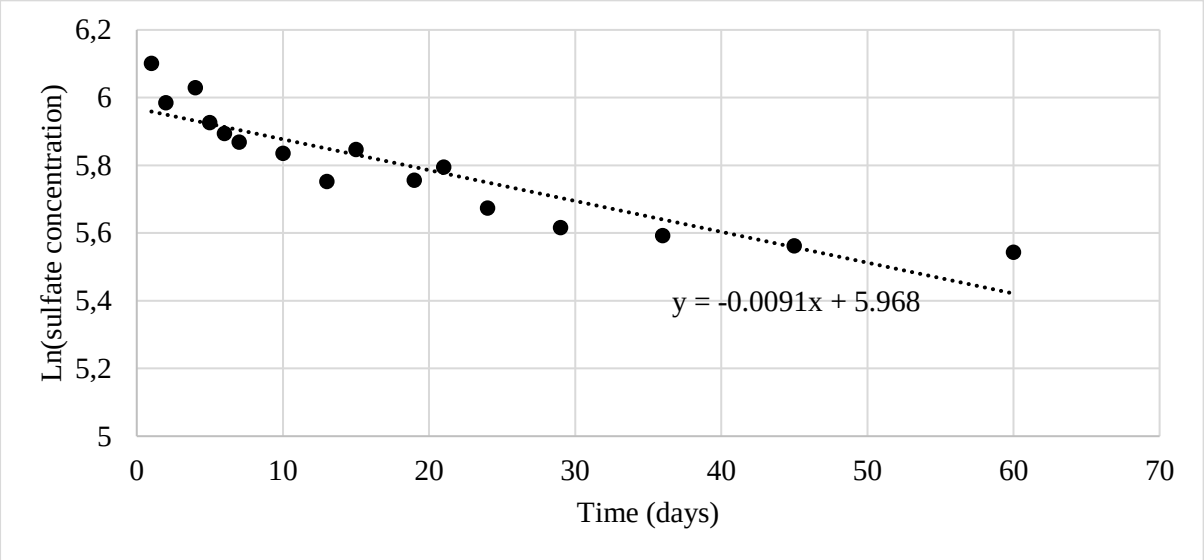


Figure 6-2: Integrated rate law for first order sulfate reduction reaction

6.1.6 Conclusions

The sulfate reduction reaction facilitated by SRM in a BOF slag neutralized solution of AMD was seen to follow first order reaction kinetics, with a rate law constant of approximately 0.0091 day^{-1}, corresponding to a sulfate reduction of approximately 0.0033 g/day. This is much lower than what is found in nutrient rich SRM environments (activated sludge processes), which sit at 12,5 g/day (Ingvorsen, Nielsen and Joulian, 2003). This rate could potentially be increased through the use of a simpler substrate/carbon source, and nutrients that are immediately available in solution as opposed to nutrients that had to have undergone hydrolysis/degradation to be liberated into solution. For the purpose of this experiment, this was not explored due to the end-user application of this technology

6.1.7 Acknowledgements

This work was conducted in part while D.G. Grubb served as the Vice President of Research and Development at Phoenix Services LLC. The authors would like to thank Phoenix Slag Services of South

Africa (Iwan Vermeulen) for their financial, technical support, and research materials; and Illovo Sugar (Mark Napier) and our confidential mining partner for AMD materials and other support. Gratitude is also extended to the Water Research Commission (WRC; Project No. K5/2757) of South Africa. The financial assistance of the National Research Foundation (NRF) toward this research is also hereby acknowledged. The opinions expressed and the conclusions drawn, are those of the authors and are not necessarily to be attributed to the NRF.

6.2 Part 2: Biological sulfate reduction of AMD in a continuous system using sugarcane bagasse as a substrate and nutrient source

6.2.1 Abstract

Sulfate reducing microorganisms (SRMs), like most living things, are highly sensitive to their environment – their functioning being almost entirely dependent on the provision/presence of favourable conditions. When used in effluent treatment, these conditions are rarely met without external alteration via temperature, pH, ionic concentration, salinity or nutrient availability increase or decrease. Creating favourable conditions for these organisms is a cost intensive process, not always able to be undertaken in systems which are aimed at being kept as cost efficient as possible due to historical or political issues – acid mine drainage (AMD) treatment being one of them. Although AMD treated with SRM has been successful in the past; the harsh conditions – especially the low pH – of typical AMD streams frequently act as inhibitors to SRM functioning. In addition, the constant provision of nutrients and carbon as substrates for the SRM is not always doable, as this results in a high capital and operational cost. The research presented here is focused on the functioning of SRMs in an AMD treatment scheme which used two byproducts as the pH adjustment and nutrient additive reagents, *viz*. basic oxygen furnace (BOF) slag and sugarcane bagasse. The treatment regime was successful, with the SRMs reducing sulfate at a rate of 8.875 mg/L.hour, resulting in a continuous average removal of sulfate from the stream of 37%. The carbon, nitrogen, phosphorous and chemical oxygen demand needs of the SRM community were achieved with relation to the extent of reduction that was required – lowering the sulfate content to below 300 ppm. The system functioned with no addition of reagents throughout a 104-day period, treating a total of approximately 150 L of AMD in a 50 L system containing 4 kg of bagasse, with a flowrate of 1 L/day of raw AMD.

6.2.2 Introduction

Microorganisms play an important role in the natural cycle of multiple chemical substances such as nitrogen, carbon, sulfur, iron, water and phosphorous (Seyfaee *et al.*, 2021). Elements within these biogeochemical cycles flow in various forms from non-living/abiotic components of the biosphere to living/biotic components (and back). In order for living components of major ecosystems – e.g., lakes or forests – to survive, all chemical elements that make up living cells must be recycled continuously. Within each cycle there is considered a large nutrient pool and a smaller exchange pool, the latter of

which is concerned with a more-active portion involved in the rapid transfer between biotic and abiotic aspects of an ecosystem (The Editors of Encyclopaedia Britannica, 2020). The microorganisms associated with these cycles and active exchanges – organisms which convert elemental nutrients into "useable" forms (such as ammonia, sulfate, carbon dioxide) – therefore play a leading role in the cycling of nutrients.

The cycles (and therefore the organisms which facilitate them) commonly present themselves in industrial processes in the same manner they present in nature. In some cases these organisms are used in a controlled manner to facilitate desirable reactions – using the biological processes of bacteria to facilitate desirable outcomes as an alternative to other artificial technologies (Deniz and Keskin-Gundogdu, 2017). The bacteria of the sulfur cycle - in particular sulfate reducing microbes (SRM) and sulfide oxidizing bacteria (SOB) - are of immense importance from both the industrial and environmental point of views. It is true that in some cases SRM can cause serious problems in many industries due to the by-production of sulfide, which is highly reactive, corrosive and toxic (Gupta and J.Germida, 2021); however, these organisms can also act in a beneficial way by removing sulfate (SRM use sulfate as a terminal electron acceptor in the degradation of organic compounds, enabling a form of anoxic respiration (Dev, Roy and Bhattacharya, 2016)) and heavy metals from waste streams.

Solutions which are engineered to allow for this type biological treatment of wastewater and other effluent, need to ensure a favorable environment for these bacteria to function and multiply within, thereby ensuring maximum sulfate reduction and subsequent immobilization of toxic ions via metal sulfide precipitation (Doble and Kumar, 2005). Factors which influence SRM functioning include temperature, salinity, sulfate concentration, pH and the "quality" (susceptibility to microbial attack) of the organic matter which is used by/provided to the bacteria as a substrate or carbon source (Goldhaber, 2003). In addition, the health and functioning of larger microbial communities – which are essential in assisting the sulfate reduction process via anaerobic degradation of substrates to simpler, more accessible molecules – are also influenced by factors such as availability of nutrients, growth stage, physiological state of bacterial cells, presence of competitive ions, and concentration of biomass (Dhir, 2018). In this regard, conditions of the effluent or environment under which the effluent is being treated/remediated by SRM might have to be altered to allow for improved SRM operation and ultimately greater sulfate and metal removal.

This research focusses on one factor which influences SRM growth and functioning: pH. The treatment regime explored herein, is intended to be deployed at abandoned mine sites where little to no contribution in the way of monitoring, additional reagents that could add to cost, or troubleshooting is desired. The aims of this research are thus related to determining the functioning of the SRM and extent of AMD remediation that can be achieved in an isolated, possibly nutrient deficient, system. Due to the

nature of AMD treatment (generally aimed at being kept as low cost as possible (Moodley *et al.*, 2018), this type of regime is an attractive option as it allows for low operational and capital costs.

A list of the objectives of the research performed and discussed in this section is given below. "SRM functioning" in this research refers to sulfate removal (extent and rate) and sulfide production. As such the objectives are as follows:

1. To determine the extent of metal addition/dissolution of BOF slag immersed in AMD and whether SRM are able to function at these (potentially) higher metal concentrations (related both to the level of metal concentrations in AMD as well as the higher concentrations caused by BOF slag dissolution).
2. To determine the extent of SRM functioning in a BOF slag neutralized solution at a pH level of between 5 and 8. In addition, the following questions is asked:
    a. What extent of AMD remediation occurs via SRM functioning and is this comparable to performance in other systems?
3. To determine whether the macro and micronutrients in the system (introduced into the system via sugarcane bagasse, BOF slag and AMD addition) is sufficient to maintain SRM functioning. In this regard, the following questions are considered:
    a. Does the COD:SO_4^{2-} ratio reach the value of 0,67 as reported as the ideal ratio in literature (Vela, Zaiat and Foresti, 2002)?
    b. What is the carbon, nitrogen, sulfate and phosphorous content of the system at the start of the process following the introduction of sugarcane bagasse

6.2.3 Background

Multiple researchers list pH as one of the most important/influential factors in ensuring optimal or maximum SRM action (Johnson *et al.*, 2009; Liu, Gong and Liu, 2014; Ayangbenro, Olanrewaju and Babalola, 2019). With particular reference to the treatment of acidic mine wastewaters (acid mine drainage (AMD), the first aim of this research was to determine SRM functioning in a basic oxygen furnace (BOF) slag neutralized stream (a stream in which BOF slag has been used as an alkalinity generator to increase pH to within a 5 – 8 pH range). This material can be contacted (directly or indirectly) with AMD (or other acidic media), initiating dissolution or leaching of the slag and releasing hydroxyl and silicate ions into the resulting solution (Naidu, 2019) thereby increasing the pH. BOF slag is a cheaper, more environmentally sustainable pH adjustment chemical, which is produced in large quantities as an industrial byproduct (Naidu et al., 2021). It has applications in multiple wastewater treatment programs (Naidu et al., 2020), and is thus a desirable alternative to other pH adjustment chemicals such as caustic soda and lime. Much research has already been undertaken to explore the option of using BOF slag as a pH adjustor (Ziemkiewicz, Skousen and Simmons, 2003; Name and Sheridan, 2014; Ramla and Sheridan, 2015; Naidu, van Dyk and Sheridan, 2021), indicating that this is

a promising reagent to facilitate pH increase. However, the raising of the pH of AMD in isolation, is not able to remove sulfate to within agricultural or potable water standards in South Africa (Department of Water Affairs and Forestry, 1996c), and thus a further polishing step must be undertaken for discharge to the environment should that be desired. The effectiveness of SRM in AMD post-pH adjustment using BOF slag is unknown, partly due to the fact that a variety of metals exist in the slag that could be liberated into solution during the leaching/dissolution process. It has been reported that the effect of heavy metals on SRM can be toxic/inhibitory at higher concentrations (Utgikar *et al.*, 2002). Determining whether SRM can function at these imposed metals concentrations is therefore the second aim of this research.

In many non-municipal waste streams undergoing biological treatment, nutrients are required to be added to the system to allow for microbial cell synthesis and growth. In the system used for the research presented here, no additional nutrients are aimed to be added – only the micro and macronutrients contained in the stream will be available to the microbial community. Approximately 12.2 g of nitrogen and 2.3g of phosphorus is needed per 100 g of cell biomass (Metcalf & Eddy *et al.*, 2014), and thus the third aim of this research is to determine whether the components found to naturally occur in the studied system are sufficient in providing these nutrients in practice.

6.2.3.1 SRM in AMD

AMD from abandoned/inactive mines is a major environmental issue in many countries with large-scale mining activities (Moreno-González *et al.*, 2022). Although AMD quality varies from mine to mine, it is generally characterized by low pH levels, high sulfate and high metal content (Moodley *et al.*, 2018; Naidu *et al.*, 2018), which in turn contributes to high levels of salinity (Favas, Martino and Prasad, 2018; Rossouw, Sheridan and Hille, 2019). The aforementioned factors which characterize AMD all (directly or indirectly) contribute to SRM health and functioning, in the following ways:

pH: Although there are some species of SRM that have been described as acidophilic and alkaliphilic, most of the known SRM grow optimally at neutral pH, or are neutrophilic (Sánchez-Andrea *et al.*, 2013). In addition, acidophilic SRM have only been reported to function at pH levels of above 3 (Sen and Johnson, 1999), whereas some AMD streams have been reported to reach pH levels of 2.38 (Naidu *et al.*, 2018). Thus, the low pH of typical AMD affected waters, have a detrimental effect on SRM functioning.

Sulfate: High sulfate concentrations allow for sufficient availability of sulfate to facilitate anoxic respiration via Equation 6-3 (Kikot *et al.*, 2010) or as shown in one of the two pathways depicted diagrammatically in Figure 6-3 (Goldhaber, 2003). SRM therefore have ample accessibility to sulfate in order to perform their elementary anaerobic processes (respiration). The type of SRM (or sulfate reducing microbe (SRM)) is not determined in this study, and therefore sulfate reduction could be occurring via either dissimilatory sulfate reduction (DSR) or assimilatory sulfate reduction (ASR). It is

hypothesized that due to the surplus of sulfate present, ASR may be favoured (Li *et al.*, 2020). If sulfide is found in the stream, this would also mean that DSR is occurring.

$$\text{Organic matter} + SO_4^{2-} \rightarrow CH_3COO^- + HS^- + HCO_3^-$$

Equation 6-3

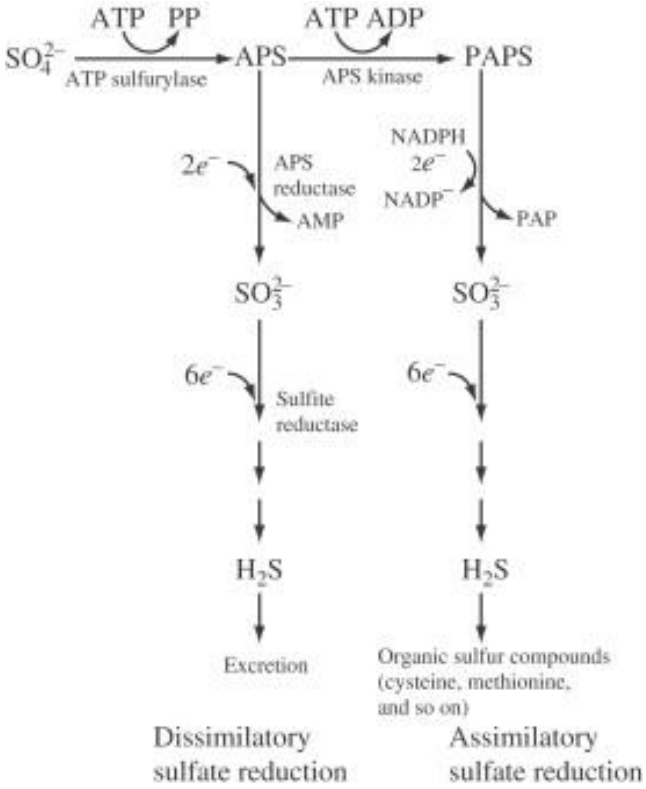


Figure 6-3: Biochemical pathway of dissimilatory and assimilatory reduction (Goldhaber, 2003)

Salinity: Increased salinity has been reported to decrease sulfate reduction rates by 41% (Van Den Brand *et al.*, 2015). Thus, high salinity levels are detrimental to SRM functioning.

The addition of BOF slag to an AMD stream allows for the lowering of salinity (through the precipitation of metal ions which contribute to the saline nature of the AMD), as well as an increase in pH (Ziemkiewicz, 1998). BOF slag addition to AMD is therefore expected to assist in SRM functioning, sulfate reduction and subsequent sulfate removal. A further point to note is that although SRM are able to generate their own alkalinity (Jimenez-Castaneda *et al.*, 2020) – sulfate reduction is a proton consuming process, thus the concentration of protons in environment decreases which generates alkalinity (Tran *et al.*, 2021) – the proton consuming process/reaction cannot begin at low pH levels.

In addition to favorable pH, sulfate and salinity levels; SRM also require a carbon, and a nitrogen source (concentrations of which should also be kept favorable) (Van Den Brand *et al.*, 2015). Due to the cost saving and sustainable nature of this research, another industrial byproduct carbon source was deemed appropriate for use in this regard – sugarcane bagasse. This was chosen due to local availability of the product, price, as well as the fact that this material contains both carbon and nitrogen elements.

Using this carbon source, the efficacy/performance of SRM in a BOF slag neutralized AMD system was analyzed. As mentioned, no further addition of nutrients was done.

Although acidic and high metal content effluent is the focus of this research, the findings presented within could also have applicability in domestic wastewater treatment plants or in anaerobic sludge reactor pretreatment regimes, where control of pH also plays a dominant role in bacterial functioning (van den Brand *et al.,* 2015).

6.2.4 Materials

BOF slag was sourced from a steel slag management company (Phoenix Slag) in Johannesburg South Africa. This slag was obtained in different size classes (milled prior to distribution) and two size classes of slag were used to perform this study – BOF slag with aperture size < 1 mm (fines) and BOF slag with aperture size > 4.75 mm and < 13.2 mm.

The larger size class was chosen to avoid blockages due to cementation in the system, as well as to act as a porous packing material for a packed bed reactor. BOF slag fines were chosen and used to allow for quick additions of alkalinity to the system during times of low pH. The composition of the BOF slag was not pertinent to this study, however X-ray diffraction and X-ray fluorescence were used to identify the components and the amount of components in the slag particles.

These analyses were performed by the Earth Lab at the University of the Witwatersrand using a Malvern Panalytical Wavelength Dispersive (WD) XRF machine. Sample preparation included drying of the particles and pulverizing them using a crusher. XRD was performed by the School of Chemistry at the University of the Witwatersrand, using a Bruker Discover D8 machine (external laboratory).

Sugarcane bagasse was sourced from Illovo sugar in Eston, South Africa. This material was not processed in any way before use. A C, N, S, and P analysis was performed on this sugarcane bagasse using a Leco Elemental Analyzer (this was performed by Leco Africa). This analysis was pertinent to the study as it gave an indication of the amount of C and N that was being provided to the SRM.

AMD was sourced from a coal mine dump in Witwatersrand, South Africa. An Inductive Coupled Plasma- Mass Spectroscopy analysis was performed to analyze elemental concentrations of this AMD (performed by an external laboratory), and A Merck Pharo 300 spectrophotometer was used to analyze iron, sulfide and sulfate concentrations. Merck test kits were used to analyze for these anions and cations. Additionally, CeBER (Center for bioprocess engineering research, 2016) methods were used to analyze sulfate. Merck test kits were also used to analyze chemical oxygen demand (COD) content of the AMD stream after it had been put into contact with sugarcane bagasse.

SRM was cultivated using mixed cultures of SRM obtained from the Northern Wastewater Treatment Works, Emmerantia Dam in Johannesburg, South Africa and from previous AMD/SRM experiments.

This mixed culture was grown in nutrient rich media (containing 5 g of sodium citrate, 4.5 mL of sodium lactate, 1 g of yeast extract and 4.5 g of Magnesium sulfate heptahydrate in 1 L of deionized water). An attempt was made to desensitize the culture to AMD and BOF slag conditions by adding 3 mL of a diluted BOF slag neutralized AMD to the sample every 2 days.

6.2.5 Methods

Sugarcane bagasse was contacted with AMD in a reaction vessel with dimensions 41.5 × 22 × 30 cm. 4 kg of sugarcane bagasse was packed in this vessel, allowing for an available liquid volume of 14.4 L Contact was allowed for 24 hours to facilitate a degree of hydrolysis (break down of hemicellulose and release of xylose, and other organic acids).

The vessel was doped with SRM inoculum and sealed using silicone tape. Continuous oxidation reduction potential (ORP) readings were taken in this vessel using an Orbipac CPF82D Memosens ORP meter fitted to the tank. An initial reference COD measurement was taken from this vessel.

The vessel described above was then set-up in a continuous system following the schematic shown in Figure 6-4.

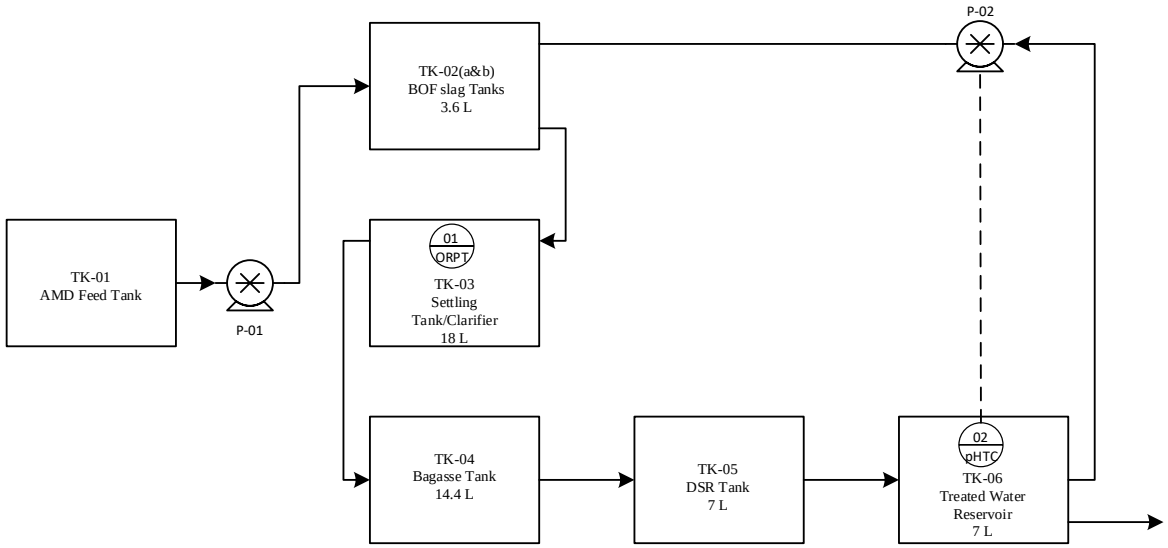


Figure 6-4: Sulfate Reduction Continuous Process Set-up Process Flow and Instrumentation Diagram

Raw AMD was pumped into the system via P-01 at 1 L/day, allowing for a residence time of 50 days. A variable recycle stream from TK-06 to TK-02 via P-01 was controlled using a continuous pH measurement in TK-06. The pH in TK-06 was aimed at being kept constant at 7, by recycling treated water to TK-02 (which picked up alkalinity from the BOF slag packing). This stream was then mixed with raw AMD in TK-03, allowing for a rise in pH. The higher the flow through TK-06, the higher the pH rise in TK-03.

The reaction time between the BOF slag and treated water was assumed to be negligible as it did not affect the residence time of the system overall. The system was commissioned using potable water as a recycle stream with an AMD inlet of approximately 5 L/day for ~ 10 days.

During this time period, the system was allowed to stabilize, and no samples were taken. All tanks in the system were sealed to prevent ingress of oxygen.

Samples were taken at the outlet of TK-04, TK-05 and TK-06 daily and analyzed for sulfate, COD and sulfide.

6.2.6 Results and Discussion

6.2.6.1 Material analysis

The BOF slag sourced from Phoenix Slag Services had an oxidic composition as shown in Table 6-3.

Table 6-3: Oxide Content of BOF slag sourced from Phoenix Slag Services

Oxide	wt.%
CaO	41.6
Fe_2O_3	20.5
SiO_2	14.4
MgO	7.2
Al_2O_3	2.8
SO_3	0.4
Loss on ignition (LOI)	5

Due to the nature of the BOF slag particle (size and mineral matrix), complete dissolution did not occur during the 50-day cycle, thus not all oxides were hydrolyzed. The addition of sulfur to the system via SO_3 dissolution (from the slag) was deemed negligible due to the high pH levels reached in the system (up to 11) and the high rate of ensuing sulfate precipitation.

The AMD sourced from the coal mine dump in Mpumalanga, South Africa had an elemental composition as shown in Table 6-4.

This solution had a sulfate concentration of 16301 mg/L (measured using spectrophotometric techniques). Other parameters of the AMD which was used, are shown in Table 6-5.

Phosphorous was added to this system at a rate of approximately 2 mg/day in the AMD, with the initial amount contained in the system being approximately 100 mg (due to 50 L of AMD being added at commissioning). The addition of metals occurred during BOF slag dissolution, as shown in Figure 6-5.

Table 6-4: Elemental composition of AMD used in study

Element	**Ag**	**Al**	**As**	**B**	**Ba**	**Be**	**Bi**	**Ca**
Unit	µg/L	µg/L	µg/L	µg/L	µg/L	µg/L	µg/L	µg/L
Concentration	112	479003	<2	2726	23	66	<2	141375
Element	**Cd**	**Ce**	**Co**	**Cr**	**Cs**	**Cu**	**Dy**	**Er**
Unit	µg/L	µg/L	µg/L	µg/L	µg/L	µg/L	µg/L	µg/L
Concentration	15	7021	1239	76	32	767	359	198
Element	**Eu**	**Fe**	**Ga**	**Gd**	**Ge**	**Hf**	**Hg**	**Ho**
Unit	µg/L	µg/L	µg/L	µg/L	µg/L	µg/L	µg/L	µg/L
Concentration	70	5261380	<2	553	<5	6,4	<5	68
Element	**In**	**K**	**La**	**Li**	**Lu**	**Mg**	**Mn**	**Mo**
Unit	µg/L	µg/L	µg/L	µg/L	µg/L	µg/L	µg/L	µg/L
Concentration	<2	9671	600	425	18	93906	197140	<10
Element	**Na**	**Nb**	**Nd**	**Ni**	**P**	**Pb**	**Pr**	**Rb**
Unit	µg/L	µg/L	µg/L	µg/L	µg/L	µg/L	µg/L	µg/L
Concentration	35266	23	1192	914	<2000	33	260	191
Element	**Sb**	**Sc**	**Se**	**Si**	**Sm**	**Sn**	**Sr**	**Zr**
Unit	µg/L	µg/L	µg/L	µg/L	µg/L	µg/L	µg/L	µg/L
Concentration	3,4	<2	<5	17686	311	4	1084	15
Element	**Ta**	**Tb**	**Te**	**Th**	**Ti**	**Tl**	**Tm**	**U**
Unit	µg/L	µg/L	µg/L	µg/L	µg/L	µg/L	µg/L	µg/L
Concentration	<2	64	2,4	12,5	3373	<2	23	16
Element	**V**	**W**	**Y**	**Yb**	**Zn**			
Unit	µg/L	µg/L	µg/L	µg/L	µg/L			
Concentration	79	8,4	2070	132	9186			

Table 6-5: AMD sourced from Mpumalanga, South Africa characteristics

Parameter	**Value**
Redox Potential (mV)	391
Dissolved Oxygen (mg/L)	2.5
Total Dissolved Solids	29112
Sulfide (mg/L)	0.019
Conductivity (mS/M)	1300
pH	2.38
Total Suspended Solids	290
Acidity (H+)	362
Turbidity	54
Total Organic Carbon (TOC)	<0.1
Sulfate (mg/L)	16 301
Hydroxypropyl cellulose	<1

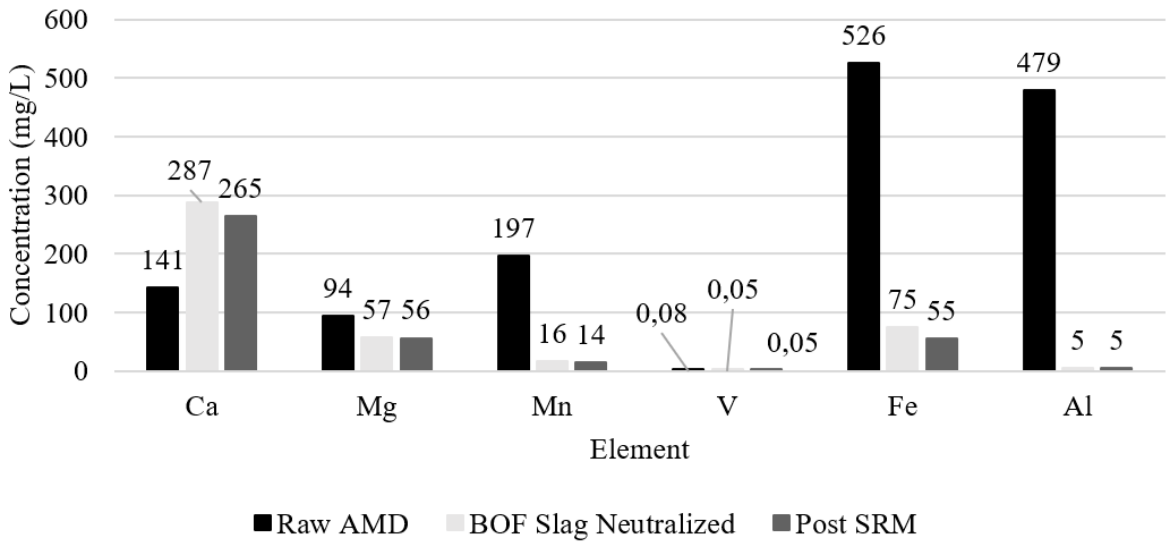


Figure 6-5: Difference in metal concentration between Raw AMD, AMD that had been BOF slag neutralized to a pH of 5,7 and given at least 1 hour settling time, and AMD after having undergone sulfate reduction via microbial action

The addition of BOF slag to the system only caused an increase in calcium (of the elements that were analyzed) (as shown in Figure 6-5). All other metals of interest decreased, most likely due to pH increase and counterion availability – resulting in precipitation. It must be noted that in other studies which were performed on a larger scale, the level of Mg in the system was also seen to increase or remain present in high levels (Naidu *et al.*, 2019). The amount of Mg removed is directly related to the pH that the system reaches (Naidu, van Dyk and Sheridan, 2021), since a pH of >9 was achieved successfully in this system before dilution with additional AMD, the Mg content decreasing is therefore expected. Sulfate removal and sulfide production occurred following BOF slag dissolution and therefore it was confirmed that SRM can survive and function in AMD and BOF slag laden waters. In must be noted that the pH of the effluent exiting the BOF slag tanks (TK-02) was much higher than that of the effluent entering the DSR Tank (TK-05), sitting at an average pH of >11. Thus, large amounts of precipitation (and therefore removal of metals) occurred over the settling tank (TK-03).

6.2.6.2 Nutrient utilization

The sugarcane bagasse sourced from Illovo Sugar in Eston, South Africa had an elemental composition as shown in Table 6-6.

Table 6-6: LECO elemental analysis of Sugarcane Bagasse from Illovo Sugar

Sample	N (%)	C (%)	S (%)	P (%)
Sugar Cane Bagasse	0.36	32.78	0.12	2,3

As displayed in Table 6-4, Table 6-5, and Table 6-6, there was a presence of inorganic nutrients (P, N, S, K, Mg, Ca, Na) and organic nutrients (organic carbon) in the combined system. The amount of carbon

in the system was approximately 1.3 kg, the amount of phosphorous in the system was approximately 92.3 g (considering addition from the AMD stream as well), and the amount of nitrogen in the system was 144 g. The percentage of this that was available (accessible) to the bacterial consortium was unknown. Regardless of the amount of bagasse that underwent decomposition in the dilute acid stream, the limiting reagent for bacterial growth would still be nitrogen (using the Biomass:N:P ratio given by Metcalf & Eddy et al. (2014)). Thus, the amount of cell growth, and subsequent sulfate reduction would be dependent on the nitrogen content of the stream.

The initial COD content of the system was 326.4 mg/L. COD measurements were taken every 10 days (approximately).

The COD and sulfate concentration in the system over time is shown in Figure 6-6. The sulfate concentration was lowered from 16301 mg/L to a final value of 234 mg/L; however, this was not solely due to sulfate reduction via SRM action. The BOF slag raised the pH of the system, allowing for the precipitation of multiple ionic compounds – many of which were sulfidic in nature, due to the high availability of sulfate in the system.

In addition, the AMD stream was also diluted with treated water, further lowering the sulfate concentration within the system. The sulfate concentration entering the bagasse tank (after pH induced precipitation and dilution) seemed to be maintained at an average of 465 mg/L (coefficient of variance being 12%). If it is assumed that this inlet was relatively constant (very little variation was noted in this stream), the sulfate removed via DSR, ASR or other biological process over time across the system would be as shown in Figure 6-7.

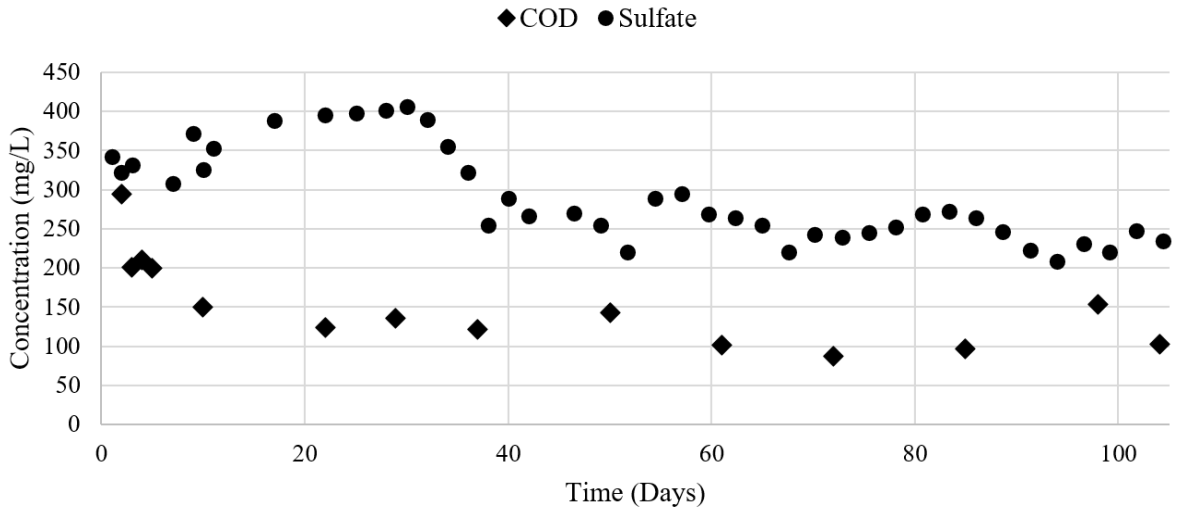


Figure 6-6: Sulfate and COD concentration of samples taken from the outlet of the Bagasse Tank over time

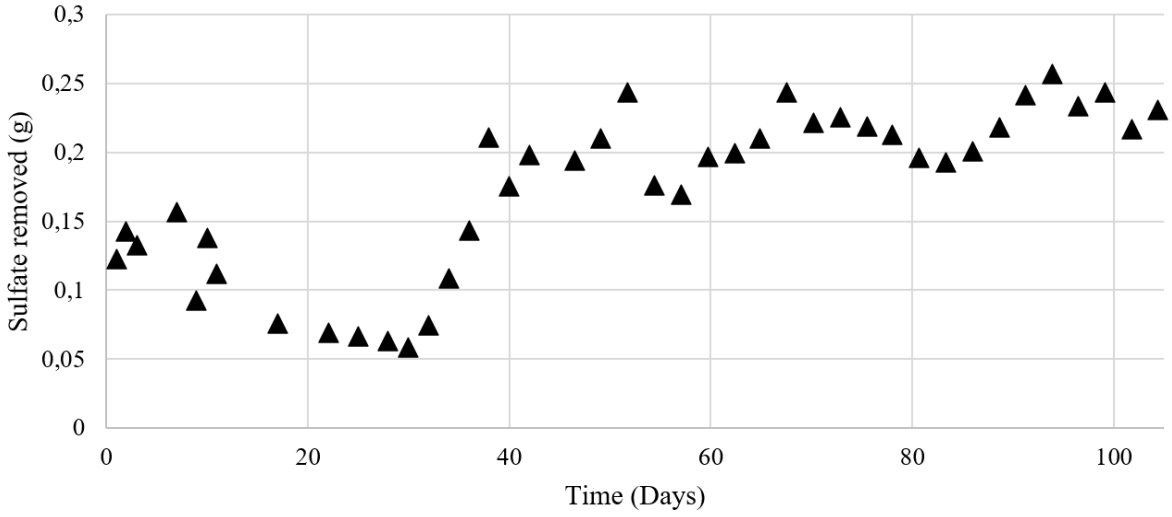


Figure 6-7: Mass of sulfate removed in a 50L system via biological functioning per day (non-cumulative) where sugarcane bagasse is used as the carbon, nitrogen and phosphorous source, and AMD is used as the sulfate source

From approximately day 40, a relatively stable sulfate removal was seen in the system, corresponding to an average sulfate removal of 0.008875 g/hour, 0.21 g/day; or a volumetric sulfate reduction rate (VSRR) of 8.875 mg/L.hour (coefficient of variance being 10.75 %).

This VSRR found in this system was similar to what has been reported in literature for initial sulfate concentrations of 1 g/L or lower using suspended culture (Oyekola, van Hille and Harrison, 2010).

Using Figure 6-6 and Figure 6-7 as bases, it can be deduced that although sulfate removal occurred at a specific rate, the COD level (removal of COD) in the system did not correspond to the 0,67 COD:sulfate ratio. Thus, it is deduced that COD was continually released from the bagasse into the system, as it was being used. The amount of COD in the system was always in excess of what was needed to be digested to achieve the amount of sulfate removal via sulfate reduction. Therefore, it can be concluded that the COD available in the stream was not a limiting factor for the biological removal of sulfate. This finding could mean one, or both of two things:

1. The phosphorous, nitrogen or other micronutrient content in the system was not sufficient to allow for adequate SRM growth that would result in a higher or complete sulfate reduction.
2. The toxicity presented by the metals in the stream, hindered the growth and performance of the SRM, such that complete DSR or ASR of the sulfate in the stream could not occur.

6.2.6.3 SRM Functioning and AMD treatment

The sulfate across the system was lowered by an average of 37% (the variation of which is shown across the 104 days of testing in Figure 6-7). Although it is known that sulfate ions are able to adhere to the surface of cellulose (Abushammala and Mao, 2019), the presence of sulfide in the system (which was found between the concentrations of 5 and 13 mg/L) confirms that biological dissimilatory sulfide reduction was able to, and did occur in the laboratory scale set up shown in Figure 6-4. The amount of

dissolved sulfide detected in the system does not account for the entire amount of sulfate that was removed, however, the ORP readings in the DSR tank were consistently < - 300 mV. This indicates that a highly anaerobic environment was maintained in the bagasse tank. The subsequent tanks all had ORP readings that were higher than this (although still negative), and thus the sulfide in the stream could have easily been liberated as H_2S or undergone re-oxidation. The latter was confirmed by the increase in average sulfate concentrations over TK-04, TK-05 and TK-06. The sulfate concentrations in these vessels (on average over the period) were 351, 287 and 293 mg/L respectively. The higher concentration in the bagasse tank (TK-04) was attributed to the toxic nature of the sulfide which was visually present in high amounts within this tank, (coating the bagasse fibers).

6.2.7 Conclusion and Recommendations

After the study was completed, the following points were confirmed in relation to the original objectives:

1. The only metal (from the elements which were analyzed) that increased in the system was calcium. SRM functioning was observed after the increase in concentration of Ca, and therefore it can be concluded that under the conditions imposed in the study, an increase in metal concentration (attributed to BOF slag leaching) still allows for SRM functioning which results in sulfate reduction and removal.
2. AMD remediation was confirmed at an average of 37% removal of sulfate (post BOF slag neutralization and subsequent metal precipitation). This, in conjunction with the presence of sulfide in an anaerobic environment, validated the supposition that SRM were functional at an acceptable rate in this environment. The VSRR found was 8.875 mg/L.hour which was similar to values found in literature – again confirming the functionality of SRM in this environment.
3. A total of 1.3 kg of carbon, 92.3 g of Phosphorous and 144 g of nitrogen was found in the system. The COD:sulfate ratio obtained was between 0.3 and 0.9, however the COD in the system did not diminish at the rate found in literature. It is therefore concluded that at more favourable conditions, greater sulfate reduction could be achieved if all the organic matter was able to be digested.

Although the system could be improved by the addition of more nutrients and a more readily accessible carbon source, this experiment was considered a success given the context in which this technology is aimed to be deployed. Although sulfate reduction did not reach a maximum, it was evident that the nutrients found in the system - at the achieved BOF slag neutralized pH levels of > 5 – were sufficient in polishing the AMD stream to sulfate levels of below 300 mg/L. This is an acceptable and attractive treatment extent for abandoned mines.

6.2.8 Acknowledgements

This work was conducted in part while D.G. Grubb served as the Vice President of Research and Development at Phoenix Services LLC. The authors would like to thank Phoenix Slag Services of South Africa (Iwan Vermeulen) for their financial, technical support, and research materials; and Illovo Sugar (Mark Napier) and our confidential mining partner for AMD materials and other support. Gratitude is also extended to the Water Research Commission (WRC; Project No. K5/2757) of South Africa. The financial assistance of the National Research Foundation (NRF) toward this research is also hereby acknowledged. The opinions expressed and the conclusions drawn, are those of the authors and are not necessarily to be attributed to the NRF.

7 Determination of the optimal configuration of a system incorporating and integrating all three processes (pH rise from BOF slag action; precipitation of metals, sulfates, and sulfides; reduction of sulfate and formation of sulfide through SRB action)

This chapter is presented solely in the form of a design document which was submitted to the Water Research Commission (WRC) of South Africa as part of the fulfillment of the project deliverables and goals (Naidu *et al.*, 2017). This document was reviewed by the WRC project committee. Sections which refer to time-based items (progress reports/deliverable timelines etc.) have been omitted from this chapter.

The full reference for this document is given below.

Naidu, T. S., Sheridan, C., van Dyk, L., Grubb, D., Hernandez, M., & Napier, M. (2017). *Design of Acid Mine Drainage Remediation Plant (1st Deliverable)* (Issue July).

Design of Acid Mine Drainage Remediation Plant (WRC 1st Deliverable)

7.1 Executive Summary

A design for a pilot-scale process aimed at remediating 1000 L/day of acid mine drainage at an AMD Dam in Witbank, South Africa is presented here in detail. The plant design parameters are determined based on a combination of literature, previous lab-scale experimental data and space and equipment availability. The plant uses a combination of metallurgical slag, sugar-cane bagasse and sulfate reducing bacteria cultures to remediate the acidic water (to as yet undetermined limits). The process design includes 8 low-density polyethylene vessels used as reactors and sedimentation tanks which – with the combination of a recycle stream – enables pH rise of the acidic mine water, precipitation of heavy metal and sulfate complexes from the AMD and dissimilatory sulfate reduction, which lowers the sulfate concentration. Conceptually, a fraction of the remediated water is recycled back into the process to leach alkalinity from the slag which is titrated with the AMD and settled in the tanks. The outlet flows back into the AMD dam. Construction of the equipment will be done off-site, with only setup and pipe connections occurring on site. Critical equipment (pumps, electronics) will be located within the enclosure for security. All on site work will be done in accordance with the Anglo-American health and safety protocol.

7.1.1 Background

The draft design presented here details a collaborative project aimed at determining the viability of using BOF slag and sugar-cane bagasse to treat 1000 L per day of AMD

Aims

The following are the aims of the project:

1. To perform preliminary laboratory studies which will provide information for the design of a pilot plant unit.
2. To design a pilot process for treating 1000 L /day of AMD on site.
3. To construct the pilot plant to treat 1000 L /day of AMD.
4. To monitor the pilot plant in order to assess performance over a 6-month period.
5. To design and prepare a process for scale up of the original pilot plant to be based on site.

7.1.2 General

This document serves as the initial design of the pilot plant system to be constructed.

7.2 Background

7.2.1 Introduction

This project is a collaboration of the University of the Witwatersrand, Phoenix Slag, Illovo Sugar and Anglo American. The aim is to determine the viability of remediating AMD at a meso-scale in a two-

step process which combines the use of metallurgical slags and sugarcane bagasse. Previous laboratory scale experimentation has confirmed the functionality of metallurgical slag as a pH raising agent and the use of sugarcane bagasse as a carbon source for dissimilatory sulfate reduction (DSR). These experiments were done on a smaller scale and the feasibility of the process needs to be tested at a larger continuous scale in order to confirm its effectiveness and determine whether use as a large-scale remediation option is possible. This report is the first deliverable of the project and summarizes the lab scale experimental process by using the data obtained to design a pilot scale plant.

7.2.1.1 Project aims

The following are the aims of the project:

1. To perform preliminary laboratory studies which will provide information for the design of a pilot plant unit.
2. To design a pilot process for treating 1000 L /day of AMD on site.
3. To construct the pilot plant to treat 1000 L /day of AMD.
4. To monitor the pilot plant in order to assess performance over a 6-month period.
5. To design and prepare a process for scale up of the original pilot plant to be based on site.

This document serves as fulfilment of the second aim.

7.2.1.2 Scope and Limitations

Experimental data was obtained from batch and continuous lab scale processes and this data was used to determine the parameters for the pilot scale design. The data obtained was used to size the vessels based on available area at the site. These experiments were done over a period of one month, but some data from previous studies and literature were also used in the design. The experimental kinetics used to design the process were sourced over a short period of time and thus allowances had to be made to compensate for the plant operating for a much longer period. For this reason, all of the equipment sizes have been conservatively designed based on literature or data obtained.

7.3 Overview of process

7.3.1 Introduction

A process is designed to remediate Acid Mine Drainage (AMD) sourced from an AMD tailings Dam, located in Witbank, Mpumalanga. The Dam is a receptacle for acid water waste from a coal mine in the area and contains high concentrations of heavy metals and sulfate. The proposed process uses metallurgical slags to raise the pH of the acidic water, allowing metal and sulfate precipitates to form and be removed via gravitational settling. After the pH is raised sufficiently, the water is then directed to a bagasse chamber where the remainder of the sulfate is removed via DSR. The outlet of this chamber

is treated water with a relatively neutral pH and low metal and sulfate content. The system will be constructed less than 10m from the AMD tailings Dam site and will be monitored for 1 year.

7.3.2 Design Basis

Remediation of 1000 L/day of acidic mine water

7.3.3 Detailed process description

AMD (with pH of 2) from the dam will be pumped into system using a peristaltic pump. The AMD stream is designed be split equally and will feed two duplicate sedimentation vessels from the top. The sedimentation vessels are arranged in parallel. Recycled treated water will also enter the sedimentation vessels from the top after being passed through the slag which will raise its pH through the leaching of lime. This high pH water will mix with the acidic (low pH) water, and a mixture with a pH of between 5 and 9 will be obtained (optimal pH will be determined after long term experimentation). At this range of pH values, precipitation of metal sulfate complexes will occur, and the sedimentation vessels will allow for settling thereof under the action of gravitational settling.

The water exiting the sedimentation vessel will thus have a lower sulfate and heavy metal concentration than the original AMD. The outlets from the sedimentation vessels will join and enter into two bioreactors designed for dissimilatory sulfate reduction. The reactors are proposed to be duplicated and created from identical tanks as the settling chamber. Sugarcane bagasse is packed into crates and stacked throughout the lengths of the reactors and the vessels will be sealed using pond-liner which will be glued to the reactors to induce the anaerobic environment. A vent will be installed into the bioreactors to channel exhaust gases away from the reactor.

A by-product of the DSR reaction is sulfide which binds to hydrogen to produce H_2S gas. If the gas concentration nears the allowable threshold, this gas can be exhausted to a scrubbing unit which oxidizes the sulfide to produce sulfuric acid. The scrubbing unit waste is proposed to be disposed of in the outlet stream since the quantity will be small relative to the AMD being collected from the site. The reactor outlet enters a secondary sedimentation vessel in which precipitation of metal sulfides can be achieved. The outlet of this chamber enters a reservoir and is considered the end product – remediated water.

Under the action of a peristaltic pump, some of this water is pumped back into the process, entering first into a slag reactor chamber which is packed with metallurgical slag in crates, and then into the sedimentation vessels to assist with precipitation. The flowrate of this stream is determined via pH control of the sedimentation vessel – if the pH is low, the flowrate of the recycle is increased and vice versa. The recycle loop is necessary to prevents armouring of the slag. If low pH AMD is allowed to come into direct contact with the slag, the slag will be coated with metal precipitates and the alkaline

reagent will no longer be accessible to raise the pH. All vessels will be sealed (with the exception of the scrubber) and will be covered to prevent UV penetration.

The design of the process is done in detail and diagrams are presented in subsequent sections.

7.3.4 Commissioning of plant/start-up

The system will need to be commissioned with metal-free water to prevent armouring of the slag. A water tank containing clean water will be used initially and will act as the source of the recycle stream until all vessels in the process are filled to capacity and an outlet flow is obtained.

7.3.5 Health and safety

All work done will comply to Anglo American's health and safety protocols. Medical examinations of all workers allowed on site are being conducted and an environmental and health risk assessment is in the process of being reviewed.

7.4 Site Selection and layout

7.4.1 Introduction

The pilot plant will be constructed at the AMD tailings dam, located in Witbank, Mpumalanga. Topical views of the physical site are shown and discussed and a plant layout diagram, in which the proposed positioning of each vessel used in the plant is shown, is also presented.

7.4.2 Site Selection

In Figure 7-1 a top view of the entire dam is shown. The area of construction for the site is outlined.



Figure 7-1: Top view of AMD tailings dam with area of construction outlined

The dam is situated next to a large mine dump in which slurry and solid wastes are continuously deposited. Liquid mine wastes (consisting mainly of wastewater) seep through this dump, leaching out heavy metals and sulfate from the solid wastes. This liquid flows out through the bottom of the dump as toe seepage and is directed towards AMD tailings dam . There is currently no treatment option for this dam and in order to keep from overflowing, the water is continuously pumped out of the dam back

into the mine dump. The water in this dam is therefore continuously decreasing in quality and in need of remediation – making it an ideal site for an experimental plant.

The total area of the site selected is approximately 774 m^2 (18 m x 43 m), however only a portion of this is able to accommodate construction due to the positioning of trenches, fences and power equipment already situated at the site which create access constraints A piece of land approximately 5 m x 30 m, with an area of 150 m^2 is proposed to be used for construction, as shown in Figure 7-2.



Figure 7-2: Top view of area to be used for construction of pilot plant at AMD tailings dam

All process equipment is proposed to occupy 95 m^2 with the remaining area to be left open for additions or alterations to the process if they are needed.

7.4.3 Plant layout

In Figure 7-3, the proposed plant layout as seen from above is displayed. Vessels have been drawn to scale and labelled in accordance with the process diagrams which are presented in the Process Flow Diagrams section. The electrical housing box has not been sized. This will be done after initial testing of the control equipment.

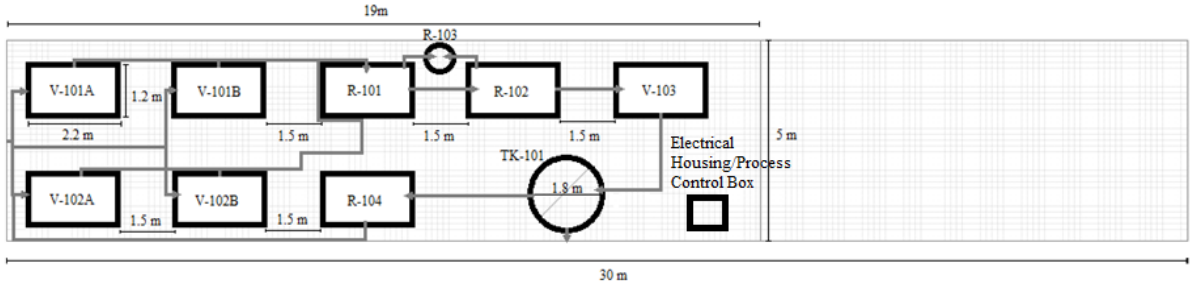


Figure 7-3: Plant layout top view

The positioning of the piping that is shown in the layout diagram includes silicon, nylon and PVC piping that will be used for construction. Different piping materials will be used for different sections of the plant and this will be further discussed in Chapter 6

7.5 Process flow diagrams

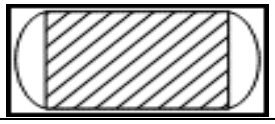
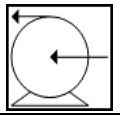
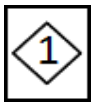
7.5.1 Introduction

The designed process is shown in a process flow diagram which details the process diagrammatically

7.5.2 Process flow diagram (PFD)

In Figure 7-4, a diagrammatic representation of the process flow and layout of the plant is shown. A key is provided in Table 7-1 which details and specifies the symbols used in the diagram.

Table 7-1: Key for Process flow diagram

Representation and description of symbols on PFD	
Symbol/Diagram	**Description**
	Settling Tank/Sedimentation Vessel
	Reaction Vessel
	Storage Vessel
	Valve
	Peristaltic Pump
	Stream Number

In Figure 7-5, a process flow diagram without symbols is provided. Images of the vessels have been used instead of diagrammatic representations.

P-101	V-101A/B	V-102A/B	R-101	R-102	R-103	V-103	TK-101	P-102	R-104
AMD Feed Pump	Sedimentation Vessel	Standby Sedimentation Vessel	Bagasse Reactor	Secondary Bagasse reactor	Hydrogen Sulfide Scrubber	Secondary Sedimentation Tank	Storage Tank for Remediated Water	Recycle Pump	Slag Chamber

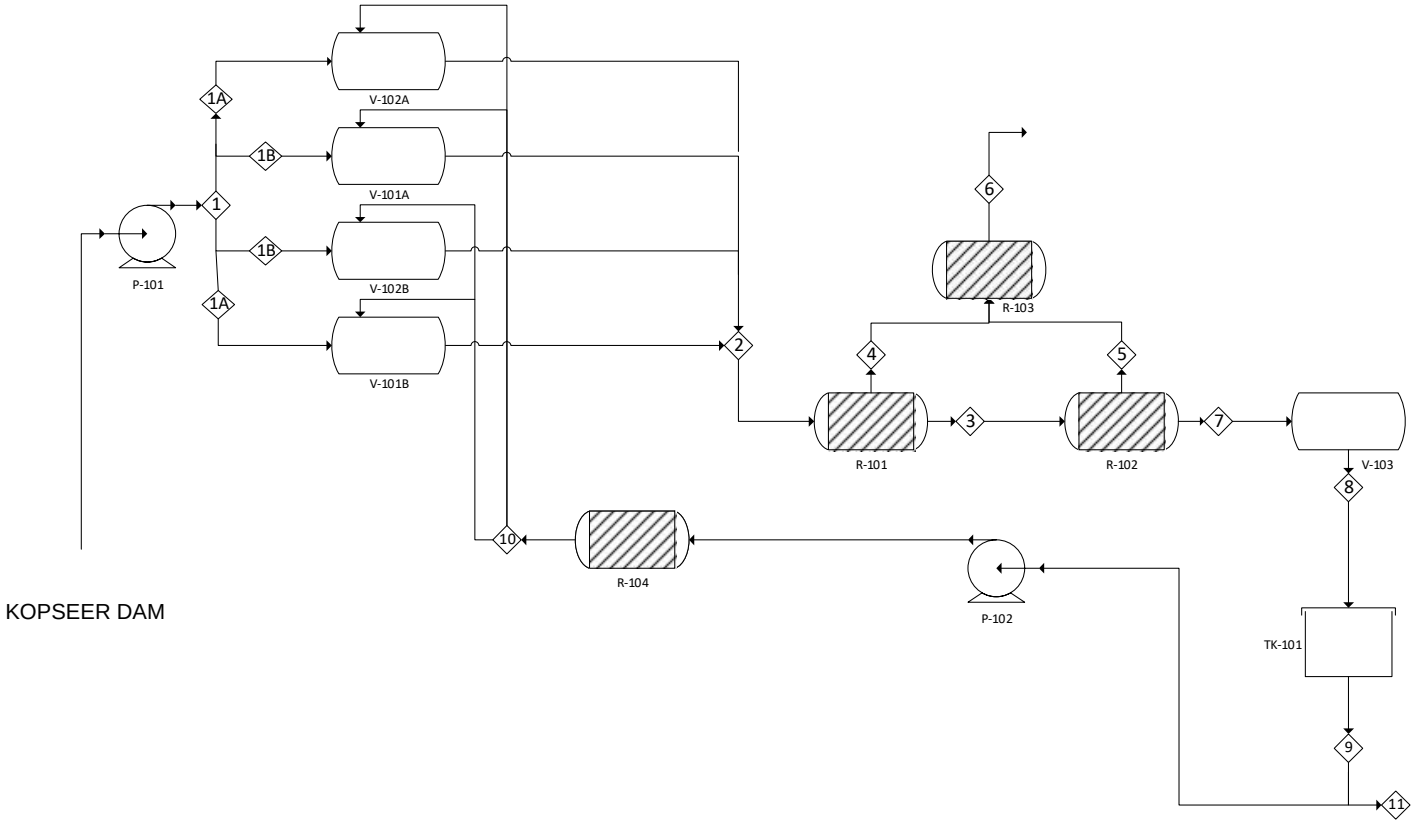


Figure 7-4: Process flow diagram

P-101	V-101A/B	V-102A/B	R-101	R-102	R-103	V-103	TK-101	P-102	R-104
AMD Feed Pump	Sedimentation Vessel	Standby Sedimentation Vessel	Bagasse Reactor	Secondary Bagasse reactor	Hydrogen Sulfide Scrubber	Secondary Sedimentation Tank	Storage Tank for Remediated Water	Recycle Pump	Slag Chamber

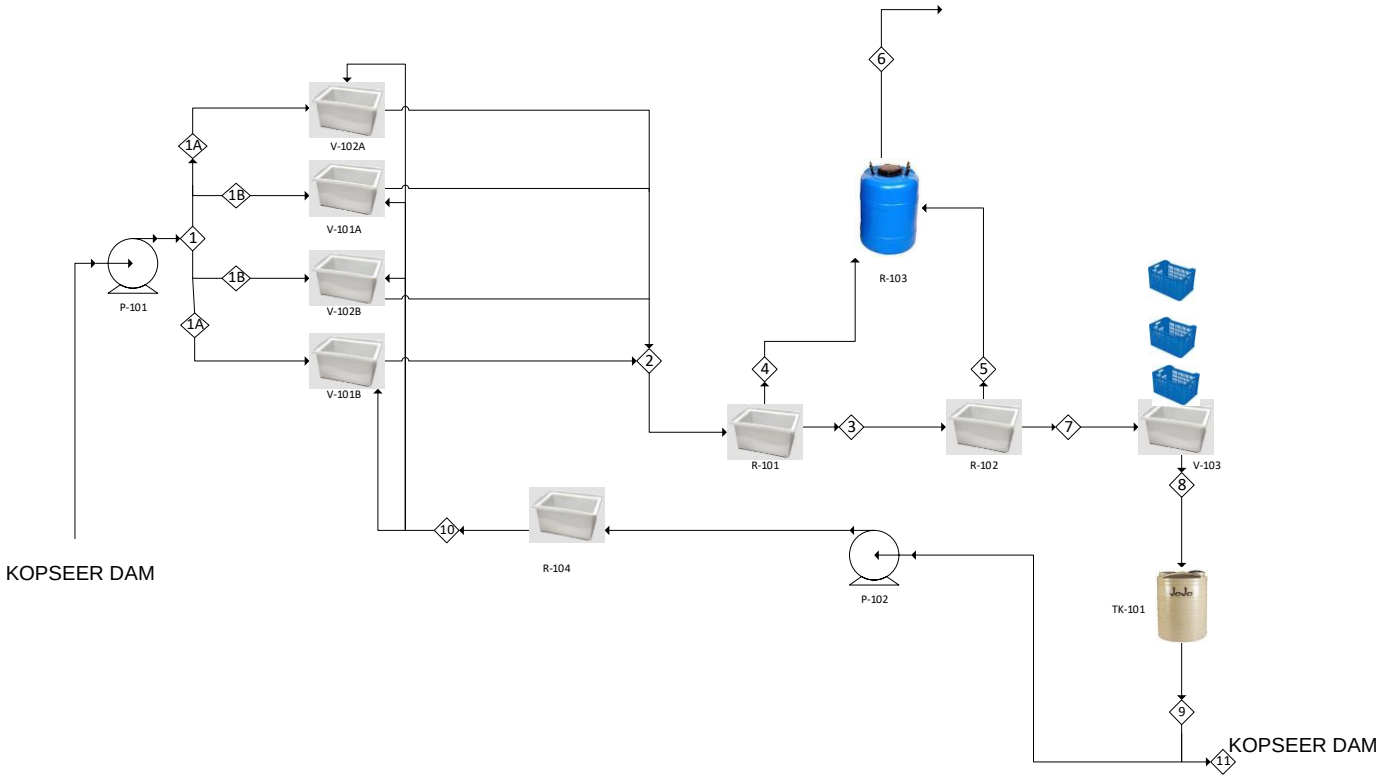


Figure 7-5: Process Flow Diagram depicting process equipment

7.6 Equipment design

7.6.1 Introduction

All major process equipment (reactors, sedimentation vessels) are sized and described in detail in this section. All reactions and settling will occur in pre-formed polyethylene vessels, which are UV and acid resistant. All vessels have the same dimensions; however, sizing was calculated to ensure they adhere to the minimum allowable size for the reactor or settling tank. Where these vessels are not large enough, multiple are used in series or parallel depending on the point they are located within process. All vessels will be sealed to avoid re-oxidation of any sulfide that may be present in the streams and will be covered to ensure no UV light is able to penetrate.

7.6.2 Settling Tank/Sedimentation Vessel

This system is represented by symbols V-101A, V-101B, V-102A and V-102B on the PFD and P&ID.

7.6.2.1 Overview & 2D Diagram

Feed into the settling tank consists of two streams; fresh AMD and recycled treated water which must first enter into the pH raising/slag chamber. Before pH rise occurs, the recycled water is at a pH of 7.5 and contains approximately 11 mg/L of dissolved iron, 200 mg/L of dissolved magnesium and 53 mg/L of dissolved manganese. The sulfate content of this stream is aimed at being kept below 100 mg/L. Calcium content of this stream is high at approximately 500 mg/L. After exiting the slag chamber (before entering the sedimentation tank) the quality and characteristics of this feed changes due to the sudden rise in pH. The calcium content can reach levels of above 1600 mg/L but all other heavy metal concentrations decrease. The settling tank contains a large volume of water moving at a low velocity, as shown in Figure 7-6.

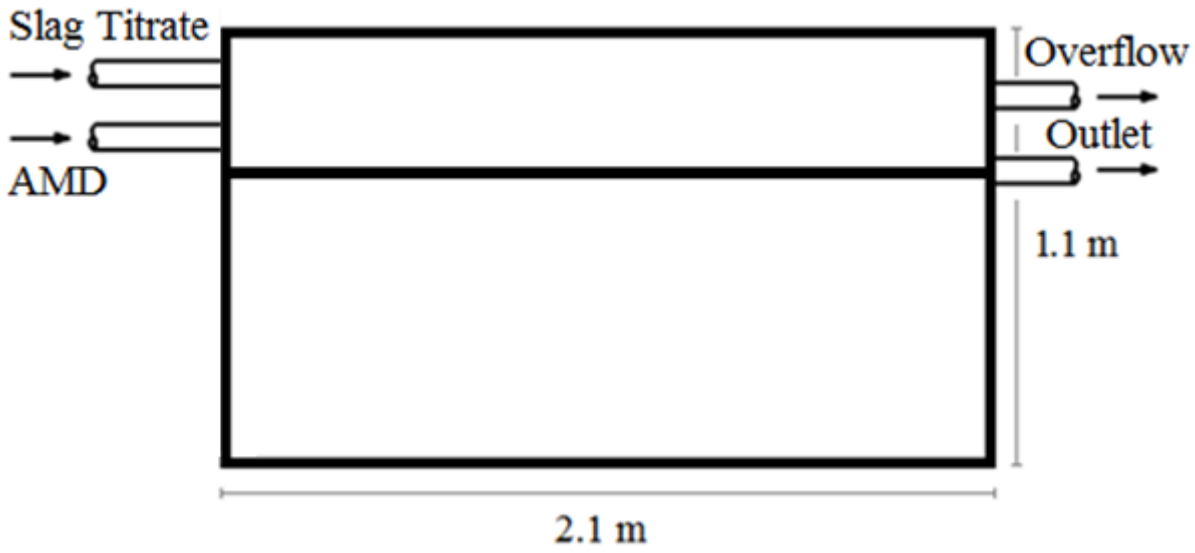


Figure 7-6: Gravity Settling tank to be used for heavy metal oxide/sulfate/sulfide/carbonate settling

The low pH AMD and high pH slag titrate would enter the vessel, mix and reach an average pH level. This pH level would be higher than the original AMD pH and thus, following mixing, precipitation of the heavy metals would occur. As the precipitate particles form in the liquid, they would settle (under the action of gravity) to the bottom of the tank. Smaller particles settle at a lower rate and may possibly be carried further forward before they reach the bottom of the tank. The very fine particles are carried away in the liquid overflow. Future designs may incorporate a mechanism which will allow easier separation of the precipitates.

7.6.2.2 Sizing

The smallest particle (ferric sulfate) was used to determine the ideal size of the sedimentation vessel. Ferric sulfate has a theoretical settling velocity of 0.000288m/min (Haman and Zazueta, 2014), which gives a calculated maximum settling area of 4.82 m^2 (calculations are shown in Appendix B). This value incorporates a safety factor, as the vessel should be large enough to hold all precipitate that is formed, without causing blockages or overflows (breakthrough of sediment). Two vessels will be used, each with a height of 1.1m, a length of 2.1m, and a width of 1.2 m, to achieve the desired sedimentation.

7.6.2.3 Materials & Mechanical Design

According to data obtained from lab-scale experiments, a total of 15 kg/day of metal precipitates could potentially be formed and removed in the settling tank when treating 1000 L/day of AMD. For this reason, two sedimentation systems will be constructed; to be used alternatingly, while cleaning of the other occurs. Cleaning of these vessels will occur weekly or when needed to avoid blockages. The inlet into the settling basin will minimize entrance velocities by the addition of a baffle just below the inlet position. This will allow very little turbulence to be created, and will distribute the water across the basin as uniformly as possible. Data obtained from experimentation indicates that precipitation of iron sulfate occurs after 24 hours of pH change. In order to ensure maximum precipitation and removal of metals, the vessel will have a residence time of at least 48 hours.

The material used for the sedimentation chamber will be linear low-density polyethylene (LLDPE) which is resistant to a 70% solution of sulfuric acid. This material will be able to withstand the corrosive nature of the AMD.

7.6.3 Bagasse Reactor

The bagasse reactors are represented by symbols R-101 and R-102 on the plant layout diagram, PFD and P&ID.

7.6.3.1 Overview & 2D Diagram

The bagasse reactor contains sugarcane bagasse and a culture of sulfate reducing bacteria which enables sulfate reduction. The bagasse is placed in removable, perforated crates and stacked inside the reactor. These racks do not impede flow and allow for spacing between the bagasse stacks to facilitate sulfate reduction. Lab scale experiments have shown greater sulfate removal when liquid is not in direct contact with carbon source for a portion of the flow. An internal side view of the reactor is shown in Figure 7-7 which incorporates this aspect.

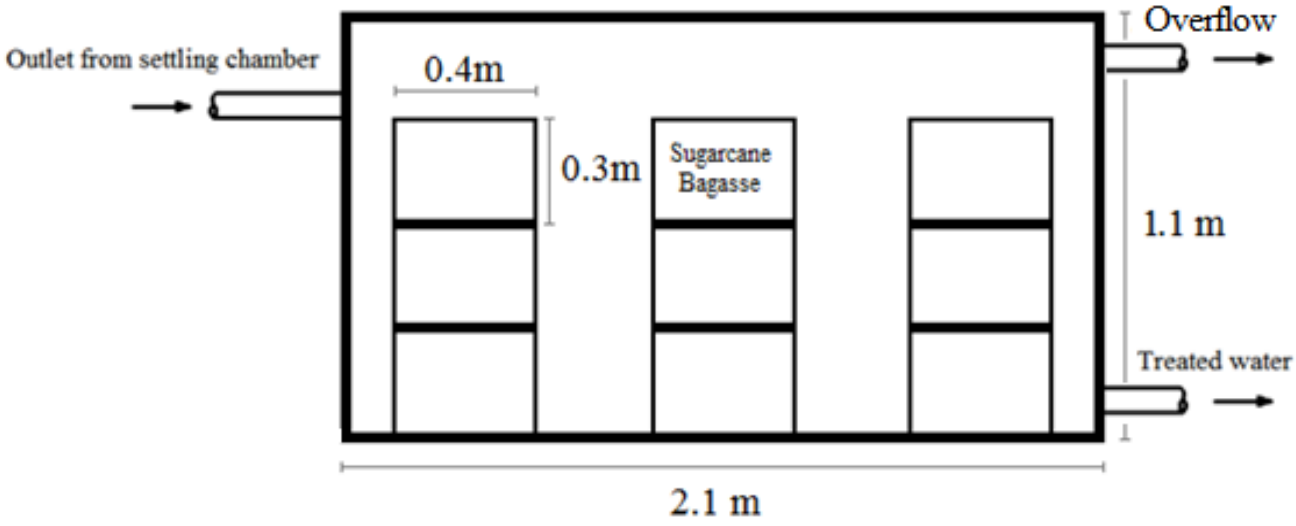


Figure 7-7: Side view of bagasse reactor

The inlet into the reactor is situated above the base and feeds liquid which flows via gravity out of the main settling tank. A gas vent is fitted to these reactors (which are sealed) and the gas produced from this system is passed through a scrubber before it is liberated into the environment.

7.6.3.2 Sizing

Using data obtained from experimentation, the volume of the reactor is calculated to be 1650 L. A detailed calculation is shown in Appendix A. The pre-made rectangular vessel with a length of 2.1 m, width of 1.2 m and height of 1.1 m will be used. This size reactor can be used to facilitate the reaction, independent of sugarcane bagasse loading – i.e. providing an alternative carbon source with a negligible volume. Since sugarcane bagasse mass (and relative volume) has to be considered, the experimental data is used to ensure scale up of the reactor is feasible.

Lab scale experimentation has shown a removal rate of sulfate of 22 mg/hour in a 50 Litre vessel with a residence time of 24 hours. If these results are used, a 1000 litre vessel will be needed to treat a flowrate of 1000 L/day of AMD. Thus, the proposed reactor vessel will be sufficient for the process. To achieve a final concentration of approximately 100 mg/L only one reactor will be needed, however two of these reactors will be set up in series to facilitate the removal in order to increase the non-contact space between the bagasse and the liquid. In this way, the sulfate removal is theorized to occur at a faster rate.

Both reactors will be inoculated with a functional strain of SRB culture which has been cultivated and acclimated using AMD tailings dam AMD samples (these cultures are currently being maintained using sodium sulfate and sodium acetate and their functioning is being monitored). Using short term experimental results, a mass of 25 kg of bagasse must be used in each of these reactors to achieve a final sulfate concentration of under 100 mg/L. This mass of bagasse will not be depleted immediately and will take approximately two weeks to degrade. The true replacement schedule is unknown and will form a research question.

All carbon containing compounds within the bagasse can theoretically be used by the SRB. Thus, since the bagasse generally has a water content of 50% or below, theoretically 3 kg of bagasse is needed in total per day to treat 1000 L of AMD. Including an over-estimation parameter to accommodate inefficiency of SRB functioning and cellulose breakdown, 90 kg of bagasse will be needed in total per month. To accommodate this, the bagasse is proposed to be changed every 17 days, pending observation of the system.

7.6.3.3 Materials & Mechanical Design

The sulfate reduction reaction will occur in two bioreactors arranged in series as opposed to one larger reactor. This is due to the challenges associated with maintaining homogeneity in large systems. The shape of the vessels will be rectangular, each having a height of 1.1 m and a length of 2.1 m. Cell washout will not be prevented, but it is assumed that SRB cell growth is equal to cell wash out.

All parts of the reactors will be constructed from linear low-density polyethylene (LLDPE) which is resistant to 70% sulfuric acid solution. No metals will be used due to the highly corrosive environment. The system will be sealed using pond liner.

7.6.4 Hydrogen Sulfide Scrubber

A low risk of hydrogen sulfide being released in a short period of time into the environment exists and for this reason a hydrogen sulfide scrubber is incorporated into the design. To negate any uncontainable H_2S release, the scrubber consists of a 200 L plastic drum containing water, hydrogen peroxide or ammonia. Exhaust gas from the bagasse reactors will be directed into the base of the vessel and allowed to bubble through the liquid. H_2S gas exhibits high dissociation and reactivity, and the gas will react with the scrubbing liquid to form sulfuric acid and water. The tank used will be constructed from polyethylene to prevent degradation of the vessel. The scrubber is represented by symbol R-103 in the PFD and P&ID.

7.6.5 Slag Reactor

This reactor is represented by symbol R-104 on the PFD and P&ID.

7.6.5.1 Overview and 2D Diagram

The slag reactor allows a rise in pH of the feed via hydroxide enrichment and hydronium ion depletion. An approximate rate of pH rise has been determined from previous experiments and this rate reduces over time as slag depletion occurs. A large slag reactor is used which will be packed with crates containing slag particles to allow for easier replacement and removal. The reactor is set up as shown in Figure 7-8.

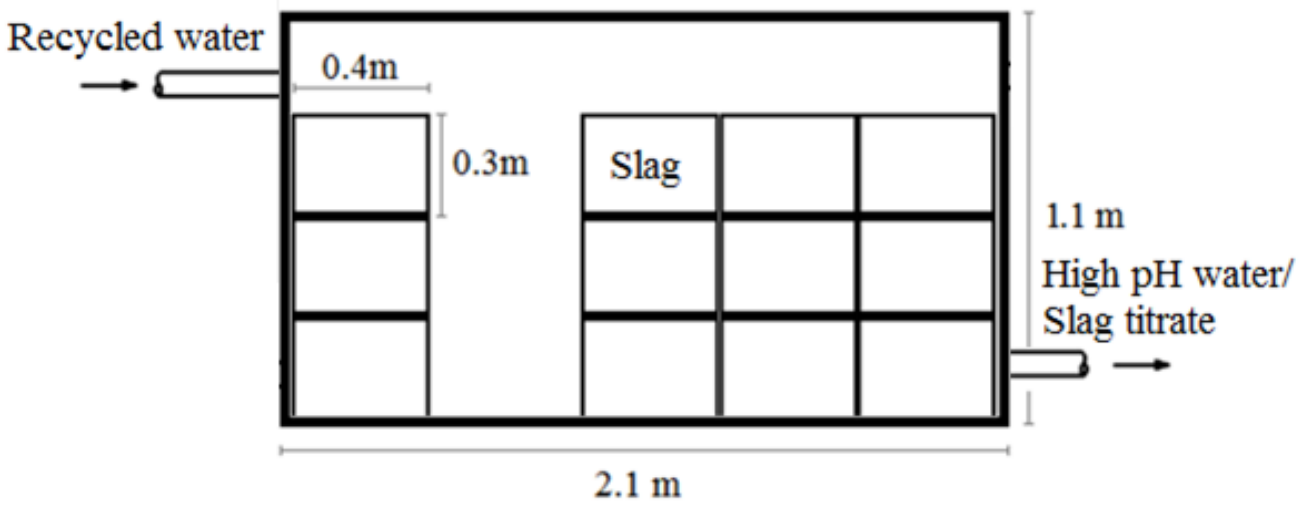


Figure 7-8: Side view of slag reactor

Each crate will contain 10 kg or more of slag which is above 8mm in aperture. The crates will allow for easy and quick replacement of the slag. The crates act like cartridges and replacement is simple, and requires little physical exertion. Settling in the reactor may occur due to the presence of heavy metals, and this can be cleaned out when necessary.

7.6.5.2 Sizing

Using the data obtained from lab scale experiments, 15kg of slag should be sufficient to raise the pH of 1000L of AMD to 9. This is determined using breakthrough curves which saw a drop from pH 11 to pH 10 after treating approximately 100 L of neutral pH water with 300 g of slag. A titration curve was also used to determine the ratio of clean water to AMD needed to reach a pH of 9. A pH of 9 will allow for sufficient heavy metal precipitation and will still be within range of the SRB pH functionality.

A 2,772 m^3 vessel will be used as the slag reactor vessel, which will allow for a maximum of 30 crates. If the reactor is packed to a maximum capacity, 25 kg of slag can be filled in each crate, giving a total slag mass of 750 kg. This will allow 50 days of treatment before depletion becomes noticeable. This option is at full reactor capacity and can be used for prolonged periods where regular replacement of slag is not possible or feasible. In order to create ease of replacement for general use however, each crate will only be filled with 10kg, and only 24 crates will be fitted in the reactor - giving a total slag mass of 240 kg. This will be sufficient for 16 days of remediation at the highest recycle rate. Every week 12 crates (120 kg) can be replaced. In this way, the slag would always be present in excess. This would prevent depletion of slag which would result in large increases of the recycle stream flowrate.

7.6.5.3 Materials & Mechanical Design

The slag reactors will be constructed out of acid resistant plastic (linear low-density polyethylene). The inlet of the reactor will be just above the base of reactor and the outlet will be just below the level of water.

7.6.6 Treated Water Reservoir

The reservoir is represented by symbol TK-101 on the PFD and P&ID.

7.6.6.1 Overview

The treated water will exit the bagasse reactor and enter into a water reservoir which would then drain back into the AMD tailings dam . The reservoir would be sealed and would not allow for hydrogen sulfide gas liberation or oxidation of any sulfide ions. The flow of the recycle stream from the reservoir to the slag reactor is controlled via pH of the settling tank. The outlet water flows back into the AMD tailings dam via an overflow outlet. This overflow would be the product stream of the system.

7.6.6.2 Sizing

The reservoir will have a volume of 225 L. A Jojo tank (or similar) will be used as the vessel.

7.6.6.3 Materials and Mechanical Design

The reservoir will be constructed from acid resistant and UV resistant plastic and will be sealable.

7.7 Piping, Valves and Pumps

7.7.1 Piping

Piping will consist primarily of PVC tubing with a small amount of silicon tubing used to pump water from the AMD tailings dam to the settling tank. Nylon tubing may also be used in certain parts of the plant to disallow oxygen from entering the system as this would interfere with the SRB functioning as well oxidize any reduced sulfate in the process. The material used for each piping stream is shown in Table 7-2. The lengths provided are estimations obtained from the plant layout diagram and may increase based on the positioning of the trenches already built on site.

Table 7-2: Piping materials of different streams and respective lengths

Stream Number	Piping Material	Approximate Length (meters)
1	Silicon	4
1A & 1B	PVC	4
2	PVC	3
3	PVC or nylon	2
4 & 5	Silicon	3
7	PVC or nylon	3
8	PVC or nylon	3
9	PVC or nylon	3
10	Silicon	5
11	Silicon	3

7.7.2 Pumping

Pumping will be done using peristaltic pumping to avoid direct contact with any liquid (which will cause corrosion and degradation of materials not resistant to acid). The environment at the dam is highly corrosive and no metal will be used in the construction of the plant. Two peristaltic pumps will be used in the process (P-101 and P-102 in PFD). P-101 will have a constant speed and the speed of P-102 will be controlled via the pH data obtained from the settling tank. Other pumps can be added optionally to

- pump water from the bagasse chamber into the reservoir
- pump water from slag chamber to slag chamber
- pump water from slag chamber into the settling chamber

(all optional pumps can be removed if the plant is setup in a way that allows for gravity flow)

The pumps will be housed in the electrical/process control box which will be constructed of acid and UV resistant plastic.

7.7.3 Valves

Multiple polyethylene or Teflon ball and joint valves and three-way valves will be used to control the flow in the system. The flow will be switched off and on depending on configuration and replacement scheduling. Additional clamp valves may be used where necessary to alter and control the flow between the various operations, especially on silicon tubing.

7.8 Control philosophy

7.8.1 Introduction

The monitoring and control philosophy will be one of providing a low level of automation and an overview of the status of the various streams within the plant, in terms of pH, temperature and conductivity. Programming of the system will be required to ensure trouble free operation. The following monitoring and controls will be in effect.

1. Flow, pH, temperature and conductivity
2. Drives indications, interlocking and control

7.8.2 General philosophy

The general interface between the operator and the supervisory system is that plant automation will be geared towards a high level of operator action and low level of automated control.

Automated control will be accomplished via monitoring of the pH inside of the settling tanks. The pH of the settling tank will control the flow of the recycle stream into the slag chamber by controlling the speed of the peristaltic pump (P-102). pH, conductivity and temperature will also be monitored, but these will be purely for recording purposes. Other control aspects may be added as the plant commences operation.

7.8.3 Control box

The operator interface to the plant will consist of visual display units and keyboards. All stream displays will be inside the control housing/box, but there may be some displays situated at the point of analysis for convenience. The interface will enable the operator to start, control and stop the plant as well as allow the operator to monitor the process continuously and remotely. The HMI will provide an alarm display and management system. In addition to this, all digital and some trend displays of certain analogue variable will be accessible to the operator by means of a data logger and a 3G network connection. The software will be designed in such a way to ensure easy back up and restoration.

7.8.4 Interlocks

Interlocks are suitably configured process conditions or integral devices which must signify a healthy plant operational state before a certain piece of equipment can be operated. A process interlock is proposed to be used in the system to stop the AMD and recycle streams if the pH of the water exiting the sedimentation tanks are too low or too high as this will result in death of the SRB.

7.8.5 Piping and instrumentation diagram

The diagram shown in Figure 7-9 is a detailed representation of the pilot plant. Valves, sample points, piping and instrumentation are shown. Table 7-3 provides a key which details the symbols used in the P&ID. All piping and cord will be enclosed in a hard conduit.

Table 7-3: Key for piping and instrumentation diagram

Utility Connections Key	
Symbol/Diagram	**Description**
	Sampling Point
	pH Transmitter
	Temperature Transmitter
	Pressure Transmitter
	Conductivity Transmitter
	pH Indicator
	Conductivity Indicator
	Temperature Indicator
	Stream Number
	Butterfly Valve
	3-Way Valve

P-101	V-101A/B	V-102A/B	R-101	R-102	R-103	V-103	TK-101	P-102	R-104
AMD Feed Pump	Sedimentation Vessel	Standby Sedimentation Vessel	Bagasse Reactor	Secondary Bagasse reactor	Hydrogen Sulfide Scrubber	Secondary Sedimentation Tank	Storage Tank for Remediated Water	Recycle Pump	Slag Chamber

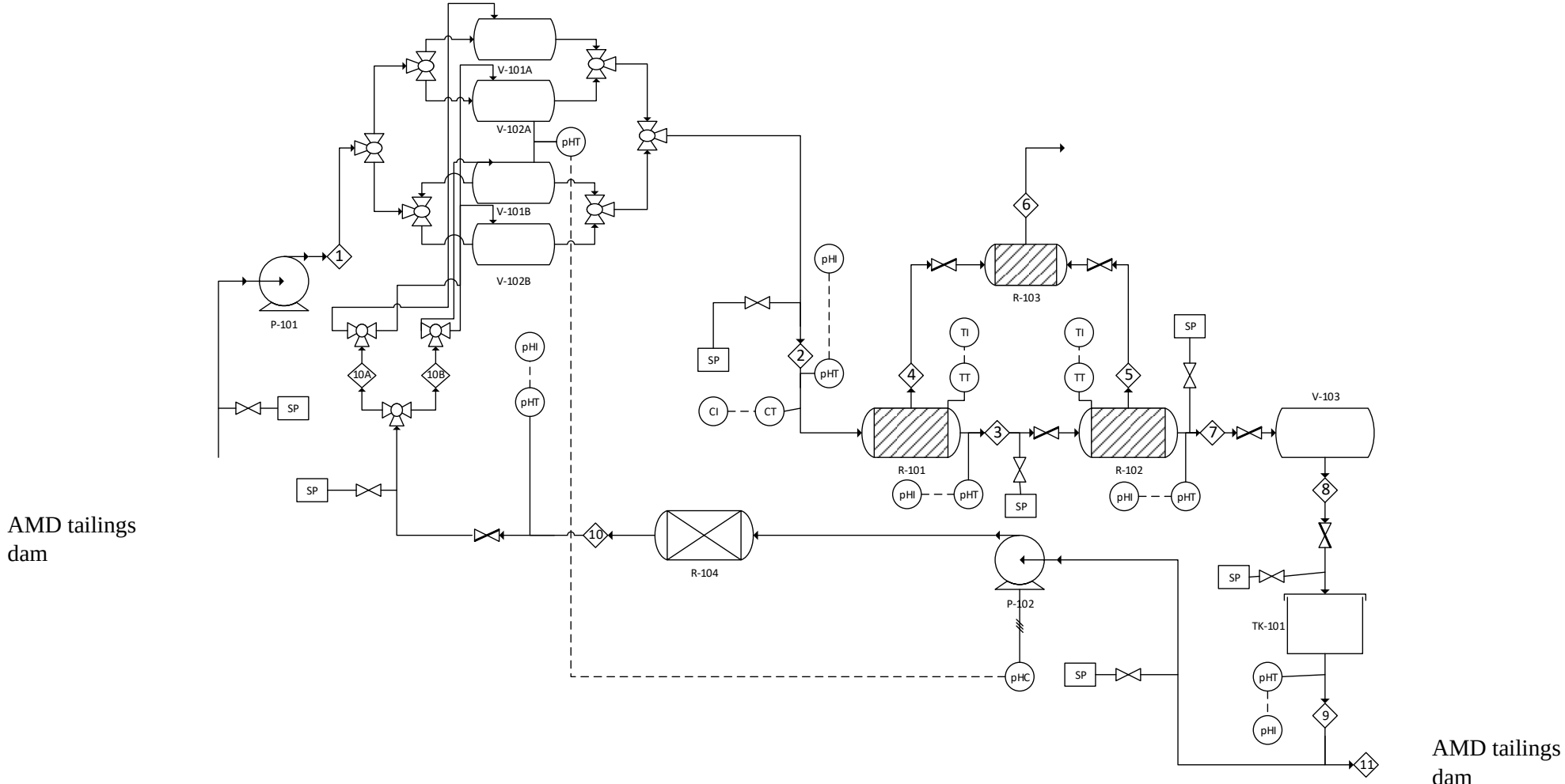


Figure 7-9: Piping and instrumentation diagram

7.9 Waste Management

Spent slag will be disposed of on site in the large mine dump situated next to dam. Treated water and scrubber water will be disposed of in the AMD tailings dam. Both the treated water and the scrubber water are of better quality than the AMD tailings dam water and thus any disposal into the dam is allowable. The waste bagasse will be disposed of in the mine dump site. Solid precipitate will be disposed of with the slag in the mine dump situated next to the dam. A schedule for waste disposal will be created based on process performance.

7.10 Costing

A list of parts needed to construct the pilot plant, as well as their quantity and cost is provided in Table 7-4. Prices marked with an * have not been quoted for and estimations have been provided in those cases.

Table 7-4: Parts and pricing list for pilot plant

Part	Description	Quantity	Cost	Supplier	Total
	Plastic rectangular reaction/sedimentation vessel	8	R6000	Pioneer Plastics, 5 Potgieter St, Rosslyn, Pretoria, 0200, South Africa	R48000
	Industrial pH electrode	3	R6000	Hanna Instruments (Pty) Ltd, 6 Vernon Road, Morninghill, South Africa	R18000
	pH electrode + meter	5	R600	Microrobotics South Africa, Centurion	R3000
	pH transmitter	3	R3000	Test & Measurement Instruments cc	R9000
	programmable logic controller	1	R12000	Siemens	R12000

Part	Description	Quantity	Cost	Supplier	Total
	Industrial Conductivity meter	1	R7000	Hanna Instruments (Pty) Ltd, 6 Vernon Road, Morninghill, South Africa	R7000
	Temperature probe and arduino kit	5	R800	Microrobotics South Africa, Centurion	R4000
	Piping	All fittings	*R5000	-	R5000
	Valves	All fittings	*R1500	-	R1500
	Crates	70	R85	Shawson's Plastics, South Africa	R5950
	Pumps	2	*R60000	Watson and Marlow	R120000
	Plastic scrubber vessel	1	R160	Pioneer Plastics, 5 Potgieter St, Rosslyn, Pretoria, 0200, South Africa	R160

Part	Description	Quantity	Cost	Supplier	Total
	Weather meter kit	1	R1300	Microrobotics South Africa, Centurion	R1300
	Aluminium tape	All fittings	*R3000	-	R3000
	Plastic pond liner sheets	All fittings	*R3000	-	R3000
	Water Reservoir	1	R2400	Plumblink, South Africa	R2400
	Electronic Housing	1	R6000	-	R6000
	Laptop	1	R6000	Incredible Connection	R6000
Total (rounded)					R256 000

7.11 Appendix A (WRC Report 1): Bagasse reactor sizing (literature based)

When conditions are ideal, the size of the reactor(s) (which is modelled as a plug flow reactor) is given by Equation 7-1 (Fogler, 1999) .

$$\boldsymbol{V = F_{A_0} \int_0^X \frac{dX}{-r_A}}$$

Equation 7-1

Where:

F_{A_0} is the initial molar flowrate of sulfate

r_A is the rate law, and

X is the desired conversion

$-r_A$ is given by Equation 7-2 and C_A is given by Equation 7-3 below.

$$\boldsymbol{-r_A = kC_A^2}$$

Equation 7-2

$-r_A$ is given by Equation 7-2 and C_A is given by Equation 7-3 below.

$$\boldsymbol{C_A = C_{A_0}(1 - X)}$$

Equation 7-3

Using Equation 7-2 and Equation 7-3, Equation 7-1 is simplified to:

$$\boldsymbol{V = \frac{F_{A_0}}{kC^2{}_{A_0}} \int_0^X \frac{dX}{(1 - X)^2}}$$

A k value from experimental data is determined to be 0.005497 mol/day. X is calculated using an experimental value of sulfate entering the bagasse reactor (approximately 15000 mg/L), and is determined to be 0.93. The initial concentration of sulfate is 15.62 mL/L, and the initial molar flowrate of sulfate is measured as 15.615 mol/day.

7.12 Appendix B (WRC Report 1): Sedimentation tank sizing

Equation 7-4 is used to calculate the settling velocity of Iron sulfate (Haman and Zazueta, 2014) and then Equation 7-5 is used to calculate the area required for the settling/sedimentation tank.

$$\boldsymbol{V_p = 0.00135\left(d^2\right)(SG-1)(0.0254)}$$

Equation 7-4

Where

V_p = settling velocity of particles in water(m/min)

d = particle diameter (microns) (2 micron for ferric sulfate)

SG = specific gravity of particle

$$\boldsymbol{Area = 1.604\left(\frac{Q}{V_p}\right)}$$

Equation 7-5

Where:

$Area$ is the surface area of the settling tank in ft^2

Q is the flowrate into the tank in gal/min

V_p is the settling velocity of the particle in in/min

8 The design, construction and monitoring of a laboratory scale system treating up to 25 L/day

This chapter is presented solely as a journal article (peer reviewed) titled “Sugar and Steel By-Product Utilization in Acid Mine Drainage Remediation” which was published in the American Society of Civil Engineers Journal of Hazardous, Toxic, and Radioactive Waste (Naidu, van Dyk, *et al.*, 2020). No supplementary or additional material is required for the achievement of this objective (Objective 5). The full reference for the article is shown below. The author contribution statement for this publication can be found in Appendix I.

Naidu, T. S., van Dyk, L. D., *et al.* (2020) ‘Sugar and Steel By-Product Utilization in Acid Mine Drainage Remediation’, *Journal of Hazardous, toxic and radioactive waste*, 24(1), pp. 1–10. doi: 10.1061/(ASCE)HZ.2153-5515.0000472.

Sugar and Steel By-Product Utilization in Acid Mine Drainage Remediation

8.1 Abstract

In this research two industrial byproducts produced close to South African mining regions were used to treat acid mine drainage (AMD): steel slag and sugarcane bagasse, i.e., the shredded cane stalk residual after sugar extraction. Basic oxygen furnace (BOF) slag has a high alkalinity which makes it ideal for neutralizing acids. Sugarcane bagasse has a high surface area and its slow decomposition makes it an ideal host media and long-term carbohydrate source for sulfate reducing bacteria (SRB). Accordingly, this research explored the viability of remediating AMD in a two-step continuous process combining both materials. A design was proposed and tested, in which a mixture of BOF slag eluate (generated from a treated water recycle loop) and raw AMD was used to initially buffer the AMD solution and precipitate heavy metals in a sedimentation tank. This avoided toxic shocking the SRBs in a subsequent sugarcane bagasse bioreactor. Overflow from the sedimentation tank was then passed through a packed bed containing sugarcane bagasse inoculated with SRBs as a polishing step to remove sulfate, precipitate metal sulfides and elevate pH to near neutral pH conditions. The effluent from this vessel represents the treated water and a fraction was recycled through a packed bed of BOF slag to create an alkaline eluate for pre-treatment of the raw AMD solution. The effect of AMD composition and slag particle size on the treatment was studied. Operation of the designed process at the laboratory scale, between 1 and 10.4 L/day has confirmed the buffering of the AMD solution to a pH of between 7 and 8, and the removal of heavy metals and sulfate to levels of below 10 mg/L for Al, Fe, Mg, Mn and <200 mg/L for sulfate. Ca increased in the system, attributed to the dissolution of slag. SRB functioned well in the system with a maximum sulfate reduction of 35% (accounting for 2% of overall sulfate removal) occurring across the sugarcane bagasse bioreactor. Precipitation and sedimentation accounted for the bulk of sulfate removal with over 90% of sulfate being removed across the sedimentation tank. Residence times of between 44 and 4 days were achieved for different conditions - smaller particle sizes of slag exhibiting better performances in terms of recycle rate and residence times.

Keywords: Acid mine drainage, BOF slag, sugarcane bagasse, sulfate reducing bacteria, dissimilatory sulfate reduction

8.2 Introduction

Water scarcity currently affects over 40% of the Earth's population – a value that is projected to rise with increasing drought and desertification due to climate change over the next three decades (Alamanos et al. 2018; United Nations Development Programme 2019). It is expected that by 2050 one in four people will be affected by water shortages. Ongoing environmental impacts from mining sites have contaminated vast amounts of drinking water and aquifers, creating long-standing public health risks and destroying aquatic and terrestrial habitats throughout the globe (Meegoda et al. 2011; Sumi and Gestring 2013).

Acid mine drainage (AMD) or acid rock drainage (ARD) is formed when rocks and waste mine materials that contain sulfide components, oxidize on exposure to water or air (Naicker et al. 2003). Waters that have been contaminated with AMD are characterized by a low pH, high acidity and high concentrations of sulfates and metals such as iron, manganese, aluminium, magnesium, calcium and iridium (Feng et al. 2004). Polluted waters very often require treatment (Peppas et al. 2000; Potgieter-Vermaak et al. 2006). AMD has long been considered an environmental hazard (Sheoran and Sheoran 2006) due to its long-term impairments to waterways and to the biodiversity of ecosystems that rely on these waterways (Akcil and Koldas 2006).

The United Nations (UN) has recently classified AMD as the second biggest problem that the Earth faces (Tuffnell 2017), and there are many abandoned mine sites in countries such as Australia, Canada, South Africa and the United States of America (USA) which are afflicted by this environmental challenge (Naidoo et al. 2009). The fundamental role of water in human activity means that the successful achievement of a large portion of the Sustainable Development Goals (SDG's) (recently proposed by the UN) will depend heavily on water availability (Vorosmarty et al. 2018) and thus innovative treatment methods (that are low cost and effective) for AMD have come to the forefront in many research areas.

One such remediation method involving the use of by-products from both the sugar and steel making industries has been tested on AMD from the Witwatersrand coal mining industry, in Mpumalanga, South Africa (Naidu et al. 2018; Name and Sheridan 2014). Waters from this region have varying conditions but like most AMDs are characterized by low pH levels and high concentrations of sulfates and metals (Feng et al. 2004). The industrial by-products, basic oxygen furnace (BOF) slag and sugarcane bagasse are regionally available in large volumes in south-eastern South Africa (SA), and in other tropical and subtropical areas throughout the world afflicted with AMD production (Grubb et al. 2018).

Between 160–240 metric tons (Mt) of BOF slag are produced worldwide every year – a problem for the iron and steelmaking industry, as BOF slag reportedly has few reuse avenues (Fernández-González et al. 2019). BOF slag characterized by 10-15 wt.% lime/portlandite and various alkaline silicates and

oxides [which originate from the fluxing agents that are added to the steel-making process (Piatak et al. 2015)], is able to generate highly alkaline solutions via hydration, and can be used to buffer and elevate the pH of AMD (Riley and Mayes 2015; Roadcap et al. 2005). Alkalinity can be generated from slag in two ways: (i) rapid hydration followed by dissociation of calcium and magnesium oxides, and; (ii) dissolution of Ca-silicate minerals which is a much slower process (Gomes et al. 2016). The hydration, dissolution and dissociation reactions that bring about this alkalinity are described by Equation 8-1 to Equation 8-7.

$$CaO + H_2O \leftrightarrow Ca(OH)_2$$

Equation 8-1

$$Ca(OH)_2 \leftrightarrow Ca^{2+} + 2OH^-$$

Equation 8-2

$$MgO + H_2O \leftrightarrow Mg(OH)_2$$

Equation 8-3

$$Mg(OH)_2 \leftrightarrow Mg^{2+} + 2OH^-$$

Equation 8-4

$$Ca_3Si_2O_7 + 7H_2O \leftrightarrow 3Ca^{2+} + 2H_4SiO_4 + 6OH^-$$

Equation 8-5

$$Ca_2SiO_4 + 4H_2O \leftrightarrow 2Ca^{2+} + H_4SiO_4 + 4OH^-$$

Equation 8-6

$$Ca_2Al(AlSi)O_7 + 5H_2O \leftrightarrow 2Ca^{2+} + SiO_2 + 2Al(OH)_3 + 4OH^-$$

Equation 8-7

As pH rises, a substantial fraction of metals precipitate as oxides, hydroxides and sulfates, lowering the metal content of the water and making the AMD solution more amenable to biological treatment by Sulfate Reducing Bacteria (SRB) cultures. Furthermore, use of BOF slag in this manner can help alleviate the global slag disposal problem [volumetric swell of fresh BOF slag limits beneficial use in construction (Ding et al. 2017)] and help preserve natural resources worldwide (Yildirim and Prezzi, 2015).

SRB can reduce sulfates to sulfides via dissimilatory sulfate reduction (DSR), promoting more metal and sulfate removal by means of metal sulfide precipitation. SRB need a substrate to function and sugarcane bagasse has shown potential in this regard (Grubb et al. 2018; Hussain and Qazi 2016).

This paper extends upon the data presented by Naidu et al. (2018) and reports on the design and implementation of a process at a laboratory scale, comprising of two main steps (neutralization and sulfate reduction) and incorporating the two waste materials in a form of waste beneficiation. The aim

of this study was to conceptualize a design for a treatment system combining BOF slag and sugarcane bagasse and to explore the effectiveness and versatility of the system by determining the extent of sulfate reduction and metal removal in two types of AMD. The effect of different particle sizes of slag and different type of slag reactor on the performance of the system was also investigated. The results from preliminary experiments and literature are used to conceptualize the design – the design procedure and findings from the operation of the set-up are presented herein.

8.3 Materials

BOF slag was sourced from Phoenix Slag Services based in Newcastle, Kwazulu Natal, South Africa. The (X-Ray Diffraction) XRD analysis of the slag sample is presented in Table 8-1. The high oxide composition of the slag allows it to be used for pH raising applications. As the oxidic compounds dissolve in the acidic medium, the oxides become hydrated forming hydroxide ions and adding alkalinity to the system. The main oxide components of BOF slag is calcium oxide (as shown in Table 8-1).

Table 8-1: XRD analysis of BOF slag

Oxide	wt.%
CaO	41.6
SiO_2	14.4
Al_2O_3	2.8
Fe_2O_3	20.5
MgO	7.2
SO_3	0.4
LOI	5

The sugarcane bagasse was collected from Illovo's sugar plant in Eston, Kwazulu Natal, South Africa and had a major sugar content as shown in Table 8-2. The various sugar components of the sugarcane bagasse make it ideal for use as a substrate/carbon source for SRB. Cellulose, hemicellulose and lignin are the main components (as shown in Table 8-2) that are broken down into simple sugars.

Table 8-2: Carbohydrate content of Illovo sugarcane bagasse

Component	wt.%
Cellulose	45.25
Hemicellulose	27.29
Lignin	18.93

The AMD was obtained from two different sources in Mpumalanga, SA. AMD was pumped from the dams or rivers into sealable, cubic storage containers and transported to the University of the Witwatersrand. The composition of the AMD as collected from the two sites is provided in Table 8-3. Only major metals are indicated in this table, but other trace metal concentrations were also found. As

shown in Table 8-3, Type A and B AMDs have a similar pH, but the sulfate content of Type A is significantly higher than Type B. All other parameters are higher in concentration in Type B AMD. Type A AMD is considered more severely polluted than Type B due to the higher concentration of sulfate which relates to a higher toxicity.

Table 8-3: Composition and pH of AMD sourced from two different AMD sources in Emalahleni, Mpumalanga, South Africa

AMD Type	pH	Aluminium (mg/L)	Calcium (mg/L)	Iron (mg/L)	Magnesium (mg/L)	Manganese (mg/L)	Sulfate (mg/L)
Type A	2.44	434.89	110.83	3039.60	105.67	88.29	12955.62
Type B	2.47	497.25	175.38	3506.88	94.04	197.68	5199.92

8.4 Methods

Design methods were used to develop a preliminary design of an AMD remediation process and experiments were performed to refine the design, testing the configuration and operation of the system. The experimental procedures and analytical techniques are presented below.

8.4.1 Preliminary Experiments

A number of evaluations were undertaken to inform the design:

- The extent of release of alkalinity from the BOF slag into the liquid and the relation between pH rise and metal ion dissolution was investigated. BOF slag was added to water and AMD in a beaker. For a range of different masses of BOF slag and volumes of liquid were investigated. A stirrer bar was used to agitate the liquid at 200 rpm. 2ml samples were taken at intervals, diluted and tested for aluminium, calcium, iron magnesium and manganese content. Experiments were repeated where necessary to keep the sample volume < 5% of total volume of system. SEM images were also taken on the BOF slag particles after stabilization of the system, and pH was monitored throughout the experiment.
- The effect of sugarcane bagasse on the pH of AMD was investigated by adding sugarcane bagasse to a solution of AMD and monitoring the pH change over time. The system was also inoculated with SRB cultures to determine if SRB could function after being exposed to raw AMD solutions. SRB was cultivated separately using a solution of sodium sulfate and sodium acetate (using a 0.7 g chemical oxygen demand/g sulfate concentration) and then added to the AMD solution (SRB solution to AMD was mixed with a 1:2 ratio). Sulfide production and sulfate reduction (concentrations) were used as indicators of SRB activity. SRB cultures were sourced from previous experiments which had used mud sediment from Emmarentia Dam in Randburg, South Africa.
- The minimum volume of slag eluate (water that has been in contact with BOF slag for a period of time) needed to titrate AMD was evaluated by determining the volume of BOF slag eluate needed

to increase the pH of AMD from 2.4 to 9. This experiment was conducted to determine whether use of a recycle stream in the process was feasible.

The results from these preliminary experiments were used to determine the design configuration shown in Figure 8-1.

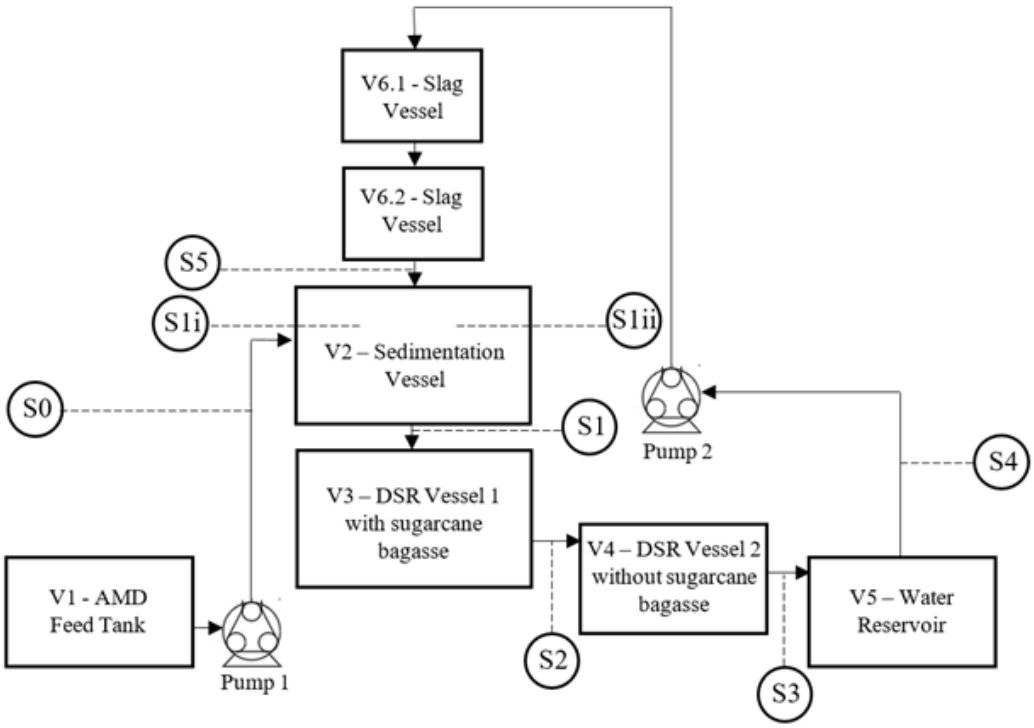


Figure 8-1: Schematic of laboratory set-up with sampling points and vessels labelled (circled numbers denote sampling locations)

8.4.2 Experimental Set-up

Figure 8-1 is a schematic of the laboratory process that was designed and tested for AMD treatment. It consists of two pumps and a number of rectangular process vessels (an AMD feed tank – V1, a slag vessel – V6.1 and V6.2, a sedimentation vessel – V2, primary and secondary DSR vessels – V3 and V4, and a water reservoir – V5) which were sealed and anaerobic. V2 (41.5 cm x 22 cm x 30 cm), V3 (41.5 cm x 22 cm x 30 cm) and V4 (30 cm x 14 cm x 20 cm) had volumes of 18 L, 14.4 L and 7 L respectively [dimensions given as (length x height x width)]. The volumes of the slag vessels changed from 1.8 L per vessel (2 vessels) to 1 L (1 vessel) on Day 64 due to a change in reactor type. V1 and V5 were not included in residence time calculations. Sample points (S1 to S5) are numbered for reference purposes in Figure 8-1. Movement of the liquid between tanks was achieved via pumping and gravity flow. The conceptualization of the experimental set-up is considered an aim of the study and was discussed further in the results section.

8.4.3 Procedure

The performance of the process was tested by operating the system under different process conditions for a total of 106 days. BOF slag particles were replaced, and sizes changed on Day 33, from size 1 (8

μm <d<13 μm) to size 2 (1.7 μm <d<3.350 μm), and on Day 64 from size 2 to size 3 (d< 1 μm) (particle size ranges were achieved using sieve analysis). On Day 64 the slag reactor type was changed from a packed bed reactor (PBR) to a continuously stirred tank reactor (CSTR) to eliminate blockages due to the small particle size. The raw AMD was changed on Day 70 from Type A to Type B. Samples were taken from sample points at different positions in the process (as shown in Figure 8-1) and analyzed for metal, sulfide and sulfate content as well as pH.

8.4.4 Analytical methods

The metal concentrations of aluminium, calcium, iron, magnesium and manganese were measured with an Agilent 2000 series atomic spectrometer (AAS). Samples were filtered, diluted on a 1:3 ratio with deionized water and acidified with 0.6 mL of nitric acid prior to AAS testing. This was done to measure the difference in concentration in dissolved and precipitated metals. pH was measured using a combined pH and ORP meter. Sulfate and sulfide concentrations were measured using turbidimetric spectrophotometric tests (using a Merck Spectroquant Pharo 300) (American Public Health Association, 1975; Center for Bioprocess Engineering Research, 2016). Samples were filtered and sometimes diluted before sulfide and sulfate testing to ensure concentrations were within an accurate range. A Scanning Electron Microscope (SEM) (FEI Quanta 200 ESEM) was used to investigate the surface of the slag particles. Standard concentration solutions were used for each test to obtain relevant calibration equations. XRD and Rietveld quantification analyses were done externally to determine the mineralogical composition of the slag. XRD sample preparation included grinding 3 g of sample and spiking it with fluorite on a 90:10 weight basis. Bagasse characterization data was obtained from the sugar mill. A Siemens D500 computer automated diffractometer was used to perform XRD.

8.5 Results and Discussion

8.5.1 Design Considerations

The first step in the design was to determine how to combine the sugarcane bagasse and BOF slag in a system, for ease of materials handling and effective treatment of the AMD. A combination of literature data and experiments were used to inform this step.

According to literature, the biological system functions best at pH levels of between 4 and 8 (Rasheed et al. 2019; Tambe et al. 2016), and thus the pH of the AMD must be increased for DSR to occur. When AMD contacts sugarcane bagasse only, it experiences a minimal rise in pH (2.4 to ~5), with bacterial functioning (determined via the presence of sulfide) only after 4 weeks. Due to the low pH, high sulfate and high metal concentrations of AMD, there was concern that passing AMD directly through the biological system could potentially toxic shock the SRBs, thus reducing DSR. Therefore, the pH of the AMD was elevated, and experiments were performed using BOF slag to determine how to best introduce alkalinity to AMD. Two options were investigated in this regard: 1) direct contact between BOF slag solids and AMD; or 2) introducing a recycle stream to create BOF slag leachate followed by

titration of the leachate with the AMD. In Figure 8-2, some results from the study (Ca and Mg concentrations in AMD or water solutions which are reacted with slag in a CSTR over time) are presented.

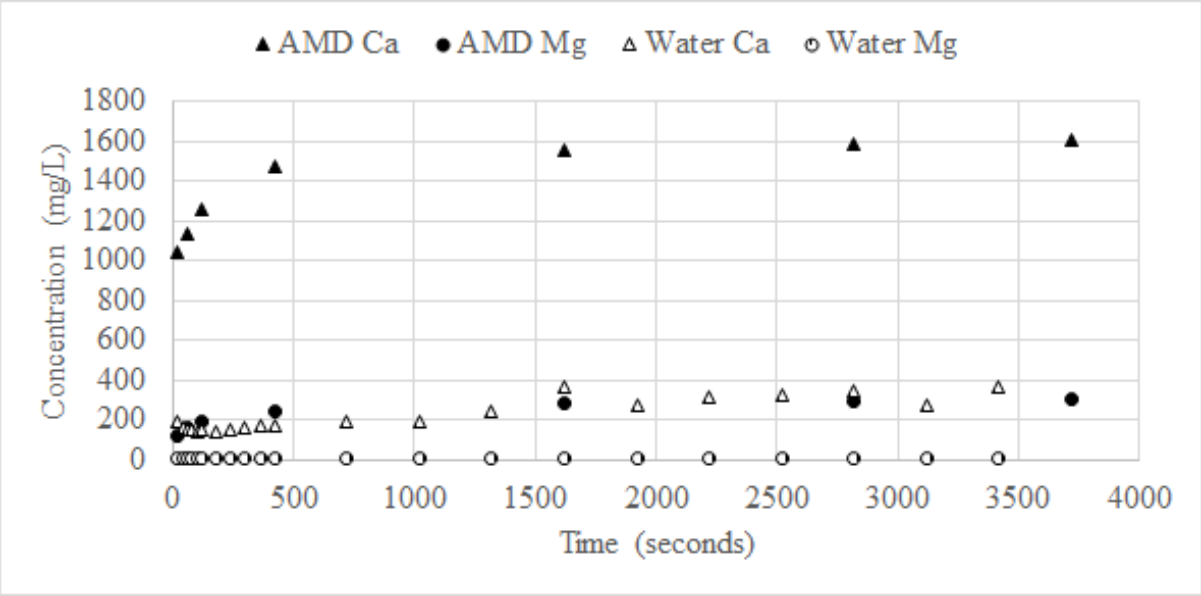


Figure 8-2: Concentrations of Mg and Ca ions in water and AMD solutions that are reacted with slag particles in a CSTR

Figure 8-2 shows that the AMD solution shows a much greater rise in concentration of Ca and Mg ions than the water solution under the same conditions (silicon is not measured as this occurs over a longer time period). The rise in pH of the AMD (to a pH of 8.5) and water (to a pH of 12.3) occurs via the dissolution and hydration reactions described in Equations 8-1 to 8-7. AMD has a higher concentration of the two metal ion species after reaction than water, as the acidity and the presence of counter-ions in the AMD (sulfate and metals) increases the forward rate of reaction resulting in greater dissolution of the slag. SEM images of the slag particles before and after pH rise of AMD are shown in Figure 8-3**.**

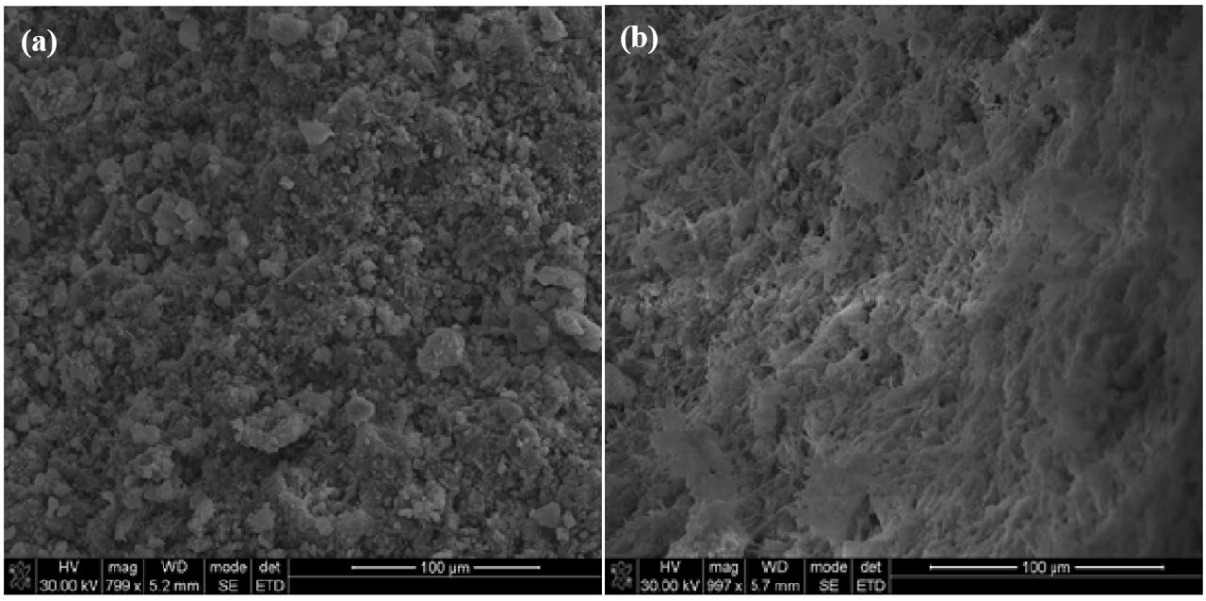


Figure 8-3: SEM imaging of (a) unreacted BOF slag compared to (b) slag reacted with AMD (particle size: 2 µm < d < 3.35 µm)

BOF slag which has been reacted with AMD (b) is visibly different to untreated slag (a), with a powder like substance shown to have formed on the surface. The formation of a precipitate on the surface of the slag limits alkalinity release and introduces operational issues relating to sludge build up and removal. To avoid this potential operational issue, a recycle loop and sedimentation vessel were added to the system. The recycle loop stream would have a pH and calcium content similar to the water stream shown in Figure 8-2. The presence of the recycle loop only allows for treated water (of a higher pH and thus lower sulfate and metal content) to pass through a BOF slag bed, increase the pH and alkalinity before contacting AMD in a separate vessel (sedimentation vessel) facilitating titration and precipitation of some sulfate and metal compounds. Investigations into the ratio of AMD to BOF slag eluate to reach a neutral pH, indicated a minimum of 1:4 in a well-mixed system. When mixing between the AMD and the BOF slag eluate (recycle stream) occurs, precipitate forms due to pH change and sedimentation occurs under the influence of gravity. The smallest particle that can form (ferric sulfate) has a settling velocity of 2.88 x 10^{-4} m/min (Haman and Zazueta 2014) and the surface area of a vessel needed to facilitate sedimentation of this particle for a flowrate of 1 L/day is 590 cm^2 (Haman and Zazueta 2014).

The pH adjusted water from the sedimentation vessel is then passed into a series of biological reactors containing SRB cultures and sugarcane bagasse as a substrate. These reactors were used as SRB cultivation vessels – SRB was cultivated in these vessels before operation began. DSR occurs in these vessels and accordingly the treated effluent serves the dual purpose of being potential released and the feedstock for stripping alkalinity from the BOF slag vessels.

Figure 8-1 is a process flow diagram of the designed laboratory scale process and shows the configuration of the reactors that were used in series to determine the extent of treatment of AMD using the slag and sugarcane bagasse. Figure 8-4 is a picture showing the laboratory system with the slag

chambers receiving the recycle stream through the top of the vessel. Performance of the system was assessed according to pH adjustment, sulfate removal, recycle ratio, metal removal.

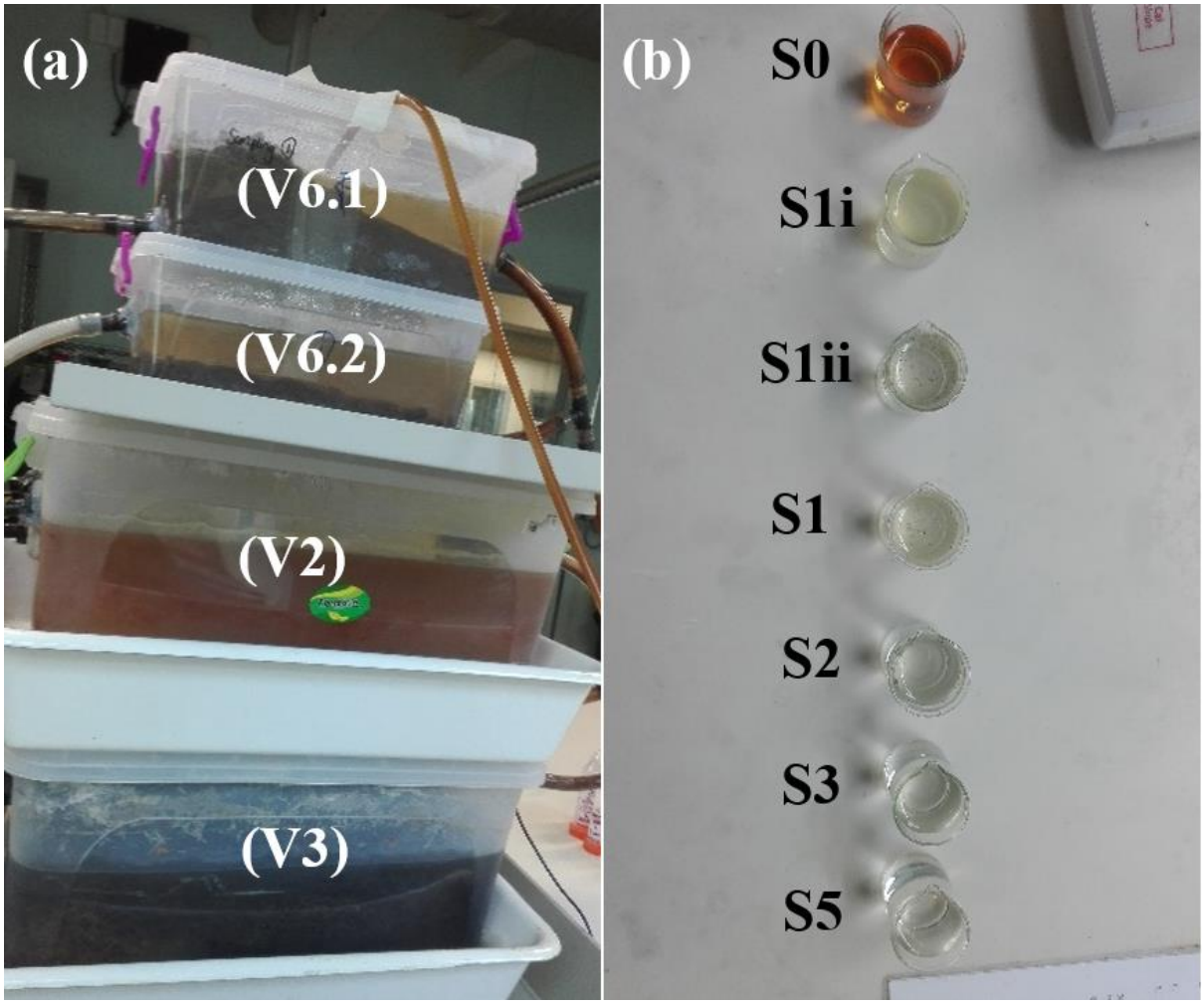


Figure 8-4: (a) Laboratory set-up with two slag chambers (V6.1 and V6.2) leading into the sedimentation vessel (V2) and then into the DSR 1 vessel (V3) which contains sugarcane bagasse; (b) top view of samples taken from each sampling point for AMD Type A and slag

The system operates as follows: Raw AMD from an AMD feed tank (V1) is pumped into a sedimentation vessel (V2). In this vessel the low pH AMD mixes with slag eluate and exhibits a rise in pH which reduces sulfate and metal levels via precipitation reactions. The outlet of the sedimentation vessel enters into a series of two DSR vessels [DSR 1 containing sugarcane bagasse (V3) and DSR 2 containing no sugarcane bagasse (V4)]. Here, DSR occurs and a portion of the sulfate remaining in the liquid is reduced to sulfide. The vessels are sealed preventing fugitive emissions of hydrogen sulfide gas. The effluent from the DSR vessels, enters into a water reservoir (V5). A portion of this water is recycled by pumping it through the slag reactor vessel (V6). This vessel is operated as a PBR and then as a CSTR. It was observed that particles in size 3 ($d<1$ μm) form a clay like substance when in contact with liquid and allowed to settle and was therefore not amenable to liquid flowing through them, hence the operation as a CSTR. The alkaline effluent from the slag vessel (V6) enters the sedimentation vessel (V2) where it mixes with raw AMD. The water that is not recycled remains in the water reservoir and

is considered treated water. The system is regulated by pH control; the pH in the sedimentation vessel controls the flowrate of AMD into the sedimentation vessel and of treated water into the slag vessel. This was accomplished by an on-off controller – when the pH in the sedimentation vessel was less than 5, the AMD pump is switched off and when the pH was greater than 7, the AMD pump is switched on to add more acidity to the system. This range was determined using literature review and data from the preliminary experiments – SRB function best at neutral pH levels and an acceptable removal of Fe (95% - 97%), Al (complete removal) and Mn (75% to 82%) was found to occur within this range.

8.5.2 Operation of laboratory scale set-up

In order to test the influence of certain system variables on the performance of the proposed treatment process design, the process was operated for 106 days with samples collected periodically from the sample points shown in Figure 8-1. The pH, sulfate and metal results, as well as the recycle ratio are presented and discussed below.

8.5.2.1 pH adjustment

pH plays a vital role in the successful functioning of the system. The rise in pH causes metal removal by precipitation and creates an amenable environment for DSR. pH control is thus an important factor to consider and was achieved by varying the flowrate of the recycle stream. A low rate of alkalinity release was observed in particle size 1 (8 μm <d< 13 μm) and thus the rate of the recycle stream was adjusted using pH control and the AMD inlet stream was kept constant at 1 L/day. This resulted in the pump operating at its maximum flowrate of 17 mL/min (24.48 L/day).

When the slag particle size was decreased, the process (pH) control was changed to keep the experiment comparable and to understand the maximum amount of AMD that could be remediated. The recycle rate was kept constant at its maximum flowrate and the AMD flowrate was controlled. The largest variation in pH occurs in the sedimentation vessel, as shown in Figure 8-5. The slag (V6) and DSR vessels (V3, V4) exhibit a buffering effect with an almost constant outlet pH (Figure 8-5**)**.

The constant outlet pH from the DSR and slag vessels could be attributed to the pH control positioning or to saturation limits of the solutions. The pH levels in the slag chamber are dependent on the dissolution of lime, portlandite and Ca-silicates. If the solution becomes saturated with metal ions, dissolution will no longer occur. The biological systems may have a similar method of functioning as changes in AMD quality and particle size of slag did little to the outlet pH.

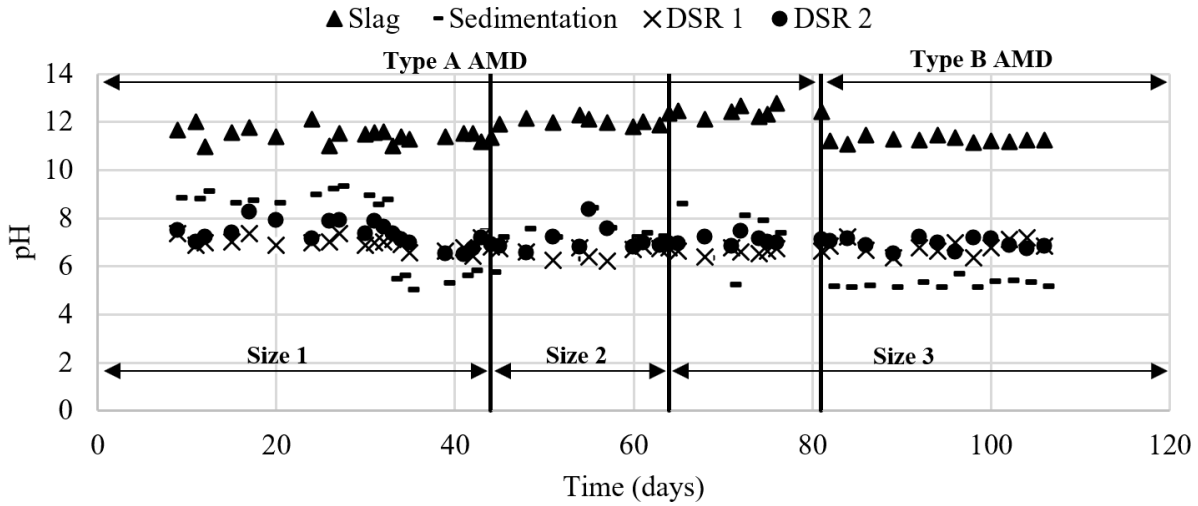


Figure 8-5: pH at the outlet of the slag (S5), sedimentation (S2), DSR 1 (S3) and DSR 2 (S4) vessels over the 106-day period

During the experiment it was noted that Mg concentration in the system did not increase. This is attributed to the precipitation chemistry of metals in varying pH solutions (with pH adjusted using BOF slag). This data is shown in Figure 8-6, with a visual representation of the experiment shown in Figure 8-7. Calcium rises as pH increases, as expected. Magnesium, however, decreases in concentration from a pH of approximately 7. The pH in the slag chambers (V6) and occasionally in the sedimentation vessel (V2) exceeds a pH of 7 and thus Mg precipitated out of solution.

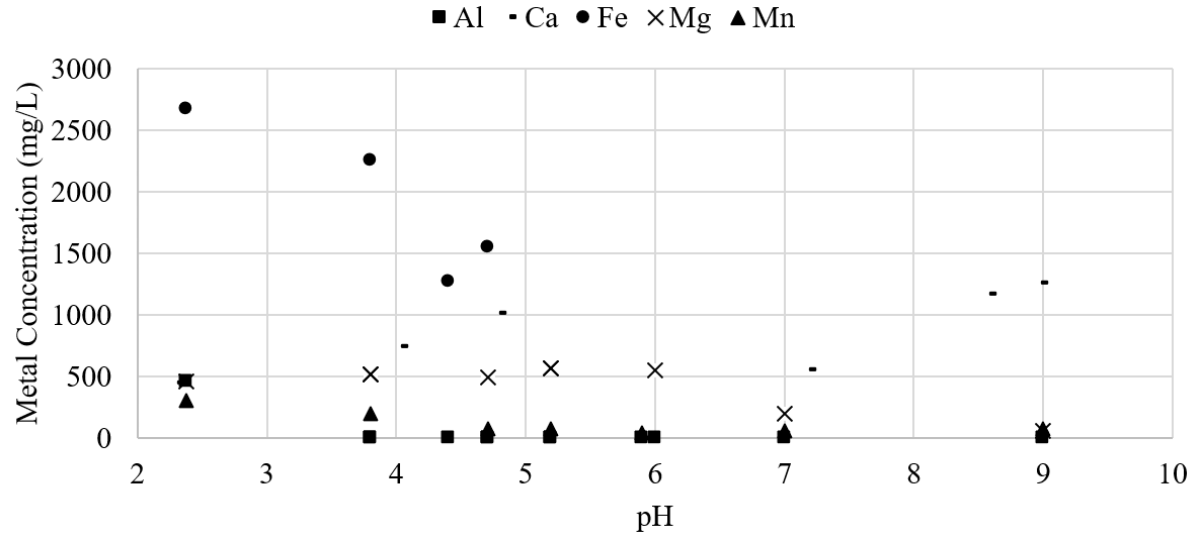


Figure 8-6: The concentration of aluminium, calcium, iron, magnesium, and manganese an AMD solution with pH change occurring through reaction with BOF slag

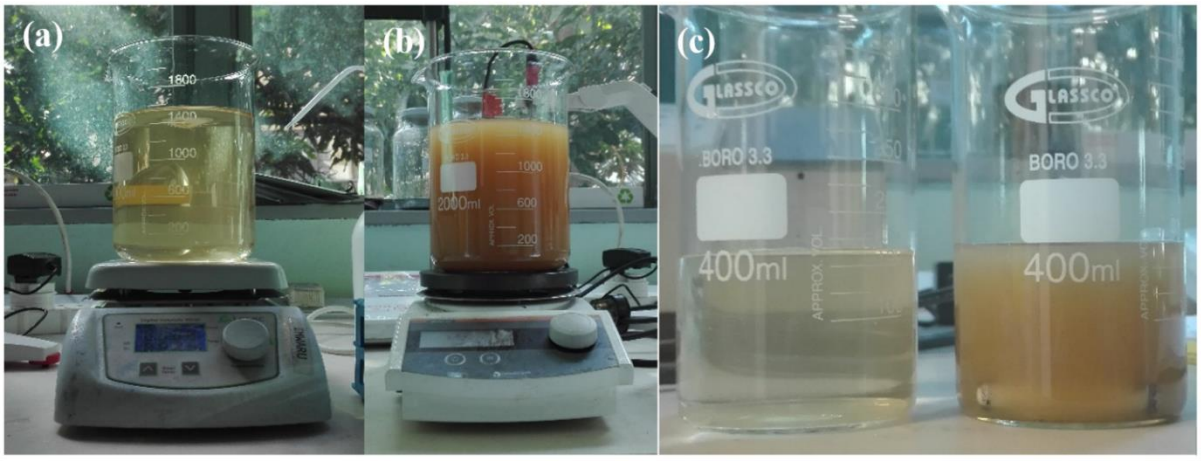


Figure 8-7: Formation of precipitation accompanying a pH rise in Type B AMD. (a) 1.5 L Untreated AMD, (b) 1.5 L AMD with addition of 3 g of slag, (c) Removal of top liquid after 2 minutes settling time (image by authors)

8.5.2.2 Sulfate removal

Sulfate removal in the system occurs via precipitation reactions and DSR. Precipitation and sedimentation accounted for the bulk of sulfate removal with over 90% of sulfate being removed across the sedimentation vessel, as shown in Figure 8-8. In the DSR vessels, sulfate removal occurs at a lower rate, accounting for less than 2% of overall sulfate removal. Sulfate removal in the DSR vessels is achieved via DSR and precipitation. A 35%, 29%, 35% and 16% sulfate removal was achieved across DSR vessel 1 for size 1 (8 µm <d< 13 µm), size 2 (1.7 µm <d< 3.35 µm), size 3 (d< 1 µm) particle size and Type B AMD respectively. DSR V2 had a lower sulfate removal percentage than DSR V1. Sulfide was detected in the DSR vessels over the 106-day period which confirmed the occurrence of DSR. The lower overall sulfate removal for Type B AMD can be attributed to a change in conditions in V3 and V4. The SRB may need to acclimatize to the new conditions over a period of time before maximum sulfate reduction can occur.

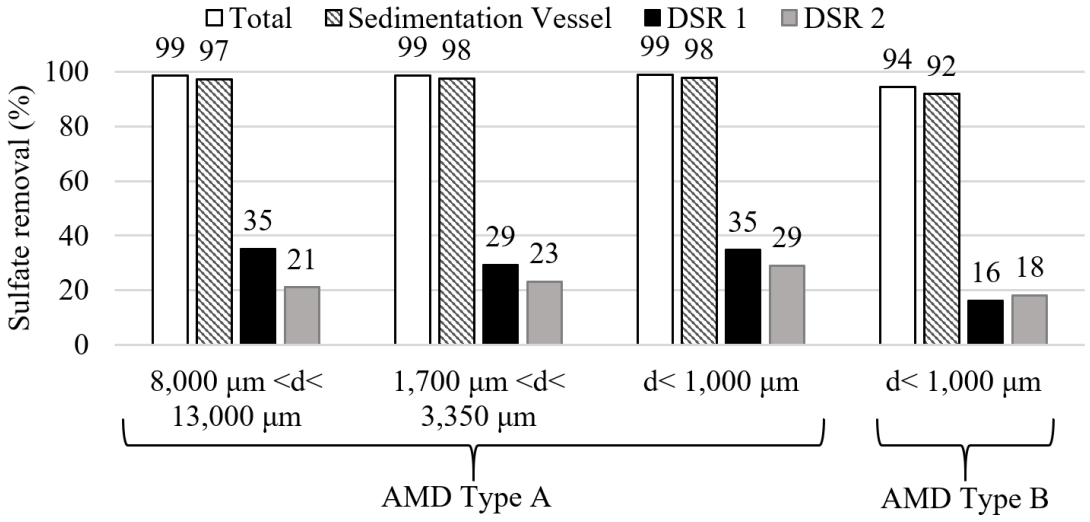


Figure 8-8: Percentage sulfate removal over entire system, sedimentation (V2), DSR1 (V3) and DSR2 (V4) vessels for system using slag with particle size 1, 2 and 3 and for AMD Type A and B

In an effort to accelerate the start-up period, the water used for start-up was AMD that had been treated using BOF slag addition. No sulfate removal occurred during the first 44 days of the process as shown in Figure 8-9. Larger particle sizes of slag resulted in lower overall sulfate and metal removal than smaller particle sizes as shown in Figure 8-10**.**

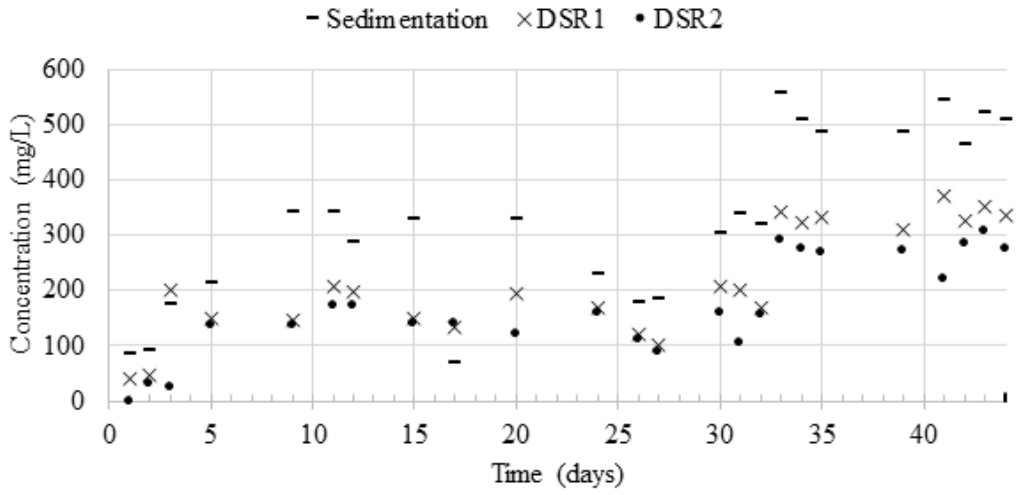


Figure 8-9: Sulfate concentration at the outlet of the sedimentation vessel (S1) and the DSR vessels (S2, S3) from start of experiment to Day 44

. Interestingly, the weaker AMD (Type B) was remediated to a lesser extent than the more severe AMD (Type A) with only 94% sulfate removal as opposed to 99%. Samples taken from the entrance, middle and outlet of the sedimentation vessel indicate that sedimentation may not be completely achieved uniformly across this surface area. Stability is not reached and there exists a very large discrepancy in concentration of sulfate between the middle of the vessel and the outlet. A larger surface area could resolve this. DSR could have also occurred to a larger extent if the size of the DSR V1 or V2 increased or if more DSR vessels are added in series.

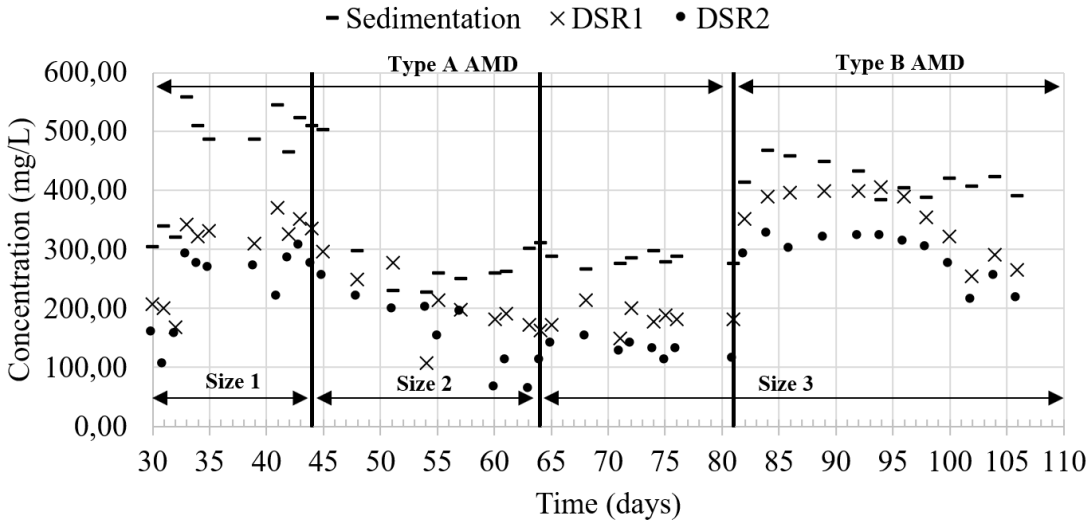


Figure 8-10: Sulfate concentration at the outlet of the sedimentation vessel (S1) and the DSR vessels (S2, S3) from Day 30 to Day 106

Dissolved sulfide was measured sporadically in the DSR vessels (V3 and V4) to confirm functioning of the SRB. The maximum sulfide concentration during operation was 14.8 mg/l found in V3 on Day 42. Sulfide concentration was generally significantly lower in V4 indicating that aeration or oxidation occurred across these reactors. No increase in sulfate concentration was detected in V4, however an increase was found in the water reservoir, confirming oxidation of sulfide. H_2S gas detectors were not triggered during operation of the system indicating that high concentrations of the gas were either not liberated from the vessels or aeration of the gas had occurred.

8.5.2.3 Water Recycle Ratio

The recycle ratio (volume recycled/volume AMD treated) changed drastically over time as shown in Table 8-4. It is thus important to note that although the overall sulfate removal remained fairly constant when the particle size of the slag was changed or when the AMD was replaced, the recycle ratio changed in order to facilitate this. A lower recycle ratio corresponds to more AMD treated in a shorter period of time, using fewer resources (slag and bagasse) and potentially requiring less power. The flowrates of the AMD inlet and recycle streams, the residence times and the recycle ratios are presented in Table 8-4.

Table 8-4: Residence time, recycle ration and flowrates of the inlet and recycle streams in the system for different particle sizes and AMD qualities

	AMD flowrate (L/day)	**Recycle Flowrate (L/day)**	**Residence Time (days)**	**Recycle Ratio**
Type A AMD with Size 1 (8 μm <d< 13 μm)	1.00	24.48	1.69	24.48
Type A AMD with Size 2 (1.7 μm <d< 3.35 μm)	2.18	24.48	1.61	11.23
Type A AMD with Size 3 (d< 1 μm)	3.76	24.48	1.43	6.51
Type B AMD with Size 3 (d< 1 μm)	10.42	24.48	1.16	2.35

8.5.2.4 Metals Removal

Metal concentration data is presented in Table 8-5. Metal removal in the system occurs via precipitation reactions of metal species with various anions as they become available and as the pH increases. Aluminium and iron exhibited a removal of over 98% for every configuration, with a final outlet concentration of below 7 mg/L and 60 mg/L respectively. Manganese exhibited a removal of over 91% for every configuration with a final outlet concentration of below 14 mg/L. Magnesium decreased in concentration, with an overall removal of over 75% for each different particle size. Only 42.6% was removed on average when Type B AMD was used. Calcium increased in every configuration with the lowest increase occurring for slag particle size 1 (8 μm <d< 13 μm) and the highest increase occurring for particle size 2 (1.7 μm <d< 3.35 μm) and Type B AMD. The increase in calcium ions corresponds to an increase in pH and a decrease in dissolved iron.

Table 8-5: Metal Concentration for size 1 (8 µm <d< 13 µm), 2 (1.7 µm <d< 3.35 µm), Size 3 (d< 1 µm) and Type B in untreated AMD and the outlet for sedimentation vessel (V2), DSR vessel 1 (V3) and DSR vessel 2 (V4)

Size 1 (8 µm <d< 13 µm)						
Metal	**AMD**	**Slag**	**Sedimentation**	**DSR 1**	**DSR 2**	**Total removal (%)**
Aluminium (mg/L)	420.64	4.94	7.62	5.74	6.08	98.55
Calcium (mg/L)	107.64	270.14	152.95	123.76	121.75	(Increase) 13.10
Iron (mg/L)	2967.75	17.66	66.45	29.82	31.31	98.94
Magnesium (mg/L)	103.13	5.37	35.13	17.67	18.89	81.68
Manganese (mg/L)	85.98	5.79	9.08	7.34	6.92	91.95
Size 2 (1.7 µm <d< 3.35 µm)						
Aluminium (mg/L)	434.89	6.81	9.87	8.06	6.72	98.45
Calcium (mg/L)	110.83	333.54	209.92	185.52	182.09	(Increase) 64.29
Iron (mg/L)	3039.60	17.67	62.76	28.12	29.95	99.01
Magnesium (mg/L)	105.67	6.15	59.47	47.85	26.11	75.29
Manganese (mg/L)	88.29	8.69	10.02	12.63	7.52	91.48
Size 3 (d< 1 µm)						
Aluminium (mg/L)	438.11	7.09	10.13	7.84	6.63	98.49
Calcium (mg/L)	111.27	429.45	235.22	190.51	176.64	(Increase) 58.75
Iron (mg/L)	3057.78	17.60	57.39	25.93	27.42	99.10
Magnesium (mg/L)	106.19	6.91	58.00	45.26	26.28	75.25
Manganese (mg/L)	88.64	8.69	7.88	12.25	7.29	91.77
Type B						
Aluminium (mg/L)	497.25		6.13	5.73	4.44	99.11
Calcium (mg/L)	175.38		311.73	286.78	288.93	(Increase) 64.75
Iron (mg/L)	3506.88		68.63	71.27	57.30	98.37
Magnesium (mg/L)	94.04		59.22	57.17	53.98	42.60
Manganese (mg/L)	197.68	7.01	15.59	13.95	13.43	93.21

Sample measurements confirmed the increased alkalinity when smaller particle slag was used, with the highest amount of calcium oxide dissolution occurring in the system using slag particle size 3 (d< 1 µm). This corresponded to the highest iron removal achieved in the system (99.1%). The removal of metals and sulfate corresponded to colour change in the liquid as shown in Figure 8-11. The AMD

becomes transparent after entering the sedimentation vessel and becomes less opaque with each subsequent treatment step (V2 to V6).

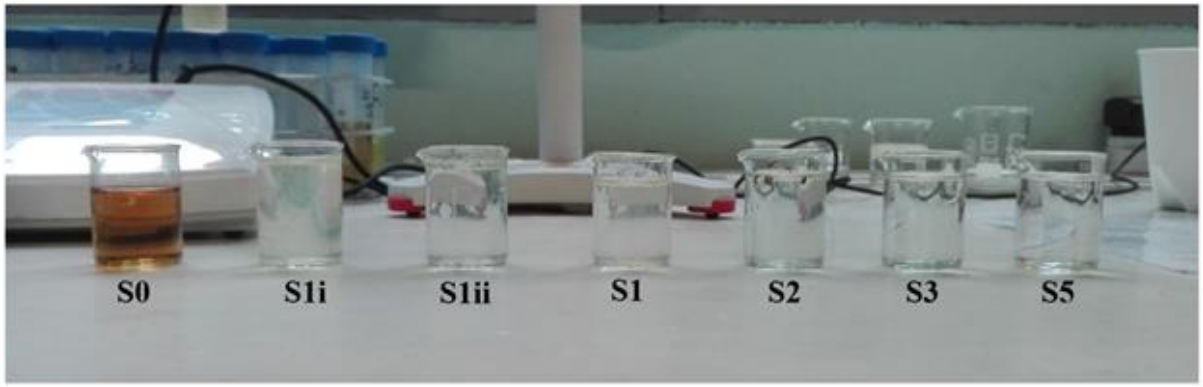


Figure 8-11: Samples from system. Left to right - Untreated AMD (Type A) (S0), sedimentation inlet (S1i), sedimentation middle (S1ii), sedimentation outlet (S1), DSR 1 outlet (S2), DSR 2 outlet (S3), slag vessel outlet (S5), (image by authors)

8.6 Conclusions

A waste beneficiation process was designed and constructed using BOF slag and sugarcane bagasse which treated AMD to maximum efficiency of 99% SO4, Al and Fe removal, 93% Mn removal, 81% Mg removal and pH buffering from approximately 2.4 to 7. The system was versatile and was able to treat two different AMD types to a level of 99% Al removal, 98% Fe removal, 93% Mn removal and 42% Mg removal.

Although a higher alkalinity was found in AMD that was put in direct contact with slag, the precipitation and settling on the surface of the slag particles were deemed too disadvantageous to successful and sustained operation of the system. Thus, a recycle stream using treated water was added to mitigate this.

AMD Type B (with a lower initial sulfate level) experienced slightly lower treatment efficiency in the system. However, AMD Type B also had the lowest recycle rate of 2.35. Changes in sizing of the process vessels and altering of the inlet and recycle flowrates have been identified as a method to increase the effectiveness of treatment for different AMD types. Changes in particle size of the slag resulted in little change to the overall outlet quality of the system, but large changes in the outlet water quality of the slag and sedimentation vessel were observed which led to corresponding changes in the recycle ratio. The largest particle size (size 1 – (8 μm <d< 13 μm)) had a recycle ratio of 24.48, the medium particle size (size 2 – (1.7 μm <d< 3.35 μm)) had a recycle ratio of 11.23 and the smallest particle size (size 3 – (d< 1 μm)) had a recycle ratio of 6.5. The change to the size 3 required a change in reactor type (from PBR to CSTR).

The maximum treatment efficiency still does not allow for water to be used in agriculture (USEPA 2018*)* and further treatment will have to be administered. This water can be used as process water at the mining site or can be fed to other AMD treatment systems where high levels of sulfate are not allowed. The aforementioned option shows potential as a low-cost pre-treatment step situated on site.

H_2S gas and sulfide concentrations were not high enough to be considered a risk, however in larger scale applications a scrubber may have to be introduced to ensure environmental health and safety.

The research has confirmed the combined use of BOF slag and sugarcane bagasse for use in an AMD remediation scheme. The results have indicated that the design proposed herein is successful as a pre-treatment process and has identified the potential for future research to further examine manners in which to improve the system. Future research will involve exploring the mechanisms of precipitation, DSR and dissolution within the process vessels and of using different process configurations to achieve a final water quality that is within agricultural or drinking water standards.

8.7 Acknowledgments

This work was conducted in part while D.G. Grubb served as the Vice President of Research and Development at Phoenix Services LLC. The authors would like to thank Phoenix Slag Services of South Africa (Iwan Vermeulen) for their financial, technical support and research materials, Illovo Sugar (Mark Napier) and our confidential mining partner for AMD materials and other support. Gratitude is also extended to the Water Research Commission (WRC; Project No. K5/2757) of South Africa. The financial assistance of the National Research Foundation (NRF) towards this research is also hereby acknowledged. Opinions expressed and conclusions arrived at, are those of the authors and are not necessarily to be attributed to the NRF.

9 The design, construction, monitoring and assessment of the long-term performance of a pilot plant used to treat 1000L/day of AMD on-site

This chapter is presented as a published conference paper titled “Acid Mine Drainage Pilot Remediation System using Waste Products from the Steel Manufacturing and Sugar Industries”, which has been peer reviewed and presented at the International Mine Water Association’s 2019 conference: “Mine Water: Technological and Ecological Challenges". This article discusses the operation of a 1000 L/day pilot plant which was deployed at a coal mine dump in Emalahleni (Naidu *et al.*, 2019). The full reference for this article is given below. The author contributions statement for this publication can be found in Appendix I.

Naidu, T. S. *et al.* (2019) ‘Acid Mine Drainage Pilot Remediation System using Waste Products from the Steel Manufacturing and Sugar Industries’, in Wolkersdorfer, C. et al. (eds) *IMWA 2019 “Mine Water: Technological and Ecological Challenges"*. Perm: International Mine Water Association, pp. 121–126. doi: 978-5-91252-145-4.

Acid Mine Drainage Pilot Remediation System using Waste Products from the Steel Manufacturing and Sugar Industries

9.1 Abstract

Acid mine drainage (AMD) has long been considered a global environmental hazard due to its long-term detrimental effects on waterways and the ecosystems that reside within them. The amount of AMD produced daily as well as the high cost associated with treatment has led the United Nations to classify AMD as the second biggest problem that the Earth faces. As such, new cost-effective remediation methods are strongly needed. This research involves such a method and focuses on the operation of a waste beneficiation treatment scheme that is being tested at pilot-scale. It incorporates the use of two waste-products which are produced in many AMD-affected countries: steel slag and sugarcane bagasse. The study has confirmed the potential of these products in the treatment of AMD through a two-step, chemical and biological process. Slag eluate contacted with raw AMD is used to initially buffer the AMD solution and precipitate heavy metals in a sedimentation tank. Overflow from the sedimentation tank is then passed through a packed bed containing sugarcane bagasse inoculated with sulfate reducing bacteria as a polishing step to remove sulfate, precipitate metal sulfides and elevate pH to near neutral conditions. A portion of the effluent is recycled through a packed bed of slag to create the eluate for pre-treatment of the raw AMD solution. The AMD used in these experiments was characterized by pH 2.6; 174 mg/L Al, 245 mg/L Ca, 4289 mg/L Fe, 334 mg/L Mn, 415 mg/L Mg and 16333 mg/L SO_4^{2-}. Operation of the pilot scale system treating 200-1000 L/day has thus far shown maximum Al, Fe, Mn and SO_4^{2-} removals of 97%, 87%, 100%, and 87% respectively. The dissolution of the slag and the alkalinity generation was found to occur mainly due to CaO and MgO dissolution. The SRB functioned in the slag eluate and a maximum sulfate reduction of 76% was found in the bioreactors. If optimized correctly, this treatment scheme could be implemented at mine sites throughout the world where these waste products are regionally available and could serve as either a low-cost pre-treatment program, or as a way for mines to recycle their acid waste for use as process or agricultural water.

9.2 Introduction

Mining is an essential global industry that gives rise to multiple downstream processes, such as extractive metallurgy, minerals processing and general metal production that are vital to almost all aspects of human life - farming, healthcare, communications, water, energy supply, transport, space technology, and construction (International Council on Mining and Metals 2018; Park et al. 2019). Mining is a large source of wealth in many areas, with countries such as Zambia, Chile, Peru, Ukraine, Uzbekistan, South Africa, Australia, and Kazakhstan all reporting that mining contributes more than 7% of their annual gross domestic product (GDP) (Ranjan 2019). Despite its acknowledged economic contributions, mining also causes significant environmental degradation and generates huge amounts of wastes that are disposed of in tailings dams or stored in impoundments. Acid mine drainage (AMD) is an example of one such mining waste. The amount of AMD produced daily as well as the high cost

associated with its treatment has necessitated new, viable and cost effective remediation schemes (Moodley 2018). In this regard, waste valorization/beneficiation has potential in (i) assisting AMD remediation schemes to remain economical, as well as in (ii) contributing to the alleviation of the burden of solid waste management in countless other industries (removal of secondary pollution which has multiple social and environmental benefits) (Nayak & Bhushan 2019).

Basic oxygen furnace slag (BOFS), containing high concentrations of oxides which have the ability to substantially increase the pH and alkalinity of acidic (Naidu *et al.*, 2018) is a final waste material in the steel making process that is in need of further processing before it can be re-used in the construction and building sector (Ding et al. 2017). BOFS cannot be used directly in construction due to volume instability issues that arise because of its high oxide content (Jiang et al. 2018). The treatment of AMD using BOFS as a lime substitute could potentially result in two valorized waste products, AMD treated to reusable water standards and BOFS treated to be reused as an aggregate in the construction industry.

This research investigates AMD treatment using BOFS by assessing the extent of remediation achieved in a pilot scale (200-1000 L/day) system. Another industrial by-product, sugarcane bagasse, is also used in the study to further remediate AMD after the BOFS treatment step and the efficacy of this biological treatment step is also evaluated. The aluminium, calcium, iron, manganese, magnesium and sulfate removal efficiency as well as the pH rise of the system are determined in order to evaluate the effectiveness of the scheme. Dissolution of the BOFS in the system is also assessed to determine the reduction of free oxide content in BOFS that causes volume instability.

9.3 Methods

Following the design and successful operation of a laboratory scale process using the same concept (Naidu, van Dyk, *et al.*, 2020), a plant designed to treat 200-1000 L/day of AMD was constructed at a mine tailings dam in Emalahleni, South Africa. The dam site, shown in Figure 9-1, comprised of two dams which are used concurrently to contain seepage from a large mine tailings dump situated at a coal mine.



Figure 9-1: (i-ii) Joint AMD dams in Emalahleni, South Africa where pilot plant is constructed (photographs by authors)

The chemical composition of the water contained within the dams changes constantly due to the varying nature of the coal tailings dump (new waste is continuously added to the dump and water seeps through this, entering the dam) as well as due to climactic conditions. The pilot plant was designed to account for the varying inlet quality so as not to impact the sensitive biological systems present in the process.

The system operates as follows (referring to Table 9-1 and Figure 9-2): AMD (stream 1) is pumped into an initial sedimentation vessel (R-102A/B) where it is mixed with a slag eluate stream (stream 10) from the slag chamber (R-101A/B). The slag eluate stream has high pH, alkalinity and hydroxide content due

to reaction between the AMD and the oxides contained within the slag. When mixed with the AMD in R-102A/B and R-103A/B, the pH of the resulting solution increases, causing (i) precipitation reactions and (ii) removal of dissolved metals and sulfates in the solution via gravitational settling.

The outlet from the sedimentation section (stream 3) contains significantly less sulfate and metal ions and is at a higher pH (close to neutral). This stream enters the biological reactors (R-104, R-105, and R-106), the first two of which contain sugarcane bagasse which act as a substrate (carbon source) for sulfate reducing bacteria (SRB). SRB are sensitive to extreme pH levels and thus the neutralization of the AMD in the sedimentation vessels (R-102, R-130) allows for SRB functioning. The biological reactors are responsible for facilitating further sulfate ion removal via dissimilatory sulfate reduction (DSR). The outlet from R-106 (stream 6) enters a water reservoir (TK-101) where the treated water is stored. Water from TK-101 either overflows into the AMD dam or is recycled into R-101A where it undergoes a reaction with the BOFS. All vessels were sealed and R-107 acted as a H_2S scrubber. Vessels marked B are replacement vessels.

Process control was setup to control the ratio of slag eluate (stream 10) to AMD feed (stream 1) in the system in order to maintain a pH of 5 in the sedimentation vessels (R-102A and R-103A). A pH of 5 was chosen to (i) keep the recycle flowrate at a sustainable level, (ii) allow for ideal functioning of the biological entities (namely sulfate reducing bacteria (SRB)) which function best at a pH between 4 and 7, and (iii) allow for a suitable amount of precipitation of metals in the bioreactors (metals need to be present in the bioreactors to allow for metal sulfide precipitation). A depiction of the layout of the plant is shown in Figure 9-3.

Table 9-1: Description of Process flow diagram elements (Figure 9-2)

Diagram Number	R-101A/B	R-102A/B	R-103A/B	R-104	R-105	R-106	R-107	TK-101	P-101	P-102
Element	Slag reactor and replacement	First sedimentation vessel (and replacement)	Second sedimentation vessel (and replacement)	Biological Reactor 1	Biological Reactor 2	Biological Reactor 3	Hydrogen Sulfide Scrubber	Water reservoir	AMD Pump	Recycle pump

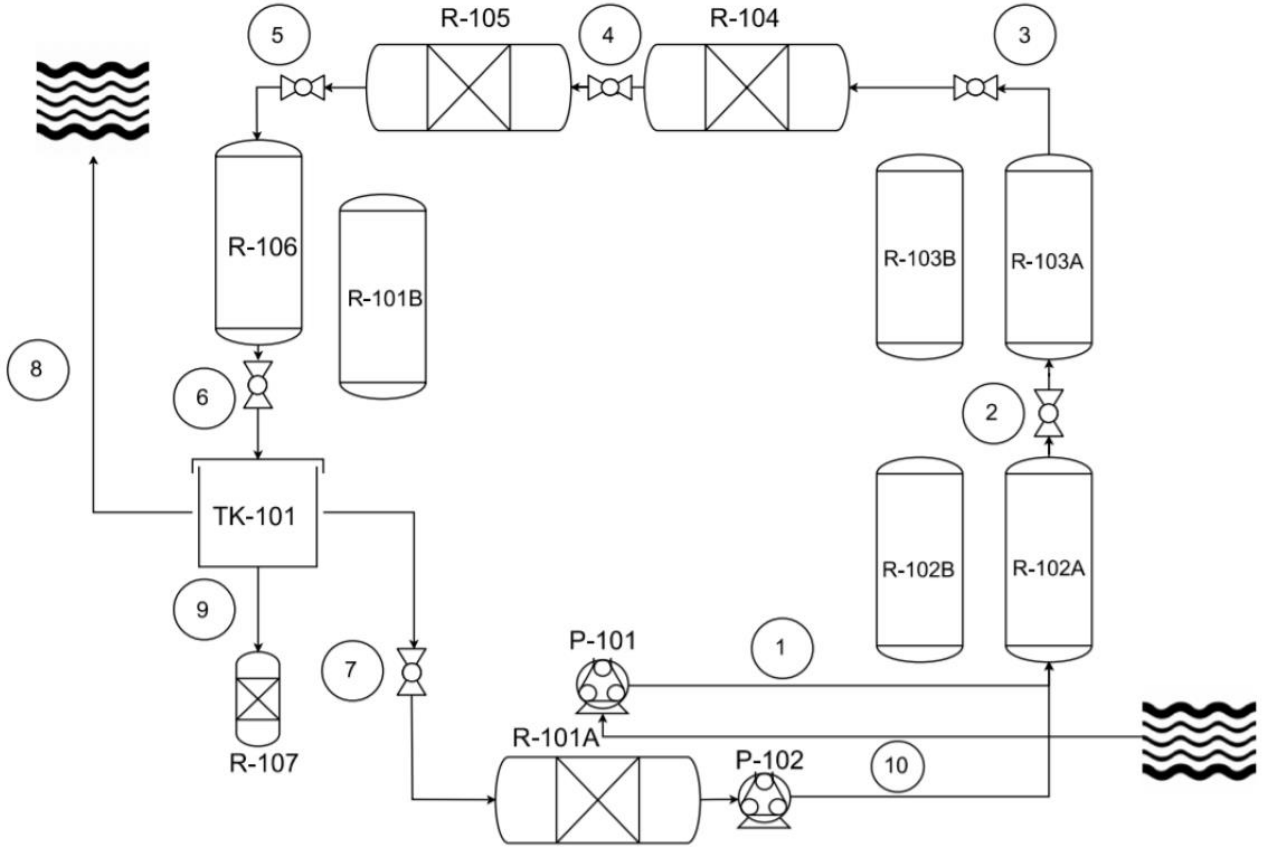


Figure 9-2: Process flow diagram (PFD) of pilot plant to treat AMD constructed at site



Figure 9-3: ((i) and (ii)) AMD remediation pilot plant at mine dam site

Data collected from the plant for a 196-day period is discussed in the Results and discussion section below.

9.4 Results and discussion

9.4.1 Flowrate and residence time

The total volume of the system was approximately 13 000 L. Flowrates and residence times for the period are displayed in Table 9-2.

Table 9-2: Flowrate and Residence Time in System

Time Period (days)	Flowrate of AMD (L/day)	Flowrate of Slag Eluent (L/day)	Residence Time (AMD and Slag Eluent) (days)
34	600	1000	8.1
34-43	270	1000	10.2
43-76	270	1200	8.8
76-120	270	2000	5.7
120-139	0	2400	5.4

From day 120 onwards, the residence time for both the slag eluent and AMD streams was 5.4 days or lower. The flowrate into the system was determined by process control operation.

9.4.2 Extent of remediation

The inlet quality of the AMD changed continuously but had average Al, Ca, Fe, Mn, Mg, SO_4^{2-} and V concentrations of 174 ± 99.8, 245 ± 128.4, 4289 ± 313.3, 334 ± 136.0, 415 ± 104.2, 16333 ± 1072 and 0.06 ± 0.01 mg/L respectively. The average pH of the untreated AMD was 2.6. The pH levels changed across each vessel as well as over time, but the average pH in each vessel was 5.4 (R-101), 3.2 (R-102), 3 (R-103), 4.6 (R-104), 4.6 (R-105), 4 (R-106) and 4 (TK-101). The change in pH of the AMD is due to hydration reactions that occur between the AMD and the BOFS and the subsequent dissociation that results in the release of hydroxide units.

The fluctuation in pH across the system over time (as shown in Figure 9-4) is attributed to the varying amount of oxide containing BOFS particles that come into contact (and are able to react) with the AMD. This varying amount is determined by the process control over the plant. When the pH of the sedimentation vessel (R-102) is lower than 5, the flowrate of the entering slag eluate (stream 10) increases until it reaches a maximum of 2400 L/day and the flowrate of the AMD stream (stream 1) decreases until 0 in order to facilitate a higher ratio of slag eluate to AMD. For pH levels higher than 5 the opposite is true.

Process control over the system became automatically effective after 120 days and thus fluctuations occurred. In addition to this, precipitation and settling in the BOFS reactor limited the release of further oxides. This was combatted by removing sedimentation and allowing only treated water (with a lower ion content and thus less ability to form precipitates) to flow through the BOFS reactor. The metal and sulfate levels across the system fluctuate along with pH levels (as shown in Figure 9-4). Metal and sulfate concentrations are dependent on the pH levels, making pH control in the system extremely important.

High pH levels allow for more precipitation reactions to occur, removing a higher quantity of sulfates and metals, and pH levels between 4 and 7 allow for optimum SRB activity.

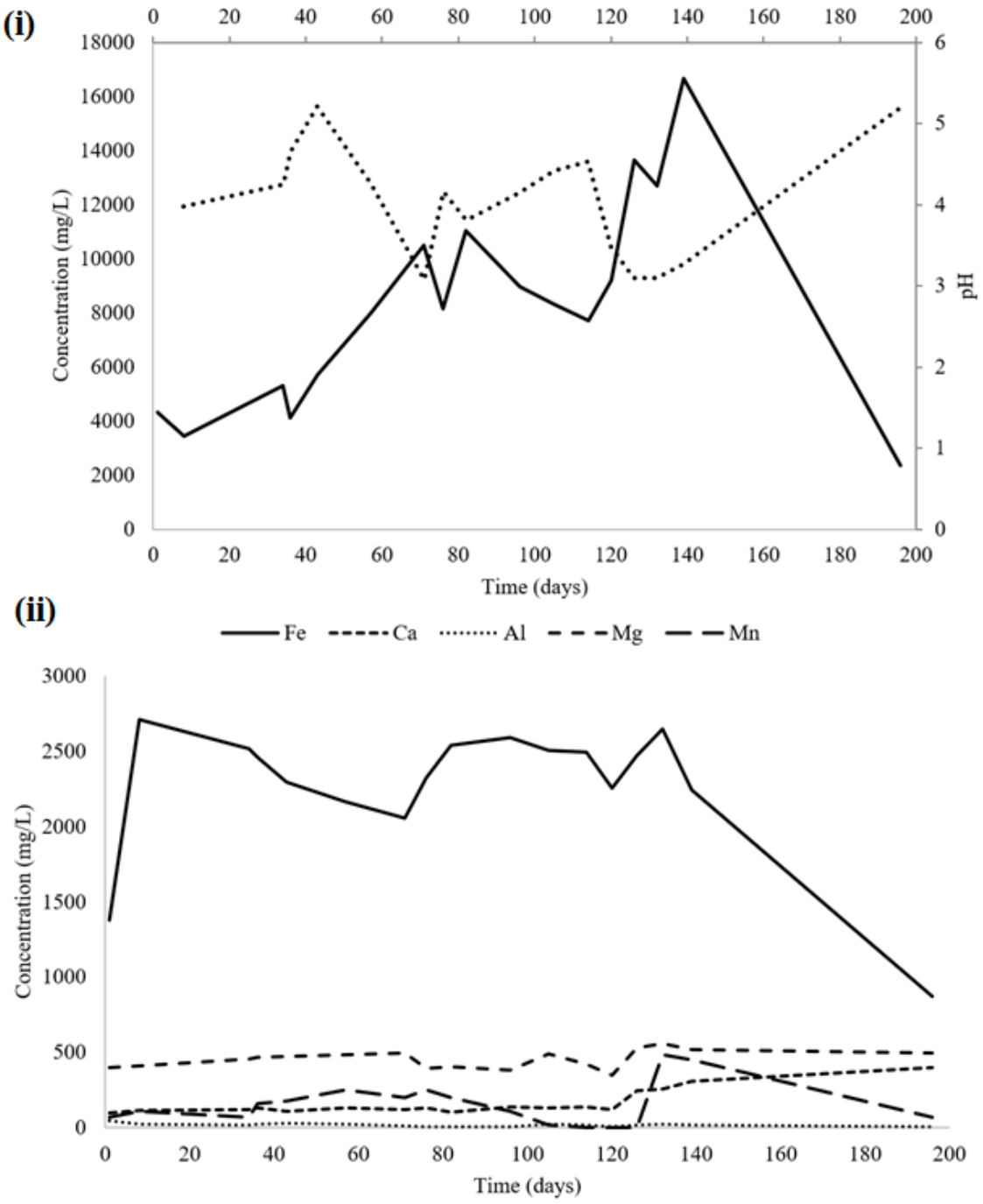


Figure 9-4: (i) pH and sulfate concentration in the water reservoir (TK-101) over the 196-day period (ii) Metal concentrations in the water reservoir (TK-101) over the 196-day period

The extent of treatment in each vessel at the end of the 196-day period is shown in Table 9-3 in terms of % removal of each component (based on the initial and last reading).

Bold indicates an increase in concentration.

Table 9-3: Extent of Remediation across each Process Vessel (%removal of components)

Component	R-102A/B (%)	R-103A/B (%)	R-104 (%)	R-105 (%)	R-106 (%)	TK-101 (%)	R-101A/B (%)
Mn	69.23	70.5	76.51	78.32	77.3	79.9	83.32
Mg	0.79	**4.77**	**0.34**	**16.06**	**12.44**	**19.54**	**23.31**
Al	95.22	95.86	96.61	97.07	96.08	95.45	90.03
Ca	**185.32**	**167.87**	**69.13**	**123.12**	**69.74**	**62.43**	**226.45**
Fe	56.28	69.72	77.96	82.72	83.39	79.61	86.61
SO_4^{2-}	55.63	72.52	80.24	81.95	83.53	84.69	87.1
pH	5.26	5.34	5.24	5.49	5.11	5.2	7.24

The extent of remediation changed considerably over time at site, and this was attributed to the fluctuating conditions (changing feed quality, climate and availability of electricity to run equipment). The best treatment (for a combination of components) was observed after approximately 4000 hours (167 days) of operation and showed an 84% removal of sulfate, 80% removal of dissolved Fe, 62% increase of Ca, 95% removal of Al, 20% increase of Mg and a 80% removal of Mn. The maximum removals in terms of Al, Fe, Mn and sulfate were 97%, 87%, 100% and 87% respectively (across different reactors). Vanadium did not exhibit any considerable changes and Mg and Ca concentrations consistently increase in the system. The chemical section of the plant (R-102, R-103) was able to remove up to 72% of sulfate and the biological section (R-104, R-105, R-106) could remove a further 11% (76% sulfate removal over the 3 reactors).

9.4.3 Dissolution of BOFS

As shown in Table 9-3, the Mg and Ca concentrations increased within the system, confirming the hydration reaction between the treated AMD and the oxidic compounds within the slag. According to literature, alkalinity can be generated from BOFS via hydration followed by dissociation of calcium and magnesium oxides (Gomes et al. 2016). The BOFS contained 41.6 mass% CaO and 7.2 mass% MgO (other oxides are present, but only Ca and Mg have been considered due to the rise in their concentrations). The hydration, dissolution and dissociation reactions that bring about alkalinity from CaO and MgO components are described by Equation 9-1 to Equation 9-4.

$$CaO + H_2O \leftrightarrow Ca(OH)_2$$

Equation 9-1

$$Ca(OH)_2 \leftrightarrow Ca^{2+} + 2OH$$

Equation 9-2

$$MgO + H_2O \leftrightarrow Mg(OH)_2$$

Equation 9-3

$$Mg(OH)_2 \leftrightarrow Mg^{2+} + 2OH^-$$

Equation 9-4

Ca in the system increased by 226% and Mg increased by 23% signifying that CaO and MgO compounds could contribute to the bulk of the pH rise and that oxidic compounds are being removed from the slag.

9.5 Conclusions

The extent of treatment of AMD using a two-step, chemical and biological process at a pilot plant (200-1000 L/day) scale was evaluated successfully and determined to have a maximum removal capacity of 97% for Al, 87% for Fe, 100% for Mn and 87% for SO_4^{2-}. SRB functioned well in the BOFS neutralized solution and the biological reactors exhibited a maximum sulfate removal of 76%. Some oxide compounds in BOFS underwent hydration (and subsequent dissociation) reactions with the treated AMD, potentially removing a degree of volume instability from the material. Although ideal functioning did not occur until after 4000 hours of operation, the experiment confirmed functionality of the scheme at a pilot plant scale. Issues relating to the poor performance [sedimentation in BOFS chamber (R-101)] in the first 4000 hours were identified and deemed to be easily correctable. Further work will focus on achieving successful pH control in the system in order to optimize the metal and sulfate removal as well as exploring manners through which to regenerate the sludge produced in the sedimentation vessels.

9.6 Acknowledgements

The authors would like to thank Phoenix Slag Services of South Africa (Iwan Vermeulen) for their financial, technical support and research materials, Illovo Sugar (Mark Napier) and our confidential mining partner for AMD materials and other support. Gratitude is also extended to the Water Research Commission (WRC; Project No. K5/2757) of South Africa. The financial assistance of the National Research Foundation (NRF) towards this research is also hereby acknowledged. Opinions expressed and conclusions arrived at, are those of the author and are not necessarily to be attributed to the NRF.

10 Preparation of a process for scale-up on site based on the pilot and lab scale studies

This chapter is presented in the form of a WRC report (2757/1/21) which has been reviewed, accepted and published under the title “Design of Acid Mine Drainage Remediation Plant” (ISBN 978-0-6392-0264-8). This report contains data and discussions pertaining to all the aims of this project, and thus there are some sections and findings/conclusions which have been duplicated. The design of a scaled-up process was compiled using the data obtained in each experimental section (pertaining to each individual objective) and thus this report contains summaries and discussion pertaining to previous objectives as well. The process design section is presented on page 218 (section 10.6). Administrative sections which are not relevant to this dissertation (timelines, contents, acknowledgements etc.) which were included at length in the original document (due to WRC specific requirements), as well as literature review section, have been omitted. This chapter is numbered to allow for easy referencing (as per original document), but apart from the omitted sections which are not relevant to the completion of this thesis, this report is presented as was submitted.

This chapter also contains waste management, process control and cost elements pertaining to a large-scale process. The full reference for this document is given below. The author contributions statement for this publication is given in Appendix I.

Naidu, T. S., Sheridan, C. M., & van Dyk, L. D. (2021). Design of Acid Mine Drainage Remediation Plant (Issue 2757). WRC. http://www.wrc.org.za/wp-content/uploads/mdocs/2757 final.pdf

Design of Acid Mine Drainage Remediation Plant

10.1 Executive Summary

10.1.1 Background

Mining is an essential global industry that has given rise to multiple downstream processes - extractive metallurgy, minerals processing and wide-ranging metal production - that are vital to almost all aspects of human life (farming, healthcare, communications, water, energy supply, transport, space technology and construction) (International Council on Mining and Metals, 2018; I. Park *et al.*, 2019). Mining is a large source of wealth in many areas, with countries such as Zambia, Chile, Peru, Ukraine, Uzbekistan, South Africa, Australia, and Kazakhstan all reporting that this industry contributes more than 7% of their annual gross domestic product (GDP) (Ranjan, 2019). Despite its acknowledged economic contributions however, mining also causes significant environmental degradation and generates multiple waste streams that are disposed of in tailings dams or stored in impoundments. Acid mine drainage (AMD) is an example of one such mining waste and the amount of this that is produced daily as well as the high cost associated with its treatment, has necessitated the development of new, viable and cost-effective remediation schemes (Moodley *et al.*, 2018). In this regard, waste valorisation/beneficiation has potential in (i) assisting AMD remediation schemes to remain economical, as well (ii) contributing to the alleviation of the burden of solid waste management in countless other industries (removal of secondary pollution which has multiple social and environmental benefits) (Nayak and Bhushan, 2019).

Basic oxygen furnace slag (BOFS) is a final waste material in the steel making process and contains high concentrations of oxides which have the ability to substantially increase the pH and alkalinity of acidic waters (Naidu, Dyk, Sheridan, & Grubb, 2018; Naidu, Dyk, & Sheridan, 2018). It is in need of further processing before it can be re-used in the construction and building sector (Ding *et al.*, 2017). BOFS cannot be used directly in construction due to volume instability problems that arise due to its high oxide content (Jiang *et al.*, 2018). Thus, the treatment of AMD using BOFS as a lime substitute could potentially result in two valorised waste products, AMD treated or pre-treated to reusable water standards and BOFS treated to be reused as an aggregate in the construction industry.

This research investigated AMD treatment or pre-treatment using BOFS by assessing the extent of remediation achieved in a laboratory (1-25 L/day) and pilot scale (200-1000 L/day) system. Another industrial by-product, sugarcane bagasse, was also used in the study to further remediate AMD after the BOFS treatment step and the efficacy of this biological treatment step is also evaluated. The aluminium, calcium, iron, manganese, magnesium, and sulfate removal efficiency as well as the pH and alkalinity rise of the system were determined in order to evaluate the effectiveness of the scheme. Dissolution of the BOFS in the system was also assessed to determine the reduction of free oxide content in BOFS

that causes volume instability. Following the collection and interpretation of laboratory and pilot scale data, a larger scale design for the process was proposed.

10.1.2 Aims

The following were the aims of the project:

1. To perform preliminary laboratory studies which will provide information for the design of a pilot plant unit.
2. To design a pilot process for treating 1000 L /day of AMD on site.
3. To construct the pilot plant to treat 1000 L /day of AMD.
4. To monitor the pilot plant in order to assess performance over a 6-month period.
5. To design and prepare a process for scale up of the original pilot plant to be based on site.

10.1.3 Methodology

Different methods were used to assess and achieve each of the aims listed. The methodology has thus been divided into the preliminary phase (which included a laboratory scale phase) and the pilot scale phase.

10.1.3.1Phase 1 – Preliminary Phase

1. Determine the mechanism and kinetics of BOFS dissolution
2. Determine the mechanism and kinetics of precipitation reactions
3. Determine the functionality of sulfate reduction at large scales using sugarcane bagasse
4. Design, construction and optimization of laboratory scale system

10.1.3.2Phase 2 – Pilot scale and larger scale phase

1. Design, construction and optimization of a process for treating 1000L/day of AMD on-site
2. Propose a design for a larger scale plant using findings from Phase 1 and 2 to treat more than 1000 L/day

These aims were partially or fully achieved to allow a larger scale design to be developed.

10.1.4 Results and Discussion

The results from the laboratory scale plant and the findings from the preliminary experiments were favourable and sufficient to inform the design of the larger pilot plant. AMD was treated to a maximum efficiency of 99% SO_4^{2-}, Al and Fe removal, 93% Mn removal, 81% Mg removal and pH buffering occurred from approximately 2.4 to 7 in the laboratory scale processes. The system was versatile and was able to treat two different AMD types to a level of 99% Al removal, 98% Fe removal, 93% Mn removal and 42% Mg removal. It was also versatile in that the pH level could be altered depending on desired outlet quality (higher pH's could be achieved via the addition of more BOFS or by allowing a longer reaction time in order to achieve different metals removal capacities). The pilot scale design was

changed slightly by using different volumes for different reactors (the biological reactor increased in size relative to the settling tank etc.) and by changing the pH setpoint in order to lower the recycle rate and ensure some metals were still present in the biological reactor (the pH setpoint was lowered such that less metals would precipitate as sulfate and hydroxide species in the settling tank, leaving some to facilitate the removal of sulfide via precipitation in the subsequent DSR reactor).

During the operation of the pilot plant, complementary experiments were also undertaken. The results from both of these operations in conjunction with the original results were used to inform the larger scale design. The extent of treatment of AMD at the pilot plant (treating 200-1000 L/day) scale was evaluated and determined to have a maximum removal capacity of 97% for Al, 87% for Fe, 100% for Mn and 87% for SO_4^{2-}. The final design was altered slightly from the initial laboratory scale design and the pilot scale design to promote further treatment and reduce energy costs related to pumping and recycling.

10.1.5 General

All aims were addressed and achieved.

10.1.6 Conclusions

The final design differed from the original design in the following ways: (i) it did not make use of a recycle effluent stream, (ii) it did not include a secondary settling vessel or a tertiary biological vessel. By assessing the results from the various stages of research comprising the study, it was concluded that the combination of the two waste materials (sugarcane bagasse and basic oxygen furnace slag) was successful in the treatment of acid mine drainage – however the extent of treatment due to the biological step (sugarcane bagasse and sulfate reducing bacteria (SRB)) was deemed poor or low, as sulfate and metal removal during this step were not solely attributed to DSR (due to the suspected inability of the system to maintain a suitable chemical oxygen demand (COD) to sulfate ratio). Nevertheless, all combinations that were explored yielded favourable results overall (improvement of water quality and water treated to an acceptable standard based on the needs of the mine). The configuration that yielded the best results was suggested for the final design. It should be noted that the bulk of the treatment occurred in the BOFS treatment step and this treatment extent could be changed easily by controlling pH levels (by controlling the addition of BOFS). Thus, the different modules in the process can also be used in isolation as pre-treatment steps – treating AMD at mine sites for reuse as process water, agricultural water or as a pre-treatment step before entering into traditional wastewater treatment plants (WWTP).

10.1.7 Recommendations

The main recommendation for the upscale design (final aim of the project) is that a full analysis of the site of implementation be done beforehand in order to (i) determine the quality of effluent water that is needed, (ii) determine what particle size would be best suited to the quality of AMD at site and the

geographical area, and (iii) check the conditions in terms of power availability and safety in the area. These factors will determine which of the proposed designs to use. In addition, further studies regarding the optimization of the process control aspect and the use of spent BOFS as an aggregate will need to be conducted to improve the efficiency and optimization of the overall system. It is also recommended that the treated water be used for agricultural purposes as it is nutrient rich.

10.2 Design Methodology

10.2.1 Introduction

In order to properly determine a feasible and working design for a combined biological and chemical AMD treatment system, a number of preliminary small-scale, batch experimental steps were taken to inform a larger scale design. The treatment or pre-treatment extent of volumes of below 100 mℓ of AMD was initially determined and these results were used to formulate a design scheme that could eventually potentially treat up to 10 000 ℓ/day. Batch experimental tests led to a continuous process that could treat between 1 and 25 ℓ/day which was monitored continuously for over a 1-year period. The results and observations from this study were used to inform the design of a larger scale plant, designed to treat between 250 and 1000 ℓ/day. This plant was constructed and then monitored for a period of 8 months. During this period, complementary data were also obtained from additional batch studies. The results from all studies have been used to inform the design of a plant that can treat up to 10 000 ℓ/day plant. This section briefly summarizes each step of the process undertaken to advise a final design. **This section refers solely to the design methodology - detailed descriptions of the materials and methods used for laboratory work, field work and complementary data are provided in the relevant chapters.**

10.2.2 Preliminary Experiments

Initial batch and continuous experiments were undertaken to determine the manner in which the BOFS and sugarcane bagasse could be combined to achieve maximum treatment. This phase included combining the two materials in one reaction vessel and then combining them in series, to determine which configuration would yield the most favourable results.

During this phase it was observed that (i) precipitation of various metal salts occurred rapidly during a pH rise and (ii) SRB functioning was inhibited by the low pH of raw AMD. The findings suggested that introducing the AMD directly into the system (into direct contact with the BOFS or sugarcane bagasse) would not be an option. This was due to the fact that the AMD had too low of a pH (it would kill any bacteria present in the sugarcane bagasse reactor and thus render this treatment null) and upon exposure to BOFS would precipitate metal oxides and sulfates almost instantaneously (resulting in a layering or armouring of the BOFS particles and preventing further release of alkaline components). A recycle stream (containing treated water) was conceptualized to combat the issues of armouring of the slag and potentially toxic shocking the biological system containing SRB.

A schematic which shows the preliminary design configuration is presented in Figure 10-1.

10.2.2.1Schematic representation of preliminary design

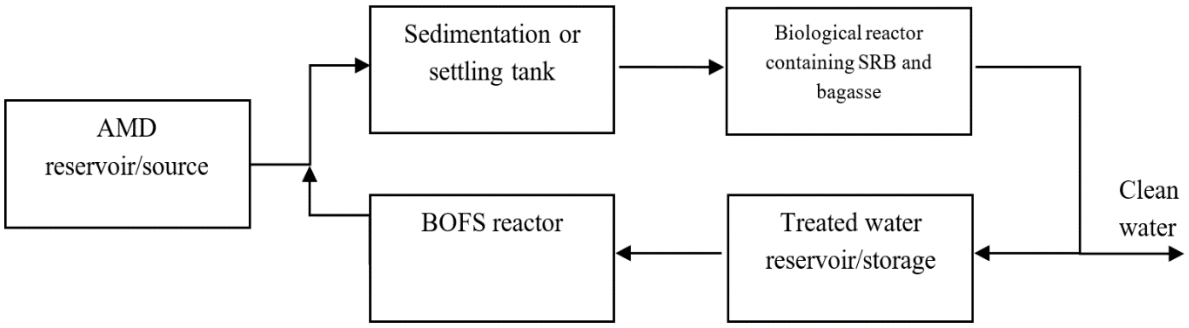


Figure 10-1: Preliminary design block flow diagram

This recycle stream necessitated the use of clean water for start-up procedures but allowed for less manual work to be done with regards to removing precipitate/sedimentation that had formed and replacement of the slag. Figure 10-1 describes the configuration that was proposed – and initially tested – to prevent precipitation and toxic shock of the system. Instead of entering the system in direct contact with one of the reagents, the raw AMD is mixed in a settling tank with the slag eluate. The water in this tank undergoes precipitation reactions (due to the increase in pH), removing a large amount of sulfates and various metal species. The water exiting the tank thus has an increased pH and is of significantly better quality – making it suitable for further treatment using biological means. Under the action of sulfate reduction, the sulfate and any metals still contained in the AMD are removed and the water exiting the biological reactor is considered treated. This water can be released back or can enter the system again as a recycle stream, coming into contact with BOFS in a BOFS packed bed reactor. This water has a very low concentration of sulfates and metals and thus precipitation and armouring of the slag does not occur.

10.2.3 Laboratory Scale (1-25 ℓ/day)

The preliminary design was tested in a continuous laboratory-scale setup for a period of a year. The remediation setup comprised of two pumps and a number of process vessels (an AMD feed tank, slag vessels, sedimentation vessels, primary and secondary DSR vessels, water reservoir and outlet storage tank) which were sealed and anaerobic. The typical setup is shown in Figure 10-2, where S1 - S5 denote sampling points.

Multiple configurations were tested:

- Vessels of different sizes
- Different reactor types
- Vessels in series
- Different qualities of AMD
- Different particle sizes of BOFS and

- Different reaction times.

Data was obtained from these configurations that assisted in informing the larger scale design.

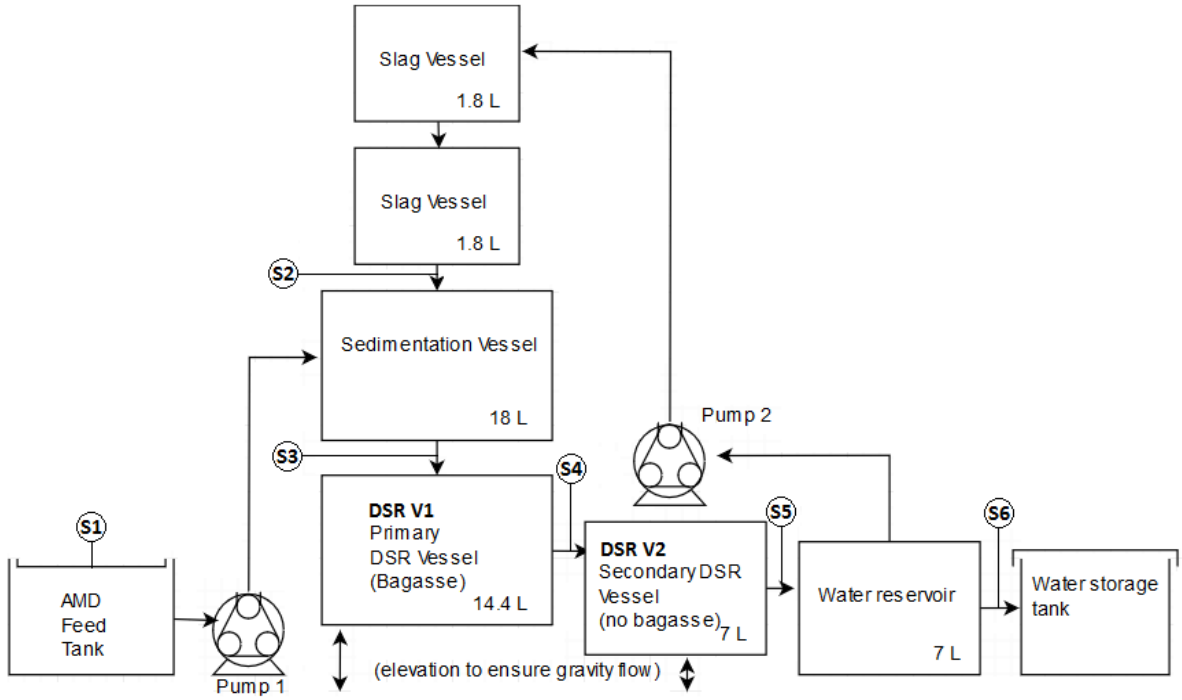


Figure 10-2: Laboratory scale set-up with vessels and sampling points denoted

AMD was treated to a maximum efficiency of 99% SO_4^{2-}, Al and Fe removal, 93% Mn removal, 81% Mg removal and pH buffering from approximately 2.4 to 7. The system was versatile and was able to treat two different AMD types to a level of 99% Al removal, 98% Fe removal, 93% Mn removal and 42% Mg removal. The main observations that altered the large-scale design were (i) the pH control data and (ii) the dissolution of the slag data. The pH levels played an important role in the treatment extent, with the pH affecting the amount of sulfate and metals removed in the settling/sedimentation phase, as well the functioning of the biological reactor. If the pH is not properly controlled in the settling tank (via determining and maintaining the correct mixing ratio between AMD and slag eluate), then the treatment extent is affected in this vessel as well as in all subsequent vessels. Low pH in the settling vessel, results in less precipitation and a higher concentration of sulfates and metals entering into the biological reactor. If the feed into the biological reactor has a low pH, the SRB in this vessel are affected (Ayangbenro, Olanrewaju and Babalola, 2019) and the sulfate reduction rate will be lowered, again leading to a higher a concentration of metals and sulfates in the discharge water. Higher concentration of metals and sulfates into the BOFS reactor will result in precipitation and possible armouring of the slag in this vessel – reducing further dissolution of pH raising or alkaline reagents. Thus, maintaining the desired pH in all vessels is of vital importance to ensuring functionality of the system.

For this reason, the following changes were introduced into the final design:

(i) The slag vessel contained an excess of slag of different particles sizes to ensure a continuous dissolution and a constant supply of high-pH, high-alkalinity eluate. A larger vessel size was proposed for this reactor.

(ii) The area and volume of the settling tanks were increased to allow for greater settling. This was also done to combat any slight variations in pH that may occur in this vessel, allowing more time for precipitation to occur and more time for smaller particles to settle. The controlled pH setpoint in the settling vessel was also changed to a lower pH (5). A pH of 5 would allow for a lower ratio of mixing between the AMD and slag eluate streams, as well as ensuring that enough dissolved metal species enter into the biological reactor to act as counterions for the precipitation of sulfide components.

(iii) The proportional size of the biological vessels (where sulfate reduction take place) were increased and the amount of bagasse used (in proportion) was also increased. A larger quantity of bagasse meant that the carbon source was available in excess and did not act as a limiting factor. The larger amount of bagasse also meant more hydrogen acceptors were present in this biological reactor which could play a role in offsetting any minor pH variations that occurred.

(iv) Lastly, a H_2S scrubber was added to combat any H_2S that could be liberated from the biological reactor. H_2S production was not an issue in the smaller scale design and was not envisioned to be an issue in the larger scale design either (due to the maximum amount of sulfide generation being within allowable limits). However, to negate any uncontainable H_2S release, the scrubber (a 200L plastic drum) contains water, hydrogen peroxide or ammonia. Gas from the bagasse reactors was directed into the base of the vessel and allowed to bubble through the liquid. H_2S gas exhibits high dissociation and reactivity, and the gas will react with the scrubbing liquid to form sulfuric acid and water. The tank used was constructed from polyethylene to prevent degradation of the vessel via corrosion. The scrubber is represented by symbol R-107 in Figure 10-3.

10.2.4 Pilot Scale (200 - 1000 ℓ/day)

Following the design and successful operation of the laboratory scale process, the plant designed to treat 200-1000 ℓ/day of AMD was constructed at a site in Emalahleni, South Africa. The site comprises of two dams which are used concurrently to contain seepage from a large mine tailings dump.

The system operated as follows (referring to Table 10-1 and Figure 10-3): AMD (stream 1) was pumped into an initial sedimentation vessel (R-102A/B) where it was mixed with a slag eluate stream (stream 10) from the slag chamber (R-101A/B). The slag eluate stream had a high pH, alkalinity and hydroxide content due to reaction between the AMD and the oxides contained within the slag. When mixed with

the AMD in R-102A/B and R-103A/B, the pH of the resulting solution increased, causing (i) precipitation reactions and (ii) removal of dissolved metals and sulfates in the solution via gravitational settling. The outlet from the sedimentation section (stream 3) contained significantly less sulfate and metal ions and was at a higher pH (close to neutral). This stream entered the biological reactors (R-104, R-105, and R-106), the first two of which contained sugarcane bagasse. The outlet from R-106 (stream 6) entered a water reservoir (TK-101) where the treated water was stored. Water from TK-101 either overflowed into the AMD dam or was recycled into R-101A where it underwent a reaction with the BOFS.

All vessels were sealed and R-107 acted as a H_2S scrubber. Vessels marked B were replacement vessels that were included in the design and were to be used when cleaning of the system occurred. When sludge build up (of precipitates) occurred in R-102A and R103-A, the inlet and recycle flow (stream 1 and 10) could be redirected to R-102B and R-103B to allow for continuous operation. In a similar way, when slag replacement had to occur in R-101A, stream 7 could be redirected to R-101B (already containing slag). Due to operational limitations these vessels were never used, with sludge removal and slag replacement occurring in intervals during the operational period.

Table 10-1: Description of process flow diagram elements in Figure 10-3

Diagram Number	R-101A/B	R102A/B	R103A/B	R-104	R-105	R-106	R-107	TK-101	P-101	P-102
Element	Slag reactor and replacement	First sedimentation vessel (and replacement)	Second sedimentation vessel (and replacement)	Biological Reactor 1	Biological Reactor 2	Biological Reactor 3	Hydrogen Sulfide Scrubber	Water reservoir	AMD Pump	Recycle pump

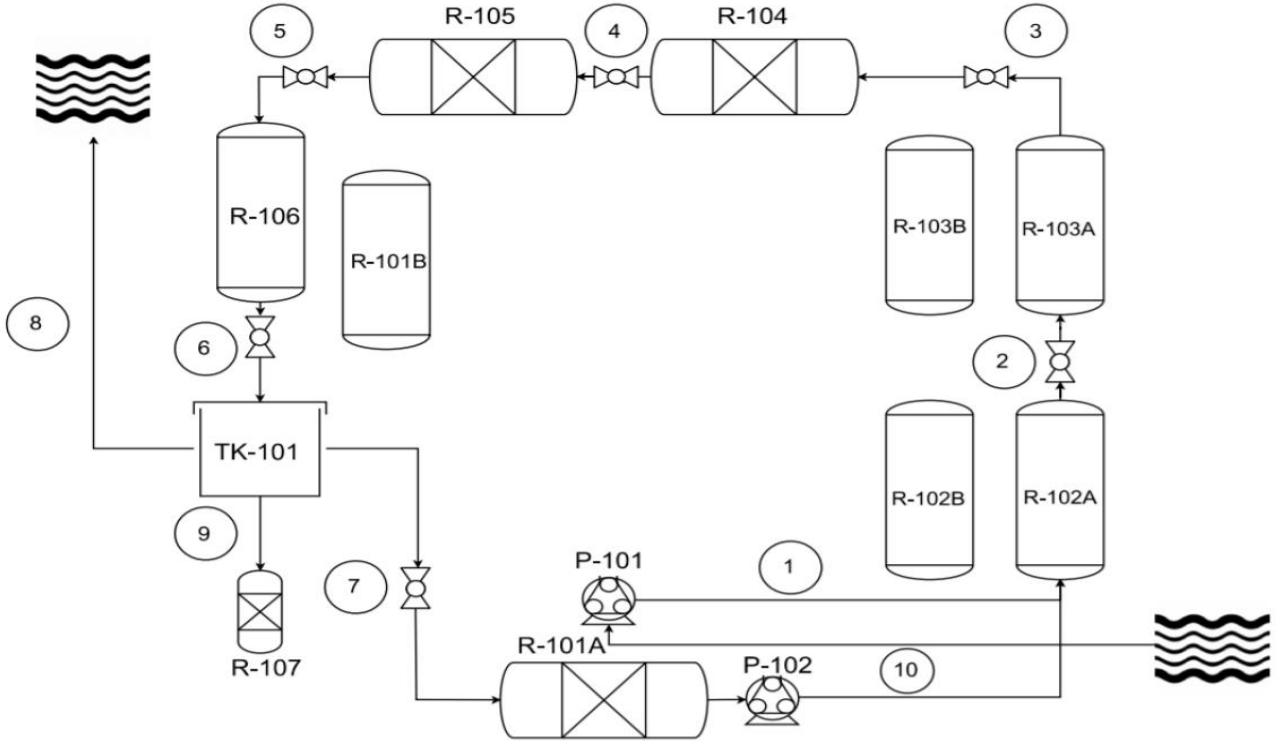


Figure 10-3: Process flow diagram (PFD) of pilot plant to treat AMD constructed at site

A process control element was used to vary the ratio of slag eluate (stream 10) to AMD feed (stream 1) that was mixed (and underwent a titration reaction) in the sedimentation vessels (R-102 and R-103) in order to maintain a pH of 5 in these vessels. A pH of 5 was chosen to (i) keep the recycle flowrate at a sustainable level, (ii) allow for ideal functioning of SRB, and (iii) allow for a suitable amount of precipitation of metals in the bioreactors (metals need to be present in the bioreactors to allow for metal sulfide precipitation). A depiction of the layout of the plant is shown in Figure 10-4.



Figure 10-4: AMD remediation pilot plant at mine dam site (photographs taken by authors)

The extent of treatment of AMD at the pilot plant (200-1000 ℓ/day) scale was evaluated and determined to have a maximum removal capacity of 97% for Al, 87% for Fe, 100% for Mn and 87% for SO_4^{2-}. SRB functioned in the BOFS neutralized solution, and the biological reactors showed a maximum sulfate removal of 76%. These were comparable to the laboratory scale data obtained, however significant differences were noted which were attributed to multiple technical issues which were experienced at site.

10.2.5 Complementary Experiments

Further experiments conducted during the pilot scale period included (i) determining the dissolution mechanism of the slag in the medium used, (ii) determining the alkalinity content of the precipitate which formed in the settling tank and (iii) determining the best process control configuration to maintain the ideal pH. These were relevant as the dissolution of the slag which produces hydroxyl units in the system to increase the pH of the AMD, is the limiting factor. It was found that the alkalinity (and ability

to in increase the pH of the system) was much higher when BOFS was dissolved directly in AMD as opposed to when dissolved in water or treated water. It was also found that smaller particle sizes of slag, although exhibiting a much quicker dissolution rate, cemented in liquid when left stagnant which prevented further dissolution. The smaller particle sizes also remained suspended in the liquid for longer periods of time and partially dissolved slag particles were frequently found in the sediment which formed at the bottom of the settling tanks. The sedimentation therefore contains a large amount of alkaline material which can be recycled to act as a pH raising reagent in the system. The process control mechanism was also investigated and a proportional only controller with pH controlled in the slag reactor as opposed to the settling tank was found to operate the best.

The findings and observations from each section have been used in the proposal of a design to treat 10 000 ℓ/day.

10.2.6 Analytical Techniques

The following analytical techniques were used to obtain measurements throughout the project period.

- Metal concentrations (Al, Ca, Fe, Mg, Mn) were measured with an Agilent 2000 series atomic spectrometer (AAS). Samples were filtered with 0.45 μm filters, diluted on a 1:3 ratio with deionized water and acidified with 0.6 mℓ of nitric acid prior to analysis. This was done to measure the difference in concentration in dissolved and precipitated metals in the samples. Sludge samples were acidified using nitric acid prior to measurement.
- Sulfate and sulfide concentrations were measured using turbidimetric spectrophotometric tests (using a Merck Spectroquant Pharo 300) (American Public Health Association, 1975; Center for bioprocess engineering research, 2016). Samples were filtered and sometimes diluted before testing to ensure concentrations were within an accurate range.
- A Scanning Electron Microscope (SEM) (FEI Quanta 200 ESEM) was used to investigate the surface of the slag particles. Standard concentration solutions were used for each test to obtain relevant calibration equations. Samples were mounted onto a metal plate using carbon tape and coated with carbon and gold palladium. Energy Dispersive X-Ray Spectroscopy (EDS) was used/performed during SEM analysis to determine the elemental composition on the slag surface (this was a qualitative assessment).
- XRD and Rietveld quantification analyses were done externally to determine the mineralogical composition of the slag. XRD sample preparation included grinding 3 g of sample and spiking it with fluorite on a 90:10 weight basis. Bagasse characterization data was obtained from the sugar mill. A Siemens D500 computer automated diffractometer was used to perform XRD.
- The pH and oxidation reduction potential (ORP) were measured using a DF Robot combined pH and ORP meter.
- Alkalinity/Acidity was measured using potentiometric titration. The titration sample (20 mℓ)

was continuously stirred and an initial pH determined and 0.02 N H_2SO_4 was added in varying proportions and pH was monitored until a pH of 4.5 (for total alkalinity calculations) was achieved. The total volume of H_2SO_4 added was recorded and used in calculating total alkalinity using Equation 10-1. For acidity, 0.1 N NaOH solution was used as a titrant.

$$\boldsymbol{Total\ alkalinity/acidity\ as\ CaCO_3 = \frac{(B/A) \times N \times 50 \times 1000}{ml\ sample}}$$

Equation 10-1

Where B is the total volume of standard acid used in titration to pH 4.5 or A is the total volume of standard base used, N is the normality of the standard solution of the acid or the base titrant, 50 is the mg equivalent of $CaCO_3$ and 1000 is used to convert from mℓ to ℓ (Smith, 2018).

- Flowrates were determined via calibrations of the peristaltic pumps which were used.
- Particle size distributions were obtained from Phoenix Slag Services.
- COD measurements were obtained using 1 mL sample together with Merck Millipore COD reagents 1.14679.0495 (A) and 1.14680.0495 (B) as well as COD cell test kit 114690. These were premixed solutions containing potassium dichromate that reacted with oxidizable material contained in the test sample. The solution containing both sample and reagents were heated to 148°C and then cooled before being tested. The concentration of unconsumed yellow $Cr_2O_7^{2-}$ ions was then determined photometrically (Merck Spectroquant ® Pharo 300) and using stoichiometry, giving the mg/ℓ of COD of the sample (Center for bioprocess engineering research, 2016; Decker, Askew and Merck, 2017).

10.2.7 Summary

A summary of the design methodology is as follows:

- Testing/evaluation of individual reagents (sugarcane bagasse with SRB and BOFS) to determine their efficacy and ideal conditions.
- Combining the reagents to determine the most feasible model for combined treatment.
- Testing the model at a laboratory scale (treating up to 25 ℓ/day)
    - Identifying shortcomings, proposing alternatives and testing alternatives
    - Proposing a model/design for the larger scale (pilot) plant based on findings
- Designing, constructing, and monitoring the pilot scale design (treating up to 250 – 1000 ℓ/day)
    - Identifying shortcomings, proposing, and testing alternatives where possible
- Proposing a design for a large scale (treating up to 10 000 ℓ/day) plant based on the findings from the previous steps.

10.3 Laboratory Scale Plant

10.3.1 Introduction

The construction and operation of a laboratory-scale plant was essential to the design process, as this allowed for the behaviour of the system to be monitored and improved before proposing a larger scale design based on the initial concept. The laboratory scale processes were tested over a period of 156 days and assessed multiple different aspects of operation, namely: reactor type, particle size, pH dependency and variation in feed quality. As discussed, the data obtained from the laboratory work was used to compile a pilot scale design. This section discusses the focal merits of the laboratory phase of the work. This small-scale study has also been the basis of a journal article and a conference paper (Naidu et al., 2018; Naidu, Van Dyk, Sheridan, & Grubb, n.d.).

10.3.2 Methodology

As mentioned, initial testing (conducted prior to laboratory scale design) revealed the shortcomings of introducing the AMD into contact with either the BOFS or the SRB and sugarcane bagasse directly. The schematic shown in Figure 10-1 was thus followed, whereby a recycle stream of treated water was reacted with BOFS and then used as a titrant for AMD. The (approximately) neutral water that was generated as a result of this reaction was then passed through the sugarcane bagasse and SRB. In this way, denaturing of both reagents (BOFS and sugarcane bagasse with SRB) was avoided.

Plastic vessels (to avoid corrosion) were used as reactors during the laboratory scale investigation. Vessels contained in the laboratory plant are listed below with volumes in brackets:

- Sedimentation vessel/settling tank (18 L)
- Primary biological (sulfate reduction) vessel containing sugarcane bagasse (14.4 L)
- Secondary biological (sulfate reduction) vessel/sulfide precipitation vessel (7 L)
- Water reservoir/storage tank (7 L)
- 2 x Slag packed bed reactors (PBR) containing BOFS (1.8 L) (this was changed to a 1 L continuously stirred tank reactor (CSTR) during operation).

The setup also consisted of 2 peristaltic pumps and a pH controller which controlled the pH at a set-point via on-off control. This set-point was changed throughout the operation.

The initial performance of the process was tested by operating the system under different process conditions for a total of 106 days. COD was measured in the liquid from the biological reactor containing bagasse before operation began. BOFS particles were replaced, and sizes changed on Day 33, from size 1 (8 μm <d<13 μm) to size 2 (1.7 μm <d<3.35 μm), and on Day 64 from size 2 to size 3 (d< 1 μm) (particle size ranges were achieved using sieve analysis). On Day 64 the BOFS reactor type was changed from a PBR to a CSTR to eliminate blockages due to the small particle size. The raw AMD was changed on Day 70 from Type A to Type B (the compositions of the different AMD are

shown in Table 10-2). Samples were taken from sample points at different positions in the process (as shown in Figure 10-2) and analysed for metal, sulfide and sulfate content as well as pH and redox/ORP. Following this, the plant was run for a period of a further 50 days using a CSTR and size 3 (d< 1 μm) BOFS in order to assess pH control functionality and options.

Table 10-2: Composition and pH of AMD sourced from two different AMD sources in Emalahleni, Mpumalanga, South Africa

AMD Type	pH	Aluminium (mg/L)	Calcium (mg/L)	Iron (mg/L)	Magnesium (mg/L)	Manganese (mg/L)	Sulfate (mg/L)
Type A	2.44	434.89	110.83	3039.60	105.67	88.29	12955.62
Type B	2.47	497.25	175.38	3506.88	94.04	197.68	5199.92

SRB was cultivated separately using a solution of sodium sulfate and sodium acetate (using a 0.7 g COD/g sulfate concentration) and then added to the AMD solution (SRB solution to AMD was mixed with a 1:2 ratio). Sulfide production and sulfate reduction (concentrations) were used as indicators of SRB activity. This inoculum was then added to the biological reactor containing sugarcane bagasse. SRB cultures were sourced from previous experiments which had used mud sediment from Emmarentia Dam in Randburg, South Africa.

10.3.3 Reactor Type

BOFS dissolution was not found to occur sufficiently in unagitated systems and thus a constant flow or constant agitation was required to achieve the necessary level of reaction – corresponding to a rise in alkalinity and pH of the system. In this regard, two types of reactors were investigated – a CSTR and a PBR.

10.3.3.1Packed Bed Reactor

The system was initially designed to house a PBR which would facilitate the acid-base reaction between the BOFS and the AMD/treated water. Use of a PBR was tested initially in the continuous process using the configuration showed in Figure 10-2 and monitored over a period of time. Treated water from the reservoir was pumped into this reactor and came into contact with the BOFS where a dissolution reaction took place. The pH, metal and sulfate content was observed for this period and it was found that without agitation of the slag, the pH did not reach a level high enough to titrate the AMD to the desired pH. The recycle ratio could not be sustained by the low concentrations of hydroxide groups found in the BOFS eluate from this reactor – i.e. because dissolution of the slag was not occurring sufficiently (due to the reactor type and BOFS particle size), the amount of hydroxide units in the slag eluate was not enough to fully neutralize the AMD to the desired pH. Thus, either a higher recycle ratio

(and conversely a longer reaction time in the slag reactor) needed to be used, or a way to increase the dissolution of the slag needed to be implemented. The PBR used in the laboratory had a small volume in relation to the total volume of the system and did not contain enough BOFS (or water) to facilitate the required rise in pH. As the requirement of the system grew (AMD needing higher and higher volumes of slag eluate to be neutralized), the flowrate through the PBR increased – effectively decreasing the residence time and the time allowed for the dissolution reaction (this meant that the solution did not have a high enough pH and there were not sufficient hydroxyl units in the solution to increase the alkalinity of the AMD by the required amount). It was concluded that for a PBR to be effective, it would have to (i) contain a substantial excess of BOFS and (ii) be of a great enough volume that water contained within this chamber would have enough time to allow dissolution of the BOFS and generate sufficient alkalinity to neutralise the AMD.

It was also found that particle size played an important role in dissolution. When an assortment of particle sizes (including fines or particles with a diameter less than 1 mm) were used as the packing material, hindrance of flow due to cementation was observed in the reactor. When only larger particle sizes (particles with a diameter of 1 cm or above) were used, void space and flow did not present any problems as no fines were present to create cementation and hinder flow. In addition, the space between particles increased allowing for constant and uniform flow through the reactor. The pH increase of the water entering the reactor, however, was very low when larger particles were used. This was attributed to the decreased surface area of the BOFS particles. It was noted that in situations of high flowrate (turbulent flow), cementation was not an issue and the fine particles remained suspended in the solution. Residence times of between 44 and 4 days were achieved for different conditions - smaller particle sizes of slag exhibiting better performances in terms of recycle rate and residence times. The flowrates and residence times are presented in Table 10-3 below.

Table 10-3: Residence time, recycle ration, and flowrates of inlet and recycle streams in system for different particle sizes and AMD qualities

AMD Type	Size class and Particle Size (µm)	AMD flowrate (L/Day)	Recycle flowrate (L/Day)	Residence Time (Days)	Recycle Ratio
A	1 (8 µm < d< 13 µm)	1	24.48	1.69	24.48
A	2 (1.7 µm < d< 3.35 µm)	2.18	24.48	1.61	11.23
A	3 (d < 1 µm)	3.76	24.48	1.43	6.51
B	3 (d < 1 µm)	10.42	24.48	1.16	2.35

10.3.3.2Continuously Stirred Tank Reactor

The PBR reactor was replaced with a CSTR during the operation of the laboratory scale system. This was done to increase the alkalinity of the BOFS eluate and thus increase the pH of the system. A dosing system was used whereby BOFS fines were added to the CSTR at intervals in order to maintain the pH in the settling tank at a certain level. This system was highly effective and increased the efficiency of the system by 3.76 (3.76 times more AMD could be treated to the same conditions using the CSTR than when using the PBR) and thus in terms of treatment capacity, the CSTR was more effective. This system, however, was more energy intensive as a dosing schedule needed to be determined and energy was used to constantly agitate or stir the system. Using fines which are suspended in fluid also did not allow for a complete dissolution reaction to occur and the sedimentation in the settling tank will contain a high concentration of partially dissolved BOFS particles. In order to minimize reagent loss in relation to this, it was proposed that a recycle stream may need to be added to the system, whereby the sludge which forms in the settling tank is used again as an alkalinity source due to its content of unreacted BOFS. This is similar to a high-density sludge (HDS) system which is discussed in a subsequent section.

10.3.3.3Summary (Reactor Type)

Due to the increased energy demands and impracticality of agitation at a large scale, the PBR design was used for the pilot scale set-up. The volume of the tank (in relation to the rest of the plant) was increased, as well as the amount of BOFS in the vessel. This was done to combat the initial issues experienced with the PBR in the laboratory scale system.

10.3.4 Particle Size

BOFS is available in a variety of different particle sizes from different steel manufacturing sites. The typical size distribution found at the Phoenix Slag Services site is shown in Table 10-4 and all particle sizes cost the same (R146 per ton (Vermeulen and Phoenix Slag Services, 2018)). Different size classes (mentioned above and shown in Table 10-3) were tested in the BOFS reactor in order to ascertain which particle sizes were best suited to treat AMD. When the recycle rate was kept constant, it was found that a smaller particle size coupled with agitation allowed for better performance in the system in terms of lower residence times – this is shown in Table 10-3.

Due to the distribution of the BOFS found at the Phoenix site, as well as the impracticality of using a constantly agitated vessel for large volumes, an assortment of large and fine particle sizes was initially used for the pilot scale design. It was deemed necessary to use particles with a diameter of 13.2 mm and below as this was the size class that Phoenix Slag Services indicated they would be most likely to supply on a continued basis. Particles with a diameter of below 13.2 mm were thus used and further divided into 3 classes (1, 2 and 3 representing the larger, medium and smaller particles in this range). Particles were divided into further groups as these size classes each have different uses as aggregates.

Table 10-4: Particle size distribution of BOFS from Phoenix Slag Services

Size Group	Diameter (mm)	Mass (g)	% Distribution
1	37.5 < d	0	0
2	26.5 < d < 37.5	0	0
3	19 < d < 26.5	0	0
4	13.2 < d < 19	470.5	25.8
5	4.75 < d < 13.2	999.2	54.9
6	2 < d <4.75	316.6	17.3
7	0.425 < d < 2	28.5	1.6
8	0.075 < d < 0.425	2.5	0.1
9	d < 0.075	2.3	0.1

The residence time calculations took into account the recycle stream flowrate. The particle size classes 1, 2 and 3 that were used in the study, correspond to size groups 5, 6 and 7 + 8 + 9 from the original distribution, respectively.

10.3.5 pH Dependency

The pH in the system was of vital importance to the extent of treatment achieved in each vessel. As discussed briefly before (in Chapter 3), the pH in the settling tank determined the amount of metals and sulfates which are removed, the pH in the biological reactor determined the functioning of the SRB and the pH of the slag eluate determined the recycle ratio and rate of the treated water going back into the system. For this reason, determining an ideal pH level was essential.

The metal species contained within the AMD precipitated out of solution at different pH's. The calcium which entered the system via dissolution of the slag was also able to precipitate out of solution due to the availability of excess sulfate which acted as a counterion at certain pH's. This is shown in Figure 10-5.

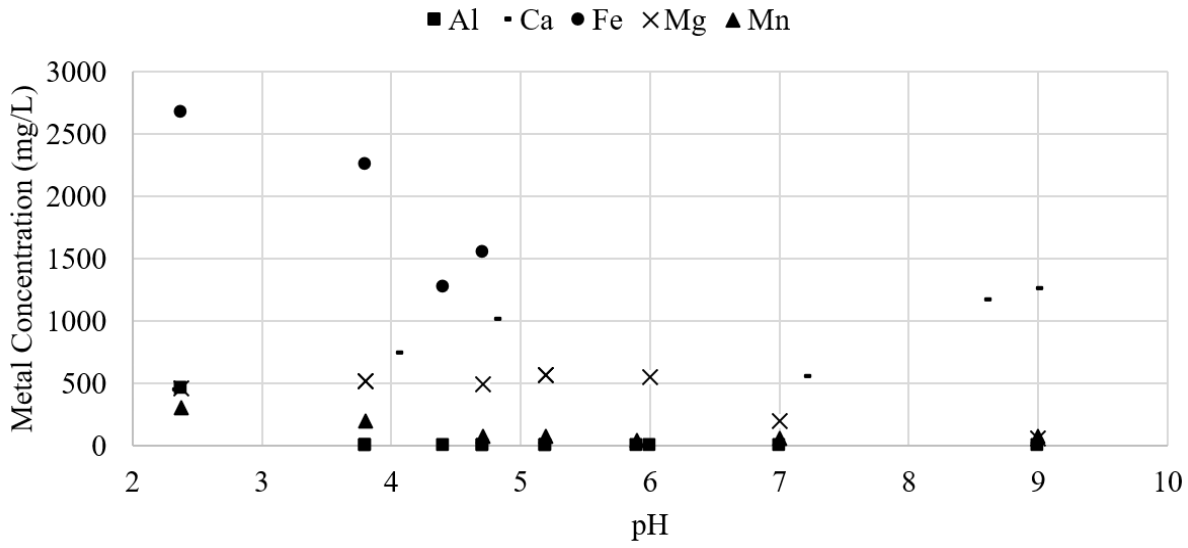


Figure 10-5: Dissolved metal concentration in AMD solutions at different pH levels when pH is altered using BOFS fines

As depicted, the ideal pH for removal of all prominent dissolved metals in AMD occurs at a pH of 7. During the first stage of the biological process however, organic acids are released into the system from the bagasse which lowers the pH slightly. Because of this, it was initially theorized that a set level of 9 should be achieved in the settling tank. This was tested and deemed too energy intensive (due to the high recycle rate) to be feasible. A pH of 7 was therefore chosen for subsequent experiments. This pH was able to be maintained, however it was found that a higher degree of metals and sulfate could be removed in the biological reactor if a higher concentration of metals were available to bond with the sulfidic components produced as a result of DSR. Thus, a pH of 5 was chosen as the setpoint in the settling tank for the design of the pilot plant. This would have the added benefit of lowering the recycle rate – effectively increasing the amount of water treated and decreasing the energy consumption of the plant. The pH dependency is linked closely to the process control philosophy and mechanism. This is discussed in detail in a subsequent section.

10.3.6 Variation in Feed Quality

During operation of the laboratory scale system, two different types of AMD were tested. The composition and characteristics of which are shown in Table 10-2. The two different AMD sources had similar pH levels but different metal and sulfate concentrations. Behaviour of the system when treating the two AMD's were different, but the same (or very similar) conditions were able to be maintained in each case. The treatment efficiency of Type B AMD was approximately 2.77 times better than the treatment efficiency of Type A AMD (2.77 times more AMD was able to be treated using a constant recycle flowrate of 24 L/day). This indicated that the design of the system and the process control was versatile and could potentially be implemented at different sites with different AMD qualities.

10.3.7 Summary of Treatment

As mentioned, different types of AMD were tested in the laboratory scale configuration (the characteristics and composition of these AMDs are given in Table 10-2) as well as different particle sizes (size 1, 2 and 3 as shown in Table 10-3). The main/overall results of the conceptualized design testing these different variables over the experimental period were favourable, with removal of most metals and sulfates occurring to levels of over 90%. The total removal of the prominent metals and sulfate from the system when different particle sizes and different AMD qualities is shown in Figure 10-6. Relative standard deviation (RSD), mean and number of repetitions (sampling times) are shown in Table 10-5. As depicted, all metals and sulfates (with the exception of Mg and Ca) were found to have an average of > 90% removal for all configurations of particle size and AMD type. Ca increased in concentration for all configurations which is attributed to the continuous influx of Ca into the system from the dissolution of the calcium oxide in the BOFS. A value of 2.61 mg/L of COD was found in the primary bioreactor before testing – giving a COD measurement of 12.56 mg COD/kg of bagasse. Bagasse was not replaced during the 106-day period and thus (according to the COD to sulfate ratio of 0.7) the sulfate removed in this reaction could not be attributed solely to biological sulfate reduction. It was determined that some reduction did occur – due to the presence of sulfide components – however further precipitation of sulfates could also have occurred in the bioreactors, as well as adsorption.

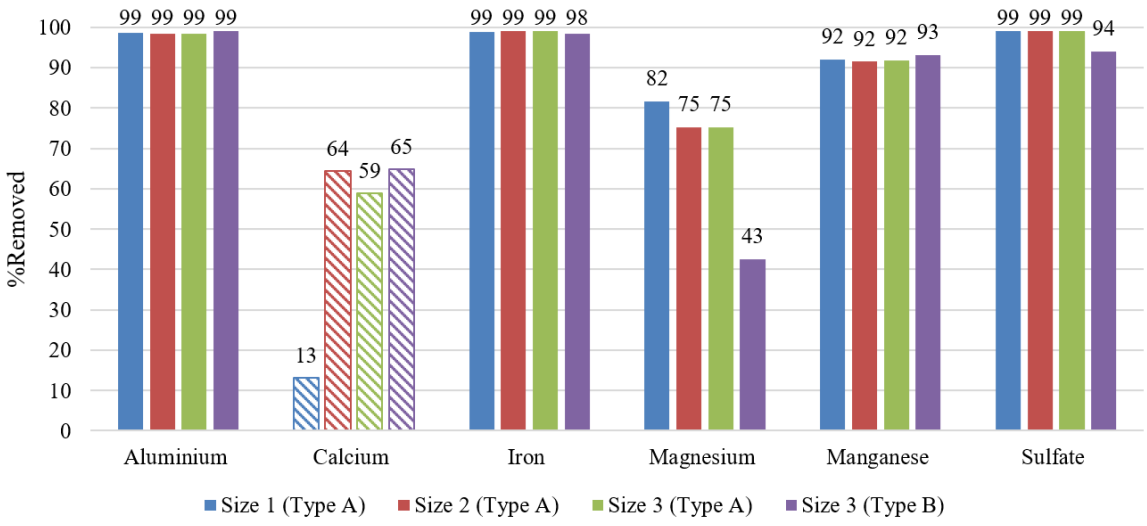


Figure 10-6: Percentage of (i) removal of total Al, Fe, Mg, Mn and sulfate in the laboratory scale system when different particle sizes and AMD qualities are used, and (ii) addition of Ca to the treated water due to BOFS dissolution (data prepared using averages for the 106-day period)

Mg removal was also not as high as the other metals, due firstly to the dissolution of magnesium oxides in the BOFS and also due to the pH in the system not being high enough to facilitate complete precipitation. The operation of the system was considered a success with the data being obtained giving valuable information regarding necessary changes that would have to be made in the large-scale design. RSD values show that the outlet conditions were not constant during the operation of the plant.

Table 10-5: Standard deviations and repetitions for outlet conditions from laboratory scale plant operation

Size 1/Type A				Size 2/Type A			
Metal/ Component	**Mean (mg/ L)**	**Repetitions**	**RSD**	**Metal/ Component**	**Mean (mg/ L)**	**Repetitions**	**RSD**
Aluminium	6.08	24	0.28	**Aluminium**	6.72	10	0.06
Calcium	121.75	24	0.33	**Calcium**	182.09	10	0.04
Iron	31.31	24	0.66	**Iron**	29.95	10	0.52
Magnesium	18.89	24	1.07	**Magnesium**	26.11	10	0.49
Manganese	6.92	24	0.42	**Manganese**	7.52	10	0.31
Sulfate	168.53	24	0.52	**Sulfate**	157.13	10	0.40
Sulfide	3.77	3	0.47	**Sulfide**	7.24	10	0.55
Vanadium	0.05	8	0.20	**Vanadium**	0.05	10	0.00
pH	7.42	24	0.09	**pH**	7.10	10	0.07
Size 3/Type A				**Size 3/Type B**			
Metal/ Component	**Mean (mg/ L)**	**Repetitions**	**RSD**	**Metal/ Component**	**Mean (mg/ L)**	**Repetitions**	**RSD**
Aluminium	6.63	8	0.03	**Aluminium**	4.44	12	0.14
Calcium	176.64	8	0.06	**Calcium**	288.93	12	0.10
Iron	27.42	8	0.24	**Iron**	57.53	12	0.50
Magnesium	26.11	8	0.49	**Magnesium**	53.98	12	0.19
Manganese	26.28	8	0.16	**Manganese**	13.34	12	0.25
Sulfate	130.32	8	0.10	**Sulfate**	287.77	12	0.13
Sulfide	7.18	8	0.26	**Sulfide**	1.26	3	3.83
				Vanadium	0.05	12	0.20
pH	7.09	8	0.03	**pH**	6.92	12	0.22

In the biological vessels, sulfate removal occurred at a lower rate than the settling vessel, accounting for less than 2% of overall sulfate removal. Sulfate removal in the biological vessels could have been

achieved via sulfate reduction, sulfate precipitation, sulfide precipitation as well as adsorption of sulfate or sulfide to the surface of the organic carbon source.

A 35%, 29%, 35% and 16% sulfate removal was achieved across DSR vessel 1 for size 1 (8 μm <d< 13 μm), size 2 (1.7 μm <d< 3.35 μm), size 3 (d< 1 μm) particle size and Type B AMD respectively. DSR vessel 2 had a lower sulfate removal percentage than DSR vessel 1. Sulfide was detected in the biological vessels over the 106-day period which confirmed the occurrence of sulfate reduction. The lower overall sulfate removal for Type B AMD was attributed to a change in conditions - SRB may need to acclimatize to the new conditions over a period of time before maximum sulfate reduction can occur.

10.4 Pilot Scale Plant

10.4.1 Introduction

After operation of the laboratory scale work, the initial design was modified and used in the construction of a pilot plant at a coal dump site in Witbank, Mpumalanga. This section discusses the operation of the plant at the site with regards to technical issues that were experienced, data obtained and any findings or observations that were made which have contributed to the design of the 10 000 L/day plant. This work was also used as the basis of a conference paper (Naidu *et al.*, 2019). The design used is shown in Figure 10-3.

10.4.2 Methodology

Data obtained from the laboratory scale operation allowed changes to be made to the design where necessary. Vessel sizes were increased to allow for larger areas for settling and the availability of more carbon for the SRB in the biological reactor. The full design methodology and sizing for the pilot scale plant can be found in Appendix A. The biological reactors used in the pilot scale were each inoculated with 100 L of inoculum before operation commenced. This inoculum was cultivated in 25 L vessels using the same methodology as described in the Laboratory Scale Plant Methodology Section.

10.4.2.1Construction and Commissioning

The system was constructed using 2200 L chemical and heat resistant plastic (linear low-density polyethylene (LLDP)) vessels as the reactors and JoJo tanks for the water reservoir and H_2S Scrubber. Construction took place over a 4-month period from January 2018 to April 2018. The system was tested with water at the Phoenix Slag Services site in Wadevile before being transferred to the site in March. Once the equipment had been transported and connected at the site, clean water was needed in order to provide a sufficient volume of water (of the right composition) to be used as the recycle stream. AMD could not be used as this would result in possible fouling of the BOFS and poisoning of the SRB in the biological reactors. Clean water was not available at site and process water had to be used instead. This water had a pH of 3 and was contaminated by various metals and sulfate which caused thick layers of precipitation over the BOFS that prevented the dissolution of the slag and the raise in the pH of the system. This delayed the optimal performance of the plant for a period of time. The plant operated for a total of 196 days.

10.4.2.2Flowrate and Residence Time

The total volume of the system was approximately 13 000 L. Flowrates and residence times for the period are displayed in Table 10-6.

Table 10-6: Flowrate and residence time in system

Time Period (days)	Flowrate of AMD (L/day)	Flowrate of Slag Eluent (L/day)	Residence Time (AMD and Slag Eluent) (days)
34	600	1000	8.1
34-43	270	1000	10.2
43-76	270	1200	8.8
76-120	270	2000	5.7
120 onwards	0	2400	5.4

From day 120 onwards, the residence time for both the BOFS eluate and AMD streams was 5.4 days or lower. The flowrate into the system was determined by process control operation.

10.4.3 Extent of Remediation

The inlet quality of the AMD changed continuously but had an average concentration and pH as shown in Table 10-7. The change in inlet concentration may have contributed to the variation in treatment extent over the remediation period. The pH levels changed across each vessel as well as over time, but the average pH in each vessel was 5.4 (R-101), 3.2 (R-102), 3 (R-103), 4.6 (R-104), 4.6 (R-105), 4 (R-106) and 4 (TK-101). The change in pH of the AMD is due to hydration reactions that occur between the AMD and the BOFS and the subsequent dissociation that results in the release of hydroxide units. The fluctuation in pH and metals across the system over time (as shown in Figure 10-7 and Figure 10-8) is attributed to the varying amount of oxide containing BOFS particles that come into contact (and are able to react) with the AMD.

Table 10-7: Average composition and pH of AMD in storage dams

Component	Concentration (mg/L)	RSD
Al	177.4	0.59
Ca	237.4	0.56
Fe	4320.1	0.07
Mn	331.3	0.42
Mg	412.5	0.25
SO_4^{2-}	16301	0.07
V	0.07	0.1
pH	2.6	0.07

This varying amount is determined by the process control over the plant. When the pH of the sedimentation vessel (R-102) is lower than 5, the flowrate of the entering slag eluate (stream 10) increases until it reaches a maximum of 2400 L/day and the flowrate of the AMD stream (stream 1) decreases until 0 in order to facilitate a higher ratio of slag eluate to AMD. For pH levels higher than 5 the opposite is true.

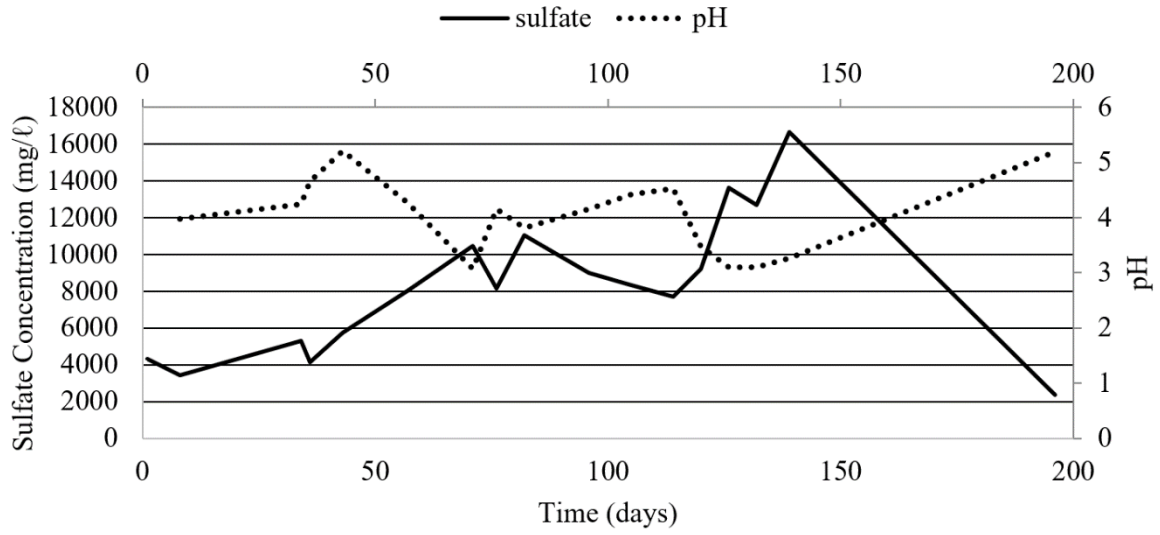


Figure 10-7: pH and sulfate concentration of the treated water from the pilot scale plant over the 196-day period (samples taken from TK-101 - treated water reservoir)

Process control over the system became automatically effective after 120 days and thus fluctuations occurred. In addition to this, precipitation and settling in the BOFS reactor limited the release of further oxides.

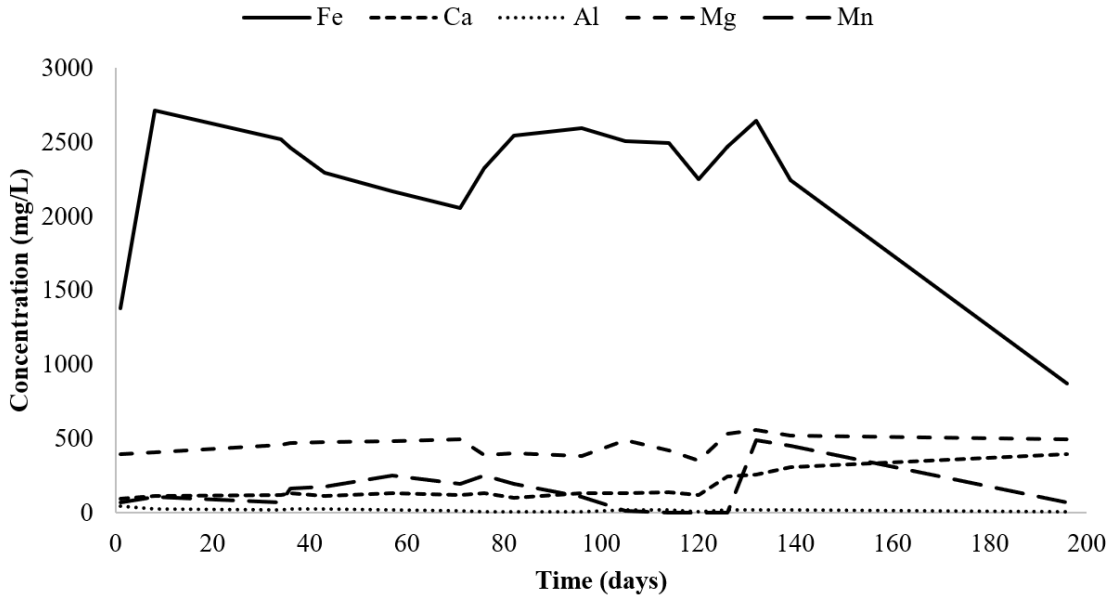


Figure 10-8: Metal concentrations in the water reservoir (TK-101) over the 196-day period

Effects of precipitation were combatted by removing sedimentation and allowing only treated water (with a lower ion content and thus less ability to form precipitates) to flow through the BOFS reactor. The metal and sulfate levels across the system fluctuate along with pH levels (as shown in Figure 10-7 and Figure 10-8). Metal and sulfate concentrations are dependent on the pH levels, making pH control in the system extremely important. High pH levels allow for more precipitation reactions to occur, removing a higher quantity of sulfates and metals, and pH levels between 4 and 7 allow for optimum SRB activity. The extent of treatment in each vessel at the end of the 196-day period is shown in Table 10-8 in terms of % removal of each component (based on the initial and last reading). Bold indicates an increase in concentration.

Table 10-8: Extent of remediation across each process vessel (%removal of components) where bold text indicates an increase in concentration and plain text indicates a decrease

Component	R-102A/B (%)	R-103A/B (%)	R-104 (%)	R-105 (%)	R-106 (%)	TK-101 (%)	R-101A/B (%)
Mn	69.23	70.50	76.51	78.32	77.30	79.90	83.32
Mg	0.79	**4.77**	**0.34**	**16.06**	**12.44**	**19.54**	**23.31**
Al	95.22	95.86	96.61	97.07	96.08	95.45	90.03
Ca	**185.32**	**167.87**	**69.13**	**123.12**	**69.74**	**62.43**	**226.45**
Fe	56.28	69.72	77.96	82.72	83.39	79.61	86.61
SO_4^{2-}	55.63	72.52	80.24	81.95	83.53	84.69	87.10
pH	5.26	5.34	5.24	5.49	5.11	5.20	7.24

The extent of remediation changed considerably over time at site, and this was attributed to the fluctuating conditions (changing feed quality, climate and availability of electricity to run equipment). The best treatment (for a combination of components) was observed after approximately 4000 hours of operation time (167 days) of operation and showed an 84% removal of sulfate, 80% removal of dissolved Fe, 62% increase of Ca, 95% removal of Al, 20% increase of Mg and a 80% removal of Mn. The maximum removals in terms of Al, Fe, Mn and sulfate were 97%, 87%, 100% and 87% respectively (across different reactors). Vanadium did not exhibit any considerable changes and Mg and Ca concentrations consistently increased in the system. The chemical section of the plant (R-102, R-103) was able to remove up to 72% of sulfate and the biological section (R-104, R-105, R-106) could remove a further 11% (76% sulfate removal over the 3 reactors).

10.4.4 Technical and Site Issues

Multiple site related issues affected the functioning of the pilot plant. These included the lack of continuous power, lack of clean water and lack of security. Multiple thefts at the site resulted in the aeration of the system (when vessel covers were stolen) and eventually in the collapse of the reactors (when the reactor steel supports were stolen). Theft of power cables in October 2018 resulted in a

complete ceasing of operation of the plant as the site management were unable to indicate when power would be restored after a period of 2 months.

These issues are summarised below:

- **Power outages**

  Start-up was aimed to take 21.5 days with the AMD pump pumping at 600 L/day and the slag recycle pump, pumping at between 2000 and 3000 L/day. This was not achieved due to power outages at site, and this process took approximately 34 days. Power outages at the plant site occurred frequently and resulted in a complete shutdown of the pumps which disrupted the continuous flow of AMD feed and recycle in the system. These outages led to a delay in the pilot plant start-up period from 21.5 days to 34 days as the pumping rate of 600 L/day AMD and the slag recycle of 2000 and 3000 L/day was not continuously maintained. Theft of power cables eventually necessitated shut down of the plant as the mine indicated they could not commit to re-establishing power at the site.

- **Theft at site**

  Anaerobic conditions were aimed to be kept stable, however due to theft at site this was not possible for a period of 2 weeks. The vessel covers were stolen and this allowed aeration of the biological system for a two-week period which compromised the anaerobic nature of the bioreactors. To address the problem, the covers were replaced with clear cheap plastic sheeting; the mine was informed of the incident and security measures to protect equipment of a valuable nature were increased (motion detections sensors were provided by the mine and the pumps and process control system were secured in locked enclosures).

- **Poor mobile network connectivity**

  Access to site via remote control was aimed to be established from the onset of operation in order to continuously monitor the plant. This was established but was not constant due to data interruptions at site. The network connectivity at site was erratic and remote access to the system was not sustainable using a data connection. This limited plant monitoring, as problems which arose at site were only identified during the weekly visits. Data had to be collected weekly with monitoring and remote access and control occurring only sporadically.

- **No potable water on site.**

  The desired pH was envisioned to be reached after 4 days, however due to the slag armouring or coating, alkalinity accessibility was limited, and the desired pH was not achieved. The system was designed for start-up with 13 000 litres of clean water, however, due to the isolation of the site and lack of access to clean water, process water (with a pH of 3 and high sulfate and metal content) was delivered to site and was used instead. This led to a large amount of precipitation and armouring of the top layer of slag in the slag vessel which in turn led to poor release of the oxide compounds in

the slag (which were responsible for the pH increase). This greatly limited the operation of the plant as oxide release was dampened in the system, preventing pH rise of the AMD entering the plant. This was rectified by removing the layer of precipitate that had formed and was preventing oxide release. The particle size of slag that was used was also not ideal for use in a packed reactor. The slag may have hindered the flow of liquid through the slag reactor. As a result, diffusion and dissolution of the alkalinity generating compounds of the slag in the liquid did not occur at fast-enough rates (similarly to what was found in the laboratory scale process). This limited the pH rise of the recycle stream and the sedimentation vessel. The hindrance of flow was due to cementing and compacting of the smaller particle sizes of slag (during the removal of the precipitation layer, hard, compacted layers of slag were found). Larger particle sizes were then added and were used to ensure more accessibility of the liquid to the slag and maintain better flow through the reactor.

The operation of the pilot plant indicated that the design was functional at larger scales and exhibited similar and comparable results to the ones obtained from the laboratory scale plant.

10.5 Complementary Data

10.5.1 Introduction

During the operation of the pilot scale plant, a number of laboratory scale experiments were undertaken to further investigate the mechanisms of sulfate removal, metal removal and pH rise in the system. It was also necessary to investigate the process control mechanism, as this played a large role in the effective functioning of both the small and large-scale plants. Findings from these complementary studies are discussed in this section. These findings have also been used to inform the 10 000 L/day design. The results from these experiments were used to form the basis of a peer reviewed conference paper which has been published in the 2020 SAIMM Mine Tailings conference proceedings (Naidu, Chauhan, *et al.*, 2020). A summary of the findings is presented below:

10.5.2 Methodology

10.5.2.1Slag dissolution

Experimentation was done (on three size classes of slag: (i) class 1 – 2 mm to 3.35 mm in diameter; (ii) class 2 – 4.75 mm to 6.7 mm in diameter and (iii) class 3 – 6.7 mm to 9.5 mm in diameter) to further understand the dissolution kinetics of BOFS and to ascribe a suitable model to predict the extent of dissolution of BOFS in media of different pH levels or acidity/alkalinity measurements. Slag leaching tests were conducted to ascertain the mechanism of dissolution. Slag samples and leaching liquids (water, AMD and hydrochloric acid) were weighed and measured out such that the liquid to solid ratio remained constant at 10:1. Initially, 40 g of slag and 400 mL of liquid were used, thereafter, 80 g of slag and 800 mL of liquid were used. The liquid was placed into a 1000 mL beaker on a magnetic stirrer, at 200 rpm and room temperature, and the pH probe was inserted into the liquid. The pH of the liquid after slag was added, was monitored continuously. 1 mL of the leaching liquid was removed as aliquots at varying time intervals for AAS analysis and titration samples of 20 mL of the leaching liquid was removed at 20 seconds into the experiment and at the end once pH stability was attained. The leached slag was put into an oven for drying at 50°C. Experiments were replicated, and where necessary multiple experiments were run to ensure change in volume after sampling did not affect the experiment. Other experiments were run using the same methodology with different volumes and masses of BOFS and leaching liquid. Lagergren and shrinking core kinetic models were applied to the data obtained from these experiments. A comparison between lime and BOFS was also performed using data from literature.

10.5.2.2Precipitate formation

Sludge formed in the various reactors was collected, acidified and assessed using the AAS procedure. This was done to determine what types of precipitates had formed. The BOFS particles from the slag dissolution reactions were also assessed using SEM and EDS. A review/literature-based study was conducted alongside these tests to determine the likely mechanism of precipitation.

10.5.3 Mechanism of pH Increase

10.5.3.1Comparison of lime and BOFS

An important thing to note in the comparison between lime (quicklime or hydrated lime) and BOFS is the availability of free lime in the sample (components that are available to hydrate and raise the pH of the media). Lime and free lime generally refer to the CaO component of the sample, however BOFS contains multiple other units in oxide and silicate form that dissolve in liquid media and contribute to the neutralization or pH rise of the media. Table 10-9 shows an approximate availability of oxides (that can readily hydrate in liquid media) in lime and BOFS. Although the free lime content in BOFS is 13 %, this only refers to the components found on the surface of the solid particle. As dissolution occurs (largely following Lagergren kinetics (Naidu, Chauhan, *et al.*, 2020)), more oxide components become available. The size of the BOFS particle used will also affect the amount of free oxide content – smaller particles have a larger availability of neutralizing/alkaline components than larger particles.

Table 10-9: Free oxide content in quicklime, hydrated lime and BOFS with particle aperture between 2000-3350 microns (determined via SEM and Energy dispersive X-ray analysis (EDA)) where Wollastonite found on the surface of the particle was not considered a free oxide (due to it's insolubility in water) (Tolonen *et al.*, 2014)**.**

Alkaline material	Oxide content (Total %)	Free oxide content (%)
Quicklime	94	91
Hydrated lime	73	71
BOFS	87	13

Although the free oxide content of BOFS is significantly less than that of normal quicklime or hydrated lime, the BOFS still exhibited success in neutralizing AMD. 80g of slag was able to raise the pH of a sample of Type A AMD with an initial pH of 2.44 to (i) a pH of 7 in 540 minutes and (ii) a pH of 10 in 1365 minutes. This is shown in Figure 10-9. The experiment shown in Figure 10-9 was repeated multiple times and it was observed that the pH in the system did not stabilize, even after 72 hours of reaction time.

The pH rise was directly related to (i) the volume of AMD, (ii) the composition of AMD, (iii) the amount of BOFS, (iv) the particle size of the BOFS and the (v) allowed reaction time. For example, 15 g of slag fines (aperture of 1000 microns or less) was able to increase the pH of 1500 mL of Type B AMD (significantly lower initial sulfate and iron concentration) to a pH of 7 in 55 minutes, and similarly 67 g of fine BOFS was able to raise 200 mL of this Type B AMD to a pH of 7 in 5 minutes.

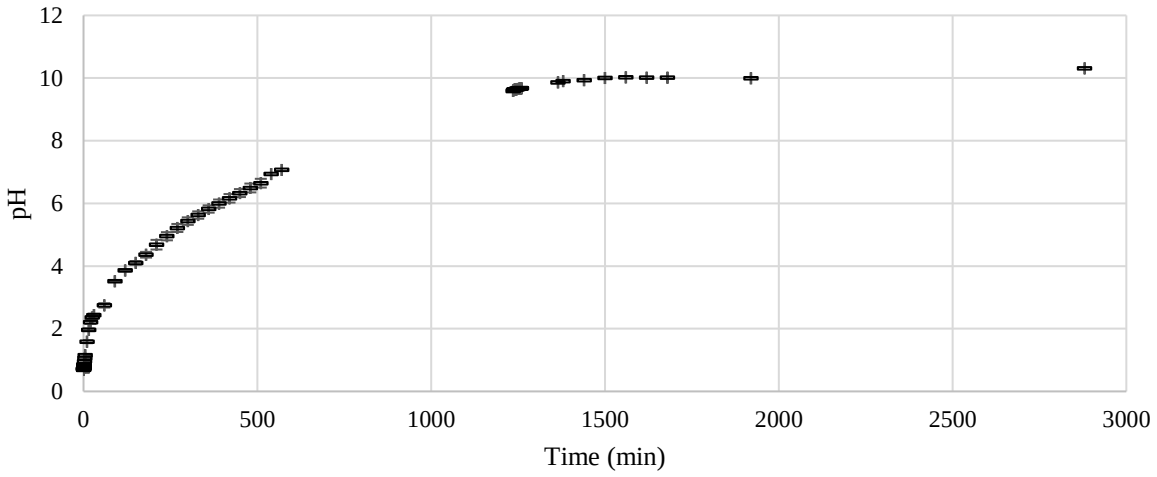


Figure 10-9: pH change over time in 800 mL of AMD in a constantly agitated reactor when 80 g of slag with particle aperture between 2000-3350 microns has been added.

The alkalinity addition corresponding to the last data point collected in the experiment shown in Figure 10-9, was 2897 units of alkalinity as $CaCO_3$ in mg/L.

The dissolution of BOFS in an acidic medium is the main mechanism of pH rise in the system, with the secondary/supporting mechanism being the hydrolysis of the sugarcane bagasse in the biological reactor.

Table 10-10: Oxide content of BOFS used in the experiment

Oxide	wt.%
CaO	41.6
Fe_2O_3	20.5
SiO_2	14.4
MgO	7.2
Al_2O_3	2.8
SO_3	0.4
Loss on ignition (LOI)	5

As shown in Table 10-8 (Section 5: Pilot Scale Plant) and Figure 10-6 (Section 4: Laboratory-Scale Plant), the Mg and Ca concentrations increased within the system, confirming the hydration reaction between the treated AMD and the oxidic compounds within the slag. According to literature, alkalinity

can be generated from BOFS via hydration followed by dissociation of calcium, magnesium and other metal oxides (Gomes *et al.*, 2016). The BOFS obtained directly from Phoenix Slag services was assessed for oxide content and shown to contain 41.6 mass% CaO and 7.2 mass% MgO (shown in Table 10-10) (XRD was performed following the procedure found in Section 3.6. The main components of BOFS were Ca, Fe, Si, Al and Mg oxides and thus Ca and Mg concentrations were primarily used as an indication of dissolution extent, as Fe and Al formed precipitated at the pH levels that were reached in the solutions. The hydration, dissolution and dissociation reactions that bring about alkalinity from CaO and MgO are described by Equation 10-2 to Equation 10-5. The iron oxide and aluminium oxide compounds also undergo dissociation similar to calcium and magnesium oxide. However, as mentioned, these components cannot be measured in the solution as they have already formed insoluble compounds and precipitated due to the pH levels that are reached in the system.

$$CaO + H_2O \leftrightarrow Ca(OH)_2$$

Equation 10-2

$$Ca(OH)_2 \leftrightarrow Ca^{2+} + 2OH^-$$

Equation 10-3

$$MgO + H_2O \leftrightarrow Mg(OH)_2$$

Equation 10-4

$$Mg(OH)_2 \leftrightarrow Mg^{2+} + 2OH^-$$

Equation 10-5

The concentrations of H^+ ions (obtained from pH measurements in the media) over time were also used to study the dissolution kinetics (using Equation 10-6). $[H^+]$ was used as this was representative of the dissolution of all oxidic compounds in the slag, regardless of pH.

$$[H^+] = 10^{-pH}$$

Equation 10-6

10.5.3.2Chemisorption Behaviour

Equation 10-7 to Equation 10-11 show the Lagergren pseudo-1st order, pseudo-2nd order models, and shrinking core diffusion through liquid film, diffusion through the ash layer and chemical reaction models that were applied and evaluated to the experimental data, respectively. It should be noted that (i) agitation was used in the batch experiments which reduced the liquid film layer diffusion limitations and (ii) BOFS dissolution is not limited to only the kinetic models tested in this report.

$$\ln\left(\frac{C_t - C_e}{C_o - C_e}\right) = -k_{1,obs}t$$

Equation 10-7

$$\frac{1}{C_o - C_e} - \frac{1}{C_t - C_e} = k_{2,obs}$$

Equation 10-8

$$k_f t = X$$

Equation 10-9

$$k_d t = 1 - 3(1 - X)^{0.67} + 2(1 - X)$$

Equation 10-10

$$k_r t = 1 - (1 - X)^{0.33}$$

Equation 10-11

It was observed that the chemical reaction model did not apply to the water and the AMD dissolution cases. Diffusion through the ash layer was found to apply best to water for Ca (all size classes) and Mg (size class 3) release from the BOFS. [H^+] kinetics were used to represent the experiment and a pseudo-1st order Lagergren model was seen to apply more often. The larger particle sizes underwent a lower rate of dissolution than the smaller particle sizes of BOFS. This can be seen in the pH data obtained over time for dissolution of different particle sizes shown in Figure 10-10.

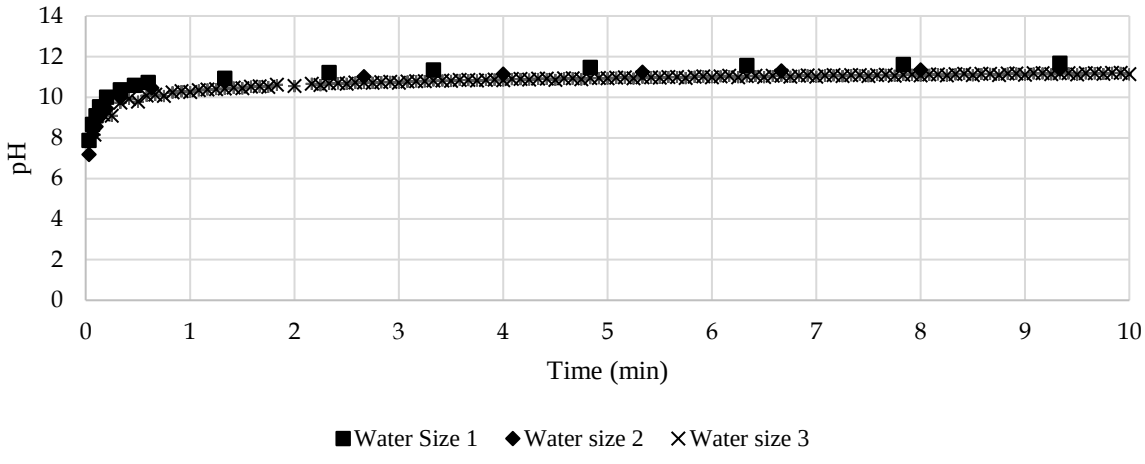


Figure 10-10: pH in water solutions during dissolution of BOFS of different particle sizes

10.5.3.3Alkalinity

The alkalinity and acidity of water, HCl and AMD were measured before and after reaction with BOFS of size class 1 (diameter from 2 mm to 3.35 mm) using titration methods. The total alkalinity and acidity calculated is summarized in Figure 10-11.

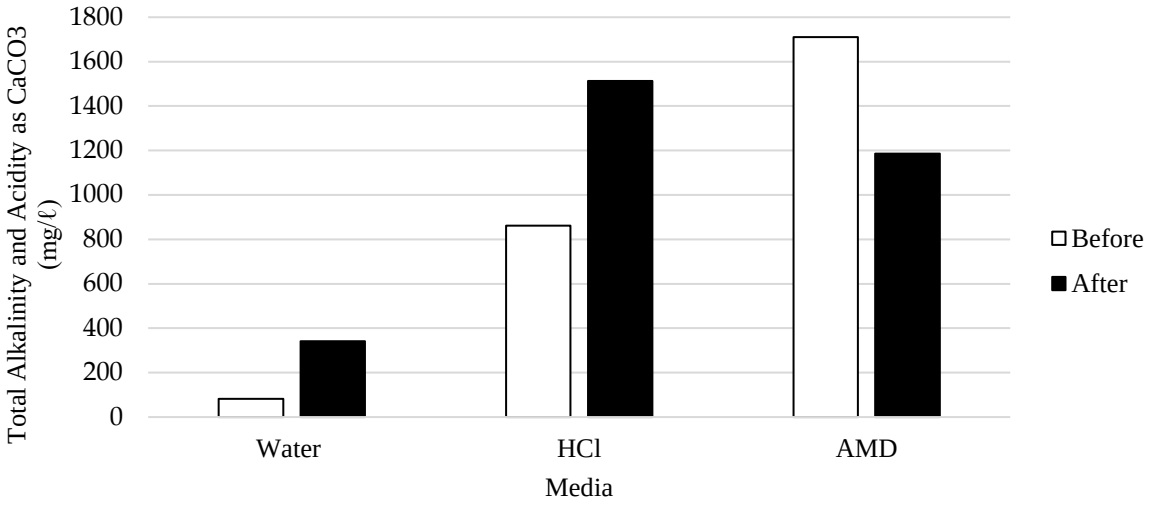


Figure 10-11: Total acidity in 800 mL of water, HCl and AMD solutions before reaction with 80 g of BOFS total alkalinity after as $CaCO_3$

As shown in Figure 10-11, the acidity in water before the BOFS reaction and the alkalinity after the BOFS reaction are much lower than the acidity and alkalinity of both acidic media. This indicates that more BOF dissolution occurs in acidic media than in neutral solutions. For application in AMD treatment, this potentially means that AMD should be reacted directly with the slag instead of using a recycle stream (as used in the laboratory and pilot-scale systems). Paradoxically, armouring of BOFS particles, which is due to precipitation of various compounds that form during neutralization reactions, prevents the direct contact between AMD and BOFS. This was observed during SEM testing.

10.5.3.4BOFS Surface Morphology

The layer of precipitation that formed on the surface of the BOFS reactor is shown in Figure 10-12. SEM images of the particles before and after reaction with water, HCl and AMD were obtained and are shown in Figure 10-13. The slag leached by water and the untreated BOFS look similar, with slightly more porosity being seen in the water leached slag.

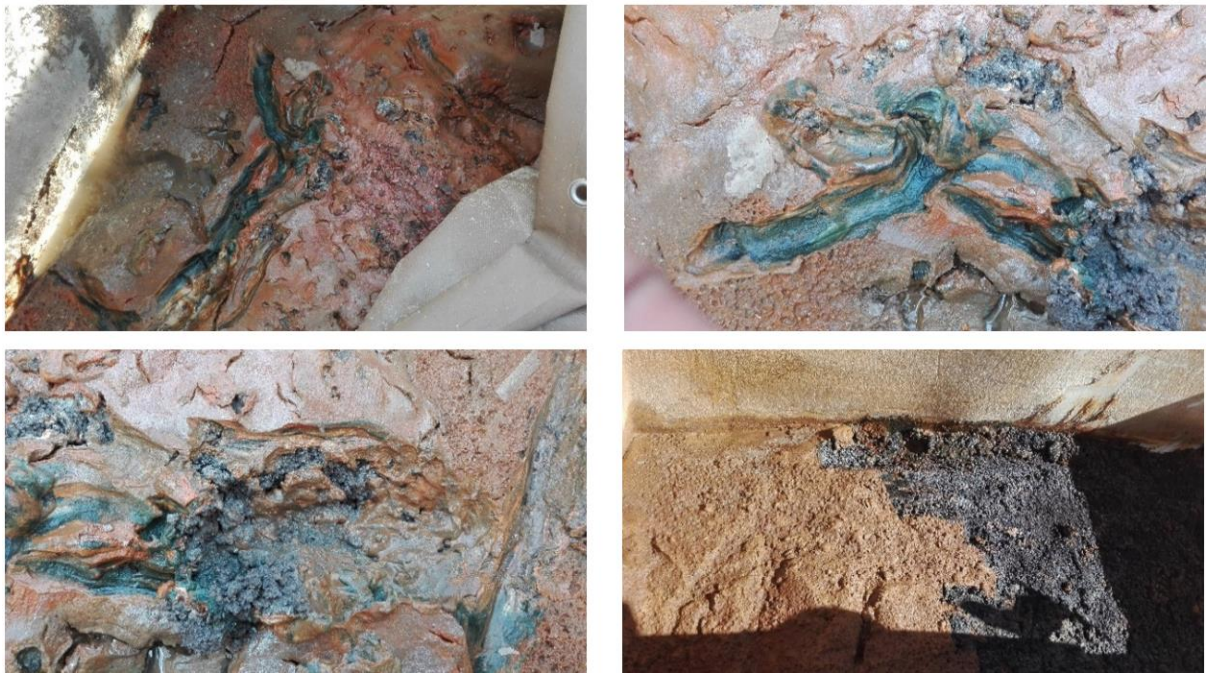


Figure 10-12: Precipitation layer on top of the BOFS in the BOFS reactor

The particles leached in HCl ((v) and (vi)) display more precipitation spots (shown by the lighter colour) and the AMD particle (iii) appears to be coated in a distinct layer identified as gypsum. It is evident that a coating of precipitates formed on the surface of the BOFS particles which were reacted with acidic media. This coating or armouring of the BOFS particles was observed in the continuous process and had a significant impact on the accessibility of the slag to react with the AMD. An agitated system could be used to prevent settling of the precipitate – in this case a recycle stream would be rendered null.

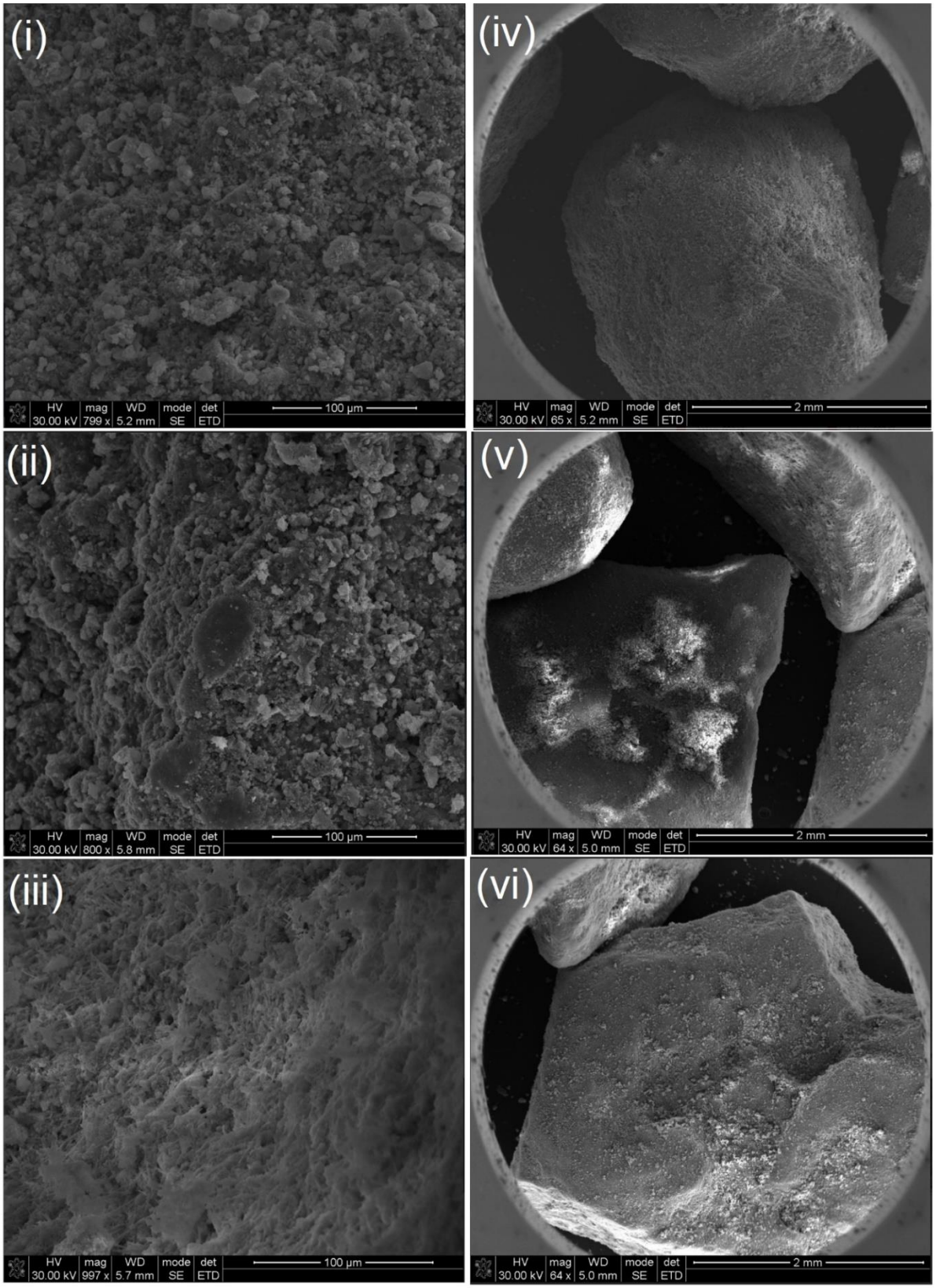


Figure 10-13: SEM images of (i) and (iv) unreacted BOFS; (ii) water leached BOFS; (iii) AMD leached BOFS; (v) and (vi) HCl leached BOFS

10.5.3.5BOFS Dissolution in Pilot and Laboratory Scale Operation

During the operation of both the laboratory and pilot-scale plants, it was observed that the pH of the system was the variable that the concentrations of metals and sulfates were dependent on. The pH, in turn, was dependent on the rate of dissolution of the BOFS.

BOFS dissolution was thus deemed the limiting factor and efforts were made to increase it by (i) increasing the amount of BOFS used, (ii) decreasing the particle sizes used and (iii) changing the reactor type from packed bed reactor (PBR) to a continuously stirred or agitated reactor (CSR). Each of these changes yielded positive results in that the rate of dissolution increased and more AMD could be treated per unit time.

In the pilot-scale system, it was noted that the calcium concentration increased with pH – an indication that the dissolution of CaO contributed to the rise in pH. Other elements (Al, Fe and even Mg) could not be assessed, as all these elements formed insoluble compounds at the pH levels that were reached. The normalised (to 100%) removal or increase in concentration through leaching from the slag is shown in Figure 10-14.

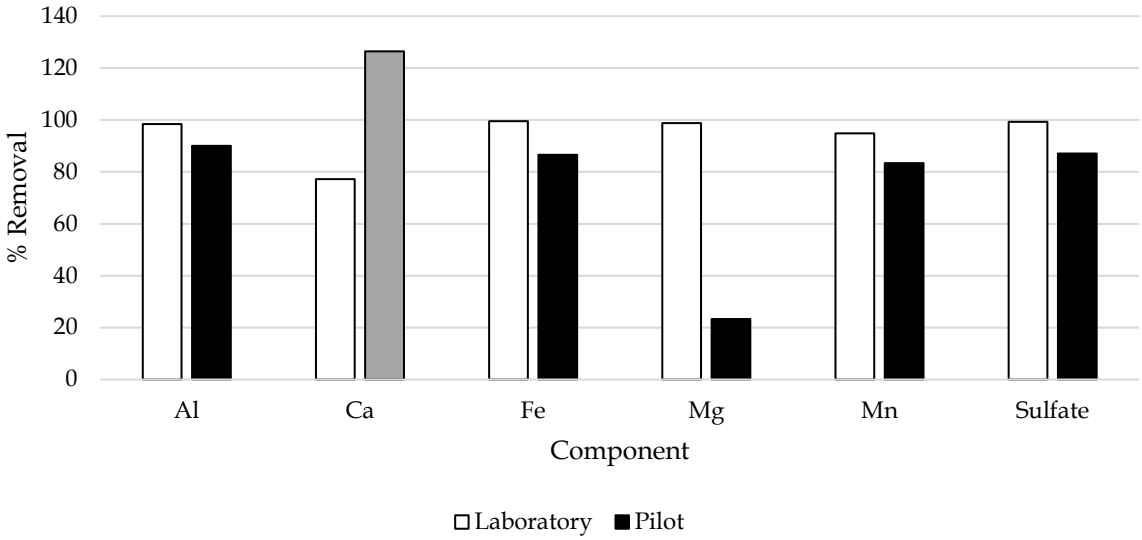


Figure 10-14: Removal (%) of Al, Ca, Fe, Mg, Mn and Sulfate across the laboratory and pilot-scale systems with Ca exhibiting an increase in the pilot-scale system (shown in grey)

As seen, the Ca concentration increased by 126% in the pilot-scale system yet decreased in the laboratory scale system. This was expected as the ratio of BOFS to AMD in the pilot scale system was much higher than that of the laboratory scale system. This ratio was changed to decrease the limiting reagent behaviour of the BOFS dissolution - the BOFS was present in excess in the pilot-scale plant whereas in the laboratory plant it was a limiting reagent. The Mg removal was also much lower in the pilot-scale and again this was due to the presence of excess BOFS as well as the low pH levels in the pilot-scale that did not cause Mg to form insoluble precipitates. Apart from the Ca and Mg, the pilot

scale and laboratory processes functioned comparably.

According to the data obtained from the laboratory and pilot-scale systems, the treatment scheme designed to remediate AMD using BOFS and sugarcane bagasse were effective and a significant improvement in the quality of the polluted water, as well as a substantial dissolution of oxides into the solution from the BOFS, was found. BOFS was effective in raising the pH of the AMD, as well as the other media (HCl, water), to ranges between 10 and 12, however the increase in alkalinity of the media was dependent on the initial acidity of the solution – the pH rise occurred fastest in water, however, greater release of alkaline elements were achieved in more acidic media. The Lagergren kinetic model presented a more accurate fit of the data than the shrinking core model, with the pseudo-first-order model seeming to better apply to acidic media using $[H^+]$ decrease and the pseudo-second-order model found to apply better to a neutral solution. Assessing the dissolution of Mg and Ca oxides individually, showed converse results, with dissolution in acidic media fitting the pseudo-second-order model better and dissolution in neutral media fitting the pseudo-first-order model better.

Shrinking core model fits were achieved in certain cases, though more accuracy in model fitting can be achieved by factoring in other variables that influence kinetics (such as temperature and pressure). The kinetic rate constants were estimated from the batch tests done, however, pH dependency was not considered in this study. By using pH buffered solutions the primary mineral kinetics may be estimated with more accuracy (Windt et al., 2011). The higher dissolution rate being found in acidic media than in water can be seen in Figure 10-15, where the concentration of Ca and Mg ions in solution are much higher in AMD than in water after being reacted with BOFS at the same conditions for the same period of time.

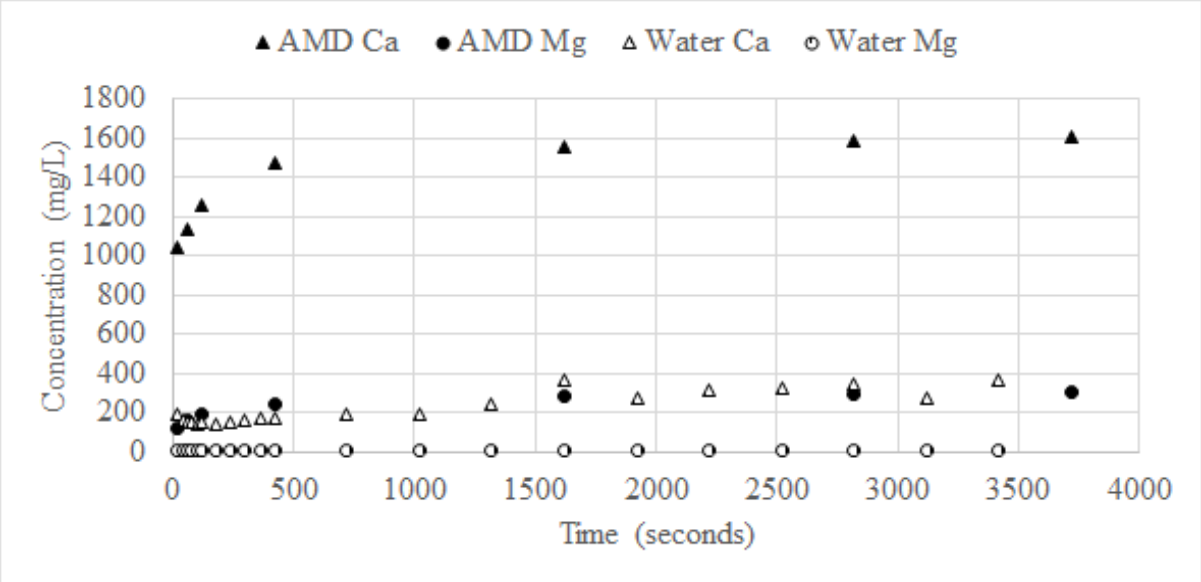


Figure 10-15: Concentrations of Mg and Ca ions in water and AMD solutions that are reacted with slag fines in a CSTR

This corresponds to the findings from alkalinity measurements taken in water, AMD and HCl media after reaction with BOFS for a period of time (Figure 10-11). The pH in each of the systems were different (the pH in the water system was the highest, followed by HCl and then AMD) after the same reaction time with the same mass of BOFS and the alkalinity readings indicate that although a lower pH is recorded in the acidic media, the solutions have a higher alkalinity than that of water. This explains the large amount of water (recycle stream) that is needed to neutralize the AMD. These observations support and explain the findings from the laboratory scale set-up which indicated that a lower recycle rate was maintained when fine particles of BOFS were stirred into the AMD. It indicates that dosing may be a less energy intensive option to using large particle sizes and a recycle stream.

10.5.4 Mechanism of Sulfate and Metal Removal

Sulfate and metals were removed from the system via precipitation reactions followed by sedimentation that occurs under the action of gravity. Due to the relatively low concentrations of sulfide that were found in the biological reactors (shown in Chapter 4) as well as the high flowrates through the plant (low residence times), SRB functioning likely did not solely account for the sulfate removal over the biological reactors. The main sulfate removal mechanism was through precipitation via pH rise and this may have continued through the biological reactors. The precipitation reactions that could have occurred are discussed below.

10.5.4.1Aluminium

The initial concentration of aluminium in the AMD (Type A) was 434 mg/L. Aluminium in acidic media most commonly forms an aqueous cation, with an oxidation number of +3 (Harding, Johnson and Janes, 2002). Addition of an alkaline material (which will hydrate and dissociate to form hydroxide units) to the solution, will first precipitate an insoluble aluminium hydroxide (by Equation 10-12):

$$Al^{3+}(aq) + 3OH^{-}(aq) = Al(OH)_3(s)$$

Equation 10-12

This was considered the main mechanism of aluminium removal in the system. It is important to note that both aluminium oxide and hydroxide species are amphoteric in nature. In acidic solutions, they will dissolve and assist with neutralizing the acid (by Equation 10-13):

$$Al(OH)_3(s) + 3H^{+}(aq) = Al^{3+}(aq) + 3H_2O(l)$$

Equation 10-13

Excess hydroxide units in the solution could also cause the aluminium hydroxide to form a tetrahydroxyaluminium ion via Equation 10-14:

$$Al(OH)_3(s) + OH^-(aq) = [Al(OH)_4]^-(aq)$$

Equation 10-14

Aluminium sulfate or sulfide could also potentially form as there is an excess of sulfate ions in the AMD. However, aluminium sulfate has a very high K_{sp} (69.2) which means it will not precipitate. Similarly, aluminium sulfide, also with a very high K_{sp} is rapidly hydrolysed in an aqueous solution to form aluminium hydroxide and hydrogen sulfide gas – thus it is unlikely that removal of aluminium occurred in this manner. Aluminium was removed from the solution almost completely (to a concentration of 10.7 mg/L) at a pH of 3.8 and redissolution did not occur even at a pH level of 9.

10.5.4.2Calcium and Magnesium

Calcium and magnesium were present in the AMD at a concentration of 110 mg/L and 115 mg/L respectively. Calcium (as well as magnesium) was also added to the solution through the dissolution (hydration and dissociation) of the BOFS. Calcium and magnesium in aqueous solutions are found in the form of a positive cation with an oxidation number of 2+. Both calcium oxide and calcium hydroxide have an intermediate solubility in water and calcium will not precipitate out of solution as either of these species. Calcium sulfate has a higher Ksp than calcium hydroxide (experimentally exhibiting a solubility of 0.274% w/w compared to calcium hydroxide which exhibited a solubility of 0.12% w/w in water at 20 ° C (Royal Society of Chemistry, 2020)), however due to the saturation of the solution with sulfates (initial Type A AMD concentration of 12955 mg/L) and the reaction of the hydroxyl group with multiple other elements – the bulk of the calcium removal is achieved via gypsum precipitation. Despite the precipitation of calcium sulfate, the calcium concentration increased in the system with increasing pH.

When the BOFS comes into contact with liquid, hydration will take place and calcium hydroxide will form. If this hydrated BOFS is then exposed to air, carbon dioxide will react with this to form calcium carbonate (by Equation 10-15) which has a low solubility in water:

$$Ca(OH)_2\,(aq) + CO_2\,(g) = CaCO_3\,(s) + H_2O\,(l)$$

Equation 10-15

The pH raising capacity of the BOFS in neutral solutions will thus be lowered if this occurs, however further reaction with an acidic media can result in the formation of carbon dioxide and water (Equation 10-16):

$$CaCO_3\,(s) + 2H^+\,(aq) = Ca^{2+}\,(aq) + CO_2\,(g) + H_2O\,(l)$$

Equation 10-16

It is thus recommended to keep the BOFS dry before use as a reagent, and once it is in use keep the particles submerged. Magnesium is most likely removed from the solution in the form of magnesium

sulfate (which has a solubility of 33.7% w/w in water) and magnesium hydroxide (which is soluble in acidic solutions but less so in basic solutions (Royal Society of Chemistry, 2020)). Magnesium decreased in solution at a pH of 9 (to a concentration of 61.7 mg/L).

10.5.4.3Iron

Under acidic conditions, the most stable oxidation state of iron is 2+. If the AMD is aerated then the redox potential of the water is such that it allows for oxidation of the ferrous iron (2+) contained in the solution to ferric iron (3+) which can then precipitate as iron hydroxide, $Fe(OH)_3$ via reactions described by Equation 10-17 and Equation 10-18 (Silver, 2012).

$$4Fe^{2+}\,(aq) + 3O_2\,(g) + 2H^{+}(aq) = 2Fe^{3+}\,(aq) + H_2O\,(l)$$

Equation 10-17

$$Fe^{3+}\,(aq) + 3OH^{-}\,(aq) = 2Fe(OH)_3\,(s)$$

Equation 10-18

Fe^{3+} has a low solubility at certain pH levels and generally precipitates out of solution. In the case that the system is anaerobic and if excess CO_3^{2-} is available in the solution (as may be the case if BOFS is hydrated and then exposed to air) the $Fe(HCO_3)_2$ salt is formed. Upon exposure to air this leads to the formation of FeCO3 and then to iron (III) oxide. During experiments, iron was almost completely removed at a pH of 7 (from an initial concentration of 3039 mg/L to 0.289 mg/L).

10.5.4.4Manganese

Under acidic conditions, the most stable oxidation state of manganese is 2+. In this reduced (Mn^{2+}) state, manganese is moderately soluble in the form of $MnSO_4$ and thus very little Mn removal is attributed to $MnSO_4$ formation and precipitation. At pH levels of 8 and above, manganese can precipitate as $MnCO_3$ and $Mn(OH)_2$. In aerated systems (under oxidizing conditions), Mn in the 3+ and 4+ can also form MnO_2, Mn_2O_3 and Mn_3O_4 even at lower pH levels – compounds which are all insoluble in water. It should be noted that is iron (II) is present in solution manganese will not precipitate at neutral conditions. Manganese in the system decreased from 88 mg/L to 52 mg/L at a pH level between 6 and 9. It should be noted that initially manganese increased in the system – this could be attributed to dissolution of manganese containing compounds in the BOFS (XRF analysis shows MN makes up 3% by weight of BOFS).

10.5.4.5Sulfate

Sulfate in the system is likely to form any of the compounds found in Table 10-11. The most likely way that sulfate is removed is via the precipitation of calcium sulfate.

Table 10-11: Solubility of sulfate compounds % weight/weight in water at 25° C

Compound	% weight/weight in water at 25° C
Magnesium Sulfate	33.7
Manganese (II) Sulfate	62.9
Iron (II) Sulfate	26.3
Calcium Sulfate	0.274
Iron (III) Sulfate	Slightly soluble
Aluminium Sulfate	36.4

The counterions which form part of the sulfate compounds which are presented in Table 10-11 (predominantly Calcium and Magnesium) become abundantly available in the solution through the dissolution and leaching of the BOFS. Once present in solution they can then bind with the sulfate ion to form a nearly insoluble product. The solubility of each sulfate compound of note (compounds which have been identified in the sample) is shown in Table 10-11, however it is likely that a small percentage of sulfate is also removed via formation and settling of small amounts of other compounds. The sulfate in the system was shown to decrease to a final level of 269 mg/L at a pH of 11.4 (after BOFS leaching and dissolution).

10.5.4.6Sediment/precipitate formed

An SEM was used on the precipitate which had formed on the surface of the BOFS particle. This precipitate is shown in Figure 10-16. An EDA was also performed on the sample.

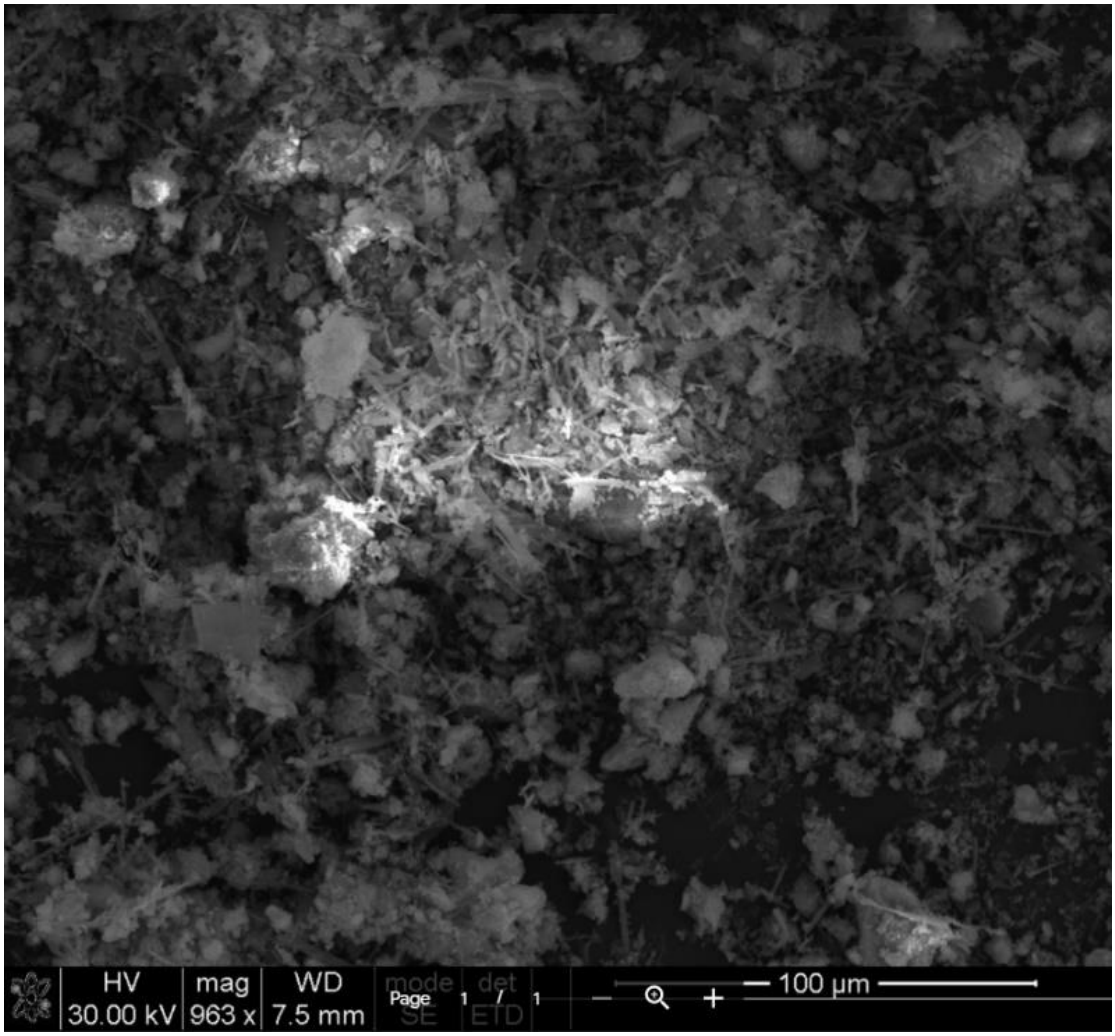


Figure 10-16: SEM of precipitate formed after reaction of BOFS and AMD for a period of 32 hours.

The results from the SEM and AAS run on the acidified precipitate, showed that aluminium, calcium, iron, magnesium, manganese, and silicate had all precipitated. The SEM and EDA were able to identify oxides and silicates but not sulfates or hydroxides, however it is likely (given the chemistry of the AMD solution and the difference in initial concentration and pH and final concentration and pH) that the majority of precipitates formed were sulfates and hydroxides.

10.5.5 Process Control Mechanism

Multiple process control configurations were tested on the system to ascertain which control mechanism best allowed the process to maintain a constant, desired pH. The diagrams (Figure 10-17 and Figure 10-18) show the different configurations that were tested, where pHT denotes the position of the pH transmitter and pHC denotes the position of the pH controller.

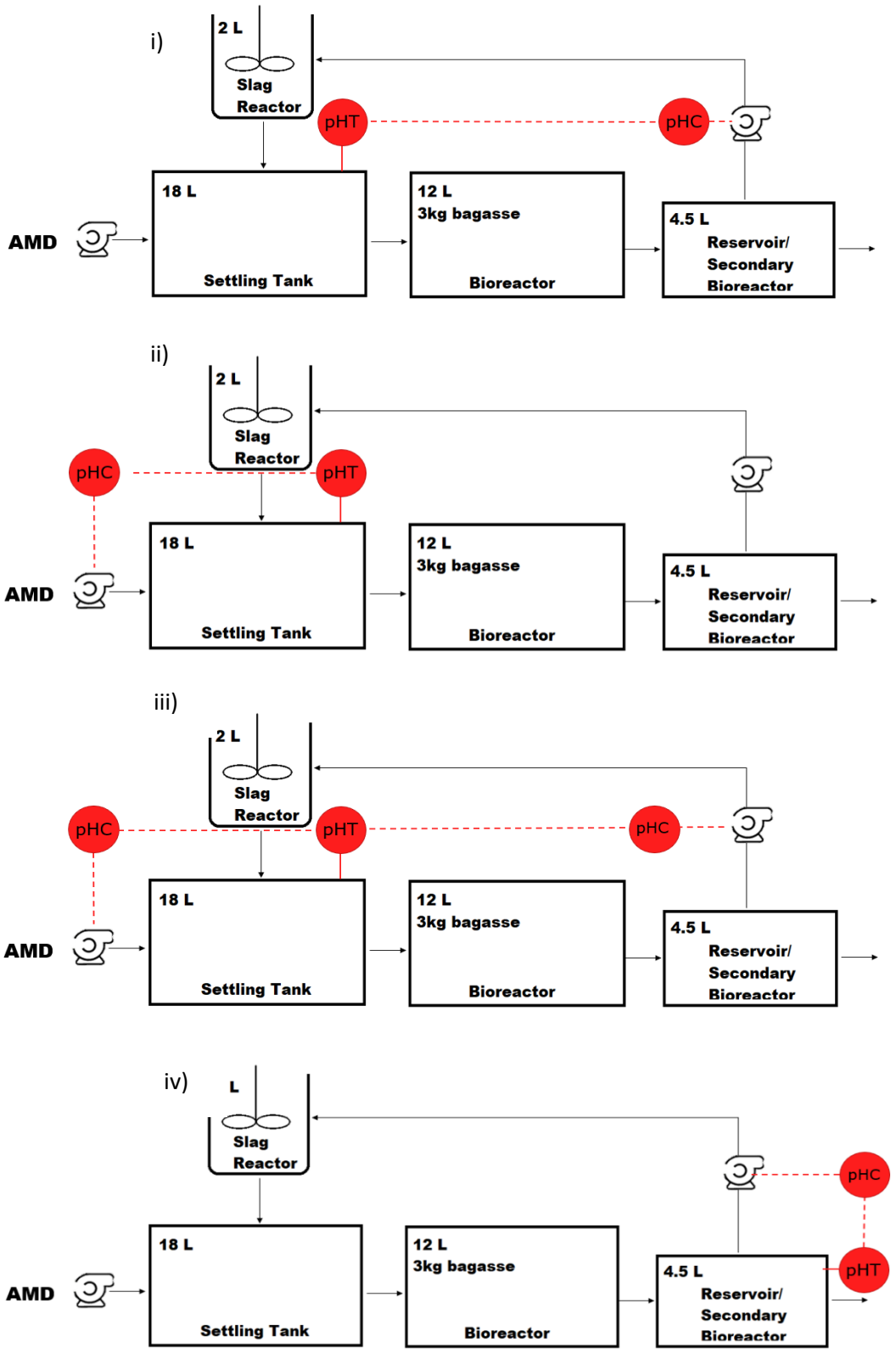


Figure 10-17: (i) Process control with recycle flowrate controlled using the pH in the settling tank; (ii) Process control with the AMD flowrate controlled using the pH in the settling tank; (iii) Process control with both the AMD and recycle flowrates being controlled using the pH in the settling tank; (iv) Process control with recycle flowrate controlled using the pH in the secondary bioreactor

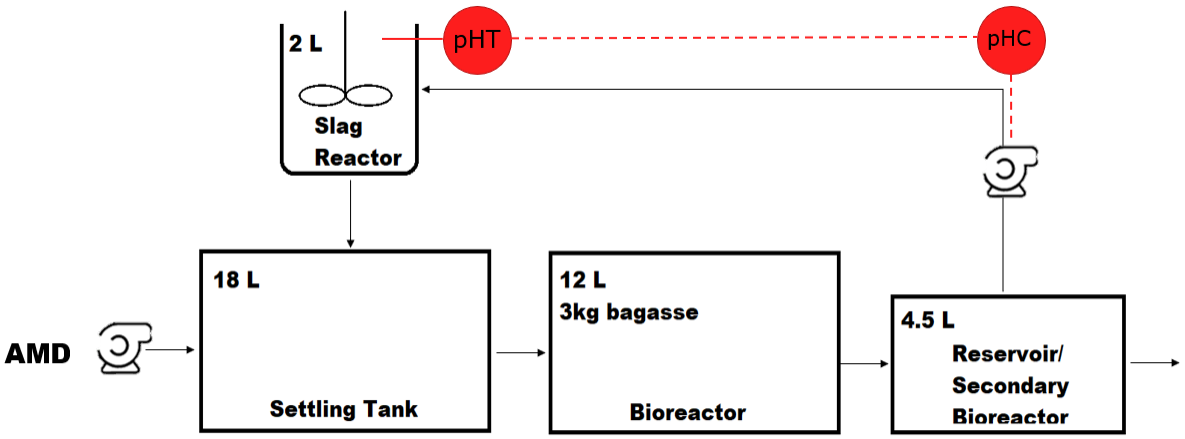


Figure 10-18: Process control with the recycle flowrate controlled using the pH setpoint in the slag reactor

The configuration shown in Figure 10-18 functioned the best with regards to maintaining a constant pH in the specified vessel. In addition to this, a proportional only control scheme was suitable for the pH control when this configuration was used. Proportional control does not incorporate integral or derivative control and makes it marginally easier to configure. The recycle flowrate (which was linked to the AMD flowrate) could also be maintained at a fairly constant rate when a proper dosing schedule was followed.

10.6 Proposed Design for Scale Up

10.6.1 Introduction

Using the data and findings obtained from the studies conducted and discussed in Chapters 2 – 5, a design for a larger scale plant is proposed in this section. The design is a general proposal for a plant that will treat more than 1000 L/day and less than 10 000 L/day of AMD with a quality similar to that found at site (Type A AMD). Some design elements have not been changed due to seamless functioning of these sections of the plant in the laboratory and pilot scale trials, but all reactors and vessels are discussed in detail. In some instances, a technical design is not proposed and a descriptive design is provided instead. A simple schematic of the proposed design is shown in Figure 10-21. The process control philosophy for the proposed plant is also discussed in this section. The design is proposed to be modular, as the treated water from each vessel has reuse avenues, and thus the mine or site in question may need to only deploy part of the treatment program to achieve the desired treatment extent.

10.6.2 Settling Tank

The initial settling tank designs did not display any issues during the operation of the laboratory or pilot scale plants; thus, the design of this section can remain largely the same. There are some design considerations to consider, and these are discussed.

10.6.2.1Primary settling tank(s)

The rectangular tanks that were used during the pilot study functioned well, however for the larger scale design a circular settling tank is proposed due to the lower frequency of maintenance and ease of sludge removal found when using this type of settler. The main considerations of a circular sedimentation/settling tanks (method of introducing flow, energy dissipation, flow distribution and sludge removal) are discussed:

10.6.3 Method of introducing flow

If a circular tank is used, the AMD and slag eluent mixture must be introduced in the centre of the tank (Tchobanoglous *et al.*, 2014). Periphery addition is sometimes used but primary settling tanks generally favour the centre tank addition design. The pipe used to transport the water to the centre of the tank can be (i) suspended from a bridge above the reactor or (ii) fixed in place beneath the reactor floor. It is suggested that the feed pipe enters the settler from the bottom as this nullifies the need for large energy dissipation devices (discussed in 7.2.1.2). The proposed vessel set-up is shown in Figure 10-19.

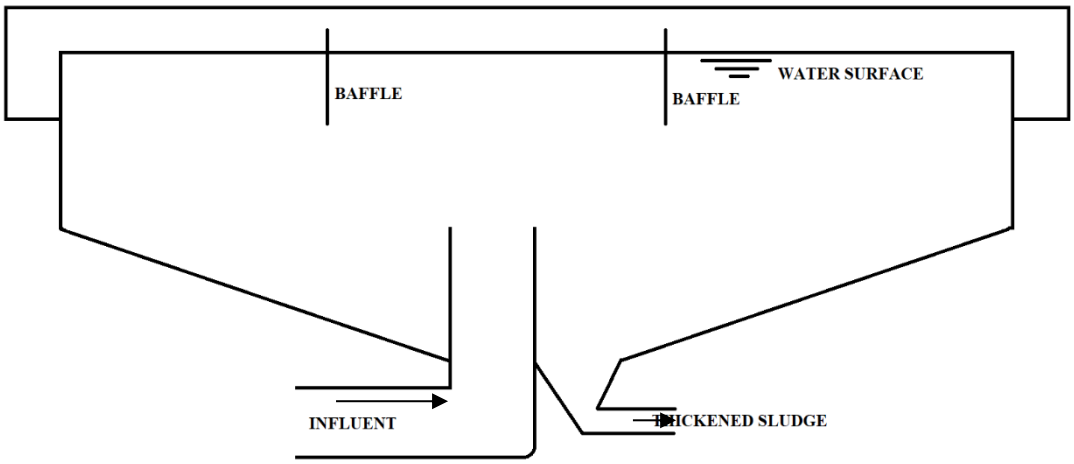


Figure 10-19: Basic design of the proposed settling vessel

10.6.4 Energy dissipation and flow distribution

An energy-dissipating device would have to be used in conjunction with the centre tank addition design when water is added from above the reactor. This design will allow the settling tank to receive influent from the centre column and discharge it tangentially into the top section of the settling tank. It is also proposed to include baffles in the construction of the primary settler in order to direct the flow of the clarified water (this is shown in Figure 10-19).

10.6.5 Sludge removal

In order to facilitate sludge removal, the bottom of the circular settling tank needs to be sloped to form an inverted cone structure. The solids that form and settle at the bottom of the tank can be scraped or can flow to a small hopper located at the bottom of the tank in the centre. To minimize the cost of sludge removal, an airlift pump can be used periodically to remove the sludge contained in the hopper.

Findings from the assessment of the sludge in the primary settling tanks from the laboratory and pilot scale studies indicated that a significant amount of alkalinity remains in the sedimentation layer or sludge blanket and this could be used as an additional pH raising reagent. If this sludge is recycled back into the settling tank or slag reactor before being removed, further reaction between BOFS particles and AMD can occur, reducing the amount of fresh slag needed during replacement. The recycling can be facilitated by a sludge outlet stream that leads either directly to the slag reactor or to a rotary vane feeder which will dose the slag reactor.

10.6.6 Sizing

Using the same design principle as followed for the pilot scale plant (scaling up), the area needed for the settling tank (to facilitate settling for a flowrate of 10 000 L/day) is 48.2 m^2 (the surface area for the pilot plant was 4.82 m^2). It is thus proposed that 5 settling tanks each with a diameter of 3.6 m be used for the larger design. The allowable detention time in a settling tank is usually < 8 hours, however the

pilot scale which had detention time of > 8 hours functioned well in terms of settling, thus a height of 1 m is deemed acceptable for the settling vessels.

10.6.7 Secondary settling tank

A rectangular tank was also used for the secondary settler to both facilitate further sulfate reduction and to remove any remaining metal sulfides or biological matter that had formed in the biological section of the plant. This vessel was tested at laboratory and pilot scale and the removal capacity was comparatively low, with the concentration of some ions increasing in the system instead of decreasing. For this reason, a secondary settler is deemed unnecessary for the application of the design. However, should secondary filtration be required (this will be based on the quality of the effluent needed) it is recommended that a packed bed filter or a high-pressure sand filter is used.

10.6.8 Packed bed filter

This filter will make use of a packing material to remove biological components from the treatment scheme by means of the formation of a biofilm on the packing material of choice. Research done on the BOFS indicates that it contains small amount of chromium and nickel that may act as an anti-microbial substance. If a packed bed filter is used as a form of removal of biological matter from the outlet stream, it is suggested that BOFS be used as part of the packing material.

10.6.9 BOF Slag Reactor

There were multiple issues relating to the BOFS reactor that were experienced during the laboratory and pilot scale studies – the main issue being that of mass transfer between the BOFS and the treated water. It was discovered that treated water which had a significantly lower acidity and higher pH than untreated AMD, was not as effective at dissolving the BOFS as raw AMD was. This caused the ratio between the recycle stream and the feed stream to be very high (high recycle compared to a low AMD inlet). When AMD was added directly to the slag, the alkalinity release and dissolution occurred much faster and to a higher degree. The pH of the AMD thus rose higher and more quickly than when AMD was mixed in the settling tank with slag eluent. Adding AMD directly to the slag, however, introduced the armouring and precipitation problem, whereby precipitation that formed either coated the slag particles, significantly lowering or preventing further dissolution, or formed a thick layer or precipitate/sedimentation on the surface of the BOFS bed, again preventing access to fresh BOFS. When AMD was added directly to the slag, then an agitated system was needed to keep the precipitated metal salts suspended in solution until it the liquid reached the settling tank. For the purposes of the upscale design, a continuously mixed reactor is proposed. The other option (a packed bed reactor) is also discussed briefly.

10.6.9.1Continuously mixed or stirred tank reactor

An abrasion resistant tank fitted with a rubber coated stirrer will need to be used for this application. AMD will be pumped into this tank at a fixed rate with the addition of fine BOFS being controlled via

pH control of the CSTR or the settling tank. The addition of the slag will be facilitated by a rotary vane feeder. The fines used will need to be less than 0.8 mm in diameter which will ensure that these particles remain suspended in the solution and do not settle in the reactor. During laboratory scale operation it was found that the particles sized between 0.8 and 1 mm settled in the CSTR. Using this option will give more control of operation and easier materials handling. The recycle stream will also be rendered null in this instance.

10.6.9.1.1 Sizing

It must be noted that sizing of this reactor may change with changes in site (AMD quality and BOFS particle size), different treatment requirements (composition of outlet stream) and modularity of the plant (whether or not the process includes all three process vessels – BOFS chamber, settling tank and DSR chamber). For application at the AMD tailings dam site – treating AMD with all processes (BOFS, settling and DSR chambers) – the sizing is done according to the results from lab experimentation.

During experimentation, 1 g of BOFS (aperture size between 2000 and 3350 μm) was required to increase the pH of AMD to 7 in 540 minutes. The size of this reactor would thus need to be 3750 L to facilitate the treatment of 10000 L/day with a dosing rate of 694.44 g/min or 1000 kg per day. This dosing schedule must be followed when no sludge recycling is done.

10.6.9.2Packed bed reactor

The alternative would be to use a PBR packed with larger sized particles and containing no fines. This option will require a slag replacement schedule and a recycle stream as AMD will not be pumped directly into this chamber. If this option is used, it is recommended that an additional CSTR is used to stir the AMD into the slag eluent before it enters the settling tank to promote further reaction between the BOFS eluent and the AMD.

10.6.9.2.1 Sizing

In the case where a PBR is chosen as the BOFS reactor, the reactor will have to be constructed in a modular fashion to allow for removal and replacement of the slag at intervals. The reaction time allowed will dictate the size of the reactor – lower reaction times will mean a larger reactor. It should also be noted that as the “free lime” or accessible oxides at the surface of the BOFS particles get consumed, the reaction time will increase.

Taking this into account, 3 reactors each 2000 L in volume, containing 2000 kg each of BOFS (aperture size between 2000 and 3350 μm) are proposed for this larger scale design. The BOFS should be placed in permeable bags (500 kg) or crates that can be lifted via crane. This sizing mimics the pilot scale design, but contains more BOFS of a larger particle size, and allows for a maintenance/replacement schedule.

10.6.9.3High density sludge process

Sludge recycling (discussed in the settling tank section (7.2.1)) may necessitate the use of a high-density sludge (HDS) process. This process incorporates two additional vessels aimed at maximizing the use of the BOFS before disposal. In this process the sludge which is extracted from the settling tank must be added to a vessel which contains fresh BOFS. This forces contact between the solids and promotes coagulation of fresh BOFS particles onto the recycled precipitates and unreacted BOFS particles – (the fact that the fresh and recycled particles are combined will force the precipitation reactions to occur on the surface of the existing particles, thereby increasing their size and density). This vessel will then lead into the BOFS reactor vessel where AMD can be added and the process can occur normally. A further vessel which is aerated can then also be added to promote oxidation of ferrous iron to ferric iron. A schematic of this system is shown in Figure 10-20.

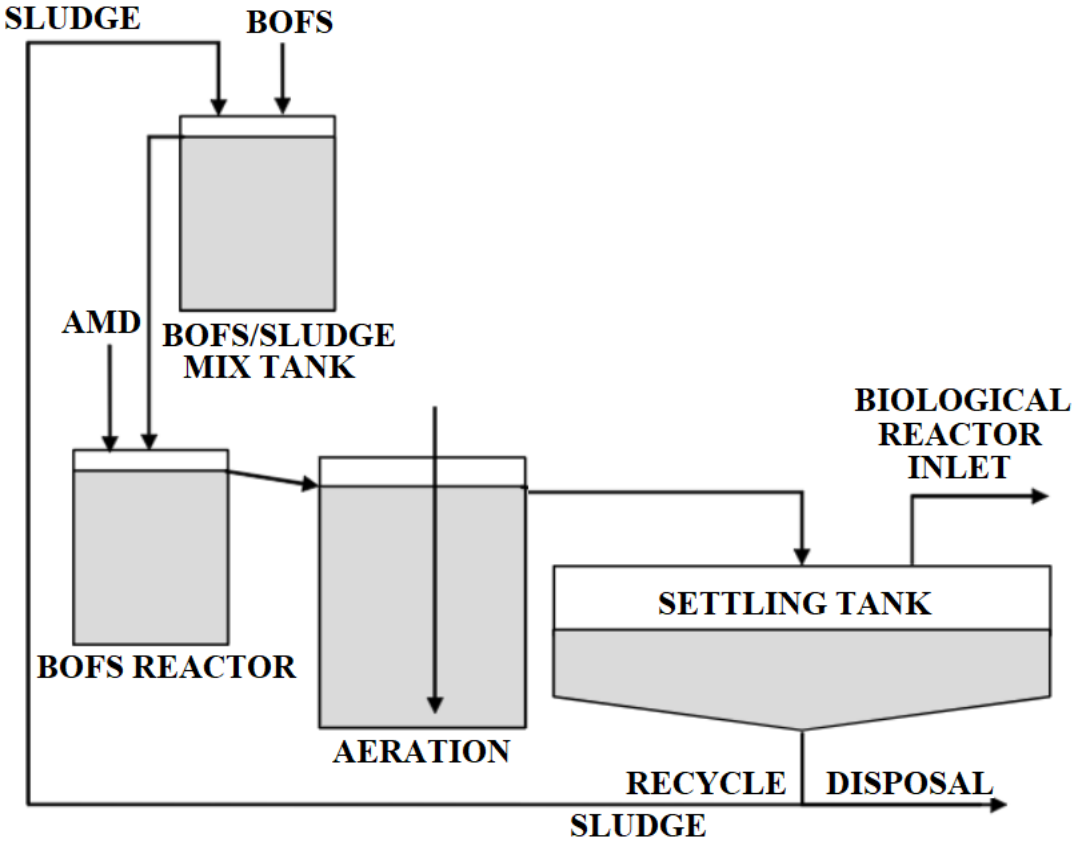


Figure 10-20: Schematic of HDS system with recycle stream proposed to be used in the larger scale design, using BOFS as a lime source

10.6.10Biological Reactors

Biological sulfate reduction may not have been the sole cause of the sulfate removal across the biological reactors, due to (i) low sulfide levels, (ii) high flowrates and (iii) low COD from the available sugarcane bagasse. This was the main issue which was found during the operation of the biological reactors at the laboratory or pilot scales. It is thus recommended that the design for these reactors change

in terms of sizing and amount of bagasse added. These reactors will operate as (i) sealed downflow or up-flow pack bed reactors or (ii) plug flow closed reactors and contain sugarcane bagasse as a packing. The bagasse will have to be replaced at intervals and the spent bagasse can be used as a fuel source or disposed of. The design of the biological section differs from the pilot plant design in that it only contains two reactors. The third reactor has been deemed unnecessary as a sulfate reduction reactor and as a secondary settling vessel. As discussed, a secondary settler or filter can be added easily to the design if the effluent water quality needs to be improved.

A hydrogen sulfide scrubber is still part of the biological reactor design and acts as a precautionary system.

10.6.10.1 Sizing

Approximately 72% of sulfate removal occurred due to pH rise as a result of BOFS dissolution in the pilot scale plant. Using the average AMD concentration of 16301 mg/L, this would mean a further 4564 mg/L of sulfate remained in the solution. In order to lower this to within irrigation water standards (576 mg/L - discussed in Chapter 9 (Rodda, Armitage and Carden, 2014)), a further 3988 mg/L will have to be removed via sulfate reduction in the biological reactors. The maximum COD measured in the biological reactor was 12 g/kg of bagasse, literature however, reports sugarcane bagasse as having 18g of COD/kg of bagasse (Vats, Khan and Ahmad, 2019). Using this value and taking the ratio of COD: sulfate as 0.7:1 - conservatively, 1550 kg of bagasse will be needed daily to treat 10000 L/day of AMD. This will mean a regular replacement schedule. Using a 2-day hydraulic residence time (HRT), the combined volumes of the biological section will need to be 20 000 L. This can be achieved using a modular approach, which will also make replacement of bagasse easier to facilitate.

10.6.11Schematic of Proposed Design

The diagram in Figure 10-21 and Table 10-12 shows a basic representation of the layout of the proposed design. The design is much simpler than both the laboratory and the pilot scale processes and does not incorporate a recycle stream. However, it should be noted that this process can function with the use of a recycle stream in conjunction to a PBR BOFS reactor using large particles of BOFS (as opposed to a continuously stirred reactor using fine particles). If this design is preferred, then the same layout as the pilot plant will be used.

Table 10-12: Description of schematic of upscale design shown in Figure 10-21

Diagram Number	R-101	R-102	R-103	R-104	R-105	P-101	P-102
Element	Slag reactor	Clarifier/Settling Tank	Biological Reactor 1	Biological Reactor 2	Hydrogen Sulfide Scrubber	AMD Pump	Recycle pump (rotary vane pump)

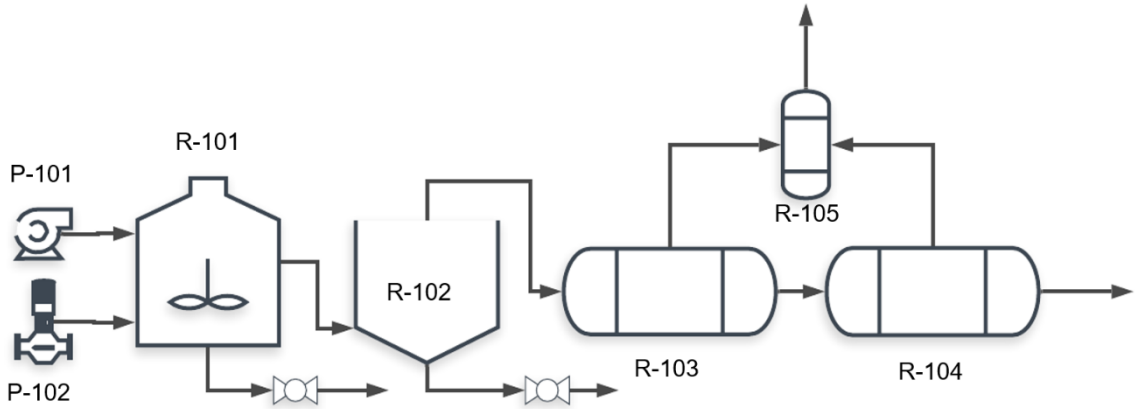


Figure 10-21: Schematic of proposed larger scale (10000 L/day) design

10.6.12Process Control

The mechanism proposed to be used for the process control over the larger system is as follows:

- The pH in the slag reactor will be monitored and transmitted to a programmable logic controller (PLC)
- The PLC will alter the speed of the rotary vane pump used to dose the slag reactor based on the pH chosen as the setpoint and how different the measure pH is to this value.
    - If the pH in the vessel is higher than the setpoint, the speed of the pump will decrease and if the pH is lower than the setpoint, the speed of the pump will increase
- Proportional only control can be used for this set-up.

10.6.13Materials of Construction

Where possible, the equipment must be constructed out of LLDPE or HDPE. If this is not an option, the equipment will need to be rubber lined and coated. The pump used to pump the AMD will have to be peristaltic to ensure no corrosion occurs due to exposure of highly acidic waters over long periods of time.

10.6.14Costing of Reagents

As mentioned in Section 2.1.1, the cost of lime (as dolomite, calcite, gypsum or hydrated lime) ranges between R203 and R533 per 1000 kg (Kalkor, 2021), whereas the price of BOFS (with different particle size ranges) is R146 per 1000 kg (Vermeulen and Phoenix Slag Services, 2018). When using a CSTR with no recycle HDS stream, the cost of reagents per day to treat AMD in this reactor would be R146. This will likely be lower due to the HDS as well as the fact that the waste or by-product generated in this reactor is valuable as an aggregate.

The cost of sugarcane bagasse is reported as approximately R1300/1000 kg (Gralimex Import, 2017). This means that per day, the cost for biological treatment would be R2015.

10.7 Waste Generation, Disposal and Re-use Routes

10.7.1 Avenues for Sludge Re-use

The sludge produced in the system due to pH change and precipitation is rich in sulfates and minerals with a particularly high composition of calcium sulfate, making it ideal for agricultural use. This sludge could be used (i) as a source of calcium and sulfur for plant nutrition, (ii) for improving the quality of acidic soils, (iii) for treating aluminium toxicity (although the sludge does contain aluminium components, the gypsum content may be enough to negate this (Wulff-zottele *et al.*, 2014)), (iv) for improving soil structure, (v) for improving water filtration and (vi) for preventing runoff and erosion. The sludge will also have remnants of the BOFS and multiple studies have shown that BOFS is suitable for soil amendments, treatments and nutrient support (Tsai and Kao, 2009; Goodarzi and Salimi, 2015; Pistocchi *et al.*, 2017).

If sludge is not reused in this manner, it will need to be disposed of or stored in an impoundment. However, it should be noted that if an HDS process is implemented, the amount of sludge (needed to treat larger volumes of water) will be much less due to the recycling of the sludge. This also means the waste sludge will be more chemically stable and contain less leachable components – making waste disposal marginally safer than traditional lime dosing plants (Kuyucak *et al.*, 2012).

10.7.2 Avenues for Water Re-use

The process was designed in such a way that outlet streams from each of the treatment vessels (slag chamber, sedimentation chamber and DSR chamber) can be accessed – i.e. it is a modular system. Thus, depending on the treatment needs of the mine or dam in question, the modules can be replaced, added or omitted as necessary. Each stage in the process achieves a different level of treatment and the outlet from each vessel therefore has different options for reuse. These are discussed below.

10.7.3 Drinking/potable water

According to WHO and South African drinking water standards (Table 10-13) – the quality of water exiting the slag chamber (from the pilot and laboratory scale plants) is not suitable for use as drinking water – thus further treatment is needed before this water is suitable for human consumption. Reverse osmosis, ultra or nanofiltration could be used as further treatment methods for this water. In some instances, mines have water treatment plants on site - however, some streams of AMD are too severely polluted and treatment via the WWTP is not feasible. In these cases, the proposed design/process can be used as a low cost, pre-treatment step before the water enters the established WWTP.

Table 10-13: WHO and SANS 241 drinking water standards compared to quality of slag vessel outlet

Components	WHO Max (mg/L)	SANS 241 (mg/L)	Pilot Plant (outlet from slag vessel) (mg/L)	Laboratory Plant (outlet from slag vessel) (mg/L)
Aluminium	0.2	0.3	0 (Undetected)	4.94
Calcium	2-80	150	401.96	270.14
Iron	0.3	0.3	50	17.66
Magnesium	20	70	425.97	5.37
Manganese	0.5	0.1	143.53	5.79
Sulfate	500	250	2435	109.11
pH	6.5 – 8.5	5-9.7	9.06	11.49

(Mamba, Rietveld and Verberk, 2008; World Health Organization, 2009; Verlicchi and Grillini, 2020)

10.7.4 Irrigation/Agricultural Water

If the outlet water has the same composition as that of the laboratory plant slag vessel outlet, it can be used for irrigation purposes with just a small amount of pH adjustment (from 11.49 to 8.4) (according to the South African irrigation water standards shown in Table 10-14). Using the outlet from the primary DSR vessel may be more suitable for this purpose as the concentrations (with the exception of iron) and pH are all within range.

Producing irrigation water from AMD treatment may be a necessary route to take, considering the lack of water resources in some regions where AMD generation poses a serious environmental problem (Martins *et al.*, 2010). This option for reuse is recommended (above others), as the treated water from the system contains nutrients from the slag and DSR vessels that could aid in crop growth - reducing the need (and associated cost) of fertilizers.

In the case where this system is used for production of water for irrigation purposes, hydraulic residence times will need to be selected to ensure treatment occurs to the acceptable level (complying to maximum recommended values for compounds of interest for waters for irrigation purposes).

Table 10-14: South African irrigation water standards compared to quality of slag vessel and DSR vessel outlet

Components	Maximum range of SA irrigation water standards (mg/L)	Pilot Plant (outlet from slag vessel) (mg/L)	Laboratory Plant (outlet from slag vessel) (mg/L)	Laboratory Plant (outlet from Sedimentation vessel) (mg/L)	Laboratory Plant (outlet from DSR vessel) (mg/L)
Aluminium	20	0 (Undetected)	4.94	9.87	5.74
Calcium	824	401.96	270.14	209.92	123.76
Iron	20	50	17.66	62.76	29.82
Magnesium	225	425.97	5.37	59.47	17.67
Manganese	10	143.53	5.79	10.02	7.34
Sulfate	576	2435	109.11	289.17	213.58
pH	6.5-8.4	9.06	11.49	7.28	7.10

(Rodda, Armitage and Carden, 2014)

10.7.5 Process water

Another option for re-use/use of the treated water is use as process water at the mine site. This would include (Water for Africa, 2009):

- Water used for extraction activities
- Water used for beneficiation activities
- Water used for utility areas
- Water used for waste management or tailings areas
- Water used in general site areas

All these activities or areas at a mining site can make use of process water and potable water is not necessarily needed for these purposes. Thus, the treated water from the system could be used in one of these avenues. The mine site in question would have to stipulate whether the composition and quality of the treated or semi-treated water would be suitable for use in these specific areas. Outlet from the sedimentation vessel can also be used as process water depending on the method and purpose of reuse. Partially treated water from the sedimentation vessel will not be suitable for agricultural or drinking water (as shown in Table 10-13) and will only be viable for process water use or further treatment.

10.7.6 Avenues for Slag Re-Use

The spent BOFS from the process is valuable as a construction material and can be used as an aggregate in cement, concrete or as road ballast (Xue *et al.*, 2006; Naidu, Sheridan and van Dyk, 2020). Trade routes will have to be established to transport spent slag; however this material can also be used closer to the mine in the development of tailings dams or impoundments.

10.8 Summary

10.8.1 Conclusions

The proposed study was envisioned to begin with an initial concept and end with a tangible design of a system that could treat AMD to agricultural or process water standards using the two waste materials, sugarcane bagasse and BOFS. Both the laboratory and the pilot-scale plants were successful, and the final proposed design is based on findings from the previous smaller-scale set-ups. The waste or by-products were successful in remediating AMD in a continuous process and the possibility of upscale of the design is recognised. The following points are presented as the main conclusions of the study:

- The level of metal and sulfate removal in the settling tanks is dependent on the pH in the tank which is dependent on the alkalinity released from the BOFS. If a higher or lower degree of removal is required in this step, the desired pH (which is controlled) can be altered in order to achieve this.
- The biological reactors are designed as a polishing step. The bulk of the removal of the sulfates occur within the settling tanks due to pH rise, but the polishing below 1000 mg/L can only occur in the biological reactors. These reactors function best at pH values between 4 and 8 and the amount of removal of sulfate that occurs in these reactors is based largely on residence time. If a higher degree of sulfate removal is required, the reactors can be made larger or vessels can be added in series to facilitate this. In addition to this, these reactors function best in anaerobic conditions and need to remain sealed. When aeration occurs, previously precipitated compounds can re-dissolve in the solution. These reactors will also need to contain the suitable amount of organic carbon source to allow for the desirable level of sulfate reduction (0.7g COD/g sulfate)
- The particle size of BOFS and whether agitation is present or not, influences how long the liquid must be in contact with the slag to dissolve enough oxides to increase the alkalinity of the system and thus raise the pH. Any particle size can be used, but different reactor types must be used to facilitate this.
- The reaction times found in the systems that were tested were not long enough to completely dissolve the BOFS, even when fine particles were used. Thus, the sludge that forms in the settling tank contains a large amount of alkaline containing particles. This sludge can be

recycled and further used as an oxide source before being disposed of. If this option is chosen, an addition of an HDS system must take place.

- The controlled pH can be anywhere in the system, however the recommended vessel for control is the slag reactor.
- Replacement rates for the reagents will vary depending on the treatment volume.
- There are further reuse avenues for all waste streams in this process:
    - The BOFS can be used as an aggregate in construction
    - The bagasse can be used a fuel source
    - The sludge can be further processed to extract valuable rare earth metals
    - The treated AMD can be used as agricultural or process water or can enter into a commercial water treatment plant for further remediation

10.8.2 Recommendations

Further studies regarding the optimization of the process control aspect and the use of spent BOFS as an aggregate will need to be conducted to improve the efficiency of the system. It is also recommended that the treated water be used for agricultural purposes as it is nutrient rich. Previous studies have indicated that BOFS or BOFS leachate can be used as a fertilizer or for soil enrichment and treatment due to the high concentrations of calcium, magnesium and silicates it contains (Japanese Society of Soil Science and Plant Nutrition, 2002; Ito, 2015). The treated water also contains some organics, in the form of acids or sugars which is beneficial for the growth of certain plants.

11 Conclusions

11.1 Application of Research

Twenty years prior to the submission of this doctoral dissertation – in 2002 – AMD had just begun to surface in the Gauteng province of South Africa, with discharge of acidic waters occurring at various locations around the Western Basin (Africa Groundwater Atlas, 2018). After a decade of research and attempts by the government and other organizations to combat this problem, the issue of uncontrolled decant of AMD was still being felt keenly in all areas of Gauteng and other parts of South Africa. Environmental experts stated that if not treated, the AMD discharge would put an end to irrigation farming in the lower reaches of the Orange River and the Hartbeespoort Dam within the next 20 years (Mashala, 2012). At the time, AMD accounted for about 4% of the total flow of the Vaal.

In 2022, the halfway point of the time-based prediction made in 2012, the AMD issue is seemingly at an inflection point. With regards to farming concerns, partially treated AMD has recently shown potential in hydroponics applications (Naidu, 2020) – a positive outcome that could combat a host of mining related issues, including land reclamation, agricultural shortages and water pollution. However with regards to river and dam pollution, a 58km stretch of the lower Wilge River system has also recently (February 2022) been destroyed after an old coal mine in Mpumalanga decanted millions of litres of acidic water into the river system (Bega, 2022). Thus, while there are constructive steps being undertaken, these are not yet commensurate to the magnitude of the imminent consequences of historical inaction.

In light of this, the challenges that exist with regards to establishing a comprehensive solution have been identified. These are: (i) cost (relating to capital and operation, as well as continual deployment of reagents to treat the continual production of AMD) and (ii) location (relating to the part of the AMD decanting process at which the treatment regime is deployed – upstream, at the mine or downstream when AMD has already entered into water bodies and waterways).

The technology explored within this dissertation has the potential to combat both challenges: (i) the cost of the treatment scheme would be substantially lower due to very little envisioned operational involvement, as well as the cost of reagents being kept low (through the use of waste and by products, and through potential valorisation of these wastes); (ii) the technology is aimed to be deployed at the source of production – individual mining sites – allowing for treatment of the streams before they enter larger water bodies.

11.2 Fulfillment of objectives

The objectives that were set to better define the proposed AMD treatment system and ascertain its level of effectiveness in passive AMD treatment were achieved through the procedures outlined in Chapter

3 and minor sections in other chapters. Fulfilment of the aims are briefly summarized below with reference to the order in which they were presented in Chapter 1 (and in the body of the dissertation):

Determine the kinetics of the slag dissolution reaction in acidic and neutral solutions.

Determination of the kinetics of the slag dissolution reaction in acidic and neutral solutions found that the Lagergren kinetic model presented the best fit of the data with the pseudo-first-order model seeming to better apply to acidic media using H^+ (hydrogen ion) decrease, and the pseudo-second-order model was found to apply better to a neutral solution. When the dissolution of Mg and Ca oxides were assessed individually, the results showed the inverse. Dissolution in acidic media fit the pseudo-second-order model better and dissolution in neutral media fit the pseudo-first-order model better. The kinetic rate constants for these models were all determined, and an assessment of the model fitting was done – showing that (i) the chemical reaction model did not apply to any case, (ii) H^+ kinetics had the highest coefficient of determination values and, lastly, (iii) the pseudo-first order model was seen to apply most often.

Identify and study the kinetics of the precipitation reactions which occur when the pH of the AMD treatment system rises.

The kinetics of the precipitation reactions which occurred during BOF slag induced pH increase, yielded differing governing equations for each metal component. The presence of multiple metal species justified the application of a singular equation relating the concentration of the metal to the pH of the system. The pH of the system was then linked to the addition of BOF slag. In this manner, the kinetics of the precipitation reactions as a collective, metal species dependent model was determined. The types of metal and sulfate precipitates were also determined.

Determine the kinetics of the SRM reactions in a BOF slag neutralized solution.

The SRM reactions in a BOF slag neutralized solution were found to follow first-order reaction kinetics; the reaction being dependent on a number of criteria such as nutrient availability, redox potential, salinity, sulfide concentration, COD:Sulfate ratio and temperature (to name a few). The kinetics and functioning of these microorganisms were thus determined at a specific set of conditions; these being representative of the conditions under which they would perform in a large scale BOF slag and AMD remediation system. The behaviour of the system was found to be favourable with sulfate reduction occurring in the system without further addition of nutrients.

Determine the optimal configuration of a system incorporating and integrating all three processes (pH rise from BOF slag action; precipitation of metals, sulfates and sulfides; reduction of sulfate and formation of sulfide through SRM action).

The processes described to achieve the above-mentioned objectives were combined in a continuous system. The order of these processes was optimized to allow for maximum metal and sulfate removal, as well as allow for a neutral treated outlet stream. The optimised order was found to be: (i) BOF slag treatment, whereby AMD was contacted with BOF slag resulting in a pH increase; (ii) subsequent removal of a degree of sulfate and metal content via precipitation; (iii) biological treatment whereby microorganisms can function better under a higher (neutral) pH and lower sulfate and metal concentration environment.

Design, construct and monitor a laboratory scale system for treating up to 25 L/ of AMD per day

Operation of the designed process at a laboratory scale was possible at flowrates ranging from 1L/day to 10.4 L/day, with a flowrate of 25 L/day able to be achieved in a system with a larger volume. The operation of the laboratory scale system confirmed the neutralisation of the AMD to a pH of between 7 and 8, and the removal of heavy metals and sulfate to levels of below 10 mg/L for Al, Fe, Mg, Mn and below 200 mg/L for sulfate for the AMD samples collected.

Design, construct, monitor and assess the long-term performance of a pilot plant to process and treat 1000L/day of AMD on-site.

Operation of a pilot-scale plant treating 200-1000 L/day demonstrated Al, Fe, Mn and SO_4^{2-} removals of 97%, 87%, 100%, and 87% respectively. The dissolution of the slag and the alkalinity generation was found to occur mainly due to CaO and MgO dissolution. The SRB functioned effectively in the slag eluate and a maximum sulfate reduction of 76% was found across the bioreactors in the pilot study.

Prepare a proposed process for scale-up on site based on the pilot study.

The final design, which was proposed, differed from the original laboratory and pilot design in the following ways: (i) it did not make use of a recycle effluent stream, (ii) it did not include a secondary settling vessel or a tertiary biological vessel. All combinations that were explored during the testing period yielded favourable results overall (improvement of water quality and water treated to an acceptable standard based on the needs of the mine). The configuration that yielded the best results was suggested for the final design and included a modular system in which BOF slag was used to increase the pH of the system before SRM were used to polish the sulfate leftover in the stream to below 400 mg/L.

11.3 Recommendations

Although this work was successful in demonstrating the potential applicability of such a treatment regime, it was not without limitations. The following recommendations are suggested to combat the plethora of challenges experienced during the completion of this dissertation:

1. Further research is recommended for the re-use of spent BOF slag (post-AMD treatment) in construction. This was briefly considered; however, the slag has a very long residence time in the reactor which did not allow for representative testing during the experimental period. If the BOF slag could be confirmed for re-use in this manner, this would mean valorisation of a further waste-streams and allow for this waste to be income generating.
2. If this technology is to be deployed at active or abandoned mining sites, the use of existing mine equipment (predominantly pumps), or the systematic set-up of flow paths to allow for gravity assisted processes, is encouraged. This is primarily to avoid theft of new equipment at abandoned mines – something which occurred during the completion of this project. This is also to keep the cost of treatment low (the reaction vessels and reagents are already low-cost).
3. This technology is proposed to be deployed in a modular fashion, such that it can be applied in many different regions with AMD of differing qualities.
4. In the event a sugarcane bagasse source is not able to be obtained, any other waste organic carbon source can be tested to provide COD and a degree of nutrients to the biological section of the plant.

11.4 Concluding Remarks

The system which was proposed, designed and tested in this study was successful in treating AMD. It can serve as a precursor to multiple other treatment regimes (reverse osmosis, membrane filtration, ionic exchange), or as a stand-alone system to service smaller, isolated areas that aim to reuse the AMD affected water in processes or for irrigation. It is intended that this research be used to solve – at least partially – AMD and other sustainability problems being experienced by mining countries all over the world, however it is acknowledged that in some areas and in some applications this technology would not be appropriate for deployment. In these cases, it is intended that the theme of this research stimulate further work into the critical filed of environmentally sustainable wastewater treatment.

12 References

Abe, I. *et al.* (2004) ‘Adsorption of fluoride ions onto carbonaceous materials’, *Journal of Colloid Interface Science*, 275, pp. 35–39.

Abushammala, H. and Mao, J. (2019) ‘A review of the surface modification of cellulose and nanocellulose using aliphatic and aromatic mono- And di-isocyanates’, *Molecules*, 24(15), pp. 1–18. doi: 10.3390/molecules24152782.

Africa Groundwater Atlas (2018) *Case Study: Acid mine drainage in South Africa*. Gauteng. Available at: http://earthwise.bgs.ac.uk/index.php/Case_Study_Acid_Mine_Drainage_South_Africa#:~:text=The first discharges of acid,the hydrogeology is poorly understood.

Agency for Toxic Substances and Disease Registery (2006) *Health Statistics Review: cancer and Birth Outcomes Analysis: endicott Area Investigation*. Atlanta GA.

Aguiar, A. *et al.* (2021) ‘Sugarcane straw as a potential second generation feedstock for biorefinery and white biotechnology applications’, *Biomass and Bioenergy*, 144(June 2020). doi: 10.1016/j.biombioe.2020.105896.

Ahmed, J. K. and Ahmaruzzaman, M. (2016) ‘Journal of Water Process Engineering A review on potential usage of industrial waste materials for binding heavy metal ions from aqueous solutions’, *Journal of Water Process Engineering*, 10, pp. 39–47. doi: 10.1016/j.jwpe.2016.01.014.

Akcil, A. and Koldas, S. (2006) ‘Acid Mine Drainage (AMD): causes, treatment and case studies’, *Journal of Cleaner Production*, 14(12-13 SPEC. ISS.), pp. 1139–1145. doi: 10.1016/j.jclepro.2004.09.006.

Akin Altun, I. and Yilmaz, I. (2002) ‘Study on steel furnace slags with high MgO as additive in Portland cement’, *Cement and Concrete Research*, 32(8), pp. 1247–1249. doi: 10.1016/S0008-8846(02)00763-9.

Alanyalı, H. *et al.* (2006) ‘Application of magnetic separation to steelmaking slags for reclamation’, *Waste Management*, 26(10), pp. 1133–1139.

Alchin, D. (2006) *XIII-Water-D-Ion Exchange Resins-2 SO 3 H SO*. New Zealand. Available at: https://nzic.org.nz/ChemProcesses/water/13D.pdf.

Alexiou, I. . and Panter, K. (2004) ‘A Review of Two-Phase Applications to Define Best Practice for the Treatment of Various Waste Streams’, in *Proceedings of IWA 10th 391 World 392 Congress on Anaerobic Digestion*. Montreal, Quebec.

Allen, B. (2010) *Global Ferrous Slag Market Poised to Reach almost $28 billion by 2020*, *Smithers*.

Alokika *et al.* (2021) 'Cellulosic and hemicellulosic fractions of sugarcane bagasse: Potential, challenges and future perspective', *International Journal of Biological Macromolecules*, 169, pp. 564–582. doi: 10.1016/j.ijbiomac.2020.12.175.

American Public Health Association (1975) *Standard methods for the examination of water and wastewater*. 14th Editi. New York: APHA.

Amini, M. *et al.* (2008) 'Statistical modeling of global geogenic fluoride contamination in groundwaters', *Environmental Science and Technology*, 42, pp. 3662–3668.

Asi, I. M., Qasrawi, H. Y. and Shalabi, F. I. (2007) 'Use of steel slag aggregate in asphalt concrete mixes', *Canadian Journal of Civil Engineering*, 34(8), pp. 902–911. doi: 10.1139/l07-025.

Askri, B. *et al.* (2016) 'Isotopic and geochemical identifications of groundwater salinisation processes in Salalah coastal plain', *Chemie der Erde - Geochemistry*, 76(2), pp. 243–255. doi: 10.1016/j.chemer.2015.12.002.

Ayangbenro, A. S., Olanrewaju, O. S. and Babalola, O. O. (2019) 'Sulfate-Reducing Bacteria as an Effective Tool for Sustainable Acid Mine Bioremediation', *Frontiers in Microbiology*, 9. doi: 10.3389/fmicb.2018.01986.

Aydilek, A. (2015) *STATE HIGHWAY ADMINISTRATION RESEARCH REPORT GEOTECHNICAL AND ENVIRONMENTAL IMPACTS OF STEEL SLAG USE IN HIGHWAY CONSTRUCTION UNIVERSITY OF MARYLAND , COLLEGE PARK Project number SP209B4H FINAL REPORT*. Maryland.

Ayenagbo, K. *et al.* (2011) 'The transportation and marketing implications of sand and gravel and its environmental impact in Lome-Togo', *Journal of Economics and International Finance*, 3(3), pp. 125–138. Available at: http://www.academicjournals.org/JEIF.

Balintova, M. and Petrilakova, A. (2011) 'Study of pH influence on selective precipitation of heavy metals from acid mine drainage', *Chemical Engineering Transactions*, 25, pp. 345–350. doi: 10.3303/CET1125058.

Banks, D. *et al.* (1995) 'Natural concentrations of major and trace elements in some Norwegian bedrock groundwaters', *Applied Geochemistry*, 10, pp. 1–16.

Barakat, M. A. (2011) 'New trends in removing heavy metals from industrial wastewater', *Arabian Journal of Chemistry*, 4(4), pp. 361–377. doi: 10.1016/j.arabjc.2010.07.019.

Barati, M., Esfahani, S. and Utigard, T. A. (2011) 'Energy recovery from high temperature slags', *Energy*, 36(9), pp. 5440–5449. doi: 10.1016/j.energy.2011.07.007.

Barca, C. *et al.* (2014) 'Steel slag filters to upgrade phosphorus removal in small wastewater treatment plants : Removal mechanisms and performance', *Ecological Engineering*, 68, pp. 214–222. doi: 10.1016/j.ecoleng.2014.03.065.

Bardone, E. *et al.* (2014) 'Dilute-acid Hydrolysis of Cellulose to Glucose from Sugarcane Bagasse', *Chemical Engineering Transactions*, 38, pp. 433–438. doi: 10.3303/CET1438073.

Barker, K. J. *et al.* (1998) 'Oxygen Steelmaking Furnace Mechanical Description and Maintenance Considerations', in *Steelmaking and Refining Volume*.

Barrett, K. D. (ed.) (2015) *Fulvic and Humic Acids: Chemical Composition, Soil Applications and Ecological Effects*. Nova Science Publishers, Incorporated.

Barton, L. L. and Fauque, G. (2009) 'Chapter 2: Biochemistry, Physiology and Biotechnology of Sulfate-Reducing Bacteria', *Advances in Applied Microbiology*, 68, pp. 41–98. doi: 10.1016/S0065-2164(09)01202-7.

van Beek, C. L. *et al.* (2012) *Risk Assessment Methodologies of Soil Threats in Europe Status and options for harmonization for*. Edited by JRC Scientific and Policy Reports. Luxembourg: Office for Official Publication of the European Communities. doi: 10.2788/47096.

Bega, S. (2022) 'Coal mine acidic water spillage into Wilge River system kills "all life, everything"', *Mail & Guardian*, 24 February. Available at: https://mg.co.za/environment/2022-02-24-coal-mine-acidic-water-spillage-into-wilge-river-system-kills-all-life-everything/.

Bernardez, L. A. *et al.* (2013) 'A kinetic study on bacterial sulfate reduction', *Bioprocess and Biosystems Engineering*, 36(12), pp. 1861–1869. doi: 10.1007/s00449-013-0960-0.

Bhatnagar, A. and Sillanpää, M. (2010) 'Utilization of agro-industrial and municipal waste materials as potential adsorbents for water treatment — A review', 157, pp. 277–296. doi: 10.1016/j.cej.2010.01.007.

Bilski, J. *et al.* (2014) 'Aluminium in coal fly ash (FA), in plants grown on FA, and in the leachates from FA', *Research Journal of Chemistry and Environment*, 2(4), pp. 22–26.

Bizzo, W. A. *et al.* (2014) 'The generation of residual biomass during the production of bio-ethanol from sugarcane, its characterization and its use in energy production', *Renewable and Sustainable Energy Reviews*, 29, pp. 589–603.

Blodau, C. (2006) 'A review of acidity generation and consumption in acidic coal mine lakes and their watersheds', *Science of the Total Environment*, 369(1–3), pp. 307–332. doi: 10.1016/j.scitotenv.2006.05.004.

Bobicki, E. R. *et al.* (2012) 'Carbon capture and storage using alkaline industrial wastes', *Progress in*

Energy and Combustion Science, 38(2), pp. 302–320. doi: 10.1016/j.pecs.2011.11.002.

Bonenfant, D. *et al.* (2008) 'CO2 sequestration potential of steel slags at ambient pressure and temperature.', *Industrial and Engineering Chemistry Research*, 47, pp. 7610–7616.

Bosecker, K. (1997) 'Bioleaching: metal solubilization by microorganisms', *FEMS Microbiology Reviews*, 20(3–4), pp. 591–604.

Bosman, D. (1983) 'Lime treatment of acid mine water and associated solids/liquid separation.', *Water Science Technology*, 15, pp. 71–84.

Bowell, R. . (2004) 'A review of sulfate removal options for mine waters', *Proceedings of Mine Water Process*, pp. 1–24.

Boyer, T. H. *et al.* (2011) 'Comparison of low-cost and engineered materials for phosphorus removal from organic-rich surface water', *Water Research*, 45(16), pp. 4803–4814. doi: 10.1016/j.watres.2011.06.020.

Brand, A. S. and Roesler, J. R. (2015) 'Cement & Concrete Composites Steel furnace slag aggregate expansion and hardened concrete properties', *CEMENT AND CONCRETE COMPOSITES*, 60, pp. 1–9. doi: 10.1016/j.cemconcomp.2015.04.006.

van den Brand, T. P. H. *et al.* (2015) 'Potential for beneficial application of sulfate reducing bacteria in sulfate containing domestic wastewater treatment', *World J Microbiol Biotechnol*, 31(11), pp. 1675–1681. doi: 10.1007/s11274-015-1935-x.

Van Den Brand, T. P. H. *et al.* (2015) 'Effects of chemical oxygen demand, nutrients and salinity on sulfate-reducing bacteria', *Environmental Engineering Science*, 32(10), pp. 858–864. doi: 10.1089/ees.2014.0307.

Brant, D. L. and Ziemkiewicz, P. F. (1997) 'Passive Removal of Manganese from Acid Mine Drainage', in *America Society of Mining and Reclamation*, pp. 741–744. doi: 10.21000/JASMR97010741.

Brito, J. de and Saikia, N. (2012) *Recycled Aggregate in Concrete: Use of Industrial, Construction and Demolition Waste Green Energy and Technology*. Lisbon, Portugal: Springer Science & Business Media.

Brown;, T. *et al.* (2009) *Chemistry The Central Science*. 11th Editi. Upper Saddle River: Pearson.

Brumleve, C. and The United States Geological Survey (2011) 'AMD Environmental Issues – Underground and Surface Mining of Sulfide Minerals'. Keweenaw Bay.

Burkel, R. S. and Stoll, R. C. (1999) 'Naturally occurring arsenic in sandstone aquifer water supply

wells of North Eastern Wisconsin', *Ground Water Monitoring and Remediation*, 19(2), pp. 114–121.

Calmon, J. L. *et al.* (2013) 'Effects of BOF steel slag and other cementitious materials on the rheological properties of self-compacting cement pastes', *Construction and Building Materials*, 40, pp. 1046–1053. doi: 10.1016/j.conbuildmat.2012.11.039.

Canfield, D. E. (2004) 'The Evolution of the Earth Surface Sulfur Reservoir', *American Journal of Science*, 304, pp. 839–861.

Cao, J. *et al.* (2012) 'Influence of electron donors on the growth and activity of sulfate-reducing bacteria', *International Journal of Mineral Processing*, 106–109, pp. 58–64. doi: 10.1016/j.minpro.2012.02.005.

Carneiro, B. P. T. *et al.* (2020) 'Acid mine drainage (AMD) treatment by neutralization: Evaluation of physical-chemical performance and ecotoxicological effects on zebrafish (Danio rerio) development', *Chemosphere*, 253, pp. 1–9. doi: 10.1016/j.chemosphere.2020.126665.

Carvalho, S. Z. *et al.* (2017) 'The recycling effect of BOF slag in the portland cement properties', *Resources, Conservation and Recycling*, 127(August), pp. 216–220. doi: 10.1016/j.resconrec.2017.08.021.

Cebrian, M. E. *et al.* (1983) 'Chronic arsenic poisoning in the North of Mexico', *Human Toxicology*, 2, pp. 121–133.

Center for bioprocess engineering research (2016) 'CeBER laboratory methods manual'. CeBer.

Chamier, J. *et al.* (2015) 'Aluminium (Al) fractionation and speciation; getting closer to describing the factors influencing Al3+ in water impacted by acid mine drainage', *Chemosphere*, 130, pp. 17–23. doi: 10.1016/j.chemosphere.2015.01.026.

Chaurand, P. *et al.* (2007) 'Environmental impacts of steel slag reused in road construction : A crystallographic and molecular (XANES) approach', 139, pp. 537–542. doi: 10.1016/j.jhazmat.2006.02.060.

Chen, S. and Lin, J. (2009) 'Enhancement of metal bioleaching from contaminated sediment using silver ion', 161, pp. 893–899. doi: 10.1016/j.jhazmat.2008.04.035.

Chern, J. M. and Chien, Y. W. (2002) 'Adsorption of nitrophenol onto activated carbon: Isotherms and breakthrough curves', *Water Research*, 36(3), pp. 647–655. doi: 10.1016/S0043-1354(01)00258-5.

Cherubini, F. (2010) 'The biorefinery concept : Using biomass instead of oil for producing energy and chemicals', *Energy Conversion and Management*, 51(7), pp. 1412–1421. doi: 10.1016/j.enconman.2010.01.015.

Chief, K. *et al.* (2016) *Understanding the Gold King Mine Spill*. Arizona.

Chun-ming, C. H. I. *et al.* (2011) 'Estimating Exchangeable Sodium Percentage from Sodium Adsorption Ratio of Salt-Affected Soil in the Songnen Plain of Northeast China', *Pedosphere: An International Journal*, 21(2), pp. 271–276. doi: 10.1016/S1002-0160(11)60127-6.

Ciocan, A. (2012) 'AN OVERVIEW OF ASSESSMENT OF THE BLAST FURNACE SLAG TRANSFORMATION INTO VALUE ADDED BY-PRODUCTS ON BASIS OF ITS CHARACTERISTICS KNOWLEDGE', in *THE ANNALS OF "DUNAREA DE JOS" UNIVERSITY OF GALATI*. Galati, Romania: Galati University Press, pp. 38–48. doi: ISSN 1453-083X.

Daliakopoulos, I. N. *et al.* (2016) 'The threat of soil salinity: A European scale review', *Science of the Total Environment*, 573, pp. 727–739.

Dantas, G. A., Legey, L. F. L. and Mazzone, A. (2013) 'Energy from sugarcane bagasse in Brazil : An assessment of the productivity and cost of different technological routes', *Renewable and Sustainable Energy Reviews*, 21, pp. 356–364. doi: 10.1016/j.rser.2012.11.080.

Decker, G., Askew, E. F. and Merck (2017) 'Chemical Oxygen Demand (COD) by Dichromate Oxidation and Photometry'. Darmstadt, Germany: Merck.

Decock, C. *et al.* (2015) 'Mitigating N 2 O emissions from soil : from patching leaks to transformative action', *Soil*, 1, pp. 687–694. doi: 10.5194/soil-1-687-2015.

Demers, I. *et al.* (2015) 'Valorisation of acid mine drainage treatment sludge as remediation component to control acid generation from mine wastes, part 1: Material characterization and laboratory kinetic testing', *Minerals Engineering*, 76, pp. 109–116. doi: https://doi.org/10.1016/j.mineng.2014.10.015.

Deniz, I. and Keskin-Gundogdu, T. (2017) 'Biomimetic Design for a Bioengineered World', in Kokturk, G. and Altun, T. D. A. (eds) *Interdisciplinary Expansions in Engineering and Design With the Power of Biomimicry*. doi: DOI: 10.5772/intechopen.72912.

Department of Mineral Resources (2010) *Lime Industry in South Africa, 2010*. South Africa. Available at: https://www.dmr.gov.za/LinkClick.aspx?fileticket=YqZfpm-OvZs%3D&portalid=0.

Department of Water Affairs and Forestry (1996a) *South African Water Quality Guidelines Volume 1 Domestic Water Use*. Second Edi. Edited by S. Holmes and CSIR Environmental Services. Pretoria: Department of Water Affairs and Forestry.

Department of Water Affairs and Forestry (1996b) *South African Water Quality Guidelines Volume 3: Industrial Use*. Second. Edited by S. Holmes and CSIR Environmental Services. Pretoria: Department of Water Affairs and Forestry.

Department of Water Affairs and Forestry (1996c) *South African Water Quality Guidelines Volume 4 Agiricultural Use: Irrigation*. Second Edi. Edited by S. Holmes and CSIR Environmental Services. Pretoria: Department of Water Affairs and Forestry.

Desilva, F. J. (1996) 'Usina Ion', pp. 25–28.

Dev, S., Roy, S. and Bhattacharya, J. (2016) 'Understanding the performance of sulfate reducing bacteria based packed bed reactor by growth kinetics study and microbial profiling', *Journal of Environmental Management*, 1177, pp. 101–110. doi: https://doi.org/10.1016/j.jenvman.2016.03.049.

Dhir, B. (2018) 'Biotechnological Tools for Remediation of Acid Mine Drainage (Removal of Metals From Wastewater and Leachate)', in Prasad, M. N. V., Favas, P. J. de C., and Maiti, S. K. (eds) *Bio-Geotechnologies for Mine Site Rehabilitation*. Elsevier, pp. 67–82. doi: https://doi.org/10.1016/B978-0-12-812986-9.00004-X.

Dhunna, R. *et al.* (2014) 'Recycling Waste Bakelite as an Alternative Carbon Resource for Ironmaking Applications', *ISIJ International*, 54(3), pp. 613–619. doi: 10.2355/isijinternational.54.613.

Ding, Y. C. *et al.* (2017) 'Study on the treatment of BOF slag to replace fine aggregate in concrete', *Construction and Building Materials*, 146, pp. 644–651. doi: 10.1016/j.conbuildmat.2017.04.164.

Doble, M. and Kumar, A. (2005) 'Treatment of Waste from Metal Processing and Electrochemical Industries', in Doble, M. and Kumar, A. (eds) *Biotreatment of Industrial Effluents*. Butterworth-Heinemann, pp. 145–155. doi: https://doi.org/10.1016/B978-075067838-4/50014-2.

Doucet, F. J. (2010) 'Effective CO 2 -specific sequestration capacity of steel slags and variability in their leaching behaviour in view of industrial mineral carbonation', *Minerals Engineering*, 23(3), pp. 262–269. doi: 10.1016/j.mineng.2009.09.006.

Dryden, I. G. C. (1982) 'Chapter 17 - Refractory and insulating materials', in *The Efficient Use of Energy (Second Edition)*. Butterworth-Heinemann, pp. 394–412. doi: https://doi.org/10.1016/B978-0-408-01250-8.50026-X.

Dumas, O. *et al.* (2018) 'Respiratory effects of trichloroethylene', *Respiratory Medicine*, 134(November 2017), pp. 47–53. doi: 10.1016/j.rmed.2017.11.021.

Durand, J. F. (2012) 'The impact of gold mining on the Witwatersrand on the rivers and karst system of Gauteng and North West Province, South Africa', *Journal of African Earth Sciences*, 68, pp. 24–43. doi: 10.1016/j.jafrearsci.2012.03.013.

DWAF (1996a) *South African Water Quality Guidelines : Domestic Use (second edition)*, *Departmet of Water Affairs and Forestry, Republic of South Africa*.

DWAF (1996b) *Water Quality Guidelines Agricultural Use: Irrigation, South African Water Quality Guidelines*.

Earl, B. and Wiford, L. D. R. (2104) *Cambridge IGCSE Chemistry*. London: Hachette UK.

El-Sheshtawy, H. *et al.* (2014) 'Monitoring of oil pollution at Gemsa Bay and bioremediation capacity of bacterial isolates with biosurfactants and nanoparticles.', *Marine Pollution Bulletin*, 87, pp. 191–200.

Eloneva, S. *et al.* (2008) 'Fixation of CO2 by carbonating calcium derived from blast furnace slag.', *Energy*, 33, pp. 1677–1678.

Environment Agency (2018) *Classify different types of waste*, *Integrated Pollution Prevention and Control (IPPC)*.

España, J. S. (2007) *The Behavior of Iron and Aluminum in Acid Mine Drainage: Speciation, Mineralogy, and Environmental Significance, Thermodynamics, Solubility and Environmental Issues*. Elsevier B.V. doi: 10.1016/B978-0-444-52707-3.50009-4.

Euroslag (2012) *Steel Slag – Basic Oxygen Furnace Slag (BOS)*. Available at: http://www.euroslag.com/fileadmin/_media/images/Products/Steel_Slag_-_BOS.pdf (Accessed: 5 November 2017).

Euroslag (2017) *Properties*. Available at: http://www.euroslag.com/products/properties/ (Accessed: 5 November 2017).

Evangelou, V. P. and Zhang, Y. L. (1995) 'A review: pyrite oxidation mechanisms and acid mine drainage prevention. Crit. Rev.', *Environ. Sci. Technol.*, 25(2), pp. 141–199.

Evarts, H. (2017) *Turning Iron and Steel Manufacturing Waste Into Valuable Materials*.

Fan, C. and Li, K. (2014) 'Glass-ceramics produced from thin- fi lm transistor liquid-crystal display waste glass and blast oxygen furnace slag', *Ceramics International*, 40(5), pp. 7117–7123. doi: 10.1016/j.ceramint.2013.12.046.

Fan, J. *et al.* (2019) 'Effect of hydraulic retention time and pH on oxidation of ferrous iron in simulated ferruginous acid mine drainage treatment with inoculation of iron-oxidizing bacteria', *Water Science and Engineering*, 12(3), pp. 213–220. doi: 10.1016/j.wse.2019.09.003.

FAO and ITSP (2015) *Status of the World's Soil Resources (SWSR)- Main Report*. Rome, Italy.

Fatoki, O. S. and Awofolu, O. R. (2004) 'Levels of Cd, Hg and Zn in some surface waters from the Eastern Cape Province, South Africa', *Water SA*, 29(4), pp. 375–380. Available at: http://www.ajol.info/index.php/wsa/article/view/5042.

Favas, P. J. C., Martino, L. E. and Prasad, Majeti N.V. (2018) 'Abandoned Mine Land Reclamation—Challenges and Opportunities (Holistic Approach)', in Prasad, Majeti Narasimha Vara, Favas, P. J. de C., and Maiti, S. K. (eds) *Bio-Geotechnologies for Mine Site Rehabilitation*. Elsevier, pp. 3–31.

Feng, D., Deventer, J. S. J. Van and Aldrich, C. (2004) 'Removal of pollutants from acid mine wastewater using metallurgical by-product slags', 40, pp. 61–67. doi: 10.1016/j.seppur.2004.01.003.

Fernández-gonzález, D. *et al.* (2019) 'The treatment of Basic Oxygen Furnace (BOF) slag with concentrated solar energy', *Solar Energy*, 180(June 2018), pp. 372–382. doi: 10.1016/j.solener.2019.01.055.

Ferreira, E. B., Zanotto, E. D. and Scudeller, L. a M. (2002) 'Glass and glass-ceramic from basic oxygen furnace (BOF) slag', *Glass Science and Technology*, pp. 75–86.

Ferrerira, E. B., Zanotto, E. D. and Fredericci, C. (2000) 'Black Glass and Dark glass-ceramic and method for making'. Brazil: INPI.

Fogler, H. S. (1999) *Elements of Chemical Reaction Engineering Elements of Chemical Reaction Engineering*. Third. Edited by N. Amundson. Prentice Hall International Series.

Fu, F., Dionysiou, D. D. and Liu, H. (2014) 'The use of zero-valent iron for groundwater remediation and wastewater treatment : A review', *Journal of Hazardous Materials*, 267, pp. 194–205. doi: 10.1016/j.jhazmat.2013.12.062.

Fujita, T. *et al.* (2009) 'Immobilization of Arsenic from Novel Synthesized Scorodite—Analysis on Solubility and Stability', *Materials Transactions*, 50(2), pp. 321–331. doi: 10.2320/matertrans.M-MRA2008844.

Ganyaglo, S. *et al.* (2010) 'Hydrochemical and isotopic characterisation of groundwaters in the eastern region of Ghana', *Journal of Water Resource Protection*, 2, pp. 199–208.

Gao, Y. –. *et al.* (2015) 'Effects of salinization and crude oil contamination on soil bacterial community structure in the Yellow River Delta region, China.', *Applied Soil Ecology*, 86, pp. 165–173.

Gavrilovski, M., Radossavljevic, S. and Milic, D. (1996) 'MINERAL PROCESSING OF A CONVERTER SLAG AND ITS USE IN IRON ORE SINTERING', *Magnetic and Electrical Separation*, 7(C), pp. 201–211.

Geerdes, M., Toxopeus, H. and Van der fliet, C. (2009) *Modern Blast Furnace Ironmaking*. 2nd Editio. Amsterdam, Netherlands: IOS Press Delft University Press.

Gevaudan, J. P. *et al.* (2019) 'Copper and cobalt improve the acid resistance of alkali-activated cements', *Cement and Concrete Research*, 115(August 2018), pp. 327–338. doi:

10.1016/j.cemconres.2018.08.002.

Gogoi, H. *et al.* (2021) ‘Acid mine drainage treatment with novel high-capacity bio-based anion exchanger’, *Chemosphere*, 264, p. 128443. doi: 10.1016/j.chemosphere.2020.128443.

Goldhaber, M. B. (2003) ‘Sulfur-rich Sediments’, in Holland, H. D. and Turekian, K. K. (eds) *Treatise on Geochemistry*. Denver: Elsevier, Pergamon, pp. 257–288. doi: https://doi.org/10.1016/B0-08-043751-6/07139-5.

Gomes, H. I. *et al.* (2016) ‘Alkaline residues and the environment : a review of impacts , management practices and opportunities’, *Journal of Cleaner Production*, 112, pp. 3571–3582. doi: 10.1016/j.jclepro.2015.09.111.

Goodarzi, A. R. and Salimi, M. (2015) ‘Applied Clay Science Stabilization treatment of a dispersive clayey soil using granulated blast furnace slag and basic oxygen furnace slag’, *Applied Clay Science*, 108, pp. 61–69. doi: 10.1016/j.clay.2015.02.024.

Google Finance (2021) *Google Finance Exchange Rate Calculator and Graphical Analysis, Google Finance*. Available at: https://www.google.com/intl/en/googlefinance/disclaimer/.

Gralimex Import (2017) *Gralimex Silage Products*.

Grosu, Y. *et al.* (2018) ‘Natural and by-product materials for thermocline-based thermal energy storage system at CSP plant : Structural and thermophysical properties’, *Applied Thermal Engineering*, 136(March), pp. 185–193. doi: 10.1016/j.applthermaleng.2018.02.087.

Grubb, D. G., Landers, D. G. and Hernandez, M. (2000) ‘Utilization of Sugarcane Bagasse to Treat Acid Mine Drainage’, *GeoEng*, 0355, pp. 19–24.

Grubeša, I. N. *et al.* (2016) *Characteristics and Uses of Steel Slag in Building Construction*. Cambridge: Woodhead Publishing.

Güler, M. *et al.* (2014) ‘Long-term changes in spatial variation of soil electrical conductivity and exchangeable sodium percentage in irrigated mesic ustifluvents’, 135, pp. 1–8. doi: 10.1016/j.agwat.2013.12.011.

Günther, P. *et al.* (2003) ‘Neutralisation of Acid Leachate in a Coal Processing Plant with Calcium Carbonate’, in *Proceedings of the 8 th International Mine Water Association (IMWA) Congress*. Johannesburg, South Africa: International Mine Water Association.

Gupta, V. V. S. R. and J.Germida, J. (2021) ‘Microbial transformations of sulfur in soil’, in Gentry, T. J., Fuhrmann, J. J., and Zuberer, D. A. (eds) *Principles and Applications of Soil Microbiology*. Third Edit. Elsevier, pp. 489–522. doi: https://doi.org/10.1016/B978-0-12-820202-9.00018-6.

Gutierrez, A. *et al.* (2016) 'Advances in the valorization of waste and by-product materials as thermal energy storage (TES) materials', *Renewable and Sustainable Energy Reviews*, 59, pp. 763–783. doi: 10.1016/j.rser.2015.12.071.

Haman, D. Z. and Zazueta, F. S. (2014) 'Settling Basins for Trickle Irrigation in Florida 1', pp. 1–6.

Han, C. *et al.* (2015) 'ScienceDirect Removal kinetics of phosphorus from synthetic wastewater using basic oxygen furnace slag', *JES*, 30, pp. 21–29. doi: 10.1016/j.jes.2014.11.003.

Han, C. *et al.* (2016) 'Effects of pH on phosphorus removal capacities of basic oxygen furnace slag', *Ecological Engineering*, 89, pp. 1–6. doi: 10.1016/j.ecoleng.2016.01.004.

Hao, O. J. *et al.* (1996) 'Sulfate-reducing bacteria', *Critical Reviews in Environmental Science and Technology*, 26(2), pp. 155–187. doi: 10.1080/10643389609388489.

Harding, C., Johnson, D. A. and Janes, R. (2002) *Elements of the P Block*. llustrated. Royal Society of Chemistry.

Helle, M. *et al.* (2012) 'Optimization of steelmaking using fastmet DRI in the blast furnace', *6th Int. Congress on the Science and Technology of Ironmaking 2012, ICSTI 2012 - Including Proceedings from the 42nd Ironmaking and Raw Materials Seminar, and the 13th Brazilian Symp. on Iron Ore*, 2(12), pp. 2038–2046.

Hellström, H.-O. *et al.* (2006) 'The aluminium content of bone, and mortality risk', *Journal of Age and Ageing*, 37(2), pp. 217–220. doi: 10.1093/ageing/afm152.

Hem, J. D. (1985) 'Study and Interpretation of the Chemical Characteristics of Natural Water', in *United States Geological Survey Water Supply Paper 2254*. Third, p. 263.

Hentati, O. *et al.* (2013) 'Toxicity assessment for petroleumcontaminated soil using terrestrial invertebrates and plant bioassays.', *Environmental Monitoring and Assessment*, 185, pp. 2989–2998.

Henze, M. *et al.* (2008) *Biological Wastewater Treatment*. illustrate. IWA Publishing.

Hernandez, M. (2018) 'Upcycling Industrial Byproducts for Control of Microbially Induced Concrete Corrosion'. Colorado.

Herrmann, U., Kelly, B. and Price, H. (2004) 'Two-tank molten salt storage for parabolic trough solar power plants', *Energy*, 29, pp. 883–893. doi: 10.1016/S0360-5442(03)00193-2.

Hogg, E. H. and Wein, R. W. (1988) 'The contribution of Typha components to floating mat buoyancy', *Ecology*, 69, pp. 1025–1031. doi: 10.2307/1941258.

Horii, K. (2015) *Overview of Iron / Steel Slag Application and Development of New Utilization Technologies*.

Hu, G. *et al.* (2010) 'An ecological floating bed made from dredged lake sludge for purification of eutrophic water', *Ecological Engineering*, 36, pp. 1448–1458.

Huang, P. *et al.* (2017) 'Mechanochemical activation of serpentine for recovering Cu (II) from wastewater', *Applied Clay Science*, 149(May), pp. 1–7.

Huang, R. *et al.* (2013) 'Recovery of valuable metals from electroplating sludge with reducing additives via vitri fi cation', 129, pp. 586–592.

Huijgen, W. and Comans, R. (2003) *Carbon Dioxide Sequestration By Mineral Carbonation*. Peten, NL.

Huijgen, W., Witkamp, G. and Comans, R. (2005) 'Mineral CO2 sequestration by steel slag carbonation', *Environmental Science and Technology*, 39, pp. 9676–9682.

Hull, S. L., Oty, U. V. and Mayes, W. M. (2014) 'Rapid recovery of benthic invertebrates downstream of hyperalkaline steel slag discharges', *Hydrobiologia*, 736(1), pp. 83–97.

Humbert, P. S. (2019) 'CO2 activated steel slag-based materials : A review', 208, pp. 448–457. doi: 10.1016/j.jclepro.2018.10.058.

Hussain, A. and Qazi, J. I. (2016) 'Application of sugarcane bagasse for passive anaerobic biotreatment of sulphate rich wastewaters', *Applied Water Science*, 6(2), pp. 205–211. doi: 10.1007/s13201-014-0226-2.

IAB (2016) *Relatório de sustentabilidade*. Rio de Janeiro. Available at: http://www.acobrasil.org.br/sustentabilidade/%0A.

Indian Bureau of Mines (2016) *Yearbook 2015*.

Ingvorsen, K., Nielsen, M. Y. and Joulian, C. (2003) 'Kinetics of bacterial sulfate reduction in an activated sludge plant', *FEMS Microbiology Ecology*, 46(2), pp. 129–137. doi: 10.1016/S0168-6496(03)00209-5.

International Council on Mining and Metals (2018) *The Value of Minerals and Metals*, *miningwithprinciples*.

International Energy Agency (2010a) *CO2 emissions from fuel combustion*. Available at: http://www.iea.org/co2highlights/%0ACO2highlights.pdf.

International Energy Agency (2010b) *Energy Technology Perspectives: Scenarios & Strategies To 2050*, *International Energy Agency (IEA) Publications*. doi: 10.1049/et:20060114.

Interstate Technology and Regulatory Council (2005) *Technical and Regulatory Guidance for In Situ Chemical Oxidation of Contaminated Soil and Groundwater*. Washington.

Irving, L. (1926) ‘The precipitation of Calcium and Magnesium from Sea Water’, *Journal of the Marine Biological Association*, 14(2), pp. 441–446. doi: 10.1017/S002531540000792X.

Islam, M. and Patel, R. (2011) ‘Thermal activation of basic oxygen furnace slag and evaluation of its fluoride removal efficiency’, *Chemical Engineering Journal*, 169(1–3), pp. 68–77. doi: 10.1016/j.cej.2011.02.054.

Ito, K. (2015) ‘Steelmaking Slag for Fertilizer Usage’, (109), pp. 130–136.

Jafaripour, A., Rowson, N. A. and Ghataora, G. S. (2015) ‘International Journal of Mineral Processing Utilisation of residue gas sludge (BOS sludge) for removal of heavy metals from acid mine drainage (AMD)’, *International Journal of Mineral Processing*, 144, pp. 90–96. doi: 10.1016/j.minpro.2015.10.002.

Jang, H. *et al.* (2014) ‘A study of the possibility of using TFT-LCD waste glass as an admixture for steam-cured PHC piles’, *Magazine of Concrete Research*, 66(4), pp. 196–208.

Japanese Society of Soil Science and Plant Nutrition (2002) *Silicic Acid and Crop Production*.

Al Jazeera (2019) *Toxic City: The Cost of Gold Mining in South Africa, Al Jazeera Special Series*.

Jiang, G. *et al.* (2016) ‘Wastewater-Enhanced Microbial Corrosion of Concrete Sewers’, *Environ. Sci. Technol.*, 50(15), pp. 8084–8092.

Jiang, Y. *et al.* (2018) ‘Characteristics of steel slags and their use in cement and concrete — A review’, *Resources, Conservation & Recycling*, 136(April), pp. 187–197. doi: 10.1016/j.resconrec.2018.04.023.

Jimenez-Castaneda, M. E. *et al.* (2020) ‘Generation of Alkalinity by Stimulation of Microbial Iron Reduction in Acid Rock Drainage Systems: Impact of Natural Organic Matter Types’, *Water, Air and Soil Pollution*, 231(472). doi: https://doi.org/10.1007/s11270-020-04820-7.

Jing, Z. *et al.* (2013) ‘Bioresource Technology UASB performance and electron competition between methane-producing archaea and sulfate-reducing bacteria in treating sulfate-rich wastewater containing ethanol and acetate’, *BIORESOURCE TECHNOLOGY*, 137, pp. 349–357. doi: 10.1016/j.biortech.2013.03.137.

Johnson, D. B. *et al.* (2009) ‘Sulfidogenesis at low pH by acidophilic bacteria and its potential for the selective recovery of transition metals from mine water’, *Advanced Materials Research*, 71(Trans Tech Publications Ltd.), pp. 693–696.

Johnson, D. B. and Hallberg, K. B. (2003) ‘The microbiology of acidic mine waters.’, *Res. Microbiol.*, 154(7), pp. 466–473.

Kadlec, R. H. (2009) ‘Comparison of free water and horizontal subsurface treatment wetlands’, *Ecological Engineering*, 35(2), pp. 159–174. doi: 10.1016/j.ecoleng.2008.04.008.

Kaduková, J. and Virčíková, E. (2005) ‘Comparison of differences between copper bioaccumulation and biosorption’, *Environment International*, 31(2), pp. 227–232. doi: 10.1016/j.envint.2004.09.020.

Kalkor (2021) ‘Kalkor Price List’. South Africa. Available at: https://kalkor.co.za/pricelist/.

Kambole, C. *et al.* (2017) ‘Basic oxygen furnace slag for road pavements : A review of material characteristics and performance for effective utilisation in southern Africa’, *Construction and Building Materials*, 148, pp. 618–631. doi: 10.1016/j.conbuildmat.2017.05.036.

Kanarbik, L. *et al.* (2014) ‘Environmental effects of soil contamination by shale fuel oils’, *Environmental Science and Pollution*, pp. 1–11.

Karamanov, A. *et al.* (1994) ‘Synthesis of wall-covering glass-ceramics from waste raw material’, *Glastech. Ber. Glass Sci. Technol.*, 67(8), pp. 227–231.

Kastyuchik, A., Karam, A. and Aïder, M. (2017) ‘The effect of electro-activation and eggshell powder on the neutralization of acid mine drainage’, *Journal of Sustainable Mining*, 16(3), pp. 73–82. doi: 10.1016/j.jsm.2017.09.002.

Kaur, G. *et al.* (2018) ‘Alternative neutralisation materials for acid mine drainage treatment’, *Journal of Water Process Engineering*, 22(November 2017), pp. 46–58. doi: 10.1016/j.jwpe.2018.01.004.

Kearney, L. (2012) *Mining and minerals in South Africa, Brand South Africa*.

Kefeni, K. K., Msagati, T. A. M. and Mamba, B. B. (2017) ‘Acid mine drainage : Prevention , treatment options , and resource recovery : A review’, *Journal of Cleaner Production*, 151, pp. 475–493. doi: 10.1016/j.jclepro.2017.03.082.

Keller, K. L., Wall, J. D. and Chhabra, S. (2011) ‘Methods in Enzymology’, in *Methods in Enzymology*. California, pp. 503–517. doi: https://doi.org/10.1016/B978-0-12-385075-1.00022-6.

Keterew, K. and Brilliance Mamba, B. (2020) ‘Evaluation of charcoal ash nanoparticles pollutant removal capacity from acid mine drainage rich in iron and sulfate’, *Journal of Cleaner Production*, 251, p. 119720. doi: 10.1016/j.jclepro.2019.119720.

Kikot, P. *et al.* (2010) ‘Study of the effect of pH and dissolved heavy metals on the growth of sulfate-reducing bacteria by a fractional factorial design’, *Hydrometallurgy*, 104(3–4), pp. 494–500. doi: 10.1016/j.hydromet.2010.02.026.

Kirby, C. S. and Cravotta III, C. A. (2005) ‘Net alkalinity and net acidity 1: Theoretical considerations’, *Applied Geochemistry*, 20, pp. 1920–1940. doi: 10.1016/j.apgeochem.2005.07.002.

Kislitsyn, B. F., Sas, R. I. and Golius, T. E. (1981) ‘Synthesis of sitalls from open hearth slag’, *Journal of Glass Ceramics*, 38(1–2), pp. 13–14.

Kloppers, C. and Fedotova, T. (2001) ‘Primary de-oxidation of Basic Oxygen Furnace steel by means of carbon’, (October), pp. 321–328.

Ko, M., Chen, Y. and Jiang, J. (2015) ‘Accelerated carbonation of basic oxygen furnace slag and the effects on its mechanical properties’, *Construction and Building Materials*, 98, pp. 286–293. doi: 10.1016/j.conbuildmat.2015.08.051.

Kumar, D. S. *et al.* (2019) ‘Measurement of metallic iron in steel making slags’, *Measurement*, 131, pp. 156–161. doi: 10.1016/j.measurement.2018.08.066.

Kundak, M., Lazic, L. and Crnko, J. (2009) ‘CO 2 EMISSIONS IN THE STEEL INDUSTRY’, *METALURGIJA*, 48(3), pp. 193–197. Available at: hrcak.srce.hr/file/56088.

Kuwahara, Y. and Yamashita, H. (2013) ‘A new catalytic opportunity for waste materials : Application of waste slag based catalyst in CO 2 fixation reaction’, *Biochemical Pharmacology*, 1, pp. 50–59. doi: 10.1016/j.jcou.2013.03.001.

Kuyucak, N. *et al.* (2012) ‘Implementation of a High Density Sludge HDS Treatment Process at the Boliden Apirsa Mine Site’, in *IMWA Proceedings 1999*. Sevilla, Spain: International Mine Water Association, pp. 473–479.

Labrenz, M. *et al.* (2000) ‘Formation of sphalerite (ZnS) deposits in natural biofilms of sulfate reducing bacteria’, *Science*, 290, pp. 1745–1747.

Labuschagne, P. F., Usher, B. H. and Matfield, F. (2005) ‘Geohydrological management approaches for site closure in South African gold mines’, in *Proc. Conference on Processing and Disposal of Industrial and Mining Waste*. Falmouth, United Kingdom: Minerals Engineering International.

Lackner, K. *et al.* (2002) ‘Carbonate chemistry for sequestering fossil carbon’, *Annual Reviews of Energy and the Environment*, 27, pp. 193–232.

Lategan, V. and Grubb, D. (2018) ‘BOF Slag leachate as Wine Grape Irrigation Water’. Johannesburg, South Africa: University of Stellenbosch.

Lehigh Environmental Initiative (2011) *Overview of Chemicals Available to Treat AMD (Active), Enviro Sci Inquiry*. Available at: https://ei.lehigh.edu/envirosci/enviroissue/amd/links/chem1.html#:~:text=For example%2C iron precipitation will,4 times more or greater). (Accessed: 6 February 2022).

Lei, S. *et al.* (2009) ‘Synthesis and morphological control of MnCO3 and Mn(OH)2 by a complex homogeneous precipitation method’, *Materials Chemistry and Physics*, 113(1), pp. 445–450. doi:

https://doi.org/10.1016/j.matchemphys.2008.07.114.

Lekakh, S. *et al.* (2008) 'Kinetics of aqueous leaching and carbonization of steelmaking slag', *Metallurgical and Materials Transactions B*, 39B, pp. 125–134.

Lewis, A. E. (2010) 'Hydrometallurgy Review of metal sulphide precipitation', 104, pp. 222–234. doi: 10.1016/j.hydromet.2010.06.010.

Lewis, R. A. (1998) *Lewis' Dictionary of Toxicology*. CRC Press.

Li, J. *et al.* (2020) 'Metagenomic insights into aniline effects on microbial community and biological sulfate reduction pathways during anaerobic treatment of high-sulfate wastewater', *Science of the Total Environment*, 742.

Li, M. *et al.* (2016) 'Effect of chlorine salt on the physical and mechanical properties of inshore saline soil treated with lime', *Soils and Foundations*, 56(3), pp. 327–335. doi: 10.1016/j.sandf.2016.04.001.

Li, X. *et al.* (2018) 'The bioenergetics mechanisms and applications of sulfate-reducing bacteria in remediation of pollutants in drainage: A review', *Ecotoxicology and Environmental Safety*, 158(March), pp. 162–170. doi: 10.1016/j.ecoenv.2018.04.025.

Li, Y. (1999) 'The use of waste basic oxygen furnace slag and hydrogen peroxide to degrade 4-chlorophenolLi, Y., 1999. The use of waste basic oxygen furnace slag and hydrogen peroxide to degrade 4-chlorophenol. , 19, pp.495–502.', *The use of waste basic oxygen furnace slag and hydrogen peroxide to degrade 4-chlorophenolLi, Y., 1999. The use of waste basic oxygen furnace slag and hydrogen peroxide to degrade 4-chlorophenol. , 19, pp.495–502.*, 19, pp. 495–502.

Li, Z. *et al.* (2013) 'Cementitious property modification of basic oxygen furnace steel slag', *Construction and Building Materials*, 48, pp. 575–579. doi: 10.1016/j.conbuildmat.2013.07.068.

Liamleam, W. and Annachhatre, A. . (2007) 'Electron donors for biological sulfate reduction.', *Biotechnol. Adv.*, 25, pp. 452–463.

Lim, M. W., Lau, E. Von and Poh, P. E. (2016) 'A comprehensive guide of remediation technologies for oil contaminated soil — Present works and future directions', *MPB*, 109(1), pp. 14–45. doi: 10.1016/j.marpolbul.2016.04.023.

Lin, C. C. and Lin, H. L. (2005) 'Remediation of Soil Contaminated with the Heavy Metal Cd2+', *Journal of Hazardous Materials*, 122, pp. 7–15. doi: 10.1016/j.jhazmat.2005.02.017.

Lin, K. L. *et al.* (2009) 'Recycling thin film transistor liquid crystal display (TFT-LCD) waste glass produced as glass-ceramics', *Journal of Cleaner Production*, 17(16), pp. 1499–1503. doi: 10.1016/j.jclepro.2009.05.012.

Lin, Y., Alva, G. and Fang, G. (2018) 'Review on thermal performances and applications of thermal energy storage systems with inorganic phase change materials', *Energy*, 165, pp. 685–708. doi: 10.1016/j.energy.2018.09.128.

Lindvall, M., Rutqvist, S. and Ye, G. (2010) 'Recovery from Dusts and Slags RECOVERY OF VANADIUM FROM V-BEARING BOF-SLAG USING AN EAF', in *Recovery from Dusts and Slags - The Twelfth International Ferroalloys Congress Sustainable Future*, pp. 189–196.

Liu, J. and Wang, D. (2017) 'Influence of steel slag-silica fume composite mineral admixture on the properties of concrete', *Powder Technology*, 320, pp. 230–238. doi: 10.1016/j.powtec.2017.07.052.

Liu, X., Gong, W. and Liu, L. (2014) 'Treatment of sulfate-rich and low pH wastewater by sulfate reducing bacteria with iron shavings in a laboratory', *Water Science Technology*, 69(3), pp. 595–600. doi: 10.2166/wst.2013.754.

Liu, Z. *et al.* (2015) 'A study of waste liquid crystal display generation in mainland China', *Waste Management and Research*, pp. 1–9. doi: 10.1177/0734242X15611736.

Lu, T. *et al.* (2018) 'Use of basic oxygen furnace slag fines in the production of cementitious mortars and the effects on mortar expansion', *Construction and Building Materials*, 167, pp. 768–774. doi: 10.1016/j.conbuildmat.2018.02.102.

Lyde, T. A. S. *et al.* (2014) 'Influence of suspended matters on iron and manganese presence in the Okpara Water Dam (Benin, West Africa)', *International Journal of Water Resources and Environmental Engineering*, 6(7), pp. 193–202. doi: 10.5897/ijwree2013.0433.

Ma, J. *et al.* (2014) 'Risk assessment of petroleumcontaminated soil using soil enzyme activities and genotoxicity to Vicia faba', *Ecotoxicology*, 23, pp. 665–673.

Macías, F. *et al.* (2012) 'From highly polluted Zn-rich acid mine drainage to non-metallic waters: Implementation of a multi-step alkaline passive treatment system to remediate metal pollution', *Science of the Total Environment*, 433(2012), pp. 323–330. doi: 10.1016/j.scitotenv.2012.06.084.

Magowo, W. (2014) *THE UTILISATION OF CELLULOSIC BIOMASS IN THE TREATMENT OF ACID MINE DRAINAGE AND THE SUBSEQUENT PRODUCTION OF FERMENTABLE SUGARS FOR BIOPROCESSING*. University of the Witwatersrand. doi: 10.1038/173017a0.

Mahieux, P., Aubert, J. and Escadeillas, G. (2009) 'Utilization of weathered basic oxygen furnace slag in the production of hydraulic road binders', *Construction and Building Materials*, 23(2), pp. 742–747. doi: 10.1016/j.conbuildmat.2008.02.015.

Malkoc, E. and Nuhoglu, Y. (2006) 'Removal of Ni(II) ions from aqueous solutions using waste of tea factory: Adsorption on a fixed-bed column', *Journal of Hazardous Materials*, 135(1–3), pp. 328–

336. doi: 10.1016/j.jhazmat.2005.11.070.

Mamba, B. B., Rietveld, L. C. and Verberk, J. Q. J. C. (2008) *SA Drinking Water Standards under the microscope*.

Manso, J. M. *et al.* (2006) 'Durability of concrete made with EAF slag as aggregate', *Cement and Concrete Composites*, 28(6), pp. 528–534. doi: 10.1016/j.cemconcomp.2006.02.008.

Mar, S. S. and Okazaki, M. (2012) 'Investigation of Cd contents in several phosphate rocks used for the production of fertilizer', *Microchemical Journal*, 104, pp. 17–21. doi: 10.1016/j.microc.2012.03.020.

Maree, J. *et al.* (2013) 'Neutralisation treatment of AMD at affordable cost', *Water SA*, 39(2). doi: 1816-7950.

Maree, J. P., Tonder, G. J. van and Mitlard, P. (1996) *Underground Neutralization of Mine Water with Limestone*. WRC Report. Edited by Water Environment and Forestry Technology. Pretoria, South Africa: Water Research Commission.

Martins, M. *et al.* (2010) 'Production of irrigation water from bioremediation of acid mine drainage : comparing the performance of two representative systems', *Journal of Cleaner Production*, 18(3), pp. 248–253. doi: 10.1016/j.jclepro.2009.10.013.

Mashala, P. (2012) 'Controlling acid mine drainage in the Western Basin not enough', *Farmer's Weekly*, 6 December. Available at: https://www.farmersweekly.co.za/agri-news/south-africa/controlling-acid-mine-drainage-in-the-western-basin-not-enough/.

Masindi, V., Suhail, M. and Abu-mahfouz, A. M. (2017) 'Integrated treatment of acid mine drainage using BOF slag , lime / soda ash and reverse osmosis (RO): Implication for the production of drinking water', *Desalination*, 424(October), pp. 45–52. doi: 10.1016/j.desal.2017.10.002.

Maslehuddin, M. *et al.* (2003) 'Comparison of properties of steel slag and crushed limestone aggregate concretes', *Construction and Building Materials*, 17(2), pp. 105–112. doi: 10.1016/S0950-0618(02)00095-8.

Masoudi, S. M., Ezzati, E. and Moradzadeh, A. (2017) 'Geoeconomics of fluorspar as strategic and critical mineral in Iran', *Resources Policy*, 52(February), pp. 100–106. doi: 10.1016/j.resourpol.2016.11.007.

Matthaiou, V. *et al.* (2019) 'Valorization of steel slag towards a Fenton-like catalyst for the degradation of paraben by activated persulfate', *Chemical Engineering Journal*, 360(May 2018), pp. 728–739. doi: 10.1016/j.cej.2018.11.198.

Mayes, W. M. and Younger, P. L. (2006) 'Buffering of Alkaline Steel Slag Leachate across a Natural

Wetland', *Environmental Science and Technology*, 40(4), pp. 1237–1234. doi: 10.1021/es051304u.

Mayes, W. M., Younger, P. L. and Aumônie, J. (2008) 'Hydrogeochemistry of Alkaline Steel Slag Leachates in the UK', *Water, Air and Soil Pollution*, 195(1–4), pp. 35–50.

McCafferty, E. (2010) *Introduction to Corrosion Science*. illustrate. Springer Science & Business Media.

Mccarthy, T. S., Africa, S. and Africa, S. (2011) 'The impact of acid mine drainage in South Africa', 107, pp. 1–7. doi: 10.4102/sajs.v107i5/6.712.

Metcalf & Eddy *et al.* (2014) *Wastewater Engineering: Treatment and Resource Recovery*. Fifth. New York: McGraw-Hill Inc.

Meyer, D. *et al.* (2012) 'Phosphate removal from synthetic and real wastewater using steel slags produced in Europe', 6, pp. 2–10. doi: 10.1016/j.watres.2012.02.012.

Mihaela, C. and Rosa, E. (2019) 'A review of the implications and challenges of manganese removal from mine drainage', *Chemosphere*, 214, pp. 491–510. doi: 10.1016/j.chemosphere.2018.09.106.

Mills, K. C., Yuan, L. and Jones, R. T. (2011) 'Estimating the physical properties of slags', *Journal of the Southern African Institute of Mining and Metallurgy*, 111(10), pp. 649–658.

Mineralpedia (2020) *Pyrite, Dakota Matrix Minerals*.

Ministry of Economic Development NZ Petroleum & Minerals (2013) *Mineral Resources*.

Mo, L. *et al.* (2017) 'Accelerated carbonation and performance of concrete made with steel slag as binding materials and aggregates', *Cement and Concrete Composites*, 83, pp. 138–145. doi: 10.1016/j.cemconcomp.2017.07.018.

Mohan, D. and Pittman, C. U. (2007) 'Arsenic removal from water / wastewater using adsorbents — A critical review', 142, pp. 1–53. doi: 10.1016/j.jhazmat.2007.01.006.

Mokhena, T. C. *et al.* (2017) 'Sugarcane bagasse and cellulose polymer composites', *Sugarcane Technology and Research*, IntechOpen, pp. 225–240.

Momot, O. and Synzynys, B. (2005) 'Toxic Aluminium and Heavy Metals in Groundwater of Middle Russia: Health Risk Assessment', *International Journal of Environmental Research in Public Health*, 2(2), pp. 214–218. doi: 10.3390/ijerph2005020003.

Moodley, I. *et al.* (2018) 'Environmentally sustainable acid mine drainage remediation : Research developments with a focus on waste / by-products', *Minerals Engineering*, 126(August 2017), pp. 207–220. doi: 10.1016/j.mineng.2017.08.008.

Morel, F. M. M. and Hering, J. G. (1993) *Principles and Applications of Aquatic Chemistry: A Wiley-Interscience publication*. illustrate. New York: Wiley.

Moreno-González, R. *et al.* (2022) 'Temporal evolution of acid mine drainage (AMD) leachates from the abandoned tharsis mine (Iberian Pyrite Belt, Spain)', *Environmental Pollution*, 295, p. 118697. doi: 10.1016/j.envpol.2021.118697.

Mori, T. *et al.* (1991) 'Microbial Corrosion of Concrete Sewer Pipes, H2S Production from Sediments and Determination of Corrosion Rate', *Water Science and Technology*, 23(7), pp. 1275–1282.

Morrissey, C. (2003) 'Mining's Malignant Menace', *Review Magazine*, pp. 1–8.

Mtero, F. (2017) 'Rural livelihoods, large-scale mining and agrarian change in Mapela, Limpopo, South Africa', *Resources Policy*, 53(June), pp. 190–200.

Munawar, A. and Riwandi (2010) 'Chemical characteristics of organic wastes and their potential use for acid mine drainage remediation', *Journal of Nature Indonesia*, 12(2), pp. 167–172. doi: 10.31258/jnat.12.2.167-172.

Munns, R. and Gilliham, M. (2015) 'Salinity tolerance of crops – what is the cost?', *New Phytologist*, 208(3), pp. 668–673.

Nag, S. K. (2009) 'Quality of groundwater in parts of ARSA block, Purulia District, West Bengal', *Bhu-Jal*, 4(1), pp. 58–64.

Naicker, K., Cukrowska, E. and Mccarthy, T. S. (2003) 'Acid mine drainage arising from gold mining activity in Johannesburg , South Africa and environs', 122, pp. 29–40.

Naidoo, K. (2021) 'Indicative cost of pure hydrated powdered lime interview'. Johannesburg, South Africa: Kelnir Projects.

Naidoo, S. *et al.* (2009) 'The Global Context of AMD', in *Acid Mine Drainage in South Africa*. Springer Briefs, pp. 1–2. doi: 10.1007/978-3-319-44435-2.

Naidu, R. *et al.* (2015) 'Towards bioavailability-based soil criteria : past , present and future perspectives', *Environmental Science and Pollution Research*, 22, pp. 8779–8785. doi: 10.1007/s11356-013-1617-x.

Naidu, T. S. *et al.* (2017) *Design of Acid Mine Drainage Remediation Plant (Deliverable 1)*. Pretoria, South Africa.

Naidu, T. S. *et al.* (2018) 'Passive acid mine drainage remediation using BOF steel slag and sugarcane bagasse', in Theodossiou, N. et al. (eds) *Protection and restoration of the environment XIV*. Thessaloniki: ARISTOTLE UNIVERSITY OF THESSALONIKI, pp. 438–447. doi: 978-960-99922-

4-4.

Naidu, T. S. *et al.* (2019) ‘Acid Mine Drainage Pilot Remediation System using Waste Products from the Steel Manufacturing and Sugar Industries’, in Wolkersdorfer, C. et al. (eds) *IMWA 2019 “Mine Water: Technological and Ecological Challenges"*. Perm: International Mine Water Association, pp. 121–126. doi: 978-5-91252-145-4.

Naidu, T. S. (2019) ‘GET TALKING – ACID MINE DRAINAGE’, *Materials World Magazine*, November. Available at: https://www.iom3archive.org.uk/materials-world-magazine/news/2019/nov/27/get-talking-acid-mine-drainage.

Naidu, T. S., Chauhan, D., *et al.* (2020) ‘An assessment of basic oxygen furnace slag dissolution for application in AMD dam remediation using waste products from the steel manufacturing and sugar industries’, in Baker, J. et al. (eds) *Tailing storage conference 2020: Investing in a Sustainable Future*. Johannesburg: The Southern African Institute of Mining and Metallurgy; Camera Press, Johannesburg, pp. 51–62.

Naidu, T. S. (2020) ‘Aquaponic Farming using Nutrient Rich Mining Wastewater streams from unrehabilitated mines’. Johannesburg: University of the Witwatersrand.

Naidu, T. S., van Dyk, L. D., *et al.* (2020) ‘Sugar and Steel By-Product Utilization in Acid Mine Drainage Remediation’, *Journal of Hazardous, toxic and radioactive waste*, 24(1), pp. 1–10. doi: 10.1061/(ASCE)HZ.2153-5515.0000472.

Naidu, T. S., van Dyk, L. . and Sheridan, C. . (2021) ‘The Use of Basic Oxygen Furnace Slag as a Substitute for Lime in Acid Mine Drainage Treatment’, in van Dyk, L. et al. (eds) *Proceedings of the South African Chemical Engineering Congress 2021 (A virtual , international conference organised by the South African Institution of Chemical Engineers - an association for the advancement of Chemical Engineering in South Africa)*. Johannesburg: The South African Institution of Chemical Engineers, pp. 156–166.

Naidu, T. S., van Dyk, L. and Sheridan, C. (2018) ‘Piloting a combined metallurgical slag /sugarcane bagasse process for treating acid mine drainage’, in *IWA World Water Congress & Exhibition 2018*. Tokyo, Japan: IWA - The International Water Association. Available at: https://efbe03b3-8c3b-494d-87ee-fcbe848d67c4.filesusr.com/ugd/a621ea_14a21142540a4bb5aa6d5be84ae2252a.pdf.

Naidu, T. S., Sheridan, C. M. and van Dyk, L. D. (2020) ‘Basic oxygen furnace slag: Review of current and potential uses’, *Minerals Engineering*, 149(February), p. 106234. doi: 10.1016/j.mineng.2020.106234.

Naidu, T. S., Sheridan, C. M. and van Dyk, L. D. (2021) *Design of Acid Mine Drainage Remediation Plant*. Pretoria, South Africa: WRC. Available at: http://www.wrc.org.za/wp-

content/uploads/mdocs/2757 final.pdf.

Name, T. and Sheridan, C. (2014) ‘Remediation of acid mine drainage using metallurgical slags’, *Minerals Engineering*, 64, pp. 15–22. doi: 10.1016/j.mineng.2014.03.024.

National Center for Biotechnology Information (2021) ‘PubChem Compound Summary for CID 1117, Sulfate’. Available at: https://pubchem.ncbi.nlm.nih.gov/compound/Sulfate.

National Center for Biotechnology Information (2022a) *PubChem Compound Summary for CID 10112, Calcium carbonate, PubChem*. Available at: https://pubchem.ncbi.nlm.nih.gov/compound/Calcium-carbonate. (Accessed: 1 February 2022).

National Center for Biotechnology Information (2022b) *PubChem Compound Summary for CID 11248, Ferrous carbonate, PubChem*. Available at: https://pubchem.ncbi.nlm.nih.gov/compound/Ferrous-carbonate. (Accessed: 6 February 2022).

National Research Council (2002) *Evolutionary and Revolutionary Technologies for Mining*. Washington, DC: The National Academies Press. doi: https://doi.org/10.17226/10318.

Nayak, A. and Bhushan, B. (2019) ‘An overview of the recent trends on the waste valorization techniques for food wastes’, *Journal of Environmental Management*, 233(July 2018), pp. 352–370. doi: 10.1016/j.jenvman.2018.12.041.

Ndlovu, S., Simate, G. S. and Matinde, E. (2017) *Waste Production and Utilization in the Metal Extraction Industry*. 1st Editio. Johannesburg, South Africa: CRC Press.

Nkosi, V. (2018) *How mine dumps in South Africa affect the health of communities living nearby, The Conversation*.

Nolan, T. B. and Udall, S. L. (1962) *Chemistry of Iron in Natural Water*. Washington.

Nordstrom, D. K. (1982) ‘The effect of sulfate on aluminum concentrations in natural waters: some stability relations in the system Al2O3-SO3-H2O at 298 K’, *Geochimica et Cosmochimica Acta*, 46(4), pp. 681–692. doi: 10.1016/0016-7037(82)90168-5.

Norris, P. R. *et al.* (1996) ‘Characteristics of Sulfobacillus acidophilus sp. nov. and other moderately thermophilic mineral-sul- phide-oxidizing bacteria’, *Microbiology*, 142(4), pp. 775–783.

Núñez-Gómez, D. *et al.* (2019) ‘Adsorption of heavy metals from coal acid mine drainage by shrimp shell waste: Isotherm and continuous-flow studies’, *Journal of Environmental Chemical Engineering*, 7(1), p. 102787. doi: 10.1016/j.jece.2018.11.032.

Olsson, N. *et al.* (2018) ‘Cement and Concrete Research Unsaturated ion di ff usion in cementitious materials – The e ff ect of slag and silica fume’, 108(April), pp. 31–37. doi:

10.1016/j.cemconres.2018.03.007.

Ortiz, P. S. and Oliveira, S. de (2014) 'Exergy analysis of pretreatment processes of bioethanol production based on sugarcane bagasse', *Energy*, 76, pp. 130–138.

Othman, A., Sulaiman, A. and Sulaiman, S. K. (2017) 'The use of quicklime in acid mine drainage treatment', *Chemical Engineering Transactions*, 56, pp. 1585–1590. doi: 10.3303/CET1756265.

Othmer, K. (1995) *Kirk-Othmer Encyclopedia of Chemical Technology*. 4th Editio. New York: John Wiley and Sons.

Oyekola, O. O., van Hille, R. P. and Harrison, S. T. L. (2010) 'Kinetic analysis of biological sulphate reduction using lactate as carbon source and electron donor: Effect of sulphate concentration', *Chemical Engineering Science*, 65(16), pp. 4771–4781. doi: 10.1016/j.ces.2010.05.014.

Park, I. *et al.* (2019) 'A review of recent strategies for acid mine drainage prevention and mine tailings recycling', *Chemosphere*, 219, pp. 588–606.

Park, J. *et al.* (2016) 'Enhancement of phosphorus removal with near-neutral pH utilizing steel and ferronickel slags for application of constructed wetlands', *Ecological Engineering*, 95, pp. 612–621. doi: 10.1016/j.ecoleng.2016.06.052.

Park, J. *et al.* (2017) 'Phosphate removal in constructed wetland with rapid cooled basic oxygen furnace slag', *Chemical Engineering Journal*, 327, pp. 713–724. doi: 10.1016/j.cej.2017.06.155.

Park, J. *et al.* (2019) 'E ff ective latent heat thermal energy storage system using thin fl exible pouches', *Sustainable Cities and Society*, 45(July 2018), pp. 143–150. doi: 10.1016/j.scs.2018.10.046.

Pathirage, U. *et al.* (2012) 'Armouring by precipitates and the associated reduction in hydraulic conductivity of recycled concrete aggregates used in a novel PRB for the treatment of acidic groundwater', in *11th Australia New Zealand Conference on Geomechanics*. Melbourne.

Patil, A. *et al.* (2013) *Aluminum fact sheet*. Illinois.

Pavlineri, N., Th, N. and Tsihrintzis, V. A. (2017) 'Constructed Floating Wetlands : A review of research , design , operation and management aspects , and data meta-analysis', *Chemical Engineering Journal*, 308, pp. 1120–1132. doi: 10.1016/j.cej.2016.09.140.

Pereira, C. F. et al (2009) 'Waste stabilization/solidification of an electric arc furnace dust using fly ash-based geopolymers', 88(7), pp. 1185–1193.

Pereira, T. C. B. *et al.* (2020) 'Acid mine drainage (AM) treatment by neutralization : Evaluation of physical-chemical performance and ecotoxicological effects on zebra fish (Danio rerio) development', *Chemosphere*, 253, pp. 1–9. doi: 10.1016/j.chemosphere.2020.126665.

Pérez-López, R. *et al.* (2010) 'Neutralization of acid mine drainage using the final product from CO2 emissions capture with alkaline paper mill waste', *Journal of Hazardous Materials*, 177(1–3), pp. 762–772. doi: 10.1016/j.jhazmat.2009.12.097.

Piatak, N. M., Parsons, M. B. and Seal, R. R. (2015) *Applied Geochemistry Characteristics and environmental aspects of slag : A review*, *Applied Geochemistry*. Elsevier Ltd. doi: 10.1016/j.apgeochem.2014.04.009.

Pistocchi, C. *et al.* (2017) 'Exchangeable Sodium Percentage decrease in saline sodic soil after Basic Oxygen Furnace Slag application in a lysimeter trial', *Journal of Environmental Management*, pp. 1–11. doi: 10.1016/j.jenvman.2017.05.007.

Potgieter-Vermaak, S. S. *et al.* (2006) 'Comparison of limestone, dolomite and fly ash as pre-treatment agents for acid mine drainage', *Minerals Engineering*, 19, pp. 454–462.

Power, G., Graefe, M. and Klauber, C. (2011) 'Bauxite residue issues: I. Current management, disposal and storage practices', *Hydrometallurgy*, 108, pp. 33–45. doi: https://doi.org/10.1016/j.hydromet.2011.02.006.

Pradhan, N. *et al.* (2008) 'Heap bioleaching of chalcopyrite: A review', *Minerals Engineering*, 21(5), pp. 355–365. doi: 10.1016/j.mineng.2007.10.018.

Proctor, D. M. *et al.* (2000) 'Physical and Chemical Characteristics of Blast Furnace , Basic Oxygen Furnace , and Electric Arc Furnace Steel Industry Slags', 34(8), pp. 1576–1582. doi: 10.1021/es9906002.

Proctor, D. M. *et al.* (2010) 'Human and Ecological Risk Assessment Assessment of Human Health and Ecological Risks Posed by the Uses of Steel-Industry Slags in the Environment Assessment of Human Health and Ecological Risks Environment', *Human and Ecological Risk Assessment*, 8(4), pp. 681–711. doi: 10.1080/20028091057150.

Proffitt, T. and Campbell-Clause, J. (2012) 'Managing grapevine nutrition and vineyard soil health', p. 29.

Ptacek, C. J. *et al.* (2003) 'The Geochemistry of Acid Mine Drainage', in Holland, H. D. and Turekian, K. K. (eds) *Treatise on Geochemistry*. Elsevier, pp. 149–204.

Puente, G. de la *et al.* (1997) 'Thermal stability of oxygenated functions in activated carbons', *Journal of Analytical Applied Pyrolysis*, 43, pp. 125–138.

Qin, J. *et al.* (2019) 'Active treatment of acidic mine water to minimize environmental impacts in a densely populated downstream area', *Journal of Cleaner Production*, 210, pp. 309–316. doi: 10.1016/j.jclepro.2018.11.029.

Quader, M. A. *et al.* (2015) ‘A comprehensive review on energy ef fi cient CO 2 breakthrough technologies for sustainable green iron and steel manufacturing’, 50, pp. 594–614. doi: 10.1016/j.rser.2015.05.026.

Ramadass, K. *et al.* (2015) ‘Ecological implications of motor oil pollution: earthworm survival and soil health.’, *Soil Biology and Biochemistry*, 85, pp. 72–81.

Ramakrishna, K. R. and Viraraghavan, T. (1997) ‘Use of slag for dye removal’, *Journal of waste management*, 17, pp. 483–488.

Ramla, B. and Sheridan, C. (2015) ‘The potential utilisation of indigenous South African grasses for acid mine drainage remediation’, *Water SA*, 41(2), pp. 247–252. doi: 10.4314/wsa.v41i2.10.

Ranjan, R. (2019) ‘Assessing the impact of mining on deforestation in India’, 60(October 2018), pp. 23–35.

Rashad, A. (2016) ‘Cementitious materials and agricultural wastes as natural fi ne aggregate replacement in conventional mortar and concrete’, *Journal of Building Engineering*, 5, pp. 119–141. doi: 10.1016/j.jobe.2015.11.011.

Reardon, E. J. and Wang, Y. (2000) ‘A Limestone Reactor for fluoride removal from wastewaters’, *Journal of Environmental Science and Technology*, 34, pp. 3247–3253.

Reddy, A. S., Pradhan, R. K. and Chandra, S. (2006) ‘Utilization of Basic Oxygen Furnace (BOF) slag in the production of a hydraulic cement binder’, *International Journal of Mineral Processing*, 79(2), pp. 98–105. doi: 10.1016/j.minpro.2006.01.001.

Reddy, K. R. *et al.* (2018) ‘CO2 SEQUESTRATION USING BOF SLAG: APPLICATION IN LANDFILL COVER’, in *Protection and restoration of the environment XIV*. Thessaloniki, pp. 392–401.

Reddy, K. R., Grubb, D. G. and Kumar, G. (2018) ‘INNOVATIVE BIOGEOCHEMICAL SOIL COVER TO MITIGATE LANDFILL GAS EMISSIONS’, in *Protection and restoration of the environment XIV*. Thessaloniki, pp. 383–391.

Reis, M. *et al.* (1992) ‘Effect of hydrogen sulfide on growth of sulfate reducing bacteria’, *Biotechnol Bioeng*, 40(5), pp. 593–600. doi: 10.1002/bit.260400506.

Remus, R. and Roudier, S. (2010) *JRC REFERENCE REPORT Best Available Techniques (BAT) Reference Document for Iron and Steel Production (Integrated Pollution Prevention and Control)*. doi: 10.2791/97469.

Reuter, M., Xiao, Y. and Boin, U. (2004) ‘Recycling and environmental issues of metallurgical slags and salt fluxes’, pp. 349–356.

Riley, A. L. and Mayes, W. M. (2015) ‘Long-term evolution of highly alkaline steel slag drainage waters’, *Environmental Monitoring and Assessment*. doi: 10.1007/s10661-015-4693-1.

Rimstidt, J. D. and Vaughan, D. J. (2003) ‘Pyrite oxidation : A state-of-the-art assessment of the reaction mechanism’, *Geochimica et Cosmochimica Acta*, 67(5), pp. 873–880. doi: 10.1016/S0016-7037(02)01165-1.

Roadcap, G. *et al.* (2006) ‘Extremely alkaline (pH>12) ground water hosts diverse microbial community’, *Ground Water*, 44(4), pp. 511–517. doi: 10.1111/j.1745-6584.2006.00199.x.

Roadcap, G., Kelly, W. and Bethke, C. (2005) ‘Geochemistry of extremely alkaline (pH>12) ground water in slag-fill aquifer.’, *Groundwater*, 43, pp. 806–816.

Rodda, N., Armitage, N. and Carden, K. (2014) *Sustainable Use of Greywater in Small-Scale Agriculture and Gardens in South Africaa*. Kwazulu Natal.

Romero, M. and Rincón, J. M. (1999) ‘Surface and Bulk Crystallization of Glass-Ceramic in the Na2O-CaO-ZnO-PbO-Fe2O3-Al2O3-SiO2 System Derived from a Goethite Waste’, *Journal of American Ceramic Society*, 82(5), pp. 1313–1317. doi: 10.1007/s11947-009-0181-3.

Romero, S. C. *et al.* (2015) ‘The potential role of aluminium hydroxysulfates in the removal of contaminants in acid mine drainage’, *Chemical Geology*, 417, pp. 414–423. doi: https://doi.org/10.1016/j.chemgeo.2015.10.020.

Rossouw, S., Sheridan, C. and Hille, R. Van (2019) ‘An Evaluation of Sugarcane Bagasse as a Feedstock in a Biological Treatment System for Mine Affected Waters’, in Wolkersdorfer, C. et al. (eds) *IMWA 2019 “Mine Water: Technological and Ecological Challenges"*. Perm: International Mine Water Association, pp. 134–139.

Royal Society of Chemistry (2020) *ChemSpider*.

RSA Department of Trade and Industry (2018) ‘Status of the SA steel industry’. Cape Town, South Africa: RSA Department of Trade and Industry.

Ryan, M. J., Kney, A. D. and Carley, T. L. (2017) ‘A study of selective precipitation techniques used to recover refined iron oxide pigments for the production of paint from a synthetic acid mine drainage solution’, *Applied Geochemistry*, 79, pp. 27–35. doi: 10.1016/j.apgeochem.2017.01.019.

Saha, S., Reza, A. S. and Kanti Roy, M. (2019) ‘Hydrochemical evaluation of groundwater quality of the Tista floodplain, Rangpur, Bangladesh’, *Applied Water Science*, 9, p. 198. doi: https://doi.org/10.1007/s13201-019-1085-7.

Sánchez-Andrea, I. *et al.* (2013) ‘Enrichment and isolation of acidophilic sulfate-reducing bacteria from Tinto River sediments’, *Environ Microbiol Rep*, 5(5), pp. 672–678. doi: 10.1111/1758-

2229.12066.

Sánchez-España, J. *et al.* (2005) ‘Acid mine drainage in the Iberian Pyrite Belt (Odiel river watershed, Huelva, SW Spain): Geochemistry, mineralogy and environmental implications’, *Applied Geochemistry*, 20, pp. 1320–1356. doi: 10.1016/j.apgeochem.2005.01.011.

Sánchez España, J. *et al.* (2006) ‘The removal of dissolved metals by hydroxysulphate precipitates during oxidation and neutralization of acid mine waters, Iberian Pyrite Belt’, *Aquatic Geochemistry*, 12(3), pp. 269–298. doi: 10.1007/s10498-005-6246-7.

Sawe, B. E. (2017) *Top 10 Steel Producing Countries In The World*, *www.worldatlas.com*.

Sayed, F. N. and Polshettiwar, V. (2015) ‘Facile and Sustainable Synthesis of Shaped Iron Oxide Nanoparticles: Effect of Iron Precursor Salts on the Shapes of Iron Oxides’, *Scientific Reports*, 5(May). doi: 10.1038/srep09733.

Schippers, A. and Sand, W. (1999) ‘Bacterial Leaching of Metal Sulfides Proceeds by Two Indirect Mechanisms via Thiosulfate or via Polysulfides and Sulfur’, *Applied Environmental Microbiology*, 65(1), pp. 319–321.

Sekhar, C., Lucelinda, M. and Sandström, Å. (2009) ‘Hydrometallurgy Comparative study on different steel slags as neutralising agent in bioleaching’, *Hydrometallurgy*, 95(3–4), pp. 190–197. doi: 10.1016/j.hydromet.2008.05.042.

Sen, A. M. and Johnson, B. (1999) ‘Acidophilic sulphate-reducing bacteria: candidates for bioremediation of acid mine drainage’, *Process Metallurgy*, 9. doi: https://doi.org/10.1016/S1572-4409(99)80073-X.

Sephton, M. G., Webb, J. A. and McKnight, S. (2019) ‘Applications of Portland cement blended with fly ash and acid mine drainage treatment sludge to control acid mine drainage generation from waste rocks’, *Applied Geochemistry*, 103(February), pp. 1–14. doi: 10.1016/j.apgeochem.2019.02.005.

Seyfaee, A. *et al.* (2021) ‘Integration assessment of the hybrid sulphur cycle with a copper production plant’, *Energy Conversion and Management*, 249, p. 114832. doi: 10.1016/j.enconman.2021.114832.

Shen, D. H., Wu, C. M. and Du, J. C. (2009) ‘Laboratory investigation of basic oxygen furnace slag for substitution of aggregate in porous asphalt mixture’, *Construction and Building Materials*, 23(1), pp. 453–461. doi: 10.1016/j.conbuildmat.2007.11.001.

Shen, F. *et al.* (2003) ‘Electrochemical removal of fluoride ions from industrial wastewater’, *Journal of Chemical Engineering Sciences*, 58, pp. 987–993.

Shen, H. and Forssberg, E. (2003) ‘An overview of recovery of metals from slags’, 23, pp. 933–949. doi: 10.1016/S0956-053X(02)00164-2.

Sheoran, A. S. and Sheoran, V. (2006) 'Heavy metal removal mechanism of acid mine drainage in wetlands: A critical review', *Minerals Engineering*, 19(2), pp. 105–116. doi: 10.1016/j.mineng.2005.08.006.

Sheridan, C. *et al.* (2012) 'A comparison of charcoal- and slag-based constructed wetlands for acid mine drainage remediation', 39(3), pp. 369–374.

Shi, C., Jiménez, A. F. and Palomo, A. (2011) 'Cement and Concrete Research New cements for the 21st century : The pursuit of an alternative to Portland cement', 41, pp. 750–763. doi: 10.1016/j.cemconres.2011.03.016.

Silbergeld, E. K. (2016) 'Health risks at different scales of mining', *Toxicology Letters*, 259S, pp. 4–62.

Silver, J. (2012) *Chemistry of Iron*. Illustrate. Springer Science & Business Media.

Simate, G. S. and Ndlovu, S. (2014) 'Acid mine drainage: Challenges and opportunities', *Journal of Environmental Chemical Engineering*, 2(3), pp. 1785–1803. doi: 10.1016/j.jece.2014.07.021.

Skousen, J. G., Ziemkiewicz, P. F. and McDonald, L. M. (2019) 'Acid mine drainage formation, control and treatment: Approaches and strategies', *Extractive Industries and Society*, 6(1), pp. 241–249. doi: 10.1016/j.exis.2018.09.008.

Skousen, J. and Ziemkiewicz, P. (2005) 'Performance of 116 Passive Treatment Systems for Acid Mine Drainage', *Journal American Society of Mining and Reclamation*, 2005(1), pp. 1100–1133. doi: 10.21000/JASMR05011100.

Smith, J. (2018) 'The Determination of Acidity of Water and Waste Water Samples by Potentiometric Titration'. Johannesburg, South Africa.

Smith, P. *et al.* (2015) 'Biogeochemical cycles and biodiversity as key drivers of', *Soil*, 1, pp. 665–685. doi: 10.5194/soil-1-665-2015.

Solomon, F. (2008) *Impacts of Metals on Aquatic Ecosystems and Human Health*.

Somvanshi, A. (2015) *Concrete without sand?*, *DowntToEarth*.

Souter, L. and Watmough, S. A. (2017) 'Science of the Total Environment Geochemistry and toxicity of a large slag pile and its drainage complex in', *Science of the Total Environment*, 605–606, pp. 461–470. doi: 10.1016/j.scitotenv.2017.06.237.

Souza, A. P. de *et al.* (2014) 'Sugarcane as a Bioenergy Source: History, Performance, and Perspectives for Second-Generation Bioethanol', *Bioenergy Research*, 7, pp. 24–35.

Stadler, S. A. C., Eksteen, J. J. and Aldrich, C. (2007) 'An experimental investigation of foaming in

acidic , high Fe x O slags', 20, pp. 1121–1128. doi: 10.1016/j.mineng.2007.01.013.

Steenkamp, J. D. and Preez, L. (2015) 'Introduction to the production of clean steel', 115(May), pp. 557–561.

Strandkvist, I. (2016) *Dissolution Study of Common Ferrous Slag Minerals*. Luleå University of Technology.

Sung Ahn, J. *et al.* (2003) *Arsenic Removal Using Steel Manufacturing By-Products as Permeable Reactive Materials in Mine Tailing Containment Systems*, *Water research*. doi: 10.1016/S0043-1354(02)00637-1.

Swallow, M. J. B. and Sullivan, G. O. (2019) 'Biomimicry of vascular plants as a means of saline soil remediation', *Science of the Total Environment*, 655, pp. 84–91. doi: 10.1016/j.scitotenv.2018.11.245.

Swartz, P. (2021) 'AgLime Price List'. Johannesburg, South Africa.

Tanaka, H. (2015) 'Resources Trend and Use of Direct Reduced Iron in Steelmaking Process', *KOBELCO TECHNOLOGY REVIEW*, 33, pp. 1–7.

Tang, J. *et al.* (2011) 'Eco-toxicity of petroleum hydrocarbon contaminated soil', *Journal of Environmental Sciences*, 23, pp. 845–851.

Tang, K., Baskaran, V. and Nemati, M. (2009) 'Bacteria of the sulphur cycle: An overview of microbiology, biokinetics and their role in petroleum and mining industries', *Biochemical Engineering Journal*, 44(1), pp. 73–94. doi: 10.1016/j.bej.2008.12.011.

Tang, S. *et al.* (2015) 'ScienceDirect Effect of dissolved oxygen concentration on iron efficiency : Removal of three chloroacetic acids', *Water Research*, 73, pp. 342–352. doi: 10.1016/j.watres.2015.01.027.

Tangahu, B. V. *et al.* (2011) 'A Review on Heavy Metals (As, Pb, and Hg) Uptake by Plants through Phytoremediation', *International Journal of Chemical Engineering*, 2011, p. 31. doi: https://doi.org/10.1155/2011/939161.

Tatsuhara, T. *et al.* (2012) 'Combined neutralization – adsorption system for the disposal of hydrothermally altered excavated rock producing acidic leachate with hazardous elements', *Engineering Geology*, 139–140, pp. 76–84. doi: 10.1016/j.enggeo.2012.04.006.

Tchobanoglous, G. *et al.* (2014) *Wastewater Engineering Treatment and Resource Recovery*. 5th Editio. New York: McGraw Hill Education.

Teir, S. *et al.* (2007) 'PAPER II Dissolution of steelmaking slags in acetic acid for precipitated calcium carbonate production', 32(4), pp. 528–539. doi: 10.1016/j.energy.2006.06.023.

The Editors of Encyclopaedia Britannica (2020) ‘Biogeochemical Cycle’, in *Encyclopedia Britannica*. Available at: https://www.britannica.com/science/biogeochemical-cycle.

The Groundwater Association (1999) *Dissolved Mineral Sources and Significance, Ground Water Hydrology for Water Well Contractors*.

The Water Center (2018) *Impacts of Aluminium on Aquatic Organisms and EPA’s Aluminium Criteria, University of Pennsylvania*.

Tipping, E. *et al.* (1988) ‘Conditions required for the precipitation of aluminium in acidic natural waters’, *Water Research*, 22, pp. 585–592. doi: https://doi.org/10.1016/0043-1354(88)90059-0.

du Toit, D. (2018) *The heat of acid mine drainage, University of the Witwatersrand: Research News*.

Tolonen, E. *et al.* (2014) ‘Acid mine drainage treatment using by-products from quicklime manufacturing as neutralization chemicals’, *Chemosphere*, 117, pp. 419–424. doi: 10.1016/j.chemosphere.2014.07.090.

Tongaat Hulett and Department of Energy (RSA) (2013) ‘Sugarcane Potential: Food and Energy’. Tongaat: Department of Energy South Africa.

Tossavainen, M. *et al.* (2007) ‘Characteristics of steel slag under different cooling conditions’, 27, pp. 1335–1344. doi: 10.1016/j.wasman.2006.08.002.

Tran, T. T. T. *et al.* (2021) ‘Sulphate-Reducing Bacteria’s Response to Extreme pH Environments and the Effect of Their Activities on Microbial Corrosion’, *Applied Science*, 11(2201). doi: https://doi.org/10.3390/app11052201.

Tsai, T. T. *et al.* (2008) ‘Chemical Oxidation of Chlorinated Solvents in Contaminated Groundwater: Review’, *Practice Periodical of Hazardous, Toxic, and Radioactive Waste Management*, 12(2), pp. 116–126. doi: 10.1061/(ASCE)1090-025X(2008)12:2(116).

Tsai, T. T. *et al.* (2010) ‘Treatment of TCE-Contaminated Groundwater Using Fenton-Like Oxidation Activated with Basic Oxygen Furnace Slag’, *Journal of Environmental Engineering*, 136(3), pp. 288–294. doi: 10.1061/(ASCE)EE.1943-7870.0000137.

Tsai, T. T. and Kao, C. M. (2009) ‘Treatment of petroleum-hydrocarbon contaminated soils using hydrogen peroxide oxidation catalyzed by waste basic oxygen furnace slag’, *Journal of Hazardous Materials*, 170(1), pp. 466–472. doi: 10.1016/j.jhazmat.2009.04.073.

Tsai, T. T., Kao, C. M. and Hong, A. (2009) ‘Treatment of tetrachloroethylene-contaminated groundwater by surfactant-enhanced persulfate / BOF slag oxidation — A laboratory feasibility study’, 171, pp. 571–576. doi: 10.1016/j.jhazmat.2009.06.036.

Tsai, T. T., Kao, C. M. and Wang, J. Y. (2011) ‘Chemosphere Remediation of TCE-contaminated groundwater using acid / BOF slag enhanced chemical oxidation’, *Chemosphere*, 83(5), pp. 687–692. doi: 10.1016/j.chemosphere.2011.02.023.

Tuffnell, S. (2017) *Acid drainage: the global environmental crisis you’ve never heard of, The Conversation*.

U.S. Energy Information Administration (2016) ‘Industrial sector energy consumption’, in *International Energy Outlook 2016*, pp. 113–126.

U.S. Geological Survey (2020) ‘Lime’, *Mineral Commodity Summaries*, 1(703).

United Nations (2018) ‘Sustainable Development Goal 6 Synthesis Report 2018 on Water and Sanitation’, p. 2.

United States Environmental Protection Agency (2018) *2018 Edition of the Drinking Water Standards and Health Advisories Tables*. Washington, DC.

United States Geological Survey Mineral Resources Program (2014) *Lime Prices in The United States by Type, Index Mundi*. Available at: United States Geological Survey Mineral Resources Program (Accessed: 25 May 2021).

Upadhyay, A. *et al.* (2021) ‘Exploring barriers and drivers to the implementation of circular economy practices in the mining industry’, *Resources Policy*, 72(February), p. 102037. doi: 10.1016/j.resourpol.2021.102037.

USEPA (2016) *Advancing Sustainable Materials Management*. USA.

Utgikar, V. P. *et al.* (2002) ‘Inhibition of sulfate-reducing bacteria by metal sulfide formation in bioremediation of acid mine drainage’, *Environmental Toxicology*, 17(1), pp. 40–48. doi: doi: 10.1002/tox.10031.

Uzun, I. and Güzel, F. (2000) ‘Adsorption of Some Heavy Metal Ions from Aqueous Solution by Activated Carbon and Comparison of Percent Adsorption Results of Activated Carbon with those of Some Other Adsorbents’, *Turkish Journal of Chemistry*, 24, pp. 291–297.

Valixa, M. *et al.* (2012) ‘Microbiologically Induced Corrosion of Concrete and Protective Coatings in Gravity Sewers’, *Chinese Journal of Chemical Engineering*, 20(3), pp. 433–438.

Vallero, D. A. (1970) ‘Dropping Acid and Heavy Metal Reactions’, in *Paradigms Lost: Learning from Environmental Mistakes, Mishaps, and Misdeeds*. Elsevier, pp. 339–365. doi: 10.1016/B978-0-7506-7888-9.50011-9.

Vasil, V., Lapšev, N., Stolbichin, J. (2013) ‘Microbiological Corrosion of Underground Sewage

Facilities of Saint Petersburg', *World Applied Sciences Journal*, 23(812), pp. 184–190. doi: 10.5829/idosi.wasj.2013.23.pac.90036.

Vats, N., Khan, A. A. and Ahmad, K. (2019) 'Observation of biogas production by sugarcane bagasse and food waste in different composition combinations', *Energy*, 185, pp. 1100–1105. doi: 10.1016/j.energy.2019.07.080.

Vaughan, D.J. and Corkhill, C. (2017) 'Mineralogy of Sulphides', *Elements*, 13(2), pp. 81–87.

Vaughan, D. J. (2005) 'Sulphides', in Selley, R. C., Plimer, I. R., and Cocks, R. M. (eds) *Encyclopedia of Geology*. Elsevier, pp. 574–586.

Vela, F. J., Zaiat, M. and Foresti, E. (2002) 'Influence of the COD to sulphate ratio on the anaerobic organic matter degradation kinetics', *Water SA*, 28(2), pp. 213–216. doi: 10.4314/wsa.v28i2.4887.

Vélez-Pérez, L. S. *et al.* (2020) 'Industrial acid mine drainage and municipal wastewater co-treatment by dual-chamber microbial fuel cells', *International Journal of Hydrogen Energy*, 45, pp. 13757–13766. doi: 10.1016/j.ijhydene.2019.12.037.

Verlicchi, P. and Grillini, V. (2020) 'Surface Water and Groundwater Quality in South Africa and Mozambique — Analysis of the Most Critical Pollutants for Drinking Purposes and Challenges in Water Treatment Selection', *Water*, 12, p. 305. doi: 10.3390/w12010305.

Vermeulen, I. and Phoenix Slag Services (2018) 'Consultation with Phoenix Slag'. Johannesburg, South Africa.

Vermuelen, I. (2019) 'Consultation/Quote from Phoenix Slag'. Johannesburg, South Africa.

Wang, B. (2016) 'Sand Wars – China and developing countries need tens of billions tons of sand for urbanization and economic growth', *nextbigfuture*, October.

Wang, G. C. (2016) *The Utilization of Slag in Civil Infrastructure Construction*. North Carolina: Woodhead Publishing.

Wang, H. Y. and Chen, K. W. (2016) 'A study of the engineering properties of CLSM with a new type of slag', *Construction and Building Materials*, 102, pp. 422–427.

Wang, X. and Cai, Q. (2006) 'Steel Slag as an iron fertilizer for corn growth and soil improvement in a pot experiment.', *Journal of Pedosphere*, 16(4), pp. 519–524.

Warren, J. K. (2006) *Evaporites:Sediments, Resources and Hydrocarbons*. Illustrate. Springer Science & Business Media.

Water for Africa (2009) *The Stakeholder Accord on Water Conservation: Guideline for Baseline Water Use Determination and Target Setting in the Mining Sector SAWC G4*. Pretoria.

Wei, R. *et al.* (2017) 'Current status and potential of biomass utilization in ferrous metallurgical industry', *Renewable and Sustainable Energy Reviews*, 68(February 2016), pp. 511–524. doi: 10.1016/j.rser.2016.10.013.

Westensee, D. K. *et al.* (2018) 'The availability of second generation feedstocks for the treatment of acid mine drainage and to improve South Africa's bio-based economy', *Science of the Total Environment*, 637–638, pp. 132–136. doi: 10.1016/j.scitotenv.2018.04.410.

Windt, L. De, Chaurand, P. and Rose, J. (2011) 'Kinetics of steel slag leaching : Batch tests and modeling', *Waste Management*, 31(2), pp. 225–235. doi: 10.1016/j.wasman.2010.05.018.

Wisconsin Department of Natural Resources (no date) 'Arsenic in Drinking Water How can arsenic affect my health?' Available at: http://dnr.wi.gov/files/PDF/pubs/DG/DG0062.pdf.

Working group III of the IPCC (2005) *IPCC Special Report on Carbon Dioxide Capture and Storage*. Edited by B. Metz et al. Cambridge, UK & New York, NY: Cambridge University Press.

World Health Organization (2004) *Guidelines for Drinking Water Quality*. Geneva.

World Health Organization (2009) *Calcium and Magnesium in Drinking-water: Public Health Significance*. Edited by J. Cotruvo and J. Bartram. Spain: WHO Press.

World Steel Association (2017) *WORLD STEEL IN FIGURES 2017*. Brussels, Beligium. Available at: https://www.worldsteel.org/en/dam/jcr:0474d208-9108-4927-ace8-4ac5445c5df8/World+Steel+in+Figures+2017.pdf.

Worldsteel Association (2016) *STEEL STATISTICAL YEARBOOK 2016*.

Wu, L., Hu, C. and Liu, W. V. (2018) 'The Sustainability of Concrete in Sewer Tunnel — A Narrative Review of Acid Corrosion in the City of Edmonton , Canada', *Sustainability*, 517(10), p. 24. doi: 10.3390/su10020517.

Wulff-zottele, C. *et al.* (2014) 'Plant Physiology and Biochemistry Sulphate fertilization ameliorates long-term aluminum toxicity symptoms in perennial ryegrass (Lolium perenne)', 83, pp. 88–99. doi: 10.1016/j.plaphy.2014.07.017.

Xiang, X. *et al.* (2016) 'Preparation and application of the cement-free steel slag cementitious material', *Construction and Building Materials*, 114, pp. 874–879. doi: 10.1016/j.conbuildmat.2016.03.186.

Xu, C. C. and Da-qiang, C. (2010) 'A Brief Overview of Low CO 2 Emission Technologies for Iron and Steel Making', *Journal of Iron and Steel Research International*, 17(3), pp. 1–7. doi: 10.1016/S1006-706X(10)60064-7.

Xue, Y. *et al.* (2006) 'Experimental investigation of basic oxygen furnace slag used as aggregate in asphalt mixture', *Journal of Hazardous Materials*, 138(2), pp. 261–268. doi: 10.1016/j.jhazmat.2006.02.073.

Xue, Y. *et al.* (2009) 'Utilization of municipal solid waste incineration ash in stone mastic asphalt mixture : Pavement performance and environmental impact', *Construction and Building Materials*, 23(2), pp. 989–996. doi: 10.1016/j.conbuildmat.2008.05.009.

Xue, Y., Hou, H. and S. Zhu (2009) 'Adsorption removal of reactive dyes from aqueous solution by modified basic oxygen furnace slag', *Journal of Chemical Engineering*, 147(272–279).

Xue, Y., Hou, H. and Zhu, S. (2009) 'Characteristics and mechanisms of phosphate adsorption onto basic oxygen furnace slag', 162, pp. 973–980. doi: 10.1016/j.jhazmat.2008.05.131.

Xue, Y., Wu, S. and Zhou, M. (2013) 'Adsorption characterization of Cu (II) from aqueous solution onto basic oxygen furnace slag', *Chemical Engineering Journal*, 231, pp. 355–364. doi: 10.1016/j.cej.2013.07.045.

Xuequan, W. *et al.* (1999) 'Study on steel slag and fly ash composite Portland cement', *Cement and Concrete Research*, 29, pp. 983–987.

Yamagata, C. and Paschoal, J. O. A. (2001) 'Systematic Precipitation of Magnesium Hydroxide Using NH 4 OH to Preparing MgO-PSZ Precursor Powder', pp. 1874–1879. doi: 10.4028/www.scientific.net/MSF.805.712.

Ye, G., Kärsrud, K. and Lindvall, M. (2011) 'Overview of the VILD-project, Vanadium Recovery from BOF-slag, a Long Term Slag Project for the Swedish Steel Industry', in *FRAY INTERNATIONAL SYMPOSIUM*. ISIJ-VDEh-Jernkontoret Joint Symposium.

Yi, H. *et al.* (2012) 'An overview of utilization of steel slag', 16, pp. 791–801. doi: 10.1016/j.proenv.2012.10.108.

Yildirim, I. Z. and Prezzi, M. (2011) 'Chemical , Mineralogical , and Morphological Properties of Steel Slag', 2011. doi: 10.1155/2011/463638.

Yildrim, I. Z. and Prezzi, M. (2009) *USE OF STEEL SLAG IN SUBGRADE APPLICATIONS*.

Zagury, G. J., Neculita, C. and Management, M. W. (2007) 'Passive Treatment of Acid Mine Drainage in Bioreactors : Short Review , Applications , and Research Needs', *Journal of Environmental Quality*, 36, pp. 1–16.

Zhang, T. *et al.* (2016) 'Removal of heavy metals from acid mine drainage using chicken eggshells in column mode.', *Journal of environmental management*, 188, pp. 1–8. doi: 10.1016/j.jenvman.2016.11.076.

Zhao, J. *et al.* (2016) 'Self-cementitious property of steel slag powder blended with gypsum', *Construction and Building Materials*, 113, pp. 835–842. doi: 10.1016/j.conbuildmat.2016.03.102.

Zhou, W. *et al.* (2016) 'Bioresource Technology Enhanced phosphorus removal from wastewater by growing deep-sea bacterium combined with basic oxygen furnace slag', *Bioresource Technology*, 214, pp. 534–540. doi: 10.1016/j.biortech.2016.05.008.

Zhu, N. *et al.* (2011) 'Bioleaching of metal concentrates of waste printed circuit boards by mixed culture of acidophilic bacteria', *Journal of Hazardous Materials*, 192(2), pp. 614–619. doi: 10.1016/j.jhazmat.2011.05.062.

Ziemkiewicz, P. (1998) 'Steel Slag: Application for AMD control', *Conference on Hazardous Waste Research*, (304), pp. 44–62. Available at: https://pdfs.semanticscholar.org/f52d/f3b4d240e21fb7b9c5fc4eea8f20306e7cec.pdf.

Ziemkiewicz, P. F., Skousen, J. G. and Simmons, J. (2003) 'Long-term Performance of Passive Acid Mine Drainage Treatment Systems', *Mine Water and the Environment*, 22, pp. 118–129.

Ziemkiewicz, P. and Skousen, J. (1997) 'The Use of Steel Slag in Acid Mine Drainage Treatment and Control', pp. 46–56.

Appendix I: Author Contributions

1. "An Assessment of Basic Oxygen Furnace Slag Dissolution for Application in AMD Dam Remediation using Waste Products from the Steel Manufacturing and Sugar Industries" was peer reviewed, presented and published in the SAIMM Mine Tailings Conference in 2020.

Reference:

Naidu, T. S., Chauhan, D., *et al.* (2020) 'An assessment of basic oxygen furnace slag dissolution for application in AMD dam remediation using waste products from the steel manufacturing and sugar industries', in Baker, J. et al. (eds) *Tailing storage conference 2020: Investing in a Sustainable Future*. Johannesburg: The Southern African Institute of Mining and Metallurgy; Camera Press, Johannesburg, pp. 51–62

Authors listed on this paper:

Tamlyn Sasha Naidu (TSN)

Divya Chauhan (DC)

Fiona Xiong (FX)

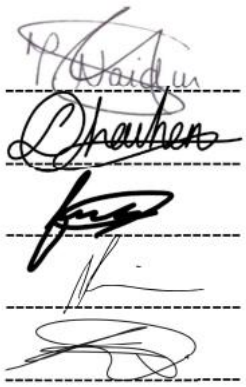
Craig Michael Sheridan (CMS)

Lizelle Doreen van Dyk (LvD)

Author Contribution Statement:

TSN, LvD and CMS conceived and planned the experiments. DC, FX and TSN carried out experimentation. TSN, DC and FX contributed to interpretation of the results and data. TSN wrote, prepared and submitted the manuscript. LvD and CMS supervised the project. LvD and CMS reviewed the manuscript.

Authors Signature:



Tamlyn Sasha Naidu (TSN)

Divya Chauhan (DC)

Fiona Xiong (FX)

Craig Michael Sheridan (CMS)

Lizelle Doreen van Dyk (LvD)

Date: 4 May 2022

2. "The Use of Basic Oxygen Furnace Slag as a Substitute for Lime in Acid Mine Drainage Treatment" was peer reviewed, presented and published at the South African Chemical Engineering Congress in 2021 (SACEC2021).

Reference:

Naidu, T. S., van Dyk, L. ., & Sheridan, C. . (2021). The Use of Basic Oxygen Furnace Slag as a Substitute for Lime in Acid Mine Drainage Treatment. In L. van Dyk, C. Sheridan, K. Harding, & J. Scholtz (Eds.), Proceedings of the South African Chemical Engineering Congress 2021 (A virtual , international conference organised by the South African Institution of Chemical Engineers - an association for the advancement of Chemical Engineering in South Africa) (pp. 156–166). The South African Institution of Chemical Engineers.

Authors listed on this paper:

Tamlyn Sasha Naidu (TSN)

Craig Michael Sheridan (CMS)

Lizelle Doreen van Dyk (LvD)

Author Contribution Statement:

TSN, LvD and CMS conceived and planned the experiments. TSN carried out experimentation. TSN performed interpretation of the results and data. TSN wrote, prepared, and submitted the manuscript. LvD and CMS supervised the project.

Authors Signature:



Tamlyn Sasha Naidu (TSN)

Craig Michael Sheridan (CMS)

Lizelle Doreen van Dyk (LvD)

Date: 4 May 2022

3. "Basic oxygen furnace slag: Review of current and potential uses" (critical review article) was peer reviewed and published in the Journal of Minerals Engineering.

Reference:

Naidu, T. S., Sheridan, C. M., & van Dyk, L. D. (2020). Basic oxygen furnace slag: Review of current and potential uses. *Minerals Engineering*, *149*(February), 106234. https://doi.org/10.1016/j.mineng.2020.106234

Authors listed on this paper:

Tamlyn Sasha Naidu (TSN)

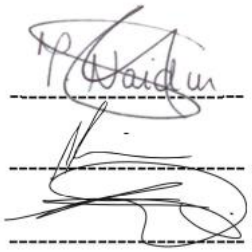
Craig Michael Sheridan (CMS)

Lizelle Doreen van Dyk (LvD)

Author Contribution Statement:

TSN and CMS conceived and planned the structure of the paper. TSN performed a literature review and the interpretation of various results and data. TSN wrote, prepared, and submitted the manuscript. LvD and CMS supervised the project and reviewed the manuscript.

Authors Signature:



Tamlyn Sasha Naidu (TSN)

Craig Michael Sheridan (CMS)

Lizelle Doreen van Dyk (LvD)

Date: 4 May 2022

4. “Passive acid mine drainage remediation using BOF steel slag and sugarcane bagasse” was peer reviewed, presented and published by the Aristotle University of Thessaloniki, at the Protection and restoration of the environment XIV conference (2018).

Reference:

Naidu, T. S., van Dyk, L. D., Sheridan, C. M., & Grubb, D. G. (2018). Passive acid mine drainage remediation using BOF steel slag and sugarcane bagasse. In N. Theodossiou, C. Christodoulatos, A. Koutsospyros, D. Karpouzos, & Z. Mallios (Eds.), Protection and restoration of the environment XIV (pp. 438–447). ARISTOTLE UNIVERSITY OF THESSALONIKI. https://doi.org/978-960-99922-4-4

Authors listed on this paper:

Tamlyn Sasha Naidu (TSN)

Craig Michael Sheridan (CMS)

Lizelle Doreen van Dyk (LvD)

Dennis Grubb (DG)

Author Contribution Statement:

TSN, LvD, DG and CMS conceived and planned the experimentation and the structure of the paper. TSN performed the experimentation. TSN, LvD, CMS and DG contributed to the interpretation of results and data. TSN wrote, prepared, and submitted the manuscript. LvD and CMS supervised the project. LvD, CMS and DG reviewed the manuscript.

Authors Signature:



Tamlyn Sasha Naidu (TSN)

Craig Michael Sheridan (CMS)

Lizelle Doreen van Dyk (LvD)

Dennis Grubb (DG)

Date: 4 May 2022

5. “Sugar and Steel By-Product Utilization in Acid Mine Drainage Remediation” was peer reviewed and published in the American Society of Civil Engineers Journal of Hazardous, Toxic, and Radioactive Waste.

Reference:

Naidu, T. S., van Dyk, L. D., Sheridan, C. M., & Grubb, D. G. (2020). Sugar and Steel By-Product Utilization in Acid Mine Drainage Remediation. Journal of Hazardous, Toxic and Radioactive Waste, 24(1), 1–10. https://doi.org/10.1061/(ASCE)HZ.2153-5515.0000472.

Authors listed on this paper:

Tamlyn Sasha Naidu (TSN)

Craig Michael Sheridan (CMS)

Lizelle Doreen van Dyk (LvD)

Dennis Grubb (DG)

Author Contribution Statement:

TSN, LvD, DG and CMS conceived and planned the experimentation and the structure of the paper. TSN performed the experimentation and TSN, LvD, CMS and DG contributed to the interpretation of results and data. TSN wrote, prepared, and submitted the manuscript. LvD and CMS supervised the project and LvD, CMS and DG reviewed the manuscript.

Authors Signature:



Tamlyn Sasha Naidu (TSN)

Craig Michael Sheridan (CMS)

Lizelle Doreen van Dyk (LvD)

Dennis Grubb (DG)

Date: 4 May 2022

6. “Acid Mine Drainage Pilot Remediation System using Waste Products from the Steel Manufacturing and Sugar Industries”, was peer reviewed and presented at the International Mine Water Association’s 2019 conference: “Mine Water: Technological and Ecological Challenges".

Reference:

Naidu, T. S., Sheridan, C. M., van Dyk, L. D., & Higginson, A. (2019). Acid Mine Drainage Pilot Remediation System using Waste Products from the Steel Manufacturing and Sugar Industries. In C. Wolkersdorfer, E. Khayrulina, S. Polyakova, & A. Bogush (Eds.), IMWA 2019 “Mine Water: Technological and Ecological Challenges" (pp. 121–126). International Mine Water Association. https://doi.org/978-5-91252-145-4

Authors listed on this paper:

Tamlyn Sasha Naidu (TSN)

Craig Michael Sheridan (CMS)

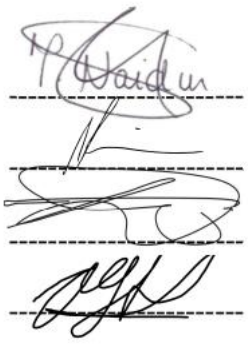
Lizelle Doreen van Dyk (LvD)

Antony Higginson (AH)

Author Contribution Statement:

TSN, LvD, and CMS conceived and planned the experimentation and the structure of the paper. TSN performed the experimentation, AH assisted with set-up of the experimentation. TSN wrote, prepared, and submitted the manuscript. LvD and CMS supervised the project and LvD, CMS and AH reviewed the manuscript.

Authors Signature:



Tamlyn Sasha Naidu (TSN)

Craig Michael Sheridan (CMS)

Lizelle Doreen van Dyk (LvD)

Antony Higginson (AH)

Date: 4 May 2022

7. "Design of Acid Mine Drainage Remediation Plant", WRC document (2757/1/21) was reviewed, accepted and published as a report by the Water Research Commission of South Africa.

Reference:

Naidu, T. S., Sheridan, C. M., & van Dyk, L. D. (2021). Design of Acid Mine Drainage Remediation Plant (Issue 2757). WRC. http://www.wrc.org.za/wp-content/uploads/mdocs/2757 final.pdf. ISBN 978-0-6392-0264-8

Authors listed on this paper:

Tamlyn Sasha Naidu (TSN)

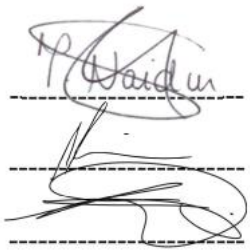
Craig Michael Sheridan (CMS)

Lizelle Doreen van Dyk (LvD)

Author Contribution Statement:

TSN, LvD, and CMS conceived and planned the experimentation. TSN performed the experimentation. TSN wrote, prepared, submitted and presented the manuscript. LvD and CMS supervised the project and LvD, CMS reviewed the manuscript.

Authors Signature:



Tamlyn Sasha Naidu (TSN)

Craig Michael Sheridan (CMS)

Lizelle Doreen van Dyk (LvD)

Date: 4 May 2022